cies within the taxon *Anopheles dirus* Peyton and Harrison (Diptera: Culicidae) in Thailand. *Proc Entomol Soc Wash* 89: 157-166.

Calado DC, Foster PG, Bergo ES, dos Santos CLS, Galardo AKR, Sallum MAM 2008. Resurrection of *Anopheles goeldii* from synonymy with *Anopheles nuneztovari* (Diptera, Culicidae) and a new record for *Anopheles dunhami* in the Brazilian Amazon. *Mem Inst Oswaldo Cruz 103*: 791-799.

Chen B, Butlin RK, Pedro PM, Wang XZ, Harbach RE 2006. Molecular variation, systematics and distribution of the *Anopheles fluviatilis* complex in southern Asia. *Med Vet Entomol 20*: 33-43.

Choochote W 2011. Evidence to support karyotypic variation of the mosquito *Anopheles peditaeniatus* in Thailand. *J Insect Sci 11*: 10.

Choochote W, Abeyewickreme W, Sucharit S, Tumrasvin W, Rongsriyam Y 1984. Laboratory hybridization of *Anopheles philippinensis* and *Anopheles annularis* in Thailand. *J Parasit Trop Med Ass Thailand 7*: 7-11.

Choochote W, Jitpakdi A, Rongsriyam Y, Komalamisra N, Pitasawat B, Palakul K 1998. Isoenzyme study and hybridization of two forms of *Anopheles sinensis* (Diptera: Culicidae) in Northern Thailand. *Southeast Asian J Trop Med Public Health 29*: 841-847.

Choochote W, Jitpakdi A, Sukontason K, Chaithong U, Wongkamchai S, Pitasawat B, Jariyapan N, Suntaravitun T, Rattanachanpichai E, Sukontason K, Leemingsawat S, Rongsriyam Y 2002. Intraspecific hybridization of two karyotypic forms of *Anopheles vagus* (Diptera: Culicidae) and the related egg surface topography. *Southeast Asian J Trop Med Public Health 33* (Suppl. 3): 29-35.

Choochote W**,** Sucharit S, Abeywickreme W 1983. Experiments in crossing two strains of *Anopheles barbirostris* van der Wulp 1884 (Diptera: Culicidae) in Thailand. *Southeast Asian J Trop Med Public Health 14*: 204-209.

Garros C, Harbach RE, Manguin S 2005. Morphological assessment and molecular phylogenetics of the Funestus and Minimus Groups of *Anopheles* (*Cellia*). *J Med Entomol 42*: 522-536.

Harbach RE 2004. The classification of genus *Anopheles* (Diptera: Culicidae): a working hypothesis of phylogenetic relationships. *Bull Entomol Res 95*: 537-553.

Harbach RE 2010. Mosquito taxonomic inventory. *Anopheles* classification. Available from: mosquito-taxonomic-inventory.info/anophelesclassification.

Harrison BA 1973. A lectotype designation and description for *Anopheles* (*An.*) *sinensis* Wiedemann 1828, with a discussion of the classification and vector status of this and some other Oriental *Anopheles. J Am Mosq Control Assoc 5*: 1-13.

Harrison BA 1980. Medical entomology studies: XIII. The *Myzomyia* series of *Anopheles* (*Cellia*) in Thailand with emphasis on intra-interspecific variations (Diptera: Culicidae)*. Contributions of the American Entomological Institute 17*: 1-195.

Harrison BA, Rattanarithikul R, Peyton EL, Mongolpanya K 1991. Taxonomic changes, revised occurrence records and notes on the Culicidae of Thailand and neighboring countries. *J Am Mosq Control Assoc 22*: 196-227.

Harrison BA, Scanlon JE 1975. Medical entomology studies II. The subgenus *Anopheles* in Thailand (Diptera: Culicidae). *Contributions of the American Entomological Institute 12*: 1-307.

Hwang UW 2007. Revisited ITS2 phylogeny of *Anopheles* (*Anopheles*) *hyrcanus* group mosquitoes: re-examination of unidentified and misidentified ITS2 sequences. *Parasitol Res 101*: 885-894.

Joshi D, Choochote W, Park MH, Kim JY, Kim TS, Suwonkerd W, Min GS 2009. The susceptibility of *Anopheles lesteri* to infection with Korean strain of *Plasmodium vivax*. *Malar J 8*: 42.

Joshi D, Kim JY, Choochote W, Park MH, Min GS 2011. Preliminary vivax malaria vector competence for three members of the *Anopheles hyrcanus* group in the Republic of Korea. *J Am Mosq Control Assoc 27*: 312-314.

Junkum A, Jitpakdi A, Jariyapan N, Komalamisra N, Somboon P, Suwonkerd W, Saejeng A, Bates PA, Choochote W 2005. Evidence to support two conspecific cytological races on *Anopheles aconitus* in Thailand. *J Vector Ecol 30*: 213-224.

Kanda T 1979. Improved techniques for the preparation of polytene chromosome for some anopheline mosquitoes. *Mosq News 39*: 568-574.

Kanojia PC, Shetty PS, Geevarghese G 2003. A long-term study on vector abundance & seasonal prevalence in relation to the occurrence of Japanese encephalitis in Gorakhpur district, Uttar Pradesh. *Indian J Med Res 117*: 104-110.

Kim SJ, Choochote W, Jitpakdi A, Junkum A, Park SJ, Min GS 2003. Establishment of a self-mating mosquito colony of *Anopheles sinensis* from Korea. *Korean J Entomol 33*: 267-271.

Kimura MA 1980. Simple method for estimating evolutionary rates of base substitution through comparative studies of nucleotide sequences. *J Mol Evol 16*: 111-120.

Klein TA, Harrison BA, Baimai V, Phunkitchar V 1984. Hybridization evidence supporting separate species status for *Anopheles nivipes* and *Anopheles philippinensis. Mosq News 44*: 466-470.

Lee WJ, Klein TA, Kim HC, Choi YM, Yoon SH, Chang KS, Chong ST, Lee IY, Jones JW, Jacobs JS, Sattabongkot J, Park JS 2007. *Anopheles kleini*, *Anopheles pullus* and *Anopheles sinensis*: potential vectors of *Plasmodium vivax* in the Republic of Korea. *J Med Entomol 44*: 1086-1090.

Ma Y, Xu J 2005. The hyrcanus group of *Anopeles* (*Anopheles*) in China (Diptera: Culicidae): species discrimination and phylogenetic relationships inferred by ribosomal DNA internal transcribed spacer 2 sequences. *J Med Entomol 42*: 610-619.

Ma Y, Yang P 2005. Taxonomic study on *Anopheles anthropophagus* from China (Diptera: Culicidae): inferred by morphology, chromosome karyotype and molecular markers. *Kun Chong Fen Lei Xue Bao 27*: 199-208.

Min GS, Choochote W, Jitpakdi A, Kim SJ, Kim W, Jung J, Junkum A 2002. Intraspecific hybridization of *Anopheles sinensis* (Diptera: Culicidae) strains from Thailand and Korea. *Mol Cells 14*: 198-204.

Park MH, Choochote W, Kim SJ, Somboon P, Saeung A, Tuetan B, Tsuda Y, Takagi M, Joshi D, Ma Y, Min GS 2008. Nonreproductive isolation among four allopatric strains of *Anopheles sinensis* in Asia. *J Am Mosq Control Assoc 24*: 489-495.

Park SJ, Choochote W, Jitpakdi A, Junkum A, Kim SJ, Jariyapan N, Park JW, Min GS 2003. Evidence for a conspecific relationship between two morphologically and cytologically different forms of Korean *Anopheles pullus* mosquito. *Mol Cells 16*: 354-360.

Paskewitz SM, Wesson DM, Collins FH 1993. The internal transcribed spacers of ribosomal DNA in five members of the *Anopheles gambiae* species complex. *Insect Mol Biol 2*: 247-257.

Rattanarithikul R, Harrison BA, Harbach RE, Panthusiri P, Coleman RE 2006. Illustrated keys to the mosquitoes of Thailand IV. *Anopheles. Southeast Asian J Trop Med Public Health 37* (Suppl. 2): 1-128.

Ree HI, Hwang UW, Lee IY, Kim TE 2001. Daily survival and human blood index of *Anopheles sinensis*, the vector species of malaria in Korea. *J Am Mosq Control Assoc 17*: 67-72.

Reid JA 1963. Notes on anopheline mosquitoes from Malaya with descriptions of three new species. *Ann Trop Med Parasitol 57*: 97-116.

Reid JA 1968. Anopheline mosquitoes of Malaya and Borneo. *Stud Inst Med Res Malaya 31*: 1-520.

Reid JA, Wilson T, Ganapathipillai A 1962. Studies on filariasis in Malaya: the mosquito vectors of periodic *Brugia malayi* in northwest Malaya. *Ann Trop Med Parasitol 56*: 323-336.

Ronquist F, Teslenko M, van der Mark P, Ayres DL, Darling A, Höhna S, Larget B, Liu L, Suchard MA, Huelsenbeck JP 2012. MrBayes 3.2: efficient Bayesian phylogenetic inference and model choice across a large model space. *Syst Biol 61*: 539-542.

Rueda LM, Li C, Kim HC, Klein TA, Foley DH, Wilkerson RC 2010. *Anopheles belenrae*, a potential vector of *Plasmodium vivax* in the Republic of Korea. *J Am Mosq Control Assoc 26*: 430-432.

Rueda LM, Wilkerson RC, Li C 2005. *Anopheles (Anopheles) lesteri* Baisas and Hu (Diptera: Culicidae): neotype designation and description. *Proc Entomol Soc Wash 107*: 604-662.

Ruiz F, Linton YM, Ponsonby DJ, Conn JE, Herrera M, Quiñones ML, Vélez ID, Wilkerson RC 2010. Molecular comparison of topotypic specimens confirms *Anopheles (Nyssorhynchus) dunhami* Causey (Diptera: Culicidae) in the Colombian Amazon. *Mem Inst Oswaldo Cruz 105*: 899-903.

Saeung A, Baimai V, Otsuka Y, Rattanarithikul R, Somboon P, Junkum A, Tuetun B, Takaoka H, Choochote W 2008. Molecular and cytogenetic evidence of three sibling species of the *Anopheles barbirostris* form A (Diptera:Culicidae) in Thailand. *Parasitol Res 102*: 499-507.

Saeung A, Otsuka Y, Baimai V, Somboon P, Pitasawat B, Tuetun B, Junkum A, Takaoka H, Choochote W 2007. Cytogenetic and molecular evidence for two species in the *Anopheles barbirostris* complex (Diptera: Culicidae) in Thailand. *Parasitol Res 101*: 1337-1344.

Saitou N, Nei M 1987. The neighbor-joining method: a new method for reconstructing phylogenetic trees. *Mol Biol Evol 4*: 406-425.

Sandosham AA 1959. *Malariology, with special reference to Malaya*, University of Malaya Press, Singapore, 322 pp.

Sasa M 1976. *Human filariasis: a global survey of epidemiology and control*, University of Tokyo Press, Tokyo, 819 pp.

Singh OP, Chandra D, Nanda N, Sharma SK, Htun PT, Adak T, Subbarao SK, Dash AP 2006. On the conspecificity of *Anopheles fluviatilis* species S with *Anopheles minimus* species C. *J Biosci 31*: 671-677.

Somboon P, Thongwat D, Choochote W, Walton C, Takagi M 2005. Crossing experiments of *Anopheles minimus* species C and putative species E. *J Am Mosq Control Assoc 21*: 5-9.

Somboon P, Tuno N, Tsuda Y, Takagi M 2000. Evidence of the specific status of *Anopheles flavirostris* (Diptera: Culicidae). *J Med Entomol 37*: 476-479.

Somboon P, Walton C, Sharpe RG, Higa Y, Tuno N, Tsuda Y, Takagi M 2001. Evidence for a new sibling species of *Anopheles minimus* from the Ryukyu Archipelago, Japan. *J Am Mosq Control Assoc 17*: 98-113.

Sucharit S, Choochote W 1982. Hybridization of *Anopheles minimus* and *Anopheles aconitus* (Diptera: Culicidae) in Thailand. *J Med Entomol 19*: 209-292.

Suwannamit S, Baimai V, Otsuka Y, Saeung A, Thongsahuan S, Tuetun B, Apiwathnasorn C, Jariyapan N, Somboon P, Takaoka H, Choochote W 2009. Cytogenetic and molecular evidence for an additional new species within the taxon *Anopheles barbirostris* (Diptera: Culicidae) in Thailand. *Parasitol Res 104*: 905-918.

Tamura K, Dudley J, Nei M, Kumar S 2007. MEGA4: Molecular Evolution Genetics Analysis (MEGA) software version 4.0. *Mol Biol Evol 24*: 1596-1599.

Thompson JD, Higgins DG, Gibson TJ 1994. CLUSTALW: improving the sensitivity of progressive multiple sequence alignment through sequence weighting, positions-specific gap penalties and weight matrix choice. *Nucleic Acids Res 22*: 4673-4680.

Thongsahuan S, Baimai V, Otsuka Y, Saeung A, Tuetun B, Jariyapan N, Suwannamit S, Somboon P, Jitpakdi A, Takaoka H, Choochote W 2009. Karyotypic variation and geographic distribution of *Anopheles campestris*-like (Diptera: Culicidae) in Thailand. *Mem Inst Oswaldo Cruz 104*: 558-566.

Thongwat D, Morgan K, O'loughlin MS, Walton C, Choochote W, Somboon P 2008. Crossing experiment supporting the specific status of *Anopheles maculatus* chromosomal form K. *J Am Mosq Control Assoc 24*: 194-202.

Whang IJ, Jung J, Park JK, Min GS, Kim W 2002. Intragenomic length variation of the ribosomal DNA intergenic spacer in a malaria vector, *Anopheles sinensis*. *Mol Cells 14*: 158-162.

White GB, Coluzzi M, Zahar AR 1975. Review of cytogenetic studies on anopheline vectors of malaria. Available from: apps.who.int/iris/bitstream/10665/65716/1/WHO_MAL_75.849.pdf.

Wilkerson RC, Li C, Rueda LM, Kim HC, Klein TA, Song GH, Strickman D 2003. Molecular confirmation of *Anopheles* (*Anopheles*) *lesteri* from the Republic of South Korea and its genetic identity with *An.* (*Ano.*) *anthropophagus* from China (Diptera: Culicidae). *Zootaxa 378*: 1-14.

Zhang HL 1990. The natural infection rate of mosquitoes by Japanese encephalitis B virus in Yunnan Province. *Zhonghua Yu Fang Yi Xue Za Zhi 24*: 265-267.

SUSCEPTIBILITY OF FIVE SPECIES MEMBERS OF THE KOREAN HYRCANUS GROUP TO *BRUGIA MALAYI*, AND HYBRIDIZATION BETWEEN *B. MALAYI*-SUSCEPTIBLE AND -REFRACTORY *ANOPHELES SINENSIS* STRAINS

Atiporn Saeung[1], Gi-Sik Min[2], Sorawat Thongsahuan[3], Kritsana Taai[1], Siripan Songsawatkiat[1] and Wej Choochote[1]

[1]Department of Parasitology, Faculty of Medicine, Chiang Mai University, Chiang Mai 50200, Thailand; [2]Department of Biological Sciences, Inha University, Incheon 402-751, South Korea; [3]Faculty of Veterinary Science (Establishment Project), Prince of Songkla University, Songkhla 90110, Thailand

*Correspondence: Dr. Wej Choochote, Department of Parasitology, Faculty of Medicine, Chiang Mai, University, Chiang Mai 50200, Thailand
E-mail: wchoocho@mail.med.cmu.ac.th; choochote.wej@gmail.com

Formatted: Complex Script Font: Italic

Abstract. Five species members of the Korean Hyrcanus Group, *i.e.*, *Anopheles pullus*, *Anopheles sinensis*, *Anopheles kleini*, *Anopheles belenrae* and *Anopheles lesteri* were tested for susceptibility to *Brugia malayi*. They were allowed to feed artificially on blood containing *B. malayi* microfilariae, and dissected 14 days after feeding. The susceptibility rates were 60%, 65%, 90%, 100% and 100% in *An. pullus*, *An. sinensis*, *An. kleini*, *An. belenrae* and *An. lesteri*, respectively. As determined by levels of susceptibility, results indicated that *An. pullus* was a moderate potential vector, while *An. sinensis*, *An. kleini*, *An. belenrae* and *An. lesteri* were high potential vectors, when compared with the 90-95% susceptibility rates of an efficient control vector, *Ochlerotatus* (= *Aedes*) *togoi*. An introgressive study of *B. malayi*-susceptible/-refractory genes was performed intensively by hybridization experiments between a high (Korean strain) and a low (Thailand strain) potential *An. sinensis* vectors, and the susceptibility rates of F_1-hybrids and backcross progenies were compared with parental stocks. The results revealed that the *B. malayi*-susceptible genes could be introgressed from a high to low potential *An. sinensis* vector by increasing the susceptibility rates from 0-5% in the parental stocks to 55% and 70% in F_1-hybrids and backcross progenies, respectively. The increase of susceptibility rates related clearly to the increase of normal larval development in the thoracic muscles of F_1-hybrids and backcross progenies.

Keywords: *Anopheles*, *Hyrcanus* Group, *Brugia malayi*, susceptibility level, hybridization, susceptible/refractory genes, Korea

Formatted: Complex Script Font: Italic

Formatted: Font: Italic

INTRODUCTION

Anophelines of the Hyrcanus Group comprises at least 27 species members and ~~has~~ have a wide distribution extending from Iberia in Europe to East and Southeast Asian regions, including some of the off-lying islands of the Indian and Pacific oceans (Harrison and Scanlon, 1975; Tanaka *et al*, 1979; Harbach, 2013). It is well known that some species members of the *Hyrcanus* Group are involved in the transmission of human diseases (*e.g*., malaria: *Plasmodium vivax*, filariasis: *Brugia malayi* and Japanese encephalitis virus), particularly in the Oriental Region and contiguous parts of the eastern Palaearctic Region (Sasa, 1976; Zhang, 1990; Ree *et al*, 2001; Kanojia *et al*, 2003; Lee *et al*, 2007; Rueda et al, 2010; Joshi *et al*, 2011).

In the Republic of Korea (ROK), at least 6 species members (*An. belenrae*, *An. kleini*, *An. lesteri*, *An. pullus*, *An. sinensis* and *An. sineroides*) of the *Hyrcanus* Group have been recognized (Tanaka *et al*, 1979; Rueda, 2005). Among these, *An. sinensis* was incriminated as a natural vector of lymphatic filariasis due to *B. malayi* in mainland ROK, whereas *An. sinensis* and *An. lesteri* were reported as natural vectors of this filarial parasite in China (Sasa, 1976). Regarding control measures in the ROK, the reduction of microfilariae in the peripheral blood of carriers interrupts the mosquito-transmitted cycle by using mass, combined with selective, treatments with a microfilaricide (diethylcarbamazine: DEC) to microfilaria positive persons. These measures were started firstly in 1964 together with remarkable economic growth followed by improved living standards, including environmental and personal hygiene. This filarial control program brought about complete elimination of this lymphatic filariasis in 2007 (Cheun *et al*, 2009). Despite complete success of the program, re-emergence at any time of this endemic disease should be kept in mind, even in thoroughly controlled endemic regions, where the environmental

Formatted: Complex Script Font: Italic
Formatted: Font: Not Italic
Formatted: Font: Italic
Formatted: Font: Italic
Formatted: Font: Italic

factor (s) favors suitable conditions for the transmission-cycle. This was reported recently in other mosquito-borne diseases, *e.g*., re-emergence of malaria due to *Plasmodium vivax* in the ROK (Chai *et al*, 1994; Park *et al*, 2000; Shim and Shin, 2002).

Regarding the information mentioned above, details of the natural vectors of *B. malayi* have been documented in only *An. sinensis* among 6 species members of the Korean Hyrcanus Group. Therefore, this information clearly emphasizes lack of knowledge on the vector competence to *B. malayi* of these anopheline mosquitoes. However, the information could be used as a robust primary guideline for a field control approach, when suspecting any anopheline species of being a transmitting vector in endemic areas of Brugian filariasis. Hence, this study reports the susceptibility to *B. malayi* of 5 species members of the Korean Hyrcanus Group (*An. belenrae*, *An. kleini*, *An. lesteri*, *An. pullus* and *An. sinensis*). In addition, this paper reported that an introgressive study of *B. malayi*-susceptible/-refractory genes between high (Korean strain) and low (Thailand strain) potential *An. sinensis* vectors was performed by hybridization experiments and comparison of susceptibility levels of F_1-hybrids and backcross progenies with parental stocks.

MATERIALS AND METHODS

Mosquito species: wild-caught, fully engorged females of *An. belenrae*, *An. kleini*, *An. pullus* and *An. sinensis* were collected from Paju City, Gyeonggi-do Province, while *An. lesteri* was collected from So-Rae District, Incheon City, ROK. Species identification of wild caught-females followed standard illustrated keys (Tanaka *et al*, 1979; Rueda, 2005). Subsequently, morphological identification (using intact morphology of eggs, larvae, pupal skins and adult females) and

molecular investigation (Joshi *et al*, 2010) were performed in F_1-progenies of iso-female lines in order to guarantee the exact identification of species. Then, the laboratory colonies of the 5 anopheline species were established by pooling 5 iso-female lines of each anopheline species, using the techniques described by (Kim *et al*, 2003). These colonies were used for studies on susceptibility to *B. malayi* throughout the experiments. Regarding an introgressive study of *B. malayi*-susceptible/-refractory genes, the parental stocks of *An. sinensis* Korean strain: a high potential vector for *B. malayi* (results obtained from this study), *An. sinensis* Thailand strain: a low potential vector for *B. malayi* (Saeung *et al*, 2013), and their F_1-hybrids and backcross progenies were used. As for the control vector, autogenous *Ochlerotatus* (= *Aedes*) *togoi* (Chanthaburi Province, eastern Thailand strain) was selected as a proven efficient laboratory vector for a wide-range of genera and species of filarial nematodes, including *B. malayi* (Jumkum *et al*, 2003).

Filarial *B. malayi:* this filarial parasite originated from a 20-year-old woman, who was a resident of Narathiwat Province, southern Thailand. Domestic cats were later infected experimentally with the parasite, which was maintained at the Department of Medical Entomology, Faculty of Tropical Medicine, Mahidol University, Bangkok, Thailand, from 1982 to 1986, when it was transferred to Mongolian jirds (*Meriones unguiculatus*) and then maintained at the animal house of the Faculty of Medicine, Chiang Mai University, Chiang Mai, Thailand (Choochote *et al*, 1986).

Blood containing *B. malayi* microfilariae: preparation of blood containing *B. malayi* microfilaria ~~was~~ followed the details as described recently (Saeung *et al*, 2013). Briefly, the jirds were intraperitoneally inoculated for at least 3 months with infective larvae of *B. malayi* and anesthetized deeply with ethylene ether. The

microfilariae were collected by injecting 3 ml of Hank's Balanced Salt Solution (HBSS, pH 7.2-7.4) into the peritoneal cavity before withdrawing by peritoneal washing. The 0.05 ml of peritoneal-washed-rich microfilariae was mixed with 5 ml of human-heparinized blood (10 units of heparin/ml of blood), taken from human volunteers who had signed the consent form. Then, the adjusted microfilarial density ranged from approximately 250 to 350 microfilariae (mf)/20 µl by using the human-heparinized blood for artificial~~ly~~ feeding all of all the mosquito species.

Infection of mosquitoes with *B. malayi* microfilariae: five-day-old adult female *Oc. togoi*, *An. belenrae*, *An. kleini*, *An. lesteri*, *An. pullus* and *An. sinensis* fasted for 24 hrs and then were allowed artificial feeding simultaneously on blood-containing *B. malayi* microfilariae (microfilarial density = 305 and 297 mf/20 µl in experiment I and II, respectively), using the techniques and apparatus previously described (Chomcharn *et al*, 1980). Likewise, 5-day-old female *An. sinensis* Korean and Thailand strains, and their F_1-hybrids and backcross progenies fasted for 24 hrs and then were allowed artificial feeding simultaneously on blood-containing *B. malayi* microfilariae (microfilarial density = 323 and 346 mf/20 µl in experiment I and II, respectively), using similar procedures as mentioned above. Fourteen days after feeding, all infected mosquitoes were dissected in normal saline solution and examined under a dissecting microscope. The number of mosquitoes with one or more infective stage larvae in any part of the body (head, thorax or abdomen) was recorded.

Determination of the possible factor (s) affecting the level of susceptibility: the thorax of infected *An. sinensis* Korean and Thailand strains, and their F_1-hybrids and backcross progenies were torn in a drop of normal saline solution and examined under a compound microscope 4 days after feeding. The first stage (L_1) larvae were

counted and scored as normal L_1 larvae if alive with intact morphology. The larvae were scored as melanized L_1 larvae if they had evidence of a retained stage and melanotic encapsulation; and scored as degenerated L_1 larvae if they demonstrated vacuolated internal organs without any evidence of melanotic encapsulation.

Ethical clearance: the protocols were approved by the Animal Ethics Committee of Faculty of Medicine, Chiang Mai University, Chiang Mai, Thailand.

RESULTS

Details of the infective rates and parasite loads of *Oc. togoi*, *An. belenrae*, *An. kleini*, *An. lesteri*, *An. pullus* and *An. sinensis* 14 days after feeding on blood containing *B. malayi* microfilariae are shown in Table 1. The 95% and 90% infective rates corresponded to an average of 16.74 and 13.06 infective (L_3) larvae per infected *Oc. togoi* in experiment I and II, respectively, which indicated that all feeding experiments were under conditions of appropriate *B. malayi* microfilarial densities in infected blood. The infective rates and average number of L_3 larvae per infected mosquito of *An. pullus*, *An. belenrae* and *An. lesteri* in experiment I, were 60% and 8.50, 100% and 8.85, and 100% and 10.90, respectively; and those in *An. kleini* and *An. sinensis* in experiment II, were 90% and 5.39, and 65% and 4.23, respectively. Comparative statistical analyses of the infective rates and average number of L_3 larvae per infected mosquito were carried out between *Oc. togoi* and 5 *An. hyrcanus* species. The results revealed that the infective rates differed significantly ($P < 0.05$) only between *Oc. togoi* and *An. pullus*, whereas the average number of L_3 larvae per infected mosquito did not differ significantly ($P < 0.05$) only between *Oc. togoi* and *An. leteri.* Notably, all infective larvae that recovered from the 2 experimental feedings were very active and found to distribute in all regions of

the head, thorax and abdomen. Also, their behavior was similar, with more than 65% of infective larvae migrating from the thorax to the head and proboscis.

Details of the infective rates and parasite loads of parental, F_1-hybrids and backcross progenies of *An. sinensis* Korean and Thailand strains, 14 days after feeding on blood containing *B. malayi* microfilariae, are shown in Table 2. The 65% and 60% infective rates corresponded to an average of 3.62 and 4.33 L_3 larvae per infected *An sinensis* Korean strain in experiment I and II, respectively, which indicated that all feeding experiments were under conditions of suitable *B. malayi* microfilarial densities in infected blood. The infective rates and average number of L_3 larvae per infected mosquito of *An. sinensis* Korean strain, *An. sinensis* Thailand strain, and their 2 F_1-hybrids [(female *An. sinensis* Korean strain x male *An. sinensis* Thailand strain)F_1 and (female *An. sinensis* Thailand strain x male *An. sinensis* Korean strain)F_1] in experiment I, were 65% and 3.62, 5% and 1, 65% and 3.92, and 55% and 5.27, respectively. Comparative statistical analyses of the infective rates and average number of L_3 larvae per infected mosquito were carried out between *An. sinensis* Korean strain and (female *An. sinensis* Korean strain x male *An. sinensis* Thailand strain)F_1, and *An. sinensis* Thailand strain and (female *An. sinensis* Thailand strain x male *An. sinensis* Korean strain)F_1. The results revealed that the infective rates and average number of L_3 larvae per infected mosquito differed significantly ($P < 0.05$) only between *An. sinensis* Thailand strain and (female *An. sinensis* Thailand strain x male *An. sinensis* Korean strain)F_1. The infective rates and average number of L_3 larvae per infected mosquito of *An. sinensis* Korean strain and *An. sinensis* Thailand strains, and their backcross progenies [(female *An. sinensis* Korean strain x male *An. sinensis* Thailand strain)F_1 x male *An. sinensis* Thailand strain], and [(female *An. sinensis* Thailand strain x male *An. sinensis* Korean

strain)F_1 x male *An. sinensis* Korean strain] in experiment II, were 60% and 4.33, 0%, 45% and 4.22, and 70% and 5.50, respectively. Comparative statistical analyses of the infective rates and average number of L_3 larvae per infected mosquito were carried out between *An. sinensis* Korean strain and [(female *An. sinensis* Korean strain x male *An. sinensis* Thailand strain)F_1 x male *An. sinensis* Thailand strain], and *An. sinensis* Thailand strain and [(female *An. sinensis* Thailand strain x male *An. sinensis* Korean strain)F_1 x male *An. sinensis* Korean strain]. The results revealed that the infective rates and average number of L_3 larvae per infected mosquito differed significantly ($P < 0.05$) only between *An. sinensis* Thailand strain and [(female *An. sinensis* Thailand strain x male *An. sinensis* Korean strain)F_1 x male *An. sinensis* Korean strain].

Parasite loads dissected 4 days after feeding on blood containing *B. malayi* microfilariae in parental, F_1-hybrids and backcross progenies of *An. sinensis* Korean and Thailand strains are detailed in Table 3 and Fig. 1. A satisfactory average number of 19.40, 21.60, 23.20 and 18.20 L_1 larvae recovered from the thoracic muscles of *An. sinensis* Korean strain, *An. sinensis* Thailand strain, (female *An. sinensis* Korean strain x male *An. sinensis* Thailand strain)F_1, and (female *An. sinensis* Thailand strain x male *An. sinensis* Korean strain)F_1, respectively, in experiment I; and 24.60, 23.80, 20.40 and 25.60 L_1 larvae obtained from the thoracic muscles of *An. sinensis* Korean strain, *An. sinensis* Thailand strain, [(female *An. sinensis* Korean strain x male *An. sinensis* Thailand strain)F_1 x male *An. sinensis* Thailand strain], and [(female *An. sinensis* Thailand strain x male *An. sinensis* Korean strain)F_1 x male *An. sinensis* Korean strain], respectively, in experiment II, indicated that all of the mosquito species were successful in taking a considerable number of microfilariae from infected blood, and subsequently they invaded the cells

of thoracic muscles. However, low degrees of normal L_1 and high degrees of abnormal L_1 (melanized and degenerated L_1) larval development in the thoracic muscles of *An. sinensis* Thailand strain (normal L_1: 16.67-23.53%, abnormal L_1: 76.47-83.33%) clearly were different from those of *An. sinensis* Korean strain (normal L_1: 48.45-56.10%, abnormal L_1: 43.90-51.55%), and their F_1-hybrids (normal L_1: 48.35-52.59%, abnormal L_1: 47.41-51.65%) and backcross progenies (normal L_1: 45.10-56.25%, abnormal L_1: 43.75-54.90%) of both directions.

DISCUSSION

In order to delineate a mosquito vector in an endemic area of filariasis, it is necessary to confirm the following evidence for a species of mosquitoes. Firstly, naturally caught specimens of a mosquito species contain infective stages of a parasite. Secondly, the same forms of infective stages develop in a laboratory-bred, clean colony of the same mosquito species after being fed on carrier blood containing parasites, and thirdly, the same mosquito species fed on human blood in an endemic area (Sasa, 1976). Therefore, from these criteria the susceptibility test in an experimental laboratory is a useful procedure for incriminating a potential vector of a certain species. Nevertheless, susceptibility alone does not imply an important role in the transmission of disease in nature, while a refractory one can rule out its significance entirely.

Vector competence to *B. malayi* of 5 species of the Korean *An. hyrcanus* group (*An. pullus*, *An. sinensis*, *An. kleini*, *An. belenrae* and *An. lesteri*), as determined by susceptibility tests using a laboratory-bred, clean mosquito colony, had not been performed and/or reported until now. The results of this investigation revealed that *An. sinensis*, *An. kleini*, *An. belenrae* and *An. lesteri* were high potential

vectors, whereas *An. pullus* was a moderate potential vector. Therefore these present results confirm the natural vector status of *An. sinensis* in the ROK, and *An. sinensis* and *An. lesteri* in China, as documented by (Sasa, 1976). Beneficial results reported herein emphasize the potential role of *An. pullus*, *An. sinensis*, *An. kleini*, *An. belenrae* and *An. lesteri* in transmitting *B. malayi* in the ROK, and *An. sinensis* and *An. lesteri* in China, where these anopheline species and *B. malayi* were found sympatrically. However, it is noteworthy that *An. sinensis*, *An. belenrae* and *An. kleini* were cryptic morphologically and only a molecular-based assay could be used robustly to recognize them (Rueda, 2005; Joshi *et al*, 2010). Remarkably, it is possible that previous identification of *An. sinensis* was based only on pure morphological characteristics, particularly in using traumatic scales of wild-caught adult females from endemic areas of Brugian filariasis, in which epidemiological and control approaches might be mixtures of 2 or 3 species depending upon the locations studied.

It has been known that the f^m (filarial susceptibility, *B. malayi*) in *Aedes* species was controlled by simple sex-linked genes with refractoriness being dominant to susceptibility. The experiments of reciprocal and backcrosses between *B. malayi*-susceptible/-refractory strains of *Stegomyia* (= *Aedes*) *aegypti*, and *B. pahangi*-susceptible *Ae. polynesiensis*/-refractory *Ae. malayensis* produced refractory progeny-females, suggesting that refractoriness is dominant to susceptibility (MacDonald and Ramachandran, 1965; MacDonald, 1976). However, those results are contrary to this study's experiments of reciprocal and backcrosses between *B. malayi*-susceptible (Korean strain)/-refractory (Thailand strain) *An. sinensis* by yielding susceptible progeny-females of both directions, indicating that susceptibility is dominant to refractoriness. The decrease in melanized and degenerated of L_1 (2

main refractory mechanisms in the thoracic muscles of the Thai *An. sinensis*) (Saeung *et al*, 2013) from 39.81-46.22% melanization and 30.25-43.52% degeneration in parental *An. sinensis* (Thailand strain) to 21.98% melanization and 29.67% degeneration in F_1-hybrids (female *An. sinensis* Thailand strain x male *An. sinensis* Korean strain) and 21.09% melanization and 22.66% degeneration in backcross progenies [(female *An. sinensis* Thailand strain x male *An. sinensis* Korean strain)F_1 x male *An. sinensis* Korean strain], when compared to 24.74-26.83% melanization and 17.07-26.81% degeneration of *An. sinensis* (Korean strain) were good supportive evidence. These results elucidated on a promising model of a *B. malayi*-anopheline-system for further investigations of various aspects concerning susceptibility/refractoriness mechanisms.

ACKNOWLEDGEMENTS

This work was supported by funding from the Thailand Research Fund (TRF Senior Research Scholar: RTA5480006) and Diamond Research Grant of the Faculty of Medicine, Chiang Mai University, awarded to W. Choochote and A. Saeung. The authors would like to thank Dr. Wattana Navacharoen, Dean of the Faculty of Medicine, Chiang Mai University, for his interest in this research.

REFERENCES

Chai IH, Lim GI, Yoon SN, Oh WL, Kim SJ, Chai JY. Ocurrence of tertian malaria in a male patient who never been abroad. *Korean J Parasitol* 1994; 32: 195-200.

Cheun HI, Kong Y, Cho SH, Lee JS, Chai JY, Lee JS, Lee JK, Kim TS. Successful control of lymphatic filariasis in the Republic of Korea. *Korean J Parasitol* 2009; 47: 323-5.

Choochote W, Sukhavat K, Somboon P, Khamboonruang C, Maleewong W, Suwanpanit P. The susceptibility of small laboratory animals to nocturnally superiodic *Brugia malayi* in Thailand. *J Parasit Trop Med Ass Thailand* 1986; 9: 35-7.

Chomcharn Y, Surathin K, Bunnag D, Sucharit S, Harinasuta T. Effects of a single dose of primaquine on a Thai strain of *Plasmodium falciparum*. *Southeast Asian J Trop Med Public Health* 1980; 11: 408-9.

Harrison BA, Scanlon JE. Medical entomology studies II. The subgenus *Anopheles* in Thailand (Diptera: Culicidae). *Contrib Am Entomol Inst* 1975; 12: 1-307.

Harbach RE. *Anopheles* classification. Mosquito taxonomic inventory, http://mosquito-taxonomic-inventory.info/anophelesclassification 2013. Accessed 10 May 2013.

Joshi D, Kim JY, Choochote W, Park MH, Min GS. Preliminary vivax malaria vector competence for three members of the *Anopheles hyrcanus* group in the Republic of Korea. *J Am Mosq Control Assoc* 2011; 27: 312-4.

Joshi D, Park MH, Saeung A, Choochote W, Min GS. Multiplex assay to identify Korean vectors of Malaria. *Mol Ecol Resour* 2010; 10: 748-50.

Jumkum A, Choochote W, Jitpakdi A, Leemingswat S, Komalamisra N, Jariyapan N, Boonyatakorn C. Comparative studies on the biology and filarial susceptibility of selected blood-feeding and autogenous *Aedes togoi* sub-colonies. *Mem Inst Oswaldo Cruz* 2003; 98: 481-5.

Kanojia PC, Shetty PS, Geevarghese G. A long-term study on vector abundance & seasonal prevalence in relation to the occurrence of Japanese encephalitis in Gorakhpur district, Uttar Pradesh. *Indian J Med Res* 2003; 117: 104-10.

Kim SJ, Choochote W, Jitpakdi A, Junkum A, Park SJ, Min GS. Establishment of a self-mating mosquito colony of *Anopheles sinensis* from Korea. *Korean J Entomol* 2003; 33: 267-71.

Lee WJ, Klein TA, Kim HC, Choi YM, Yoon SH, Chang KS, Chong ST, Lee IY, Jones JW, Jacobs JS, Sattabongkot J, Park JS. *Anopheles kleini*, *Anopheles pullus*, and *Anopheles sinensis*: potential vectors of *Plasmodium vivax* in the Republic of Korea. *J Med Entomol* 2007; 44: 1086-90.

MacDonald WW. Mosquito genetics in relation to filarial infections. In Taylor AER, Muller R eds, Genetic Aspects of Host-Parasite Relationship (Symposia of the British Society for Parasitology). Oxford, UK. Blackwell Scientific Publications. 1976, p 1-24.

MacDonald WW, Ramachandran CP. The influence of the gene f^m (Filarial susceptibility, *Brugia malayi*) on the susceptibility of *Aedes aegypti* to seven strains of *Brugia*, *Wuchereria* and *Dirofilaria*. *Ann Trop Med Parasit* 1965; 59: 64-73.

Park JW, Son JI, Hur JP, Jong JS, Hwangbo Y, Lee SW, Kee MK, Shin YH, Yang BK. An outbreak of vivax malaria in Republic of Korea in 1999. *Korean J Infec Dis* 2000; 32: 335-9.

Ree HI, Hwang UW, Lee IY, Kim TE. Daily survival and human blood index of *Anopheles sinensis*, the vector species of malaria in Korea. *J Am Mosq Control Assoc* 2001; 17: 67-72.

Rueda LM, Li C, Kim HC, Klein TA, Foley DH, Wilkerson RC. *Anopheles belenrae*, a potential vector of *Plasmodium vivax* in the Republic of Korea. *J Am Mosq Control Assoc* 2010; 26: 430-2.

Rueda LM. Two new species of *Anopheles* (*Anopheles*) Hyrcanus Group (Diptera: Culicidae) from the Republic of Korea. *Zootaxa* 2005; 941: 1-26.

Sasa M. Human filariasis: A global survey of epidemiology and control. Tokyo, University of Tokyo Press. 1976, p 433-67.

Saeung A, Hempolchom C, Baimai V, Thongsahuan S, Taai K, Jariyapan N, Chaithong U, Choochote W. Susceptibility of eight species members in the *Anopheles hyrcanus* group to nocturnally subperiodic *Brugia malayi*. *Parasit Vectors* 2013; 6: 5.

Shim JC, Shin EH. Malaria in Korea 2002. *Korean J Infec Dis* 2002; 34: 104-35.

Tanaka K, Mizusawa K, Saugstad ES. A revision of the adult and larval mosquitoes of Japan (including the Ryukyu Archipelago and the Ogasawara Islands) and Korea (Diptera: Culicidae). *Contrib Am Entomol Inst* 1979; 16: 1-985.

Zhang HL. The natural infection rate of mosquitoes by Japanese encephalitis B virus in Yunnan Province. *Zhonghua Yu Fang Yi Xue Za Zhi* 1990; 24: 265-7.

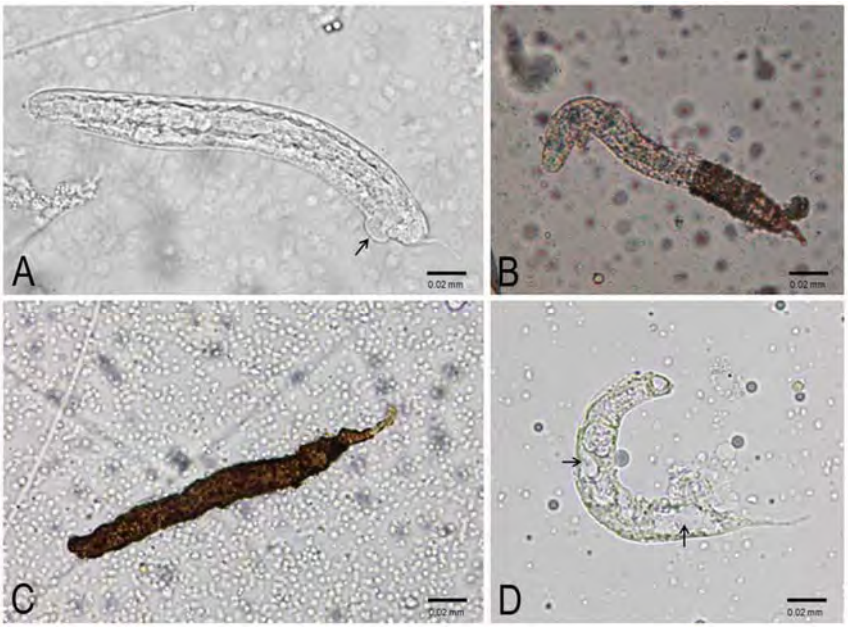

Fig 1-L_1 larvae recovered from thoracic muscle of *Anopheles sinensis* strains 4 days after infected blood meal. *An. sinensis* Korean strain: (A) Normal live larva with intact cuticle and internal organs (small arrow: protuberance of anal plug at the anal pore). *An. sinensis* Thailand strain: (B) Incomplete melanotic encapsulated larva. (C) Completely melanotic encapsulated larva. (~~E~~D) Degenerated and vacuolated internal organs (small arrow) larva.

Table 1

Infective rates and parasite loads of 5 species in the Korean *Anopheles hyrcanus* group after feeding on blood containing *Brugia malayi* microfilariae (microfilarial density = 305 and 297 mf/20 µl in experiment I and II, respectively), with all mosquitoes dissected 14 days after feeding.

Mosquito species	Infective rates (%) (No.)*	Average No. L_3 per infected mosquito (range)[+]	L_3-distribution		
			% head (No.)	% thorax (No.)	% abdomen (No.)
Experiment I					
Oc. togoi	95 (19/20)	16.47 (1-37)	61.66 (193)	20.13 (63)	18.21 (57)
An. pullus	60 (12/20)[a]	8.50 (1-16)[f]	65.69 (67)	15.68 (16)	18.63 (19)
An. belenrae	100 (20/20)[b]	8.85 (1-21) [g]	75.71 (134)	15.25(27)	9.04 (16)
An. lesteri	100 (20/20)[c]	10.90 (2-24)[h]	68.35 (149)	11.01 (24)	20.64 (45)

Table 1 (continued)

Mosquito species	Infective rates (%) (No.)*	Average No. L_3 per infected mosquito (range)[+]	L_3-distribution		
			% head (No.)	% thorax (No.)	% abdomen (No.)
Experiment II					
Oc. togoi	90 (18/20)	13.06 (1-31)	66.81 (157)	14.89 (35)	18.30 (43)
An. kleini	90 (18/20)[d]	5.39 (1-10)[i]	76.29 (74)	11.34 (11)	12.37 (12)
An. sinensis	65 (13/20)[e]	4.23 (1-17)[j]	81.82 (45)	12.73 (7)	5.45 (3)

*Fisher's exact test: b, c, d, e vs. control, $P > 0.05$; a vs. control, $P < 0.05$

[+] t-test (two-sided): h vs. control, $P > 0.05$; f, g, i, j vs. control, $P < 0.05$

Table 2

Infective rates and parasite loads in parental, reciprocal and backcross progenies of *Anopheles sinensis* strains from Korea and Thailand after feeding on blood containing *Brugia malayi* microfilariae (microfilarial density = 323 and 346 mf/20 µl in experiment I and II, respectively), with all mosquitoes dissected 14 days after feeding.

An. sinensis strains (Female x male)	Infective rates (No.)*	Average No. L_3 per infected mosquito (range)[+]	L_3-distribution		
			% head (No.)	% thorax (No.)	% abdomen (No.)
Experiment I					
Parental crosses					
SK	65 (13/20)[a]	3.62 (1-13)[e]	72.34 (34)	10.64 (5)	17.02 (8)
ST	5 (1/20)[b]	1 (1)[f]	100 (1)	-	-
Reciprocal crosses					
(SK x ST)F_1	65 (13/20)[a]	3.92 (1-16)[e]	80.39 (41)	11.76 (6)	7.84 (4)
(ST x SK)F_1	55 (11/20)[b]	5.27 (1-16)[f]	48.27 (28)	31.03 (18)	20.70 (12)

Table 2 (continued)

An. sinensis strains (Female x male)	Infective rates (No.)*	Average No. L_3 per infected mosquito (range)+	L_3-distribution		
			% head (No.)	% thorax (No.)	% abdomen (No.)
Experiment II					
Parental crosses					
SK	60 (12/20)[c]	4.33 (1-11)[g]	88.46 (46)	9.62 (5)	1.92 (1)
ST	0 (0/20)[d]	-	-	-	-
Back crosses					
(SK x ST)F_1 x ST	45 (9/20)[c]	4.22 (1-9)[g]	76.31 (29)	10.53 (4)	13.16 (5)
(ST x SK)F_1 x SK	70 (14/20)[d]	5.50 (1-18)	64.94 (50)	18.18 (14)	16.88 (13)

SK: *An. sinensis* (Korean strain); ST: *An. sinensis* (Thailand strain)

*Chi-square test: a, c vs. control, $P > 0.05$; b, d vs. control, $P < 0.05$

+ t-test (two-sided): e, g vs. control, $P > 0.05$; f vs. control, $P < 0.05$

Table 3

Parasite loads in parental, reciprocal and backcross progenies of *Anopheles sinensis* strains from Korea and Thailand dissected 4 days after feeding on blood containing *Brugia malayi* microfilariae

(microfilarial density = 323 and 346 mf/20 μl in experiment I and II, respectively).

An. sinensis strains (Female x male)	Average No. L_1 per infected thorax (range)[+]	% normal L_1 (No.)	% melanized L_1 (No.)	% degenerated L_1 (No.)
Experiment I				
Parental crosses				
SK	19.40 (5-23)	48.45 (47)	24.74 (24)	26.81 (26)
ST	21.60 (8-31)	16.67 (18)	39.81 (43)	43.52 (47)
Reciprocal crosses				
(SK x ST)F_1	23.20 (10-36)	52.59 (61)	22.41 (26)	25.00 (29)
(ST x SK)F_1	18.20 (6-19)	48.35 (44)	21.98 (20)	29.67 (27)

Table 3 (continued)

An. sinensis strains (Female x male)	Average No. L_1 per infected thorax (range)[+]	% normal L_1 (No.)	% melanized L_1 (No.)	% degenerated L_1 (No.)
Experiment II				
Parental crosses				
SK	24.60 (14-25)	56.10 (69)	26.83 (33)	17.07 (21)
ST	23.80 (9-44)	23.53 (28)	46.22 (55)	30.25 (36)
Back crosses				
(SK x ST)F_1 x ST	20.40 (7-38)	45.10 (46)	30.39 (31)	24.51 (25)
(ST x SK)F_1 x SK	25.60 (11-27)	56.25 (72)	21.09 (27)	22.66 (29)

* Dissected from 5 thoraxes

Cytogenetic, crossing and molecular evidence of two cytological forms of *Anopheles argyropus* and three cytological forms of *Anopheles pursati* (Diptera: Culicidae) in Thailand

Thongsahuan, S.[1], Otsuka, Y.[2], Baimai, V.[3], Saeung, A.[4], Hempolchom, C.[4], Taai, K.[4], Srisuka, W.[5], Dedkhad, W.[4], Sor-suwan, S.[4], Choochote, W.[4*]

[1]Faculty of Veterinary Science (Establishment Project), Prince of Songkla University, Songkhla 90110, Thailand

[2]Department of Infectious Disease Control, Faculty of Medicine, Oita University, Oita, 879-5593, Japan

[3]Department of Biology and Centre for Vectors and Vector-Borne Diseases, Faculty of Science, Mahidol University, Bangkok 10400, Thailand

[4]Department of Parasitology, Faculty of Medicine, Chiang Mai University, Chiang Mai 50200, Thailand

[5]Entomology Section, Queen Sirikit Botanic Garden, P.O. Box 7, Chiang Mai, 50180, Thailand

[*]Corresponding author e-mail: choochote.wej@gmail.com

Abstract.

Nine and 11 isolines of *Anopheles argyropus* and *Anopheles pursati*, respectively, were established from individual females collected from cow-baited traps, and the characteristics of metaphase chromosomes were investigated in their F_1-progenies. As determined by the different amounts of extra heterochromatin on sex chromosomes, 2 types of X (X_1, X_2) and Y (Y_1,Y_2), and 2 types of X (X_1, X_2) and 3 types of Y (Y_1, Y_2, Y_3) chromosomes were obtained from *An. argyropus* and *An. pursati*, respectively. These types of sex chromosomes comprised 2 [Forms A (X_1, Y_1) and B (X_1, X_2, Y_2)] and 3 [Forms A (X_1, X_2, Y_1), B (X_1, X_2, Y_2) and C (X_2, Y_3)] karyotypic forms of *An. argyropus* and *An. pursati*, respectively. All karyotypic forms acquired from *An. pursati* are new one that were discovered in this study, of which Forms A, B and C were found generally in Chiang Mai Province, while only 1 isoline of Form B was obtained in Ratchaburi Province. Form A was recovered from *An. argyropus* only in Ubon Ratchathani Province, whereas Form B from that species was found commonly in both Ubon Rathchathani and Nakhon Si Thammarat Provinces. Crossing experiments among the 2 and 3 isolines representing 2 and 3 karyotypic forms of *An. argyropus* and *An. pursati*, respectively, indicated genetic compatibility in yielding viable progenies and synaptic salivary gland polytene chromosomes through F_2-generations. The conspecific natures of these karyotypic forms in both species were further supported by very low intraspecific sequence variations (average genetic distance: *An. argyropus* = 0.003-0.007, *An. pursati* = 0.000-0.005) of ribosomal DNA (ITS2) and mitochondrial DNA (COI and COII).

INTRODUCTION

Anopheles argyropus and *Anopheles pursati* belong to the subgenus *Anopheles* of the Hyrcanus Group and Myzorhynchus Series. *An. argyropus* is distributed widely in Thailand and other countries in Asia, i.e., India (Assam), Vietnam, Cambodia, Malaysia (Malaysian Peninsular) and Indonesia (Java and Sumatra). Regarding *An. pursati*, the distribution of this anopheline species has been recorded so far from Thailand, Vietnam, Cambodia and Malaysia (Malaysian Peninsular) (Reid, 1968; Scanlon *et al*., 1968; Harrison & Scanlon, 1975; Rattanarithikul *et al*., 2006; Harbach, 2013). With regard to medical importance, these 2 anopheline species have never been incriminated as natural, suspected or potential vectors of any human diseases. However, *An. pursati* was reported recently as a high potential vector for nocturnally subperiodic *Brugia malayi*, as determined by a 60% susceptibility rate and 3.83 (1-11) parasite load (Saeung *et al*., 2013). Furthermore, these 2 anopheline species are considered as economic pests of livestock, due to their vicious and massive biting behavior when taking blood meals from cattle (Reid *et al*., 1962; Reid, 1968; Harrison & Scanlon, 1975).

Regarding metaphase chromosome investigations, two karyotypic forms of *An. argyropus*, i.e., Forms A (X_1, X_2, Y_1) and B (X_1, X_2, Y_2), were first reported from Chiang Mai and Phrae Provinces (northern Thailand), and Chiang Mai Province and Chanthaburi Province (eastern Thailand), respectively (Baimai *et al*., 1993). These 2 karyotypic variants clearly appeared to result from a gradual increase in the extra heterochromatin on X and Y chromosomes. The genetic variation at the chromosomal level, within the taxon *Anopheles* species, potentially results in the existence of species complex and causes difficulty in identifying sibling species (isomorphic species) and/or subspecies (cytological forms/races) members of the complex that results from identical

Formatted: Font: Not Bold

Formatted: Centered

morphology or minimal morphological distinction. Additionally, those members of each complex may differ in biological characteristics (e.g., microhabitats, resting and biting behavior, sensitivity or resistance to insecticides, susceptible or refractory to pathogens, etc.), which can be used to determine their vectorial capacity (Subbarao, 1998; Choochote & Saeung, 2013). Thus, inaccurate identification of individual members within the taxon *Anopheles* species complex may result in failure to distinguish between a vector and non-vector species, and lead to complications and/or unsuccessful vector control-approaches. A recent good example was reported on *Anopheles barbirostris* complex in Thailand, which emphasized on the significance of *Anopheles* species complex status. These reports comprised 5 sibling species members (*Anopheles campestris*-like and *An. barbirostris* species A1, A2, A3 and A4), all of which exhibited identical morphology at the adult stage, and only the branch summation of seta 2-VI of pupal skins could be used to separate *An. campestris*-like from *An. barbirostris* species A1, A2, A3 and A4 (average summation of seta 2-VI: *An. campestris*-like = 22.40−24.50 branches; *An. barbirostris* species A1, A2, A3 and A4 = 9.2−16.40 branches) (Harrison & Scanlon, 1975; Saeung *et al*., 2007, 2008; Suwannamit *et al*., 2009; Thongsahuan *et al*., 2009). Regarding distribution and biting behavior, *An. campestris*-like was found mostly in flat plain localities and it chose to bite humans, while *An. barbirostris* species A1, A2, A3 and A4 were rather confined in mountainous areas and they preferred to bite on cattle. Furthermore, *An. campestris*-like was a high potential vector for *Plasmodium vivax,* whereas *An. barbirostris* species A1, A2, A3 and A4 were very low potential vectors (Thongsahuan *et al*., 2011).

Regarding the above information, very little is known about the genetic proximities among 2 karyotypic variants of *An. argyropus*, and there is a complete lack

of karyotypic information of *An. pursati* in a systematic direction. Therefore, this study is the first to report, 3 new karyotypic forms [Forms A (X_1, X_2, Y_1), B (X_1, X_2, Y_2) and C (X_2, Y_3)] of *An. pursati*, and determine the genetic proximity among 2 and 3 karyotypic variants of *An. argyropus* and *An. pursati*, respectively, by crossing experiments related to comparative DNA sequencing of the second internal transcribed spacer (ITS2) of ribosomal DNA (rDNA), cytochrome *c* oxidase subunit I (COI) and cytochrome *c* oxidase subunit II (COII) of mitochondrial DNA (mtDNA).

MATERIALS AND METHODS

Formatted: Font: Not Bold

Formatted: Centered

Field collections and establishment of isoline colonies

Wild-caught, fully engorged female mosquitoes of *An. argyropus* and *An. pursati* were collected from cow-baited traps. The *An. argyropus* mosquitoes were obtained from Ubon Rathchathani Province in the northeastern region and Nakhon Si Thammarat Province in the southern region of Thailand. The *An. pursati* mosquitoes were acquired from Chiang Mai Province in the northern region and Ratchaburi Province in the western region of Thailand. A total of 9 and 11 isolines of *An. argyropus* and *An. pursati*, respectively, were established successfully and maintained in our insectary, using the techniques described by Choochote & Saeung (2013). Exact species identification was performed using intact morphology of egg, larval, pupal and adult stages from the F_1-progenies of isolines, by following the standard keys (Reid, 1968; Harrison & Scanlon, 1975; Rattanarithikul *et al*., 2006). These isolines were used for studies on the metaphase karyotype, crossing experiment and molecular analysis.

Metaphase karyotype preparation

Metaphase chromosomes were prepared from 10 samples of the early fourth-instar larval brains of F_1-progenies of each isoline in *An. argyropus* and *An. pursati*, using the techniques described by Choochote & Saeung (2013). Identification of karyotypic forms followed the standard cytotaxonomic systems of Baimai *et al.* (1993).

Crossing experiment

The 2 and 3 laboratory-raised isolines of *An. argyropus* and *An. pursati*, respectively, were selected arbitrarily from the stock isoline colonies. They were Form A (X_1, Y_1; Ur1A) and B (X_2, Y_2; Ns5B) of *An. argyropus*, and Form A (X_1, Y_1; Cm1A), B (X_2, Y_2; Rt1B) and C (X_2, Y_3; Cm7C) of *An. pursati* (Table 1). These isolines were used for crossing experiments in order to determine post-mating barriers by employing the techniques reported by Choochote & Saeung (2013).

DNA extraction and PCR amplification

Total genomic DNA was isolated from individual F_1-progeny adult female of each isoline of *An. argyropus* and *An. pursati* (Table 1) using DNeasy® Blood and Tissue Kit (QIAGEN, Japan). Primers for amplification of ITS2, COI, and COII regions were followed previous studies by Saeung *et al.* (2007). The ITS2 region of the rDNA was amplified using primer ITS2A (5'-TGT GAA CTG CAG GAC ACA T-3') and ITS2B (5'-TAT GCT TAA ATT CAGGGGGT-3') (Beebe & Saul, 1995). Amplification of the 709 bp fragment of mitochondrial COI barcoding region was conducted using the LCO1490 (5′-GGT CAA CAA ATC ATA AAG ATA TTG G-3′) and HCO2198 (5′-TAA ACT TCA GGG TGA CCA AAA AAT CA-3′) primers of Folmer *et al.* (1994).

The mitochondrial COII region was amplified using primers LEU (5′-TCT AAT ATG GCA GAT TAG TGC A-3′) and LYS (5′-ACT TGC TTT CAG TCA TCT AAT G-3′) (Sharpe *et al*., 2000). Each PCR reaction was carried out in total of 20 µl volume containing 0.5 U *Ex Taq* (Takara, Japan), 1X *Ex Taq* buffer, 2 mM of $MgCl_2$, 0.2 mM of each dNTP, 0.25 µM of each primer, and 1 µl of the extracted DNA. For ITS2, PCR program consisted of initial denaturation at 94^{o}C for 1 minute, 30 cycles at 94^{o}C for 30 seconds, 55^{o}C for 30 seconds, and 72^{o}C for 1 minute, and a final extension at 72^{o}C for 5 minutes. The amplification profile of COI and COII comprised initial denaturation at 94^{o}C for 1 minute, 30 cycles at 94^{o}C for 30 seconds, 50^{o}C for 30 seconds, and 72^{o}C for 1 minute, and a final extension at 72^{o}C for 5 minutes. The amplified products were electrophoresed in 1.5% agarose gels and stained with ethidium bromide. Finally, the amplicons were purified using the QIAquick® PCR Purification Kit (QIAGEN, Japan). The PCR products were sequenced in both directions using the BigDye® V3.1 Terminator Cycle Sequencing Kit and 3130 genetic analyzer (Applied Biosystems of Life Technologies, Japan).

Sequencing alignment and phylogenetic analysis

Sequences were aligned using the CLUSTAL W multiple alignment program (Thompson *et al*., 1994) and edited manually in BioEdit version 7.0.5.3 (Hall, 1999). All positions containing gaps and missing data were excluded from the analysis. The Kimura two-parameter (K2P) model was employed to calculate genetic distances (Kimura, 1980). Using the distances, construction of neighbor-joining trees (Saitou & Nei, 1987) and the bootstrap test with 1,000 replications were performed with the Molecular Evolutionary Genetics Analysis (MEGA) version 4.0 program (Tamura *et*

al., 2007). Bayesian analysis was conducted with MrBayes 3.2 (Ronquist *et al*., 2012) by using two replicates of 1 million generations with the nucleotide evolutionary model. The best-fit model was chosen for each gene separately using the Akaike Information Criterion (AIC) in MrModeltest version 2.3 (Nylander, 2004). The general time-reversible (GTR) with gamma distribution shape parameter (G) was selected for ITS2, whereas the GTR+I+G was the best-fit model for COI and COII. Bayesian posterior probabilities were calculated from the consensus tree after excluding the first 25% trees as burn-in. Available sequences of the Hyrcanus Group were retrieved from GenBank using BLAST (http://blast.ncbi.nlm.nih.gov/Blast.cgi) for performing the phylogenetic analysis with our sequences.

RESULTS

Formatted: Font: Not Bold

Formatted: Centered

Metaphase karyotypes

Cytogenetic observations of F_1-progenies of the 9 isolines of *An. argyropus* revealed different types of sex chromosomes, due to the addition of extra heterochromatin. There were 2 types of X (metacentric X_1 and submetacentric X_2) and 2 types of Y chromosomes (metacentric Y_1 and large submetacentric Y_2), which comprised 2 forms of metaphase karyotypes on the basis of Y chromosome configurations, i.e., Forms A (X_1, Y_1) and B (X_1, X_2, Y_2) (Table 1, Fig. 1a-f). Form A was recovered only in Ubon Ratchathani Province, northeastern region, whereas Form B was found commonly in both Ubon Rathchathani and Nakhon Si Thammarat Provinces, southern region. Likewise, 2 types of X (metacentric X_1 and submetacentric X_2) and 3 types of Y (metacentric Y_1, small submetacentric Y_2 and large submetacentric Y_3) chromosomes of *An. pursati* were recovered from a total of 11 isolines. These types of X and Y

chromosomes were designated as Forms A (X_1, X_2, Y_1), B (X_1, X_2, Y_2) and C (X_2, Y_3) (Fig. 2a-i). All karyotypic forms were found generally in Chiang Mai Province, while only 1 isoline obtained in Ratchaburi Province, western region, was X_2, Y_2 of Form B.

Crossing experiments

Table 2 shows details of hatchability, pupation, emergence and adult sex-ratio of parental, reciprocal and F_1-hybrid crosses between the 2 isolines of *An. argyropus* representing Forms A and B. Table 3 shows these details on crossing experiments among the 3 isolines of *An. pursati* representing Forms A, B and C. All crosses yielded viable progenies through the F_2-generations. No evidence of genetic incompatibility or post-mating reproductive isolation was observed among these crosses. The salivary gland polytene chromosomes of the 4^{th} instar larvae of F_1-hybrids from all crosses showed complete synapsis, without inversion loops along the whole length of all autosomes and of X chromosome (Fig. 3a-c).

DNA sequences and phylogenetic analysis

The ITS2, COI and COII sequences were available in the DDBJ/EMBL/GenBank nucleotide sequence database under accession numbers AB826053-AB826112 (Table 1). The length of ITS2 was 472 bp and 499 bp in *An. argyropus* and *An. pursati*, respectively. No intraspecific ITS2 sequence variation was observed among the 11 isolines of *An. pursati*, whereas 4 base substitutions (A↔G at position 242 and 289, C↔T at position 388, A↔C at position 435) were found among the 9 isolines of *An. argyropus*. The analysis of COI (658 bp) among the 9 isolines of *An. argyropus* revealed 13 base substitutions, while 7 base substitutions were obtained among the 11

isolines of *An. pursati*. The analysis of COII (685 bp) among the 9 isolines of *An. argyropus* showed 8 base substitutions, whilst 2 base substitutions derived from the 11 isolines of *An. pursati*. All the substitutions were not specific to karyotypic forms. The evolutionary relationships among the karyotypic forms of *An. argyropus* and *An. pursati* were determined using neighbor-joining (NJ) and Bayesian analysis (BA). Both phylogenetic methods showed the same tree topologies, therefore, only the Bayesian tree result was shown for all DNA regions (Fig. 4-6). The 9 isolines of *An. argyropus* were grouped as a monophyletic clade, with high branch support in all DNA regions (100% in NJ, 98-100% in BA). Likewise, all 11 isolines of *An. pursati* were placed within the same clade, with high branch support in all DNA regions (99-100% in NJ, 100% in BA). The average genetic distances within 2 and 3 karyotypic forms of *An. argyropus* and *An. pursati* were 0.003 and 0.000, 0.007 and 0.005, and 0.004 and 0.001, based on ITS2, COI and COII sequences, respectively. The phylogenetic tree revealed that *An. pursati* was more closely related to *Anopheles nitidus* and *Anopheles nigerrimus* than to *An. argyropus* based on ITS2 and COI sequences. However, both species were well separated from other species members of the Hyrcanus Group in all DNA regions.

DISCUSSION

Formatted: Font: Not Bold

Formatted: Centered

Cytogenetic investigations of 17 *An. argyropus* isolines from 3 different localities in Thailand (Chiang Mai and Phrae Provinces, northern region; Chanthaburi Province, eastern region) were performed firstly by Baimai *et al.* (1993). The results demonstrated that this anopheline species exhibited karyotypic variation via a gradual increase of extra heterochromatin on X and Y chromosomes, and forming 2 karyotypic forms

[Forms A (X_1, X_2, Y_1) and B (X_1, X_2, Y_2)]. In the present study, similar results of 2 karyotypic forms have been obtained by examining 9 isolines from 2 different locations (Ubon Ratchatani Province, northeastern region; Nakhon Si Thammarat Province, southern region). Remarkably, the Form A (X_2, Y_1), reported by Baimai *et al.* (1993), was not detected in any isoline colonies, as the limitation in number of samples appeared to be used in the current study. Regarding *An. pursati*, the 3 new karyotypic forms [Forms A (X_1, X_2, Y_1), B (X_1, X_2, Y_2) and C (X_2, Y_3)] were recovered from 11 isolines in 2 different localities (Chiang Mai Province, northern region; Ratchaburi Province, western region). Apparently, these distinct karyotypic forms were caused by the gradual addition of extra heterochromatin on sex chromosomes.

According to the genetic diversity at the chromosomal level of the *An. argyropus* [Forms A (X_1, Y_1) and B (X_1, X_2, Y_2)] and *An. pursati* [Forms A (X_1, X_2, Y_1), B (X_1, X_2, Y_2) and C (X_2, Y_3)] found in this study, crossing experiments among the karyotypic variants of *An. argyropus* and *An. pursati* were performed intensively by following robust systematic procedures as documented by Choochote & Saeung (2013). The results showed no post-mating reproductive isolation. All crosses yielded viable progenies through F_2-generations and synaptic salivary gland polytene chromosomes, suggesting the conspecific nature of these karyotypic variants, which comprised 2 and 3 cytological forms within the taxon *An. argyropus* and *An. pursati*, respectively. The low intraspecific sequence variations [average genetic distance = 0.003-0.007 (*An. argyropus*) and 0.000-0.005 (*An. pursati*)] of the nucleotide sequences in ribosomal DNA (ITS2) and mitochondrial DNA (COI and COII), and all isolines of *An. argyropus* and *An. pursati* were placed within each monophyletic clade and well separated from the other 10 species members (*Anopheles belenrae*, *Anopheles crawfordi*, *An.*

nigerrimus, *An. nitidus*, *Anopheles kleini*, *Anopheles lesteri*, *Anopheles paraliae*, *Anopheles peditaeniatus*, *Anopheles pullus* and *Anopheles sinensis*) of the Hyrcanus Group. This was based on neighbor-joining (NJ) and Bayesian analyses (BA), which acted as good supportive evidence. It is interesting to note that the differences in the amount and distribution of heterochromatin observed from both anopheline species were not resulted in the evolution divergence as in, for example, *Drosophila kikkawai* complex, *Anopheles dirus* complex, *Anopheles maculatus* complex and *Bactocera dorsalis* complex, as stated by Baimai (1998). The present results are in accordance with crossing experiments among karyotypic forms of other *Anopheles* species, i.e., *Anopheles vagus* Forms A and B (Choochote *et al*., 2002), *An. pullus* (= *Anopheles yatsushiroensis*) Forms A and B (Park *et al*., 2003), *An. sinensis* Forms A and B (Choochote *et al*., 1998; Min *et al*., 2002; Park *et al*., 2008b), *Anopheles aconitus* Forms B and C (Junkum *et al*., 2005), *An. barbirostris* species A1 (Forms A, B and C) and A2 (Forms A and B) (Saeung *et al*., 2007, Suwannamit *et al*., 2009), *An. campestris*-like Forms B, E and F (Thongsahuan *et al*., 2009), *An. peditaeniatus* Forms A, B, C, D, E and F (Choochote, 2011; Saeung *et al*., 2012), *An. nigerrimus* Forms A, B, C and D (Songsawatkiat *et al*., 2013) and *An. paraliae* Forms A, B, C, D and E (Taai *et al*., 2013b).

Acknowledgements

This work was supported by the Thailand Research Fund (TRF Senior Research Scholar: RTA5480006) and the Diamond Research Grant of Faculty of Medicine, Chiang Mai University to W. Choochote, A. Saeung and S. Thongsahuan. The authors would like to thank Dr. Wattana Navacharoen, Dean of the Faculty of Medicine, Chiang

Formatted: Font: Not Bold, Italic

Mai University and Assoc. Prof. Usa Chethanond, Director of the Faculty of Veterinary Science (Establishment Project), Prince of Songkla University for their interest in this research.

REFERENCES

Baimai, V. (1998). Heterochromatin accumulation and karyotypic evolution in some dipteran insects. *Zoological Studies* **37:** 75-88.

Baimai, V., Rattanarithikul, R. & Kijchalao, U. (1993). Metaphase karyotypes of *Anopheles* of Thailand and Southeast Asia: I. The *hyrcanus* group. *Journal of the American Mosquito Control Association* **9:** 59-67.

Beebe, N.W. & Saul, A. (1995). Discrimination of all members of the *Anopheles punctulatus* complex by polymerase chain reaction-restriction fragment length polymorphism analysis. *The American Journal of Tropical Medicine and Hygiene* **53:** 478-481.

Choochote, W. (2011). Evidence to support karyotypic variation of the mosquito, *Anopheles peditaeniatus* in Thailand. *Journal of Insect Science* **11:** 10.

Choochote, W., Jitpakdi, A., Rongsriyam, Y., Komalamisra, N., Pitasawat, B. & Palakul, K. (1998). Isoenzyme study and hybridization of two forms of *Anopheles sinensis* (Diptera: Culicidae) in Northern Thailand. *Southeast Asian Journal of Tropical Medicine and Public Health* **29:** 841-847.

Choochote, W., Jitpakdi, A., Sukontason, K.L., Chaithong, U., Wongkamchai, S., Pitasawat, B., Jariyapan, N., Suntaravitun, T., Rattanachanpichai, E., Sukontason, K., Leemingsawat, S. & Rongsriyam, Y. (2002). Intraspecific hybridization of two karyotypic forms of *Anopheles vagus* (Diptera: Culicidae)

Formatted: Font: Not Bold

Formatted: Centered

and the related egg surface topography. *Southeast Asian Journal of Tropical Medicine and Public Health* **33:** 29-35.

Choochote, W. & Saeung, A. (2013). Systematic techniques for the recognition of *Anopheles* species complexes. In: *Anopheles mosquitoes-New insights into malaria vectors*, Manguin S. (editors) InTech, DOI: 10.5772/54853. Available from: http://www.intechopen.com/books/anopheles-mosquitoes-new-insights-into-malaria-vectors/systematic-techniques-for-the-recognition-of-anopheles-species-complexes.

Folmer, O., Black, M., Hoeh, W., Lutz, R. & Vrijenhoek, R. (1994). DNA primers for amplification of mitochondrial cytochrome *c* oxidase subunit I from diverse metazoan invertebrates. *Molecular Marine Biology and Biotechnology* **3:** 294-299.

Hall, T.A. (1999). BioEdit: a user-friendly biological sequence alignment editor and analysis program for Windows 95/98/NT. *Nucleic Acids Symposium Series* **41:** 95-98.

Harbach, R.E. (2013). *Anopheles* classification in: *Mosquito taxonomic inventory*, Available from: http://mosquito-taxonomic-inventory.info/.

Harrison, B.A. & Scanlon, J.E. (1975). Medical entomology studies II. The subgenus *Anopheles* in Thailand (Diptera: Culicidae). *Contributions of the American Entomological Institute* **12:** 1-307.

Junkum, A., Komalamisra, N., Jitpakdi, A., Jariyapan, N., Min, G.S., Park, M.H., Cho, K.H., Somboon, P., Bates, P.A. & Choochote, W. (2005). Evidence to support two conspecific cytological races on *Anopheles aconitus* in Thailand. *Journal of Vector Ecology* **30:** 213-224.

Kimura, M. (1980). Simple method for estimating evolutionary rates of base substitution through comparative studies of nucleotide sequences. *Journal of Molecular Evolution* **16:** 111-120.

Min, G.S., Choochote, W., Jitpakdi, A., Kim, S.J., Kim, W., Jung, J. & Junkum, A. (2002). Intraspecific hybridization of *Anopheles sinensis* (Diptera: Culicidae) strains from Thailand and Korea. *Molecules and Cells* **14:** 198-204.

Nylander, J.A.A. (2004). MrModeltest v2. Program distributed by the author. Evolutionary Biology Centre, Uppsala University.

Park, S.J., Choochote, W., Jitpakdi, A., Junkum, A., Kim, S.J., Jariyapan, N., Park, J.W. & Min, G.S. (2003). Evidence for a conspecific relationship between two morphologically and cytologically different forms of Korean *Anopheles pullus* mosquito. *Molecules and Cells* **16:** 354-360.

Park, M.H., Choochote, W., Junkum, A., Joshi, D., Tuetan, B., Saeung, A., Jung, J.H. & Min, G.S. (2008a). Reproductive isolation of *Anopheles sinensis* from *Anopheles lesteri* and *Anopheles sineroides* in Korea. *Genes & Genomics* **30:** 245-252.

Park, M.H., Choochote, W., Kim, S.J., Somboon, P., Saeung, A., Tuetan, B., Tsuda, Y., Takagi, M., Joshi, D., Ma, Y. & Min, G.S. (2008b). Non reproductive isolation among four allopatric strains of *Anopheles sinensis* in Asia. *Journal of the American Mosquito Control Association* **24:** 489-495.

Rattanarithikul, R., Harrison, B.A., Harbach, R.E., Panthusiri, P. & Coleman, R.E. (2006). Illustrated keys to the mosquitoes of Thailand IV. *Anopheles*. *Southeast Asian Journal of Tropical Medicine and Public Health* **37:** 1-128.

Reid, J.A. (1968). Anopheline mosquitoes of Malaya and Borneo. *Studies from the Institute for Medical Research Malaysia* **31:** 1-520.

Reid, J.A., Wilson, T. & Ganapathipillai, A. (1962). Studies on filariasis in Malaya: The mosquito vectors of periodic *Brugia malayi* in North-West Malaya. *Annals of Tropical Medicine and Parasitology* **56:** 323-336.

Ronquist, F., Teslenko, M., van der Mark, P., Ayres, D.L., Darling, A., Höhna, S., Larget, B., Liu, L., Suchard, M.A. & Huelsenbeck, J.P. (2012). MrBayes 3.2: efficient Bayesian phylogenetic inference and model choice across a large model space. *Systematic Biology* **61:** 539-542.

Saeung, A., Baimai, V., Otsuka, Y., Rattanarithikul, R., Somboon, P., Junkum, A., Tuetun, B., Takaoka, H. & Choochote, W. (2008). Molecular and cytogenetic evidence of three sibling species of the *Anopheles barbirostris* Form A (Diptera: Culicidae) in Thailand. *Parasitology Research* **102:** 499-507.

Saeung, A., Baimai, V., Thongsahuan, S., Min, G.S., Park, M.H., Otsuka, Y., Maleewong, W., Lulitanond, V., Taai, K. & Choochote, W. (2012). Geographic distribution and genetic compatibility among six karyotypic forms of *Anopheles peditaeniatus* (Diptera: Culicidae) in Thailand. *Tropical Biomedicine* **29:** 613-625.

Saeung, A., Hempolchom, C., Baimai, V., Thongsahuan, S., Taai, K., Jariyapan, N., Chaithong, U. & Choochote, W. (2013). Susceptibility of eight species members of *Anopheles hyrcanus* group to nocturnally subperiodic *Brugia malayi*. *Parasites & Vectors* **6:** 5.

Saeung, A., Otsuka, Y., Baimai, V., Somboon, P., Pitasawat, B., Tuetun, B., Junkum, A., Takaoka, H. & Choochote, W. (2007). Cytogenetic and molecular evidence for two species in the *Anopheles barbirostris* complex (Diptera: Culicidae) in Thailand. *Parasitology Research* **101:** 1337-1344.

Saitou, N. & Nei, M. (1987) The neighbor-joining method: A new method for reconstructing phylogenetic trees. *Molecular Biology and Evolution* **4:** 406-425.

Scanlon, J.E., Peyton, E.L. & Gould, D.J. (1968). An annotated checklist of the *Anopheles* of Thailand. *Thai National Scientific Papers Fauna Series* **2:** 1-35.

Sharpe, R.G., Harbach, R.E. & Butlin, R.K. (2000). Molecular variation and phylogeny of members of the Minimus group of *Anopheles* subgenus *Cellia* (Diptera: Culicidae). *Systematic Entomology* **25:** 263-272.

Songsawatkiat, S., Baimai, V., Saeung, A., Thongsahuan, S., Otsuka, Y., Srisuka, W. & Choochote, W. (2013). Cytogenetic, hybridization and molecular evidence of four cytological forms of *Anopheles nigerrimus* (Hyrcanus Group) in Thailand and Cambodia. *Journal of Vector Ecology* **38:** 266-276.

Subbarao, S.K. (1998). Anopheline species complexes in South-East Asia. *World Health Organization Technical Publication Searo* **18:** 1-82.

Suwannamit, S., Baimai, V., Otsuka, Y., Saeung, A., Thongsahuan, S., Tuetun, B., Apiwathnasorn, C., Jariyapan, N., Somboon, P., Takaoka, H. & Choochote, W. (2009). Cytogenetic and molecular evidence for an additional new species within the taxon *Anopheles barbirostris* (Diptera: Culicidae) in Thailand. *Parasitology Research* **104:** 905-918.

Taai, K., Baimai, V., Saeung, A., Thongsahuan, S., Min, G.S., Otsuka, Y., Park, M.H., Fukuda, M., Somboon, P. & Choochote, W. (2013a). Genetic compatibility between *Anopheles lesteri* from Korea and *Anopheles paraliae* from Thailand. *Memorias do Instituto Oswaldo Cruz* **108:** 312-320.

Taai, K., Baimai, V., Thongsahuan, S., Saeung, A., Otsuka, Y., Srisuka, W., Sriwichai, P., Somboon, P., Jariyapan, N. & Choochote, W. (2013b). Metaphase karyotypes

of *Anopheles paraliae* (Diptera: Culicidae) in Thailand and evidence to support five cytological races. *Tropical Biomedicine* **30:** 238-249.

Tamura, K., Dudley, J., Nei, M. & Kumar, S. (2007). MEGA4: Molecular evolution genetics analysis (MEGA) software version 4.0. *Molecular Biology and Evolution* **24:** 1596-1599.

Thompson, J.D., Higgins, D.G. & Gibson, T.J. (1994). CLUSTAL W: improving the sensitivity of progressive multiple sequence alignment through sequence weighting, positions-specific gap penalties and weight matrix choice. *Nucleic Acids Research* **22:** 4673-4680.

Thongsahuan, S., Baimai, V., Junkum, A., Saeung, A., Min, G.S., Joshi, D., Park, M.H., Somboon, P., Suwonkerd, W., Tippawangkosol, P., Jariyapan, N. & Choochote, W. (2011). Susceptibility of *Anopheles campestris*-like and *Anopheles barbirostris* species complexes to *Plasmodium falciparum* and *Plasmodium vivax* in Thailand. *Memorias do Instituto Oswaldo Cruz* **106:** 105-112.

Thongsahuan, S., Baimai, V., Otsuka, Y., Saeung, A., Tuetun, B., Jariyapan, N., Suwannamit, S., Somboon, P., Jitpakdi, A., Takaoka, H. & Choochote, W. (2009). Karyotypic variation and geographic distribution of *Anopheles campestris*-like (Diptera: Culicidae) in Thailand. *Memorias do Instituto Oswaldo Cruz* **104:** 558-566.

Figure legends

Figure 1 Metaphase karyotypes of *Anopheles argyropus*. (a) Form A (X_1, Y_1: Ubon Ratchathani Province); (b) Form B (X_1, Y_2: Nakhon Si Thammarat Province); (c) Form B (X_2, Y_2: Nakhon Si Thammarat Province); (d) Form B (homozygous X_2, X_2: Nakhon Si Thammarat Province); (e) Diagrams of representative metaphase karyotype of Forms A; (f) Diagrams of representative metaphase karyotype of Forms B.

Figure 2 Metaphase karyotypes of *Anopheles pursati*. (a) Form A (X_1, Y_1: Chiang Mai Province); (b) Form A (X_2, Y_1: Chiang Mai Province); (c) Form B (X_1, Y_2: Chiang Mai Province); (d) Form B (X_2, Y_2: Ratchaburi Province); (e) Form C (X_2, Y_3: Chiang Mai Province); (f) Form B (heterozygous X_1, X_2: Chiang Mai Province); (g) Diagrams of representative metaphase karyotype of Forms A; (h) Diagrams of representative metaphase karyotype of Forms B; (i) Diagrams of representative metaphase karyotype of Form C.

Figure 3 Synapsis in all arms of salivary gland polytene chromosome of F_1-hybrids 4^{th} larvae of *Anopheles argyropus* and *An. pursati*. (a) *An. argyropus*: Ur1A female x Ns5B male. (b) *An. pursati*: Cm1A female x Rt1B male; (c) *An. pursati*: Cm1A female x Cm7C male.

Figure 4 Bayesian phylogenetic relationships among the 9 isolines of *Anopheles argyropus* and 11 isolines of *An. pursati* based on ITS2 sequences compared with 10 species members of the Hyrcanus Group. Numbers on branches are bootstrap values (%) of NJ analysis and Bayesian posterior probabilities. Only the values higher than 70% both on bootstrap values and posterior probabilities are shown. Branch lengths are proportional to genetic distance (scale bar).

Figure 5 Bayesian phylogenetic relationships among the 9 isolines of *Anopheles argyropus* and 11 isolines of *An. pursati* based on COI sequences compared with 8 species members of the Hyrcanus Group. Numbers on branches are bootstrap values (%) of NJ analysis and Bayesian posterior probabilities. Only the values higher than 70% both on bootstrap values and posterior probabilities are shown. Branch lengths are proportional to genetic distance (scale bar).

Figure 6 Bayesian phylogenetic relationships among the 9 isolines of *Anopheles argyropus* and 11 isolines of *An. pursati* based on COII sequences compared with 8 species members of the Hyrcanus Group. Numbers on branches are bootstrap values (%) of NJ analysis and Bayesian posterior probabilities. Only the values higher than 70% both on bootstrap values and posterior probabilities are shown. Branch lengths are proportional to genetic distance (scale bar).

Table 1 Locations, code of isolines, karyotypic forms of *Anopheles argyropus* and *An. pursati*, and their GenBank accession numbers

Location (Geograpical coordinate)	Code of isoline[a]	Karyotypic form	GenBank accession number			Reference
			ITS2	COI	COII	
An. argyropus						
Ubon Ratchathani (15° 31′ N, 105° 35′ E)	Ur1A[a]	A (X_1, Y_1)	AB826053	AB826073	AB826093	This study
	Ur2B	B (X_2, Y_2)	AB826054	AB826074	AB826094	This study
	Ur4B	B (X_2, Y_2)	AB826055	AB826075	AB826095	This study
Nakhon Si Thammarat (08° 29′ N, 100° 0′ E)	Ns5B[a]	B (X_2, Y_2)	AB826056	AB826076	AB826096	This study
	Ns8B	B (X_2, Y_2)	AB826057	AB826077	AB826097	This study
	Ns12B	B (X_2, Y_2)	AB826058	AB826078	AB826098	This study
	Ns19B	B (X_1, Y_2)	AB826059	AB826079	AB826099	This study
	Ns21B	B (X_2, Y_2)	AB826060	AB826080	AB826100	This study
	Ns24B	B (X_2, Y_2)	AB826061	AB826081	AB826101	This study

Table 1 (continued)

Location (Geograpical coordinate)	Code of isoline[a]	Karyotypic form	GenBank accession number			Reference
			ITS2	COI	COII	
An. pursati						
Chiang Mai (18° 47′ N, 98° 59′ E)	Cm1A[a]	A (X_1, Y_1)	AB826062	AB826082	AB826102	This study
	Cm2C	C (X_2, Y_3)	AB826063	AB826083	AB826103	This study
	Cm4A	A (X_2, Y_1)	AB826064	AB826084	AB826104	This study
	Cm6B	B (X_2, Y_2)	AB826065	AB826085	AB826105	This study
	Cm7C[a]	C (X_2, Y_3)	AB826066	AB826086	AB826106	This study
	Cm9A	A (X_1, Y_1)	AB826067	AB826087	AB826107	This study
	Cm10A	A (X_1, Y_1)	AB826068	AB826088	AB826108	This study
	Cm11B	B (X_1, Y_2)	AB826069	AB826089	AB826109	This study
	Cm14C	C (X_2, Y_3)	AB826070	AB826090	AB826110	This study
	Cm15C	C (X_2, Y_3)	AB826071	AB826091	AB826111	This study
Ratchaburi (13° 21′ N, 99° 22′ E)	Rt1B[a]	B (X_2, Y_2)	AB826072	AB826092	AB826112	This study

Table 1 (continued)

Location (Geograpical coordinate)	Code of isoline[a]	Karyotypic form	GenBank accession number			Reference
			ITS2	COI	COII	
An. belenrae	-	-	EU789794	-	-	Park *et al*., 2008a
An. crawfordi	Sk1B	B (X_3, Y_2)	AB779152	AB779181	AB779210	Saeung *et al*., unpubl. data
An. kleini	-	-	EU789793	-	-	Park *et al*., 2008a
An. lesteri	-	-	EU789791	-	-	Park *et al*., 2008a
	ilG1	-	-	AB733028	AB733036	Taai *et al*., 2013a
An. nigerrimus	Ur26A	A (X_3, Y_1)	AB778778	AB778791	AB778804	Songsawatkiat *et al*., 2013
An. nitidus	Ur2D	D (X_3, Y_4)	AB777782	AB777803	AB777824	Songsawatkiat *et al*., unpubl. data
An. paraliae	Sk1B	B (X_1, Y_2)	AB733487	AB733503	AB733519	Taai *et al*., 2013b
An. peditaeniatus	Cm7B	B (X_2, Y_2)	AB714990	AB715043	AB715096	Saeung *et al*., 2012
An. pullus	-	-	EU789792	-	-	Park *et al*., 2008a
	-	-	-	AY444348	AY444347	Park *et al*., 2003

Table 1 (continued)

Location (Geograpical coordinate)	Code of isoline[a]	Karyotypic form	GenBank accession number			Reference
			ITS2	COI	COII	
An. sinensis	i2ACM	A (X, Y_1)	AY130473	-	-	Min *et al*., 2002
	-	-	-	AY444351	-	Park *et al*., 2003
	i1BKR	B (X, Y_2)	-	-	AY130464	Min *et al*., 2002

[a] used in crossing experiments.

Table 2 Crossing experiments among 2 isolines of *Anopheles argyropus*

Crosses (Female x Male)	Total eggs (number)[a]	Embryonation rate[b]	Hatched n (%)	Pupation n (%)	Emergence n (%)	Total emergence n (%)	
						Female	Male
Parental cross							
Ur1A x Ur1A	398 (245, 153)	81	314 (78.89)	273 (86.94)	268 (98.17)	123 (45.90)	145 (54.10)
Ns5B x Ns5B	279 (101, 178)	77	201 (72.04)	193 (96.02)	189 (97.93)	79 (41.80)	110 (58.20)
Reciprocal cross							
Ur1A x Ns5B	416 (240, 176)	83	295 (70.91)	292 (98.98)	272 (93.15)	135 (49.63)	137 (50.37)
Ns5B x Ur1A	267 (147, 120)	80	200 (74.91)	192 (96)	180 (93.75)	76 (42.22)	104 (57.78)
F_1- hybrid cross							
(Ur1A x Ns5B)F_1 x (Ur1A x Ns5B)F_1	308 (162, 146)	88	243 (78.90)	238 (97.94)	231 (97.06)	114 (49.35)	117 (50.65)
(Ns5B x Ur1A)F_1 x (Ns5B x Ur1A)F_1	324 (130, 194)	84	266 (82.10)	266 (100)	266 (100)	125 (46.99)	141 (53.01)

[a] two selective egg-batches of inseminated females from each cross. [b] dissection from 100 eggs; n = number.

Table 3 Crossing experiments among 3 isolines of *Anopheles pursati*

Crosses (Female x Male)	Total eggs (number)[a]	Embryonation rate[b]	Hatched n (%)	Pupation n (%)	Emergence n (%)	Total emergence n (%)	
						Female	Male
Parental cross							
Cm1A x Cm1A	254 (132, 122)	81	199 (78.35)	172 (86.43)	167 (97.09)	76 (45.51)	91 (54.49)
Rt1B x Rt1B	237 (128, 109)	78	184 (77.64)	165 (89.67)	158 (95.76)	78 (49.37)	80 (50.63)
Cm7C x Cm7C	249 (113, 136)	75	187 (75.10)	183 (97.86)	181 (98.91)	92 (50.83)	89 (49.17)
Reciprocal cross							
Cm1A x Rt1B	236 (110, 126)	82	194 (82.20)	165 (85.05)	159 (96.36)	70 (44.03)	89 (55.97)
Rt1B x Cm1A	242 (124, 118)	72	172 (71.07)	163 (94.77)	148 (90.79)	78 (52.70)	70 (47.30)
Cm1A x Cm7C	221 (113, 108)	86	188 (85.07)	169 (89.89)	160 (94.67)	81 (50.63)	79 (49.37)
Cm7C x Cm1A	261 (119, 142)	88	206 (78.93)	202 (98.06)	196 (97.03)	97 (49.49)	99 (50.51)
Rt1B x Cm7C	234 (104, 130)	92	211 (90.17)	198 (93.84)	190 (95.96)	93 (48.95)	97 (51.05)
Cm7C x Rt1B	284 (167, 117)	87	233 (82.04)	226 (97.00)	221 (97.79)	112 (50.68)	109 (49.32)

Table 3 continued

Crosses (Female x Male)	Total eggs (number)[a]	Embryonation rate[b]	Hatched n (%)	Pupation n (%)	Emergence n (%)	Total emergence n (%)	
						Female	Male
F_1- hybrid cross							
(Cm1A x Rt1B)F_1 x (Cm1A x Rt1B)F_1	264 (112, 152)	81	214 (81.06)	214 (100)	201 (93.93)	90 (44.78)	111 (55.22)
(Rt1B x Cm1A)F_1 x (Rt1B x Cm1A)F_1	220 (118, 102)	94	205 (93.18)	205 (100)	201 (98.05)	94 (46.77)	107 (52.23)
(Cm1A x Cm7C)F_1 x (Cm1A x Cm7C)F_1	255 (131, 124)	90	217 (85.10)	174 (80.18)	170 (97.70)	94 (55.29)	76 (44.71)
(Cm7C x Cm1A)F_1 x (Cm7C x Cm1A)F_1	231 (103, 128)	85	189 (81.82)	157 (83.07)	151 (96.18)	72 (47.68)	79 (52.32)
(Rt1B x Cm7C)F_1 x (Rt1B x Cm7C)F_1	286 (109, 177)	89	249 (87.06)	242 (97.19)	240 (99.17)	110 (45.83)	130 (54.17)
(Cm7C x Rt1B)F_1 x (Cm7C x Rt1B)F_1	212 (103, 109)	93	197 (92.92)	177 (89.85)	175 (98.87)	80 (45.71)	95 (54.29)

[a] two selective egg-batches of inseminated females from each cross. [b] dissection from 100 eggs; n = numbers.

1

Elsevier Editorial System(tm) for Comptes rendus Biologies
Manuscript Draft

Manuscript Number:

Title: Cytogenetic, crossing and molecular evidence of four cytological races of Anopheles crawfordi (Diptera: Culicidae) in Thailand and Cambodia

Article Type: Article original / Full Length Article

Section/Category: Molecular biology and genetics

Keywords: Anopheles crawfordi, metaphase karyotypes, crossing experiments, ITS2, COI, COII

Corresponding Author: Dr. Atiporn Saeung,

Corresponding Author's Institution:

First Author: Atiporn Saeung

Order of Authors: Atiporn Saeung; Visut Baimai ; Sorawat Thongsahuan; Yasushi Otsuka; Wichai Srisuka; Kritsana Taai; Pradya Somboon; Wannapa Suwonkerd; Tho Sochanta; Wej Choochote

Abstract: Twenty-nine isolines of Anopheles crawfordi were established from wild-caught females collected from cow-baited traps in Thailand and Cambodia. Three types of X (X1, X2, X3) and 4 types of Y (Y1, Y2, Y3, and Y4) chromosomes were identified, according to differing amounts of extra heterochromatin. These sex chromosomes were formed 4 metaphase karyotypes, i.e., Forms A (X1, X2, X3, Y1), B (X1, X2, X3, Y2), C (X2, Y3) and D (X2, Y4). Forms C and D were new metaphase karyotypes that confined to Thailand, while Forms A and B appeared to be common in both Thailand and Cambodia. Crossing experiments among 4 karyotypic forms indicated genetic compatibility in yielding viable progenies and synaptic salivary gland polytene chromosomes. The results suggested the conspecific nature, comprising 4 cytological races, which further supported by very low intraspecific variations (genetic distance = 0.000-0.018) of the nucleotide sequences in ribosomal DNA (ITS2) and mitochondrial DNA (COI, COII).

Suggested Reviewers: Dr. Bruce A Harrison
Taxonomist/Public Health Entomologist, 661 Drumheller Road, Clemmons, NC 27012
skeeterdoc@gmail.com

Dr. Claire Garros
Cirad, UMR Contrôle des maladies, F-34398 Montpellier Cedex 5, France.
claire.garros@cirad.fr

Professor Dr. Hiroyuki Takaoka
Institute of Biological Sciences, Faculty of Science, University of Malaya
takaoka@oita-u.ac.jp

Opposed Reviewers:

Cytogenetic, crossing and molecular evidence of four cytological races of *Anopheles crawfordi* (Diptera: Culicidae) in Thailand and Cambodia

Atiporn Saeung[a,*], Visut Baimai[b], Sorawat Thongsahuan[c], Yasushi Otsuka[d], Wichai Srisuka[e], Kritsana Taai[a], Pradya Somboon[a], Wannapa Suwonkerd[f], Tho Sochanta[g], Wej Choochote[a]

[a]*Department of Parasitology, Faculty of Medicine, Chiang Mai University, Chiang Mai 50200, Thailand.*

[b]*Department of Biology and Centre for Vectors and Vector-Borne Diseases, Faculty of Science, Mahidol University, Bangkok 10400, Thailand.*

[c]*Faculty of Veterinary Science (Establishment Project), Prince of Songkla University, Songkhla 90110, Thailand.*

[d]*Department of Infectious Disease Control, Faculty of Medicine, Oita University, Oita, 879-5593, Japan.*

[e]*Entomology Section, Queen Sirikit Botanic Garden, P.O. Box 7, Chiang Mai, 50180, Thailand.*

[f]*Office of Disease Prevention and Control 10, Chiang Mai, 50200, Thailand.*

[g]*National Center for Malaria Control, Parasitology and Entomology, Phnom Penh, Cambodia.*

*Corresponding author: Dr. Atiporn Saeung
Department of Parasitology, Faculty of Medicine,
Chiang Mai University,
Chiang Mai 50200, Thailand
E-mail: atsaeung@mail.med.cmu.ac.th

ABSTRACT

Twenty-nine isolines of *Anopheles crawfordi* were established from wild-caught females collected from cow-baited traps in Thailand and Cambodia. Three types of X (X_1, X_2, X_3) and 4 types of Y (Y_1, Y_2, Y_3, and Y_4) chromosomes were identified, according to differing amounts of extra heterochromatin. These sex chromosomes were formed 4 metaphase karyotypes, i.e., Forms A (X_1, X_2, X_3, Y_1), B (X_1, X_2, X_3, Y_2), C (X_2, Y_3) and D (X_2, Y_4). Forms C and D were new metaphase karyotypes that confined to Thailand, while Forms A and B appeared to be common in both Thailand and Cambodia. Crossing experiments among 4 karyotypic forms indicated genetic compatibility in yielding viable progenies and synaptic salivary gland polytene chromosomes. The results suggested the conspecific nature, comprising 4 cytological races, which further supported by very low intraspecific variations (genetic distance = 0.000-0.018) of the nucleotide sequences in ribosomal DNA (ITS2) and mitochondrial DNA (COI, COII).

Keywords: Anopheles crawfordi, metaphase karyotypes, crossing experiments, ITS2, COI, COII

1. Introduction

Anopheles (*Anopheles*) *crawfordi* belongs to the Lesteri Subgroup and Hyrcanus Group of the Myzorhynchus Series. So far, the distribution of this anopheline species has been recorded from India (Assam), Thailand, Cambodia, Vietnam, Malaysia (Malaysian Peninsular) and Indonesia (Sumatra) [1-3]. Even though *An. crawfordi* could be found abundantly as a proven outdoor-biter of humans in certain localities of eastern and southern Thailand, its status as a vector of any human-diseases remains obscure and needs to be investigated more intensively [2]. However, our recent experiments indicated that this anopheline species could serve as a high potential vector of the filarial nematode, nocturnally subperiodic *Brugia malayi*, as determined by 80-85% susceptibility rates and 6.06-6.24 average number of L_3 larvae per infected mosquito [4]. These results were in agreement with previous investigators in that *An. crawfordi* could provide satisfactory susceptibility to periodic *B. malayi* in Malaysia [5-6]. Additionally, *An. crawfordi* is considered an economic pest due to its vicious biting-behavior on cattle [1-2,5].

Regarding cytogenetic aspects, investigations of *An. crawfordi* from 2 different localities in Thailand (eastern region: Chanthaburi Province; southern region: Phang Nga Province) were performed by Baimai et al. [7]. The results of their studies demonstrated that this anopheline species exhibited genetic diversity at the chromosomal level, via a gradual increase in extra heterochromatin on X and Y chromosomes. This resulted in 2 karyotypic variants (cytological forms) namely Form A (X_1, Y_1) and B (X_2, Y_2). The marked genetic variations on X and Y chromosomes within the taxon *Anopheles* potentially results in the existence of species complex. The identical morphology or minimal morphological distinction among sibling species

(isomorphic species) and subspecies (cytological races) members within each complex leads to difficulty in exactly identifying individual members. Furthermore, those members may differ in biological characteristics (e.g., microhabitats, resting and biting behaviors, sensitivity or resistance to insecticides, susceptible or refractory to pathogens, etc.), which can be used to determine their vectorial capacity. Thus, inaccurate identification of individual members within the taxon *Anopheles* species complex may result in the failure to recognize between a vector and non-vector species, and cause of complicated vector control-approach [8]. Although marked genetic variations at the chromosomal level of *An. crawfordi* have been illustrated apparently, little is known about their genetic proximities. Thus, this paper reports 2 new karyotypic forms of *An. crawfordi* [Form C (X_2, Y_3) and D (X_2, Y_4)], and performed their genetic proximities by crossing experiments among 4 karyotypic forms and comparing DNA sequences of the second internal transcribed spacer (ITS2) of ribosomal DNA (rDNA), and cytochrome *c* oxidase subunit I (COI) and cytochrome *c* oxidase subunit II (COII) of mitochondrial DNA (mtDNA).

2. Materials and methods

2.1 Field collections and establishment of isoline colonies

Wild-caught, fully engorged female mosquitoes of *An. crawfordi* were collected from cow-baited traps at 6 allopatric locations in Thailand (Chiang Mai and Nan Provinces, northern region; Chumphon, Phang Nga, Trang and Songkhla Provinces, southern region), and 2 allopatric locations in Cambodia (Ratanakiri and Mondulkiri) (Fig. 1, Table 1). A total of 29 isolines were established successfully and maintained in our insectary using the techniques described by Choochote and Saeung [9]. Exact

97 species identification was performed by using intact morphology of egg, larval, pupal
98 and adult stages from the F_1-progenies of isolines, following standard keys [1-2,10].
99 These isolines were used for studies on the metaphase karyotype, crossing experiment
100 and molecular analysis.
101
102 *2.2 Metaphase karyotype preparation*
103 Metaphase chromosomes were prepared from 10 samples of the early fourth-
104 instar larval brains of F_1-progenies of each isoline, using techniques previously
105 described by Saeung et al. [11]. Identification of karyotypic forms followed the standard
106 cytotaxonomic systems of Baimai et al. [7].
107
108 *2.3 Crossing experiment*
109 The 10 laboratory-raised isolines of *An. crawfordi* were selected arbitrarily from
110 the 29 isoline colonies, which were representative of 4 karyotypic forms, i.e., Form A
111 [Cm1A **(**X_1, Y_1**)**, Tg3A (X_3, Y_1), Pg5A (X_2, Y_1), Rt1A (X_1, Y_1)], B [Nn1B (X_1, Y_2),
112 Tg1B (X_3, Y_2), Sk1B (X_3, Y_2), Mr1B (X_2, Y_2)], C [Tg2C (X_2, Y_3)] and D [Tg4D (X_2,
113 Y_4)] (Table 1). These isolines were used for crossing experiments in order to determine
114 post-mating barriers by employing the techniques previously reported by Saeung et al.
115 [11].
116
117 *2.4 DNA extraction and PCR amplification*
118 Total genomic DNA was isolated from individual F_1-progeny adult female of
119 each isoline of *An. crawfordi* (Table 1) using DNeasy® Blood and Tissue Kit
120 (QIAGEN). Primers for amplification of ITS2, COI, and COII regions were followed

previous studies by Saeung et al. [11]. The ITS2 region of the rDNA was amplified using primer ITS2A (5'-TGT GAA CTG CAG GAC ACA T-3') and ITS2B (5'-TAT GCT TAA ATT CAGGGGGT-3') [12]. Amplification of the 709 bp fragment of mitochondrial COI barcoding region was conducted using the LCO1490 (5'-GGT CAA CAA ATC ATA AAG ATA TTG G-3') and HCO2198 (5'-TAA ACT TCA GGG TGA CCA AAA AAT CA-3') primers of Folmer et al. [13]. The mitochondrial COII region was amplified using primers LEU (5'-TCT AAT ATG GCA GAT TAG TGC A-3') and LYS (5'-ACT TGC TTT CAG TCA TCT AAT G-3') [14]. Each PCR reaction was carried out in total of 20 µl volume containing 0.5 U *Ex Taq* (Takara), 1X *Ex Taq* buffer, 2 mM of $MgCl_2$, 0.2 mM of each dNTP, 0.25 µM of each primer, and 1 µl of the extracted DNA. For ITS2, PCR program consisted of initial denaturation at 94^{o}C for 1 min, 30 cycles at 94^{o}C for 30 sec, 55^{o}C for 30 sec, and 72^{o}C for 1 min, and a final extension at 72^{o}C for 5 min. The amplification profile of COI and COII comprised initial denaturation at 94^{o}C for 1 min, 30 cycles at 94^{o}C for 30 sec, 50^{o}C for 30 sec, and 72^{o}C for 1 min, and a final extension at 72^{o}C for 5 min. The amplified products were electrophoresed in 1.5% agarose gels and stained with ethidium bromide. Finally, the amplicons were purified using the QIAquick® PCR Purification Kit (QIAGEN). The PCR products were sequenced in both directions using the BigDye® V3.1 Terminator Cycle Sequencing Kit and 3130 genetic analyzer (Applied Biosystems).

2.5 Sequencing alignment and phylogenetic analysis

Sequences were aligned using the CLUSTAL W multiple alignment program [15] and edited manually in BioEdit version 7.0.5.3 [16]. All positions containing gaps and missing data were excluded from the analysis. The Kimura two-parameter (K2P)

model was employed to calculate genetic distances [17]. Using the distances, construction of neighbor-joining trees [18] and the bootstrap test with 1,000 replications were performed with the Molecular Evolutionary Genetics Analysis (MEGA) version 4.0 program [19]. Bayesian analysis was conducted with MrBayes 3.2 [20] by using two replicates of 1 million generations with the nucleotide evolutionary model. The best-fit model was chosen for each gene separately using the Akaike Information Criterion (AIC) in MrModeltest version 2.3 [21]. The general time-reversible (GTR) with gamma distribution shape parameter (G) was selected for ITS2, whereas the GTR+I+G was the best-fit model for COI and COII. Bayesian posterior probabilities were calculated from the consensus tree after excluding the first 25% trees as burnin. Available sequences of the Hyrcanus Group were retrieved from GenBank using BLAST (http://blast.ncbi.nlm.nih.gov/Blast.cgi) for performing the phylogenetic analysis with our sequences.

3. Results

3.1 Metaphase karyotypes

Cytological observations of F_1-progenies of 29 isolines of *An. crawfordi* demonstrated distinct types of sex chromosomes due to the addition of extra heterochromatin. There were 3 types of X (metacentric X_1, submetacentric X_2 and large submetacentric X_3) and 4 types of Y chromosomes (small telocentric Y_1, large subtelocentric Y_2, small subtelocentric Y_3 and submetacentric Y_4) (Fig. 2). These types of X and Y chromosomes comprised 4 forms of metaphase karyotypes on the basis of Y chromosome configurations, designated as Form A (X_1, X_2, X_3, Y_1), B (X_1, X_2, X_3,Y_2), C (X_2,Y_3) and D (X_2, Y_4). The number of isolines of these karyotypic forms occurring

169 in different localities in 5 and 2 provinces of Thailand and Cambodia, respectively, are
170 illustrated in Fig. 1 and Table 1. Forms C and D were new metaphase karyotype
171 discovered in the present study. Forms A and B appeared to be common in both
172 Thailand and Cambodia, while Forms C and D were found confine to Trang Province,
173 southern Thailand.
174
175 *3.2 Crossing experiments*
176 Details of hatchability, pupation, emergence and adult sex ratio of parental,
177 reciprocal and F_1-hybrid crosses among the 10 isolines of *An. crawfordi* representing
178 Forms A-D are shown in Table 2. All crosses yielded viable progenies through the F_2-
179 generations. No evidence of genetic incompatibility and/or post-mating reproductive
180 isolation was observed among these crosses. The salivary gland polytene chromosomes
181 of the 4^{th} instar larvae of F_1-hybrids from all crosses showed synapsis without inversion
182 loops along the whole lengths of all autosomes and the X chromosome (Fig. 3).
183
184 *3.3 DNA sequences and phylogenetic analysis*
185 All sequences were generated from 29 isolines of the Thai and Cambodian *An.*
186 *crawfordi* populations and available in the DDBJ/EMBL/GenBank nucleotide sequence
187 database under accession numbers AB779131-AB779217 (Table 1). The length of the
188 ITS2 region ranged from 446 to 449 bp in 7 and 22 isolines from Cambodia and
189 Thailand, respectively. *An. crawfordi* from both Provinces of Cambodia differed from
190 that in Thailand by a deletion of T, C and T at position 21, 280 and 292, respectively.
191 However, they all showed the same length for COI (658 bp, excluding primers) and
192 COII (685 bp) sequences. The evolutionary relationships among the 4 karyotypic forms

193 were determined using neighbor-joining (NJ) and Bayesian analysis. Both phylogenetic
194 methods showed similar tree topologies, thus, only the Bayesian tree was shown for all
195 regions (Figures 4-6). All 29 isolines were placed within the same cluster and well
196 separated from other species members of the *An. hyrcanus* group (*An. belenrae, An.*
197 *kleini, An. lesteri, An. paraliae, An. peditaeniatus, An. pullus* and *An. sinensis*). The
198 mean intra-specific sequence divergences within (0.000-0.018) and between (0.000-
199 0.016) the 4 karyotypic forms exhibited no significant difference in these DNA regions
200 (Table 3).
201

202 # 4. Discussion

203 Investigations on the metaphase karyotypes of *An. crawfordi* from 2 different
204 locations (eastern region, Chanthaburi Province; southern region, Phang Nga Province)
205 in Thailand were reported first by Baimai et al. [7]. The results demonstrated that *An.*
206 *crawfordi* exhibited karyotypic variation via a gradual increase of extra heterochromatin
207 on X (X_1, X_2) and Y (Y_1, Y_2) chromosomes, leading to the formation of 2 karyotypic
208 forms [Form A (X_1, X_2, Y_1) and B (X_1, X_2, Y_2)]. These metaphase karyotypes could be
209 distinguished on the basis of size, shape, amount and distribution of constitutive
210 heterochromatin on sex chromosomes. Likewise, 4 distinct karyotypic forms [Form A
211 (X_1, X_2, X_3, Y_1), B (X_1, X_2, X_3, Y_2), C (X_2, Y_3) and D (X_2, Y_4)] of *An. crawfordi*
212 recovered from 29 isolines, in 6 and 2 locations in Thailand and Cambodia,
213 respectively, were due to addition of extra heterochromatin on sex chromosomes.
214 Obviously, the above information elucidates the possibility of a cytological mechanism
215 for the karyotypic evolution of the Oriental *Anopheles* by gradually adding extra
216 heterochromatin onto the arms of sex chromosomes, which is keeping with Baimai's

hypothesis [22]. Additionally, such chromosome distinction is very useful for the cytotaxonomic study of closely related species, especially sibling species and/or subspecies members within the taxon *Anopheles* species, as exemplified in others groups of Oriental anophelines [8,11,23-32]. Regarding distribution of the 4 karyotypic forms of *An. crawfordi*, Forms A and B appear to be common in all locations of both Thailand and Cambodia, while Forms C and D are confined to Trang Province, southern Thailand. Remarkably, Form A (10 isolines) was detected only in Phang Nga Province, whereas all karyotypic forms were obtained from 8 isolines in Trang Province, despite these 2 provinces being located approximately 190 km away from each another. This is the first substantial evidence that supports the richness of ecological diversity in Trang Province, which seems to be the main key for supporting specific microhabitats that favor the karyotypic evolution of *An. crawfordi*.

Crossing experiments using isoline colonies of anopheline mosquitoes, which relate to results of cytology and molecular analysis to determine post-mating barriers, have proved to be efficient classical techniques for identifying sibling species and/or subspecies members within the taxon *Anopheles* species [8,11,23-32]. Regarding this matter, crossing experiments among the 4 allopatric karyotypic forms of *An. crawfordi* were performed intensively. The results of no post-mating reproductive isolation by yielding viable progenies through F_2-generations and synaptic salivary gland polytene chromosomes strongly suggest a conspecific nature, comprising 4 cytological races within this taxon. Low intra-specific sequence divergence (genetic distance = 0.000-0.018) of ITS2, COI and COII of the 4 karyotypic forms provide good supportive evidence. Thus, our findings are in agreement with the results of crossing experiments among karyotypic forms of other anophelines previously reported by several

241 investigators, i.e., *An. vagus* [33], *An. pullus* (= *An. yatsushiroensis*) [34], *An. sinensis*
242 [35-38], *An. aconitus* [25], *An. barbirostris* species A1 and A2 [11,29], *An. campestris*-
243 like taxon [30] and *An. peditaeniatus* [31-32].

244 Up until now, numerous studies have used ribosomal and mitochondrial DNA
245 markers for phylogenetic analysis in order to determine the relationships among sibling
246 species and/or subspecies members of *Anopheles* species complexes [11,27,29-30,39-
247 43]. However, there have been no reports of evolutionary relationships among different
248 karyotypic forms of *An. crawfordi*. Thus, our report is the first on the phylogenetic
249 relationships among 4 karyotypic forms of Thai and Cambodian *An. crawfordi*
250 populations. This study provided important information on the distribution of this
251 species across different geographic regions, and highlighted that all karyotypic forms
252 represent a single species. In addition, the crossing experiments of *An. crawfordi* isoline
253 colonies using cytological markers that relate to the information of molecular
254 investigation, as a multidisciplinary approach, was reported first in this study.

255

256 **Disclosure of interest**

257 The authors declare that they have no conflicts of interest concerning this article.

258

259 **Acknowledgements**

260 This work was supported by the Thailand Research Fund (TRF Senior Research
261 Scholar: RTA5480006) and the Diamond Research Grant of Faculty of Medicine,
262 Chiang Mai University to W. Choochote and A. Saeung. The authors would like to
263 thank Dr. Wattana Navacharoen, Dean of the Faculty of Medicine, Chiang Mai
264 University, for his interest in this research.

References

[1] J.A. Reid, Anopheline mosquitoes of Malaya and Borneo, Stud. Inst. Med. Res. Malaysia. 31 (1968) 1-520.

[2] B.A. Harrison, J.E. Scanlon, Medical entomology studies II. The subgenus *Anopheles* in Thailand (Diptera: Culicidae), Contrib. Am. Entomol. Inst. 12 (1975) 1-307.

[3] R.E. Harbach, Mosquito taxonomic inventory, *Anopheles* classification, http://mosquito-taxonomic-inventory.info/anophelesclassification (2011) [Accessed 10 December 2012].

[4] A. Saeung, C. Hempolchom, V. Baimai, S. Thongsahuan, K. Taai, N. Jariyapan, U. Chaithong, W. Choochote, Susceptibility of eight species members of *Anopheles hyrcanus* group to nocturnally subperiodic *Brugia malayi*, Parasit. Vectors. 6 (2013) 5.

[5] J.A. Reid, T. Wilson, A. Ganapathipillai, Studies on filariasis in Malaya: The mosquito vectors of periodic *Brugia malayi* in North-West Malaya, Ann. Trop. Med. Parasitol. 56 (1962) 323-336.

[6] R.H. Wharton, A.B.G. Laing, W.H. Cheong, Studies on the distribution and transmission of malaria and filariasis among aborigines in Malaya, Ann. Trop. Med. Parasitol. 57 (1963) 235-254.

[7] V. Baimai, R. Rattanarithikul, U. Kijchalao, Metaphase karyotypes of *Anopheles* of Thailand and Southeast Asia: I. The *hyrcanus* group, J. Am. Mosq. Control Assoc. 9 (1993) 59-67.

[8] S.K. Subbarao, Anopheline species complexes in South-East Asia, WHO. Tech. Pub. Ser. 18 (1998) 1-82.

289 [9] W. Choochote, A. Saeung, Systematic techniques for the recognition of
290 *Anopheles* species complexes, in: M. Sylvie (Eds.), *Anopheles* mosquitoes-New
291 insights into malaria vectors, InTech, Rijeka, 2012, (in press).
292 [10] R. Rattanarithikul, B.A. Harrison, R.E. Harbach, P. Panthusiri, R.E. Coleman,
293 Illustrated keys to the mosquitoes of Thailand IV. *Anopheles*, Southeast Asian J.
294 Trop. Med. Public Health. 37 (suppl 2) (2006) 1-128.
295 [11] A. Saeung, Y. Otsuka, V. Baimai, P. Somboon, B. Pitasawat, B. Tuetun, A.
296 Junkum, H. Takaoka, W. Choochote, Cytogenetic and molecular evidence for
297 two species in the *Anopheles barbirostris* complex (Diptera: Culicidae) in
298 Thailand, Parasitol. Res. 101 (2007) 1337-1344.
299 [12] N.W. Beebe, A. Saul, Discrimination of all members of the *Anopheles*
300 *punctulatus* complex by polymerase chain reaction-restriction fragment length
301 polymorphism analysis, Am. J. Trop. Med. Hyg. 53 (1995) 478-481.
302 [13] O. Folmer, M. Black, W. Hoeh, R. Lutz, R. Vrijenhoek, DNA primers for
303 amplification of mitochondrial cytochrome *c* oxidase subunit I from diverse
304 metazoan invertebrates, Mol. Mar. Biol. Biotechnol. 3 (1994) 294-299.
305 [14] R.G. Sharpe, R.E. Harbach, R.K. Butlin, Molecular variation and phylogeny of
306 members of the Minimus group of *Anopheles* subgenus *Cellia* (Diptera:
307 Culicidae), Syst. Entomol. 25 (2000) 263-272.
308 [15] J.D. Thompson, D.G. Higgins, T.J. Gibson, CLUSTAL W: improving the
309 sensitivity of progressive multiple sequence alignment through sequence
310 weighting, positions-specific gap penalties and weight matrix choice, Nucleic
311 Acids Res. 22 (1994) 4673-4680.

312 [16] T.A. Hall, BioEdit: a user-friendly biological sequence alignment editor and
313 analysis program for Windows 95/98/NT, Nucl. Acids. Symp. Ser. 41 (1999)
314 95-98.
315 [17] M. Kimura, Simple method for estimating evolutionary rates of base
316 substitution through comparative studies of nucleotide sequences, J. Mol. Evol.
317 16 (1980) 111-120.
318 [18] N. Saitou, M. Nei, The neighbor-joining method: A new method for
319 reconstructing phylogenetic trees, Mol. Biol. Evol. 4 (1987) 406-425.
320 [19] K. Tamura, J. Dudley, M. Nei, S. Kumar, MEGA4: Molecular evolution
321 genetics analysis (MEGA) software version 4.0, Mol. Biol. Evol. 24 (2007)
322 1596-1599.
323 [20] F. Ronquist, M. Teslenko, P. van der Mark, D.L. Ayres, A. Darling, S. Höhna,
324 B. Larget, L. Liu, M.A. Suchard, J.P. Huelsenbeck, MrBayes 3.2: efficient
325 Bayesian phylogenetic inference and model choice across a large model
326 space, Syst. Biol. 61 (2012) 539-542.
327 [21] J.A.A. Nylander, MrModeltest v2. Program distributed by the author,
328 Evolutionary Biology Centre, Uppsala University, 2004.
329 [22] V. Baimai, Heterochromatin accumulation and karyotypic evolution in some
330 dipteran insects, Zool. Stud. 37 (1998) 75-88.
331 [23] T. Kanda, K. Takai, G.L. Chiang, W.H. Cheong, S. Sucharit, Hybridization and
332 some biological facts of seven strains of the *Anopheles leucosphyrus* group
333 (Reid, 1968), Jpn. J. Sanit. Zool. 32 (1981) 321-329.
334 [24] V. Baimai, R.G. Andre, B.A. Harrison, U. Kijchalao, L. Panthusiri, Crossing and
335 chromosomal evidence for two additional sibling species within the taxon

Anopheles dirus Peyton and Harrison (Diptera: Culicidae) in Thailand, Proc. Entomol. Soc. Wash. 89 (1987) 157-166.

[25] A. Junkum, N. Komalamisra, A. Jitpakdi, N. Jariyapan, G.S. Min, M.H. Park, K.H. Cho, P. Somboon, P.A. Bates, W. Choochote, Evidence to support two conspecific cytological races on *Anopheles aconitus* in Thailand, J. Vector. Ecol. 30 (2005) 213-224.

[26] P. Somboon, D. Thongwat, W. Choochote, C. Walton, M. Takagi, Crossing experiments of *Anopheles minimus* species C and putative species E, J. Am. Mosq. Control Assoc. 21 (2005) 5-9.

[27] A. Saeung, V. Baimai, Y. Otsuka, R. Rattanarithikul, P. Somboon, A. Junkum, B. Tuetun, H. Takaoka, W. Choochote, Molecular and cytogenetic evidence of three sibling species of the *Anopheles barbirostris* Form A (Diptera: Culicidae) in Thailand, Parasitol. Res. 102 (2008) 499-507.

[28] D. Thongwat, K. Morgan, M.S. O'loughlin, C. Walton, W. Choochote, P. Somboon, Crossing experiment supporting the specific status of *Anopheles maculatus* chromosomal form K, J. Am. Mosq. Control Assoc. 24 (2008) 194-202.

[29] S. Suwannamit, V. Baimai, Y. Otsuka, A. Saeung, S. Thongsahuan, B. Tuetun, C. Apiwathnasorn, N. Jariyapan, P. Somboon, H. Takaoka, W. Choochote, Cytogenetic and molecular evidence for an additional new species within the taxon *Anopheles barbirostris* (Diptera: Culicidae) in Thailand, Parasitol. Res. 104 (2009) 905-918.

[30] S. Thongsahuan, V. Baimai, Y. Otsuka, A. Saeung, B. Tuetun, N. Jariyapan, S. Suwannamit, P. Somboon, A. Jitpakdi, H. Takaoka, W. Choochote,

Karyotypic variation and geographic distribution of *Anopheles campestris*-like (Diptera: Culicidae) in Thailand, Mem. Inst. Oswaldo Cruz. 104 (2009) 558-566.

[31] W. Choochote, Evidence to support karyotypic variation of the mosquito, *Anopheles peditaeniatus* in Thailand, J. Insect Sci. 11 (2011) 10.

[32] A. Saeung, V. Baimai, S. Thongsahuan, G.S. Min, M.H. Park, Y. Otsuka, W. Maleewong, V. Lulitanond, K. Taai, W. Choochote, Geographic distribution and genetic compatibility among six karyotypic forms of *Anopheles peditaeniatus* (Diptera: Culicidae) in Thailand, Trop. Biomed. 29 (2012) 613-625.

[33] W. Choochote, A. Jitpakdi, K.L. Sukontason, U. Chaithong, S. Wongkamchai, B. Pitasawat, N. Jariyapan, T. Suntaravitun, E. Rattanachanpichai, K. Sukontason, S. Leemingsawat, Y. Rongsriyam, Intraspecific hybridization of two karyotypic forms of *Anopheles vagus* (Diptera: Culicidae) and the related egg surface topography, Southeast Asian J. Trop. Med. Public Health 33 (suppl 3) (2002) 29-35.

[34] S.J. Park, W. Choochote, A. Jitpakdi, A. Junkum, S.J. Kim, N. Jariyapan, Evidence for a conspecific relationship between two morphologically and cytologically different Forms of Korean *Anopheles pullus* mosquito, Mol. Cells. 16 (2003) 354-360.

[35] W. Choochote, A. Jitpakdi, Y. Rongsriyam, N. Komalamisra, B. Pitasawat, K. Palakul, Isoenzyme study and hybridization of two forms of *Anopheles sinensis* (Diptera: Culicidae) in Northern Thailand, Southeast Asian J. Trop. Med. Public Health. 29 (1998) 841-847.

[36] G.S. Min, W. Choochote, A. Jitpakdi, S.J. Kim, W. Kim, J. Jung, A. Junkum, Intraspecific hybridization of *Anopheles sinensis* (Diptera: Culicidae) strains from Thailand and Korea, Mol. Cells 14 (2002) 198-204.

[37] M.H. Park, W. Choochote, A. Junkum, D. Joshi, B. Tuetan, A. Saeung, J.H. Jung, G.S. Min, Reproductive isolation of *Anopheles sinensis* from *Anopheles lesteri* and *Anopheles sineroides* in Korea, Genes & Genomics 30 (2008a) 245-252.

[38] M.H. Park, W. Choochote, S.J. Kim, P. Somboon, A. Saeung, B. Tuetan, Y. Tsuda, M. Takagi, D. Joshi, Y.J. Ma, G.S. Min, Nonreproductive isolation among four allopatric strains of *Anopheles sinensis* in Asia, J. Am. Mosq. Control Assoc. 24 (2008b) 489-495.

[39] R.C. Wilkerson, P.G. Foster, C. Li, M.A. Sallum, Molecular phylogeny of neotropical *Anopheles* (*Nyssorhynchus*) *albitarsis* species complex (Diptera: Culicidae), Ann. Entomol. Soc. Am. 98 (2005) 918-925.

[40] I. Dusfour, J.R. Michaux, R.E. Harbach, S. Manguin, Speciation and phylogeography of the Southeast Asian *Anopheles sundaicus* complex, Infect. Genet. Evol. 7 (2007) 484-493.

[41] K. Morgan, S.M. O'Loughlin, F. Mun-Yik, Y.M. Linton, P. Somboon, S. Min, P.T. Htun, S. Nambanya, I. Weerasinghe, T. Sochantha, A. Prakash, C. Walton, Molecular phylogenetics and biogeography of the Neocellia Series of *Anopheles* mosquitoes in the Oriental Region, Mol. Phylogenet. Evol. 52 (2009) 588-601.

[42] C. Paredes-Esquivel, M.J. Donnelly, R.E. Harbach, H. Townson, A molecular phylogeny of mosquitoes in the *Anopheles barbirostris* Subgroup reveals cryptic

406 species: implications for identification of disease vectors, Mol. Phylogenet.
407 Evol. 50 (2009) 141-151.
408 [43] N. Nanda, O.P. Singh, V.K. Dua, A.C. Pandey, B.N. Nagpal, T. Adak, A.P.
409 Dash, S.K. Subbarao, Population cytogenetic and molecular evidence for
410 existence of a new species in *Anopheles fluviatilis* complex (Diptera: Culicidae),
411 Infect. Genet. Evol. 13 (2013) 218-223.
412
413
414
415
416

417 **Figure legends**

418 **Fig. 1.** Map of Thailand and Cambodia showing 8 provinces where samples of *An.*
419 *crawfordi* were collected and the number of isolines of the 4 karyotypic forms (A-D)
420 detected in each location.

421

422 **Fig. 2.** Metaphase karyotypes of *An. crawfordi*. (a) Form A (X_1, Y_1: Chiang Mai); (b)
423 Form A (X_3, Y_1: Chumphon); (c) Form A (X_2, Y_1: Trang); (d) Form B (X_1, Y_2: Nan);
424 (e) Form B (X_3, Y_2: Trang); (f) Form B (X_3, Y_2: Songkhla); (g) Form B (X_2, Y_2:
425 Ratanakiri); (h) Form C (X_2, Y_3: Trang); (i) Form D (X_2, Y_4: Trang); (j) Form B
426 (homozygous X_2, X_2: Mondulkiri); diagrams of representative metaphase karyotype of
427 Form C (k) and Form D (l).

428

429 **Fig. 3.** Complete synapsis in all arms of salivary gland polytene chromosome of F_1-
430 hybrid larvae of *An. crawfordi*. (a) Cm1A female x Sk1B male; (b) Cm1A female x
431 Tg2C male; (c) Cm1A female x Tg4D male; (d) Cm1A female x Rt1A male; (e) Cm1A
432 female x Mr1B male.

433

434 **Fig. 4.** Phylogenetic relationships among the 29 isolines of *An. crawfordi* from Thailand
435 and Cambodia using Bayesian analysis based on ITS2 sequences compared with 7
436 species of the Hyrcanus Group. Numbers on branches are bootstrap values (%) of NJ
437 analysis and Bayesian posterior probabilities (%). Only the values higher than 70% both
438 on bootstrap values and posterior probabilities are shown. Bars represent 0.05
439 substitutions per site.

Fig. 5. Phylogenetic relationships among the 29 isolines of *An. crawfordi* from Thailand and Cambodia using Bayesian analysis based on COI sequences compared with 5 species of the Hyrcanus Group. Numbers on branches are bootstrap values (%) of NJ analysis and Bayesian posterior probabilities (%). Only the values higher than 70% both on bootstrap values and posterior probabilities are shown. Bars represent 0.1 substitutions per site.

Fig. 6. Phylogenetic relationships among the 29 isolines of *An. crawfordi* from Thailand and Cambodia using Bayesian analysis based on COII sequences compared with 5 species of the Hyrcanus Group. Numbers on branches are bootstrap values (%) of NJ analysis and Bayesian posterior probabilities (%). Only the values higher than 70% both on bootstrap values and posterior probabilities are shown. Bars represent 0.1 substitutions per site.

Table 1

Locations in Thailand and Cambodia, code of isolines, 4 karyotypic forms (A-D) of *An. crawfordi* and their GenBank accession numbers.

Location (Geograpical coordinate)	Code of isoline[a]	Karyotypic form	Genbank accession number			Reference
			ITS2	COI	COII	
Thailand						
Chiang Mai (18° 47′ N, 98° 59′ E)	Cm1A[a]	A (X_1, Y_1)	AB779131	AB779160	AB779189	This study
Nan (19° 21′ N, 100° 39′ E)	Nn1B[a]	B (X_1, Y_2)	AB779132	AB779161	AB779190	This study
Chumphon (10° 29′ N, 99° 11′ E)	Cp1A	A (X_3, Y_1)	AB779133	AB779162	AB779191	This study
Trang (07° 33′ N, 99° 38′ E)	Tg1B[a]	B (X_3, Y_2)	AB779134	AB779163	AB779192	This study
	Tg2C[a]	C (X_2, Y_3)	AB779135	AB779164	AB779193	This study
	Tg3A[a]	A (X_3, Y_1)	AB779136	AB779165	AB779194	This study
	Tg4D[a]	D (X_2, Y_4)	AB779137	AB779166	AB779195	This study
	Tg6B	B (X_2, Y_2)	AB779138	AB779167	AB779196	This study
	Tg8D	D (X_2, Y_4)	AB779139	AB779168	AB779197	This study
	Tg11A	A (X_2, Y_1)	AB779140	AB779169	AB779198	This study
	Tg12C	C (X_2, Y_3)	AB779141	AB779170	AB779199	This study
Phang Nga (08° 27′ N, 98° 31′ E)	Pg4A	A (X_1, Y_1)	AB779142	AB779171	AB779200	This study

Table 1 (*continued*)

Location (Geograpical coordinate)	Code of isoline[a]	Karyotypic form	Genbank accession number			Reference
			ITS2	COI	COII	
	Pg5A[a]	A (X_2, Y_1)	AB779143	AB779172	AB779201	This study
	Pg6A	A (X_1, Y_1)	AB779144	AB779173	AB779202	This study
	Pg7A	A (X_2, Y_1)	AB779145	AB779174	AB779203	This study
	Pg8A	A (X_2, Y_1)	AB779146	AB779175	AB779204	This study
	Pg9A	A (X_2, Y_1)	AB779147	AB779176	AB779205	This study
	Pg11A	A (X_2, Y_1)	AB779148	AB779177	AB779206	This study
	Pg12A	A (X_1, Y_1)	AB779149	AB779178	AB779207	This study
	Pg14A	A (X_1, Y_1)	AB779150	AB779179	AB779208	This study
	Pg16A	A (X_2, Y_1)	AB779151	AB779180	AB779209	This study
Songkhla (07° 13′ N, 100° 37′ E)	Sk1B[a]	B (X_3, Y_2)	AB779152	AB779181	AB779210	This study
Cambodia						
Ratanakiri (13° 44′ N, 107° 0′ E)	Rt1A[a]	A (X_1, Y_1)	AB779153	AB779182	AB779211	This study
	Rt2B	B (X_2, Y_2)	AB779154	AB779183	AB779212	This study

Table 1 (*continued*)

Location (Geograpical coordinate)	Code of isoline[a]	Karyotypic form	Genbank accession number			Reference
			ITS2	COI	COII	
Mondulkiri (12° 27′ N, 107° 14′ E)	Rt3B	B (X_2, Y_2)	AB779155	AB779184	AB779213	This study
	Mr1B[a]	B (X_2, Y_2)	AB779156	AB779185	AB779214	This study
	Mr2A	A (X_2, Y_1)	AB779157	AB779186	AB779215	This study
	Mr3A	A (X_1, Y_1)	AB779158	AB779187	AB779216	This study
	Mr4B	A (X_2, Y_2)	AB779159	AB779188	AB779217	This study
An. belenrae	-	-	EU789794	-	-	Park et al. [37]
An. kleini	-	-	EU789793	-	-	Park et al. [37]
An. lesteri	-	-	EU789791	-	-	Park et al. [37]
	ilG1	-	-	AB733028	AB733036	Taai et al. unpublished data
An. paraliae	Sk1B	B (X_1, Y_2)	AB733487	AB733503	AB733519	Taai et al. unpublished data
An. peditaeniatus	RbB	B (X_3, Y_2)	AB539061	AB539069	AB539077	Choochote [31]
An. pullus	-	-	EU789792	-	-	Park et al. [37]
	-	-	-	AY444348	AY444347	Park et al. [34]

Table 1 (*continued*)

Location (Geograpical coordinate)	Code of isoline[a]	Karyotypic form	Genbank accession number			Reference
			ITS2	COI	COII	
An. sinensis	i2ACM	A (X, Y_1)	AY130473	-	-	Min et al. [36]
	-	-	-	AY444351	-	Park et al. [34]
	i1BKR	B (X, Y_2)	-	-	AY130464	Min et al. [36]

a: used in crossing experiments.

Table 2

Crossing experiments among 10 isolines of *An. crawfordi*.

Crosses (Female x Male)	Total eggs (number)[a]	Embryonation rate[b]	Hatched n (%)	Pupation n (%)	Emergence n (%)	Total emergence n (%)	
						Female	Male
Parental cross							
Cm1A x Cm1A	309 (179, 130)	90	272 (88.03)	258 (94.85)	248 (96.12)	111 (44.76)	137 (55.24)
Nn1B x Nn1B	251 (141, 110)	87	208 (82.87)	200 (96.15)	200 (100.00)	88 (44.00)	112 (56.00)
Tg3A x Tg3A	395 (166, 229)	92	348 (88.10)	317 (91.09)	311 (98.11)	162 (52.09)	149 (47.91)
Tg1B x Tg1B	413 (234, 179)	79	326 (78.93)	293 (89.88)	287 (97.95)	149 (51.92)	138 (48.08)
Tg2C x Tg2C	314 (200, 114)	85	264 (84.08)	259 (98.11)	256 (98.84)	111 (43.36)	145 (56.64)
Tg4D x Tg4D	228 (123, 105)	83	185 (81.14)	183 (98.92)	183 (100.00)	93 (50.82)	90 (49.18)
Pg5A x Pg5A	326 (146, 180)	88	284 (87.12)	281 (98.94)	278 (98.93)	138 (49.64)	140 (50.36)
Sk1B x Sk1B	269 (103, 166)	97	261 (97.03)	256 (98.08)	251 (98.05)	118 (47.01)	133 (52.99)
Rt1A x Rt1A	254 (156, 98)	93	236 (92.91)	231 (97.88)	229 (99.13)	127 (55.46)	102 (44.54)
Mr1B x Mr1B	269 (175, 94)	88	237 (88.10)	232 (97.89)	230 (99.14)	112 (48.70)	118 (51.30)
Reciprocal cross							
Cm1A x Nn1B	360 (217, 143)	80	284 (78.89)	281 (98.94)	281 (100.00)	132 (46.98)	149 (53.02)
Nn1B x Cm1A	283 (105, 178)	93	252 (89.05)	252 (100.00)	252 (100.00)	111 (44.05)	141 (55.95)
Cm1A x Tg3A	232 (146, 86)	94	204 (87.93)	200 (98.04)	196 (98.00)	114 (58.16)	82 (41.84)
Tg3A x Cm1A	258 (129, 129)	92	235 (91.09)	230 (97.87)	228 (99.13)	108 (47.37)	120 (52.63)
Cm1A x Tg1B	269 (151, 118)	90	221 (82.16)	217 (98.19)	213 (98.16)	96 (45.07)	117 (54.93)

Table 2 *(continued)*

Crosses (Female x Male)	Total eggs (number)[a]	Embryonation rate[b]	Hatched n (%)	Pupation n (%)	Emergence n (%)	Total emergence n (%)	
						Female	Male
Tg1B x Cm1A	278 (113, 165)	93	256 (92.09)	246 (96.09)	239 (97.15)	126 (52.72)	113 (47.28)
Cm1A x Tg2C	320 (134, 186)	95	282 (88.13)	282 (100.00)	282 (100.00)	149 (52.84)	133 (47.16)
Tg2C x Cm1A	337 (179, 158)	96	313 (92.88)	285 (91.05)	242 (84.91)	117 (48.35)	125 (51.65)
Cm1A x Tg4D	280 (120, 160)	90	252 (90.00)	232 (92.06)	230 (99.14)	112 (48.70)	118 (51.30)
Tg4D x Cm1A	282 (113, 169)	88	240 (85.11)	200 (83.33)	196 (98.00)	102 (52.04)	94 (47.96)
Cm1A x Pg5A	255 (138, 117)	95	242 (94.90)	242 (100.00)	230 (95.04)	97 (42.17)	133 (57.83)
Pg5A x Cm1A	260 (160, 100)	96	247 (95.00)	232 (93.93)	216 (93.10)	111 (51.39)	105 (48.61)
Cm1A x Sk1B	296 (170,126)	95	281 (94.93)	281 (100.00)	275 (97.86)	138 (50.18)	137 (49.82)
Sk1B x Cm1A	333 (160, 173)	90	290 (87.09)	258 (88.97)	201 (77.91)	104 (51.74)	97 (48.26)
Cm1A x Rt1A	263 (145, 118)	94	247 (93.92)	230 (93.12)	230 (100.00)	121 (52.61)	109 (47.39)
Rt1A x Cm1A	277 (163, 114)	92	255 (92.06)	247 (96.86)	230 (93.12)	118 (51.30)	112 (48.70)
Cm1A x Mr1B	287 (109, 178)	87	227 (79.09)	209 (92.07)	209 (100.00)	102 (48.80)	107 (51.20)
Mr1B x Cm1A	308 (194, 114)	78	234 (75.97)	234 (100.00)	234 (100.00)	113 (48.29)	121 (51.71)
F_1- hybrid cross							
(Cm1A x Nn1B)F_1 x (Cm1A x Nn1B)F_1	320 (136, 184)	86	243 (75.94)	221 (90.95)	221 (100.00)	104 (47.06)	117 (52.94)
(Nn1B x Cm1A)F_1x (Nn1B x Cm1A)F_1	357 (168, 189)	91	300 (84.03)	267 (89.00)	267 (100.00)	134 (50.19)	133 (49.81)
(Cm1A x Tg3A)F_1 x (Cm1A x Tg3A)F_1	296 (169, 127)	80	216 (72.97)	216 (100.00)	207 (95.83)	101 (48.79)	106 (51.21)
(Tg3A xCm1A)F_1 x (Tg3A x Cm1A)F_1	325 (126, 199)	87	260 (80.00)	257 (98.85)	257 (100.00)	131 (50.97)	126 (49.03)

Table 2 (*continued*)

Crosses (Female x Male)	Total eggs (number)[a]	Embryonation rate[b]	Hatched n (%)	Pupation n (%)	Emergence n (%)	Total emergence n (%)	
						Female	Male
(Cm1A x Tg1B)F_1 x (Cm1A x Tg1B)F_1	235 (108, 127)	91	207 (88.09)	207 (100.00)	205 (99.03)	86 (41.95)	119 (58.05)
(Tg1B x Cm1A)F_1 x (Tg1B x Cm1A)F_1	252 (145, 107)	84	171 (67.86)	169 (98.83)	166 (98.22)	86 (51.81)	80 (48.19)
(Cm1A x Tg2C)F_1 x (Cm1A x Tg2C)F_1	318 (131, 187)	83	261 (82.08)	261 (100.00)	253 (96.93)	121 (47.83)	132 (52.17)
(Tg2C x Cm1A)F_1 x (Tg2C x Cm1A)F_1	354 (164, 190)	85	290 (81.92)	287 (98.97)	276 (96.17)	132 (47.83)	144 (52.17)
(Cm1A x Tg4D)F_1 x (Cm1A x Tg4D)F_1	263 (188, 75)	80	200 (76.05)	182 (91.00)	180 (98.90)	86 (47.78)	94 (52.22)
(Tg4D x Cm1A)F_1 x (Tg4D x Cm1A)F_1	250 (150, 100)	97	212 (84.80)	212 (100.00)	210 (99.06)	116 (55.24)	94 (44.76)
(Cm1A x Pg5A)F_1 x (Cm1A x Pg5A)F_1	265 (126, 139)	91	230 (86.79)	230 (100.00)	225 (97.83)	106 (47.11)	119 (52.89)
(Pg5A x Cm1A)F_1 x (Pg5A x Cm1A)F_1	250 (102, 148)	88	195 (78.00)	183 (93.85)	172 (93.99)	86 (50.00)	86 (50.00)
(Cm1A x Sk1B)F_1 x (Cm1A x Sk1B)F_1	336 (136, 200)	85	269 (80.06)	269 (100.00)	269 (100.00)	110 (40.89)	159 (59.11)
(Sk1B x Cm1A)F_1 x (Sk1B x Cm1A)F_1	320 (162, 158)	92	269 (84.06)	269 (100.00)	269 (100.00)	134 (49.81)	135 (50.19)
(Cm1A x Rt1A)F_1 x (Cm1A x Rt1A)F_1	227 (148, 79)	84	154 (67.84)	140 (90.91)	137 (97.86)	66 (48.18)	71 (51.82)
(Rt1A x Cm1A)F_1 x (Rt1A x Cm1A)F_1	235 (108, 127)	97	218 (92.77)	218 (100.00)	218 (100.00)	116 (53.21)	102 (46.79)
(Cm1A x Mr1B)F_1 x (Cm1A x Mr1B)F_1	268 (159, 109)	79	204 (76.12)	204 (100.00)	204 (100.00)	102 (50.00)	102 (50.00)
(Mr1B x Cm1A)F_1 x (Mr1B x Cm1A)F_1	245 (100, 145)	65	152 (62.04)	150 (98.68)	147 (98.00)	69 (46.94)	78 (53.06)

a: two selective egg-batches of inseminated females from each cross; *b*: dissection from 100 eggs; n = number.

Table 3

Mean intra-specific sequence divergence using Kimura two-parameter (K2P) model among *An. crawfordi* Forms A, B, C and D from Thailand and Cambodia based on ITS2, COI and COII sequences.

	ITS2	COI	COII
Within Form			
A	0.009	0.010	0.008
B	0.014	0.018	0.012
C	0.000	0.000	0.000
D	0.000	0.000	0.000
Between Forms			
A-B	0.014	0.016	0.011
A-C	0.005	0.006	0.005
A-D	0.005	0.006	0.005
B-C	0.014	0.015	0.011
B-D	0.014	0.015	0.011
C-D	0.000	0.000	0.000

Figure 1

Click here to download high resolution image

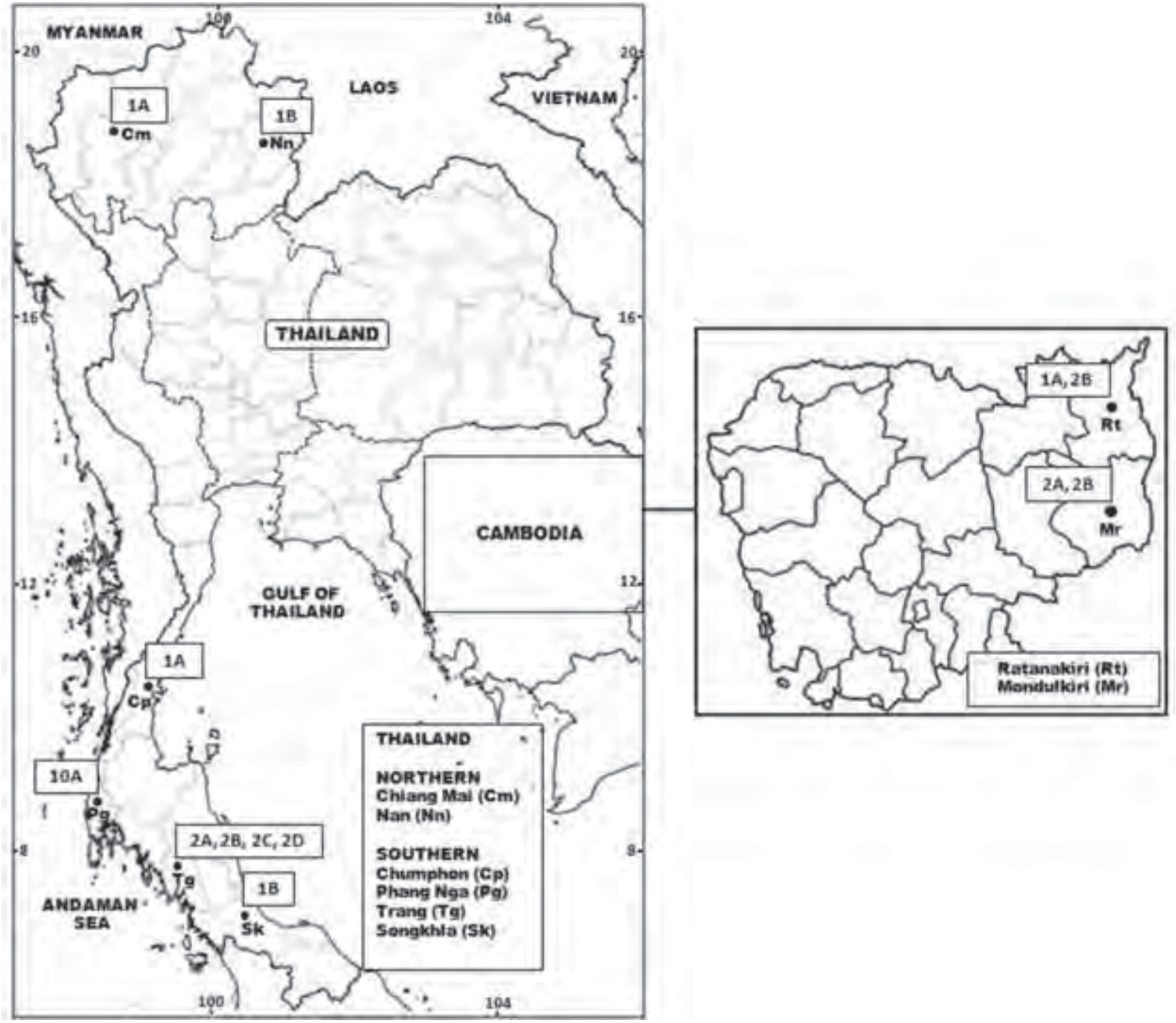

Figure 2

Click here to download high resolution image

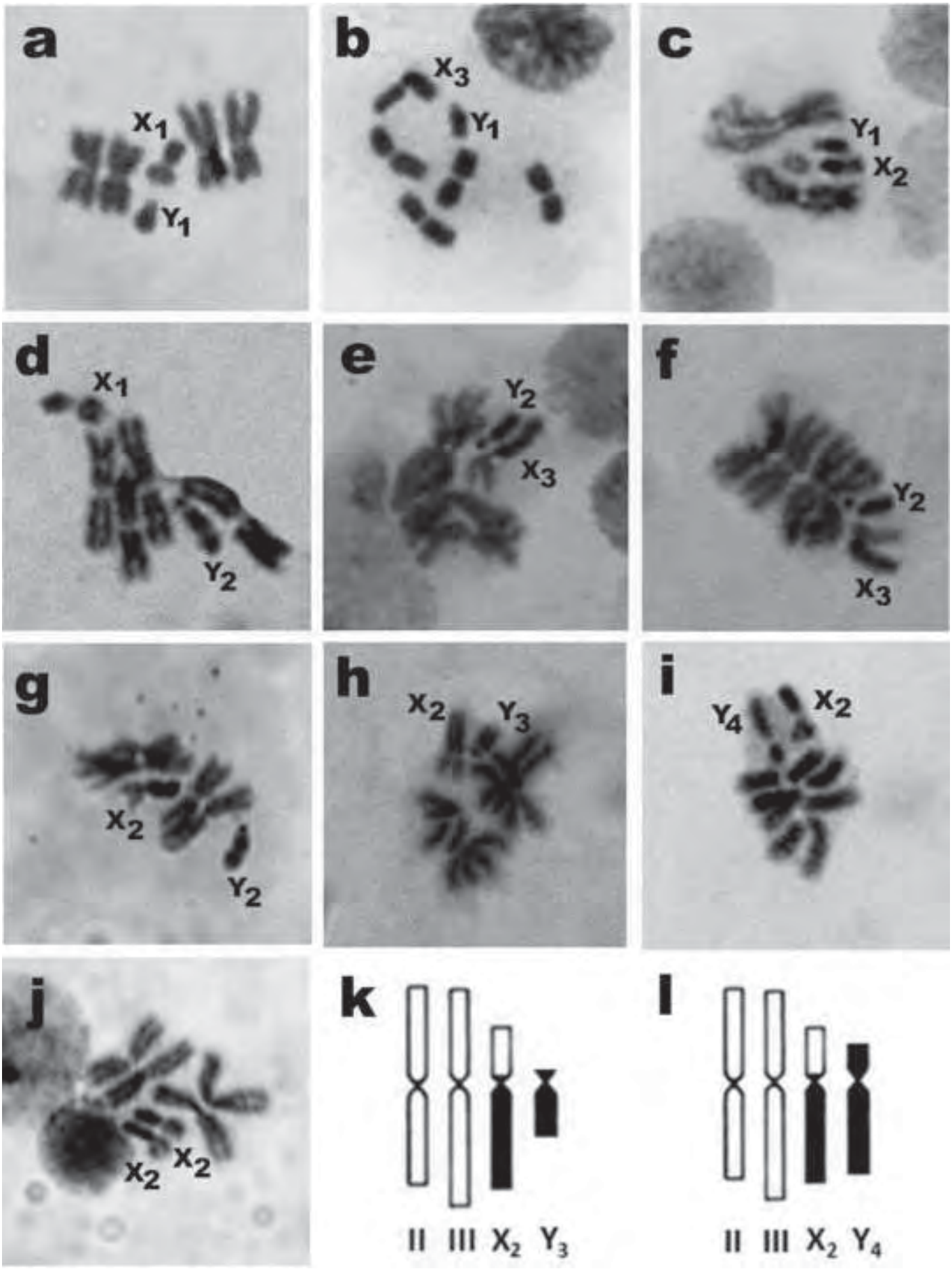

Figure 3

Click here to download high resolution image

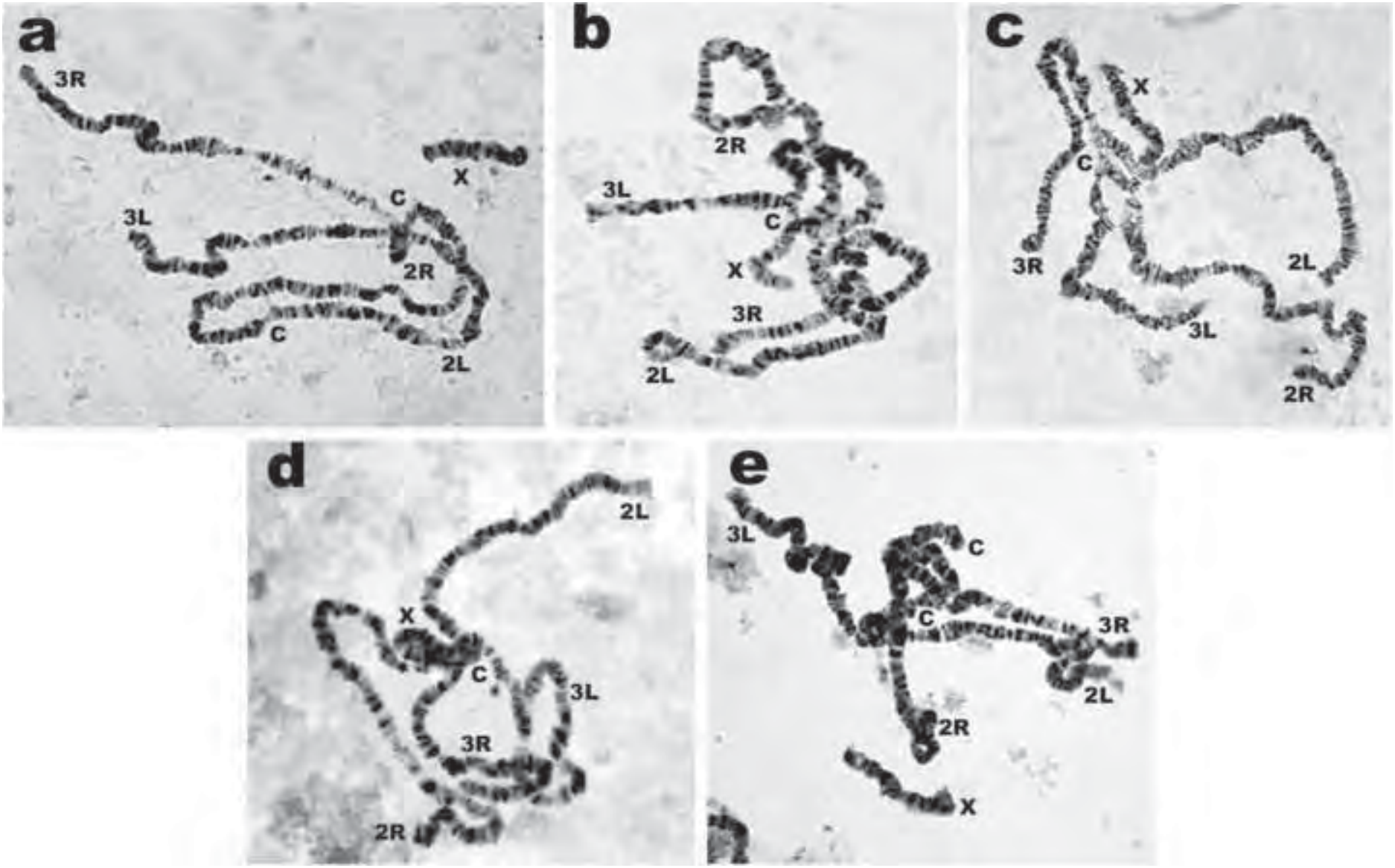

Figure 4

Click here to download high resolution image

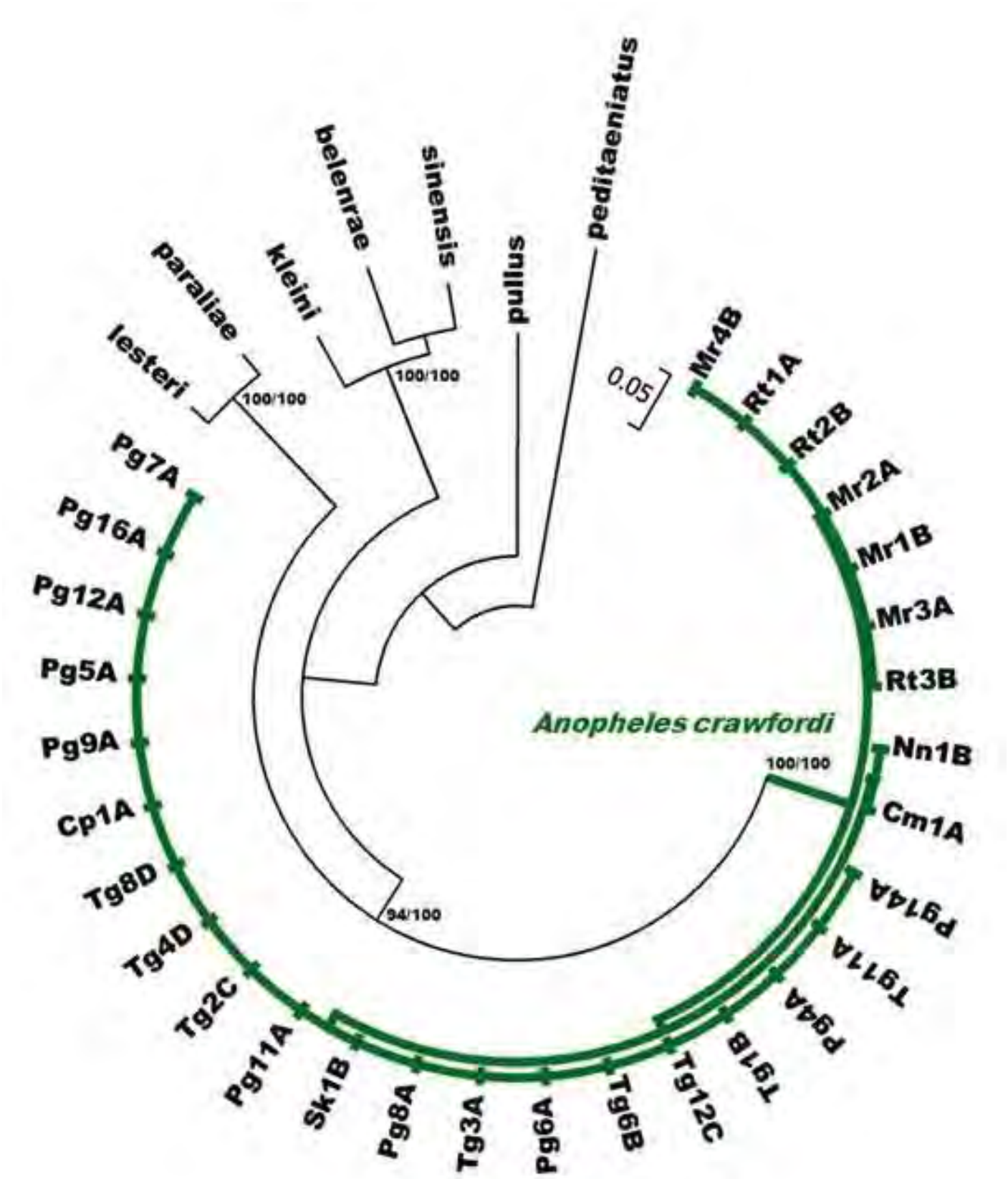

Figure 5

Click here to download high resolution image

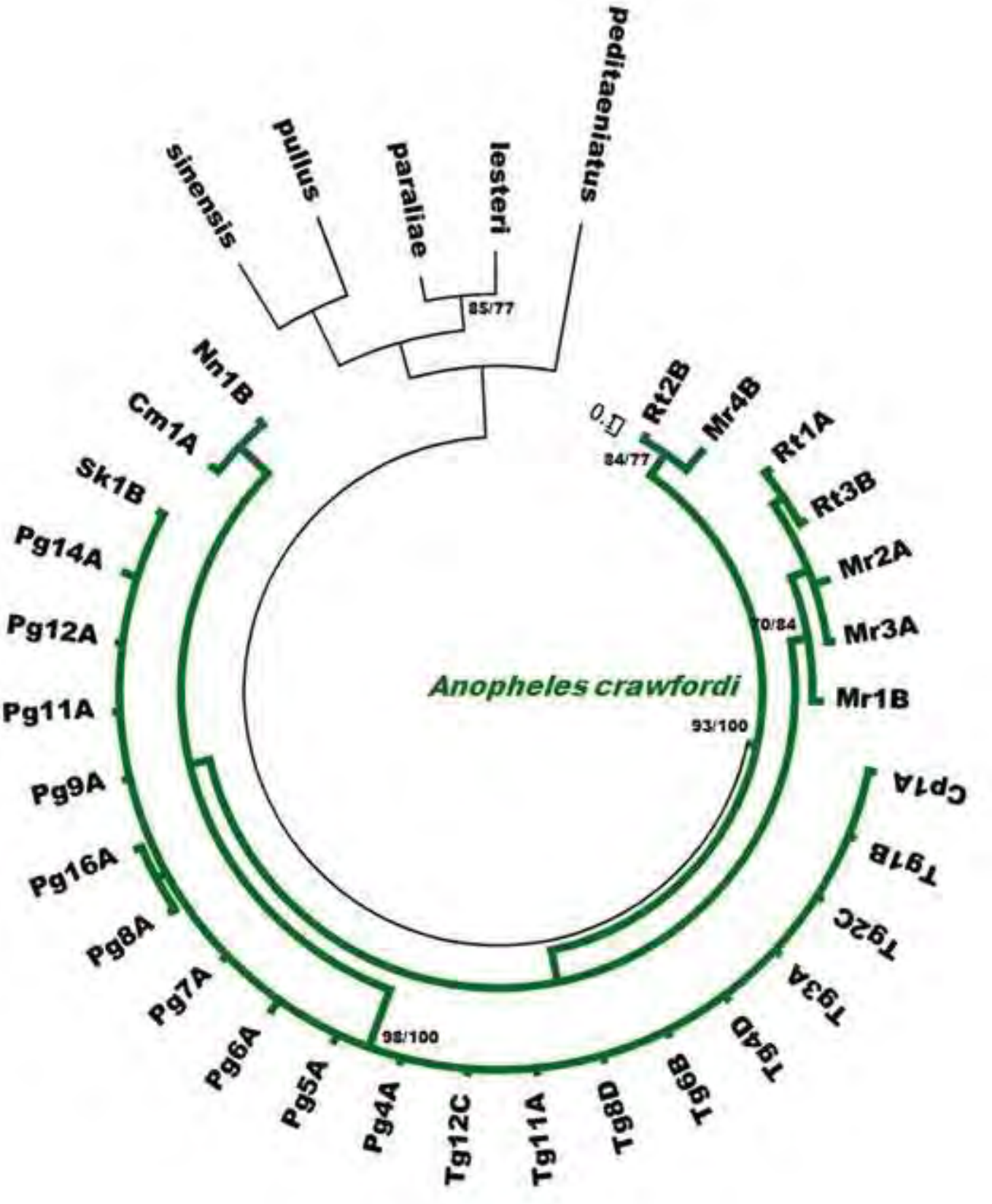

Figure 6
Click here to download high resolution image

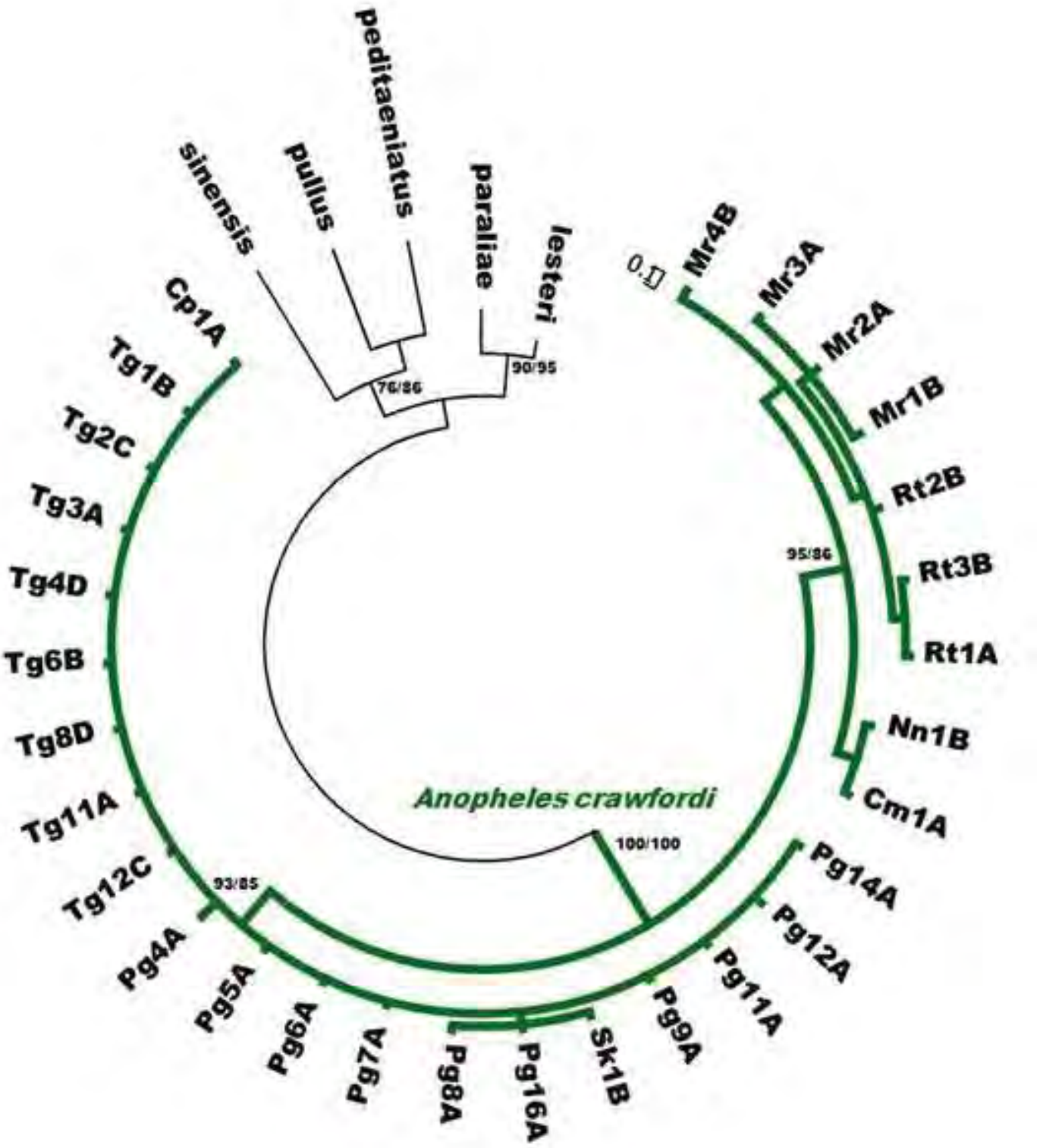

Evidence to support five cytological races of *Anopheles nitidus* in Thailand

Siripan Songsawatkiat[1a], Visut Baimai[2b], Sorawat Thongsahuan[3c], Atiporn Saeung[1d], Yasushi Otsuka[4e], Kritsana Taai[1f], Chayanit Hempolchom[1g], Wichai Srisuka[5h], Petchaboon Poolphol[6i], and Wej Choochote[1j*]

[1]Department of Parasitology, Faculty of Medicine, Chiang Mai University, Chiang Mai 50200, Thailand
[2]Department of Biology and Centre for Vectors and Vector-Borne Diseases, Faculty of Science, Mahidol University, Bangkok 10400, Thailand
[3]Faculty of Veterinary Science (Establishment Project), Prince of Songkla University, Songkhla 90110, Thailand
[4]Department of Infectious Disease Control, Faculty of Medicine, Oita University, Oita, 879-5593, Japan
[5]Entomology Section, Queen Sirikit Botanic Garden, P.O. Box 7, Chiang Mai, 50180, Thailand
[6]Office of Disease Prevention and Control 7th, Department of Disease Control, Ministry of Public Health, Thailand, Ubon Ratchathani, 34000, Thailand

Abstract

Metaphase karyotype investigation on two allopatric strains of *Anopheles nitidus* Harrison, Scanlon and Reid (Diptera: Culicidae) was conducted in Thailand during 2011-2012. Five karyotypic forms, i.e., Form A (X_1, Y_1), B (X_1,Y_2), C (X_2, Y_3), D (X_1, X_3, Y_4) and E (X_1, X_2, X_3, Y_5) were obtained from a total of 21 iso-female lines. Forms A, B and C were confined to Phang Nga province, southern Thailand, whereas Forms D and E were restricted to Ubon Ratchathani province, northeastern Thailand. Hybridization experiments among the 5 iso-female lines, which were representative of 5 karyotypic forms of *An. nitidus*, revealed genetic compatibility in providing viable progenies and synaptic salivary gland polytene chromosomes through F_2-generations. This suggested a conspecific nature comprising 5 cytological races within this taxon. The very low intra-specific sequence variations of the nucleotide sequences in ribosomal DNA [second internal transcribed spacer (ITS2)] and mitochondrial DNA [cytochrome *c* oxidase subunit I (COI) and cytochrome *c* oxidase subunit II (COII)] among 5 karyotypic forms were very good supportive evidence.

Keywords: *Anopheles nitidus*, metaphase karyotypes, hybridization experiments, second internal transcribed spacer, cytochrome *c* oxidase subunit I, cytochrome *c* oxidase subunit II

Correspondence: [a] siripann471@hotmail.com, [b] visut.bai@mahidol.ac.th, [c] sorawat_ton@hotmail.com, [d] atsaeung@mail.med.cmu.ac.th, [e] yotsuka@oita-u.ac.jp, [f] kritsana.taai@hotmail.com, [g] chayanit_hem@gmail.com, [h] wsrisuka@gmail.com, [i] siapoolphol@gmail.com, [j] wchoocho@mail.med.cmu.ac.th, *Corresponding author

Introduction

Anopheles (*Anopheles*) *nitidus* Harrison, Scanlon and Reid (Diptera: Culicidae) is a foothill anopheline species that belongs to the Nigerrimus Subgroup and Hyrcanus Group of the Myzorhynchus Series, and has a wide distribution range extending from India (Assam) to Vietnam, Cambodia, Thailand (a cosmopolitan species), Malaysia (Malaysian Peninsular and Sarawak) and Indonesia (Sumatra) (Reid 1968; Harrison and Scanlon 1975; Rattanarithikul et al. 2006; Harbach 2011). Although *An. nitidus* acts as a vicious biter of humans in some localities of Thailand, it has never been incriminated as a natural and/or suspected vector of any human-diseases, unlike other species members of the Thai *An. hyrcanus* group [e.g., *An. nigerrimus*, *An. peditaeniatus* and *An. sinensis* that one suspected vectors of *Plasmodium vivax* (Baker et al. 1987; Harbach et al. 1987; Gingrich et al. 1990; Rattanarithikul et al. 1996); and *An. nigerrimus*, a potentially natural vector of *Wuchereria bancrofti* in Phang Nga province, southern Thailand (Division of Filariasis 1998)]. Nevertheless, *An. nitidus* is considered an economic pest of cattle because of its vicious biting-behavior (Reid et al. 1962; Reid 1968; Harrison and Scanlon 1975).

Regarding cytogenetic investigations of *An. nitidus* by Baimai et al. (1993), their results revealed that at least 2 types of X (X_1, X_2) and 1 type of Y chromosomes were obtained in 2 isoline colonies caught from Muang district, Phang Nga province and Sadao district, Songkhla province, southern Thailand. As emphasized by the above information, cytogenetic evidence of *An. nitidus* is obviously lacking, particularly regarding the knowledge of genetic proximity among the karyotypic variants in a systematic direction. Thus, this paper reports herein, 5 karyotypic variants of *An. nitidus* and determine their genetic proximity by performing hybridization experiments among them relating to DNA sequence analyses of the second internal transcribed spacer (ITS2) of ribosomal DNA (rDNA), cytochrome *c* oxidase subunit I (COI) and cytochrome *c* oxidase subunit II (COII) of mitochondrial DNA (mtDNA).

Materials and Methods

Field collections and establishment of isoline colonies

Wild-caught, fully engorged female mosquitoes of *An. nitidus* were collected from cow-baited traps at 2 allopatric locations, i.e., Muang district, Phang Nga province and Nachaluai district, Ubon Ratchathani province in southern and northeastern Thailand, respectively (Figure 1, Table 1). A total of 21 isolines were established successfully and maintained in our insectary using the techniques described by Choochote et al. (1983) and Kim et al. (2003). Exact species identification was performed by using intact morphology of egg, larval, pupal and adult stages from the F_1-progenies of isolines, following standard keys (Reid 1968; Harrison and Scanlon 1975; Rattanarithikul et al. 2006). These isolines were used for studies on the metaphase karyotype, hybridization experiment and molecular analysis.

Metaphase karyotype preparation

Metaphase chromosomes were prepared from 10 samples of the early fourth-instar larval brains of F_1-progenies of each isoline, using techniques previously described by Saeung et al. (2007). Identification of karyotypic forms followed the standard cytotaxonomic systems of Baimai et al. (1993).

Hybridization experiment

The 5 laboratory-raised isolines of *An. nitidus* were selected arbitrarily from the 21 isoline colonies as representatives of the 5 karyotypic forms, i.e., Form A (Pg2A), B (Pg5B), C (Pg4C), D (Ur2D) and E (Ur5E) (Table 1). These isolines were used for hybridization experiments in order to determine post-mating barriers by employing the techniques previously reported by Saeung et al. (2007).

DNA extraction and amplification

Molecular analyses of 3 specific genomic loci (ITS2, COI and COII) were performed in order to determine intraspecific sequence variation within the taxon *An. nitidus*. Individual F_1-progeny adult female of each isoline of *An. nitidus* (Ur2D, Ur5E, Ur8E, Ur11D, Ur12D, Ur15D, Ur16E, Ur19D, Ur22E, Ur23E, Ur24D, Ur25D, Ur27D, Ur28E, Ur30E, Ur31D, Ur33E, Ur34D, Pg2A, Pg4C and Pg5B) was used for DNA extraction and amplification. Genomic DNA was extracted from each mosquito using DNeasy® Blood and Tissue Kit (QIAgen, www.qiagen.com). Primers for amplification of ITS2, COI, and COII regions were followed previous studies by Saeung et al. (2007). The ITS2 region of the rDNA was amplified using primer ITS2A (5'-TGT GAA CTG CAG GAC ACA T-3') and ITS2B (5'-TAT GCT TAA ATT CAGGGGGT-3') (Beebe and Saul 1995). The LCO1490 (5'-GGT CAA CAA ATC ATA AAG ATA TTG G-3') and HCO2198 (5'-TAA ACT TCA GGG TGA CCA AAA AAT CA-3') primers of Folmer et al. (1994) were used to amplify a fragment of mitochondrial COI barcoding region. The mitochondrial COII region was amplified using primers LEU (5'-TCT AAT ATG GCA GAT TAG TGC A-3') and LYS (5'-ACT TGC TTT CAG TCA TCT AAT G-3') (Sharpe et al. 2000). Each PCR reaction was carried out in total 20 µl volume containing 0.5 U *Ex Taq* (Takara, www.takara.co.jp), 1X *Ex Taq* buffer, 2 mM of $MgCl_2$, 0.2 mM of each dNTP, 0.25 µM of each primer, and 1 µl of the extracted DNA. For ITS2, the conditions for amplification consisted of initial denaturation at 94°C for 1 min, 30 cycles at 94°C for 30 sec, 55°C for 30 sec, and 72°C for 1 min, and a final extension at 72°C for 5 min. The amplification profile of COI and COII comprised initial denaturation at 94°C for 1 min, 30 cycles at 94°C for 30 sec, 50°C for 30 sec, and 72°C for 1 min, and a final extension at 72°C for 5 min. The amplified products were electrophoresed in 1.5% tris-acetate-EDTA (TAE) agarose gels and stained with ethidium bromide. Finally, the PCR products were purified using the QIAquick® PCR Purification Kit (QIAgen, www.qiagen.com) and their sequences directly determined using the BigDye® V3.1 Terminator Cycle Sequencing Kit and 3130 genetic analyzer (Applied Biosystems, www.appliedbiosystems.com). The sequence data obtained have been deposited in the DDBJ/EMBL/GenBank nucleotide sequence database under accession numbers AB777782-AB777844 (Table 1). The ITS2, COI and COII sequences obtained from this study were also compared with published sequences available through GenBank.

Sequencing alignment and phylogenetic analysis

Sequences of ITS2, COI and COII were aligned using the CLUSTAL W multiple alignment program (Thompson et al. 1994) and edited manually in BioEdit version 7.0.5.3 (Hall 1999). Gap sites were excluded from the following analysis. The Kimura two-parameter (K2P) model was employed to calculate genetic distances (Kimura 1980). Using the distances, construction of neighbor-joining trees (Saitou and Nei 1987) and the bootstrap test with 1,000 replications were performed with the MEGA version

4.0 program (Tamura et al. 2007). Bayesian analysis was conducted with MrBayes 3.2 (Ronquist et al. 2012) by using two replicates of 1 million generations with the nucleotide evolutionary model. The best-fit model was chosen for each gene separately using the Akaike Information Criterion (AIC) in MrModeltest version 2.3 (Nylander 2004). The general time-reversible (GTR) with gamma distribution shape parameter (G) was selected for ITS2, whereas, the GTR+I+G was the best-fit model for COI and COII. Bayesian posterior probabilities were calculated from the consensus tree after excluding the first 25% trees as burnin.

Results

Metaphase karyotype

Cytogenetic observations of F_1-progenies of the 21 isolines of *An. nitidus* revealed different types of sex chromosomes due to the addition of extra block (s) of heterochromatin. There were 3 types of X (small metacentric X_1, submetacentric X_2 and large submetacentric X_3) and 5 types of Y chromosomes (small telocentric Y_1, small subtelocentric Y_2, large subtelocentric Y_3, submetacentric Y_4 and small metacentric Y_5) (Figure 2-3). The X_1 chromosome has a small metacentric shape with one arm euchromatic, and the opposite one totally heterochromatic. The X_2 chromosome is different from the X_1 chromosome in having an extra block of heterochromatin in the heterochromatic arm, making it a long arm of submetacentric configuration. The X_3 chromosome has a large submetacentric shape that was slightly different from the X_2 chromosome in having an extra block of heterochromatin at the distal end of the long heterochromatic arm. A good comparison of the size and shape between X_2 and X_3 chromosomes could be made easily in heterozygous females (Figure 2I). Similar to the situation in the X chromosome, the Y chromosome also exhibited extensive variation in size and shape, due to differing amounts and distribution of heterochromatic block. Thus the Y_1 chromosome is an apparently small telocentric figure, which represents the simple or ancestral form (Figure 2A). The Y_2 chromosome has a small subtelocentric or acrocentric shape that slightly differs from the Y_1 chromosome, which has a very small portion of the short arm present (Figure 2B). Chromosome Y_3 has a large subtelocentric configuration that obviously differs from the Y_2 chromosome in having an extra block of heterochromatin at the distal end of the long heterochromatic arm (Figure 2C). The Y_4 chromosome is clearly submetacentric figure, with the short arm approximately 1/3 the length of the long arm (Figure 2D-E). It appears to have derived from the Y_3 chromosome by means of adding an extra block of heterochromatin onto the short arm, and transferring it to a submetacentric configuration. Chromosome Y_5 had a small metacentric shape, which was quite different from chromosomes Y_1, Y_2, Y_3 and Y_4 by having an equal herterochromatiic block on each arm (Figure 2F-G). Based on uniquely different characteristics of Y chromosome from each isoline colony, they were designated as Form A (X_1, Y_1), B (X_1, Y_2), C (X_2, Y_3), D (X_1, X_3, Y_4) and E (X_1, X_2, X_3, Y_5). Forms A, B and C were found in Phang Nga province, and Forms D and E were obtained in Ubon Ratchathani province.

Hybridization experiment

Details of hatchability, pupation, emergence and adult sex-ratio of parental, reciprocal and F_1-hybrid crosses among the 5 isolines of *An. nitidus* Forms A, B, C, D and E are shown in Table 2. All crosses yielded viable progenies through F_2-generations. No

evidence of genetic incompatibility and/or post-mating reproductive isolation was observed among these crosses. The salivary gland polytene chromosomes of the 4th stage larvae from all crosses showed synapsis without any inversion loops along the whole length of all autosomes and the X chromosome (Figure 4).

DNA sequences and phylogenetic analysis

DNA sequences were determined and analyzed for the ITS2, COI and COII regions of the 21 isolines of *An. nitidus* Forms A, B, C, D and E. They showed various lengths of ITS2, at 480 bp in 18 isolines from Ubon Ratchathani province and 481 bp in 3 isolines from Phang Nga province. The *An. nitidus* from Ubon Ratchathani province differed from that in Phang Nga province by a deletion of T at position 421. They all showed the same length in COI (658 bp) and COII (685 bp). To reveal the evolutionary relationship among the 5 karyotypic forms, neighbour-joining (NJ) and Bayesian trees were constructed in Figures 5-7. Both phylogenetic methods showed similar tree topologies, thus, only the NJ tree was shown for all regions. The results showed that all *An. nitidus* Forms A, B, C, D and E sequences were monophyletic in both trees. The average genetic distances within 5 karyotypic forms were 0.002, 0.008 and 0.006 for ITS2, COI and COII regions, respectively. The average genetic distances among 5 karyotypic forms were 0.006, 0.007 and 0.007 for ITS2, COI and COII regions, respectively. Furthermore, all karyrotypic forms of *An. nitidus* were different obviously from other inter-species members of the Hyrcanus Group, with strongly supported bootstrap probabilities (99-100%) in phylogenetic trees (Figures 5-7). Interestingly, three published ITS2 sequences (Genbank accession numbers HM488273, HM488272 and HM488268), which were identified previously as the Hyrcanus Group by Paredes-Esquivel et al. 2011 were placed within the same clade of *An. nitidus*.

Discussion

A cytogenetic investigation of *An. nitidus* in Thailand was documented first by Baimai et al. (1993). The results indicated that this anopheline species exhibited genetic diversity at the chromosomal level via a gradual increase in the extra heterochromatin block (s) on the X chromosome (X_1, X_2), whereas this event was not detected in the Y chromosomes, possibly due to the limited number of isolines used. However, this investigation of 21 *An. nitidus* isolines from 2 allopatric locations [Phang Nga province, southern region; Ubon Ratchathani province, northeastern region] in Thailand revealed 3 types of X (X_1, X_2, X_3) and 5 types of Y (Y_1, Y_2, Y_3, Y_4, Y_5) chromosomes, which were designated as Form A (X_1, Y_1), B (X_1,Y_2), C (X_2, Y_3), D (X_1, X_3, Y_4) and E ((X_1, X_2, X_3, Y_5), depending upon the uniquely distinct characteristics of Y chromosomes. The 5 different karyotypic forms of *An. nitidus* recovered in this study were due clearly to addition of the extra heterochromatin block (s) on sex chromosomes (X, Y), and in keeping with Baimai's hypothesis, which is an important mechanism in the species process of Oriental anophelines (Baimai 1998). It could be used robustly as a primary genetic marker for further identification of sibling species and/or subspecies (cytological races) within the taxon *Anopheles* (Kanda et al. 1981; Baimai et al. 1987; Subbarao 1998; Junkum et al. 2005). Interestingly, investigation of the 18 isolines from Ubon Ratchathani province, northeastern region, revealed only 2 karyotypic forms (Form D: 10 isolines; Form E: 8 isolines), whereas that of the 3 isolines from Phang Nga province, southern region, yielded 3 distinct karyotypic forms (Form A, B and C)

in each isoline, even though these 2 allopatric locations were placed approximately 800 km apart. This phenomenon appeared to elucidate the difference in ecological diversity, which favored specific microhabitats for the karyotypic evolution of *An. nitidus*. However, additional surveys are expected in order to obtain greater numbers of isolines from both provinces and/or other locations across 6 regions (northern, western, central, northeastern, eastern and southern) of Thailand. This would bring about understanding of the population-genetic structure of this anopheline species. Meanwhile, all experiments are progressing currently.

Hybridization experiments using anopheline isoline-colonies, relating to information on cytology and molecular analysis to determine post-mating barriers, have been proven so far as an efficient classical technique for recognizing sibling species and/or subspecies (cytological races) members within the taxon *Anopheles* (Kanda et al. 1981; Baimai et al. 1987; Subbarao 1998; Junkum et al. 2005; Somboon et al. 2005; Saeung et al. 2007, 2008; Thongwat et al. 2008; Suwannamit et al. 2009; Thongsahuan et al. 2009; Choochote 2011). The markedly genetic diversity at the chromosomal level of *An. nitidus*, via the addition of extra heterochromatin on sex chromosomes (X, Y) in this study, warrants intensive determination of post-mating barriers by hybridization experiments among the 5 karyotypic forms. The results of no post-mating reproductive isolation by yielding viable progenies through F_2-generations and synaptic salivary gland polytene chromosomes, along the entire length of autosomes and the X chromosome, indicate a conspecific nature comprising 5 cytological races within this taxon. The very low intra-specific sequence variations (mean genetic distance = 0.002-0.008) of the nucleotide sequences of ITS2, COI and COII of the 5 karyotypic forms are good supportive evidence. These results are agreed with previous hybridization experiments among sympatric and/or allopatric karyotypic forms of other anopheline species, i.e., *An. vagus* (Choochote et al. 2002), *An. pullus* (= *An. yatsushiroensis*) (Park et al. 2003), *An. sinensis* (Choochote et al. 1998; Min et al. 2002; Park et al. 2008b), *An. aconitus* (Junkum et al. 2005), *An. barbirostris* species A1 and A2 (Saeung et al. 2007; Suwannamit et al. 2009); *An. campestris*-like taxon (Thongsahuan et al. 2009) and *An. peditaeniatus* (Choochote 2011; Saeung et al. 2012). Thus, karyotypic variation based on extra heterochromatin in sex chromosomes seems to be a general phenomenon within Oriental *Anopheles.* This is the first report of hybridization experiment and molecular investigation of *An. nitidus* using karyotypic markers. In addition, the present study incorporated a nuclear and mitochondrial DNA sequence to increase the exact identification of this species from other inter-species members of the Hyrcanus Group (Min et al. 2002; Park et al. 2003; Park et al. 2008a; Choochote 2011). It is interesting to note that the ITS2 sequence of three specimens (TR2, TR3 and TR6) collected from Trat province, eastern Thailand, and identified as the Hyrcanus group by Paredes-Esquivel et al. 2011, were clustered together with 5 karyotypic forms of *An. nitidus* in a phylogenetic tree and presumed to be the same species as that in our study.

Acknowledgements

This work was supported by The Thailand Research Fund to W. Choochote and A. Saeung (TRF Senior Research Scholar: RTA5480006), Royal Golden Jubilee Ph.D. Program to W. Choochote and S. Songsawatkiat (PHD/0356/2552) and Faculty of Medicine Endowment Fund, Chiang Mai University, Chiang Mai, Thailand.

289 **References**

290 Baimai V. 1998. Heterochromatin accumulation and karyotypic evolution in some
291 dipteran insects. *Zoological Studies* 37: 75-88.
292 Baimai V, Andre RG, Harrison BA, Kijchalao U, Panthusiri L. 1987. Crossing and
293 chromosomal evidence for two additional sibling species within the taxon
294 *Anopheles dirus* Peyton and Harrison (Diptera: Culicidae) in Thailand.
295 *Proceedings of the Entomological Society of Washington* 89: 157-166.
296 Baimai V, Rattanarithikul R, Kijchalao U. 1993. Metaphase karyotypes of
297 *Anopheles* of Thailand and Southeast Asia: I. The *hyrcanus* group. *Journal of*
298 *the American Mosquito Control Association* 9: 59-67.
299 Baker EZ, Beier JC, Meek SR, Wirtz RA. 1987. Detection and quantification of
300 *Plasmodium falciparum* and *P. vivax* infections in Thai Kampuchean
301 *Anopheles* (Diptera: Culicidae) by enzyme linked immunosorbent assay. *Journal*
302 *of Medical Entomology* 24: 537-541.
303 Beebe NW, Saul A. 1995. Discrimination of all members of the *Anopheles*
304 *punctulatus* complex by polymerase chain reaction-restriction fragment length
305 polymorphism analysis. *American Journal of Tropical Medicine and Hygiene*
306 53: 478–481.
307 Choochote W. 2011. Evidence to support karyotypic variation of the mosquito,
308 *Anopheles peditaeniatus* in Thailand. *Journal of Insect Science* 11: 10.
309 Choochote W, Jitpakdi A, Rongsriyam Y, Komalamisra N, Pitasawat B, Palakul K.
310 1998. Isoenzyme study and hybridization of two forms of *Anopheles sinensis*
311 (Diptera: Culicidae) in Northern Thailand. *Southeast Asian Journal of Tropical*
312 *Medicine and Public Health* 29: 841-847.
313 Choochote W, Jitpakdi A, Sukontason KL, Chaithong U, Wongkamchai S,
314 Pitasawat B, Jariyapan N, Suntaravitun T, Rattanachanpichai E, Sukontason K,
315 Leemingsawat S, Rongsriyam Y. 2002. Intraspecific hybridization of two
316 karyotypic forms of *Anopheles vagus* (Diptera: Culicidae) and the related egg
317 surface topography. *Southeast Asian Journal of Tropical Medicine and Public*
318 *Health* 33: 29-35.
319 Choochote W, Sucharit S, Abeywickreme W. 1983. Experiments in crossing two strains
320 of *Anopheles barbirostris* Van der Wulp 1884 (Diptera: Culicidae) in Thailand.
321 *Southeast Asian Journal of Tropical Medicine and Public Health* 14: 204-209.
322 Division of filariasis. 1998. Department of Communicable Disease Control, Ministry
323 of Public Health. p 1-33.
324 Folmer O, Black M, Hoeh W, Lutz R, Vrijenhoek R. 1994. DNA primers for
325 amplification of mitochondrial cytochrome *c* oxidase subunit I from diverse
326 metazoan invertebrates. *Molecular Marine Biology and Biotechnology* 3: 294-
327 299.
328 Gingrich J, Weatherhead A, Sattabongkot J, Pilakasiri C, Wirtz RA. 1990.
329 Hyperendemic malaria in Thai Village: dependence of year-round transmission
330 on focal and seasonally circumscribed mosquito (Diptera: Culicidae) habitats.
331 *Journal of Medical Entomology* 27: 1016-1026.
332 Hall TA. 1999. BioEdit: a user-friendly biological sequence alignment editor and
333 analysis program for Windows 95/98/NT. *Nucleic Acids Symposium Series* 41:
334 95-98.

335 Harbach RE. 2011. Mosquito taxonomic inventory. *Anopheles* classification.
336 http://mosquito-taxonomic-inventory.info/anophelesclassification [Accessed 10
337 December 2012].
338 Harbach RE, Gingrich JB, Pang LW. 1987. Some entomological observations on
339 malaria transmission in a remote village in northwestern Thailand. *Journal of*
340 *the American Mosquito Control Association* 3: 296-301.
341 Harrison BA, Scanlon JE. 1975. Medical entomology studies II. The subgenus
342 *Anopheles* in Thailand (Diptera: Culicidae). *Contributions of the American*
343 *Entomological Institute* 12: 78.
344 Junkum A, Komalamisra N, Jitpakdi A, Jariyapan N, Min GS, Park MH, Cho KH,
345 Somboon P, Bates PA, Choochote W. 2005. Evidence to support two
346 conspecific cytological races on *Anopheles aconitus* in Thailand. *Journal of*
347 *Vector Ecology* 30: 213-224.
348 Kanda T, Takai K, Chiang GL, Cheong WH, Sucharit S. 1981. Hybridization and some
349 biological facts of seven strains of the *Anopheles leucosphyrus* group
350 (Reid, 1968). *Japanese Journal of Sanitary Zoology* 32: 321-329.
351 Kim SJ, Choochote W, Jitpakdi A, Junkum A, Park SJ, Min GS. 2003.
352 Establishment of a self-mating mosquito colony of *Anopheles sinensis* from
353 Korea. *The Korean Journal of Parasitology* 33: 267-271.
354 Kimura MA. 1980. Simple method for estimating evolutionary rates of base
355 substitution through comparative studies of nucleotide sequences. *Journal of*
356 *Molecular Evolution* 16: 111-120.
357 Min GS, Choochote W, Jitpakdi A, Kim SJ, Kim W, Jung J, Junkum A. 2002.
358 Intraspecific hybridization of *Anopheles sinensis* (Diptera: Culicidae)
359 strains from Thailand and Korea. *Molecules and Cells* 14: 198-204.
360 Nylander JAA. 2004. MrModeltest v2. Program distributed by the author. Evolutionary
361 Biology Centre, Uppsala University.
362 Paredes-Esquivel C, Harbach RE, Townson H. 2011. Molecular taxonomy of members
363 of the *Anopheles hyrcanus* group from Thailand and Indonesia. *Medical and*
364 *Veterinary Entomology* 25: 348–352.
365 Park MH, Choochote W, Junkum A, Joshi D, Tuetan B, Saeung A, Jung JH, Min GS.
366 2008a. Reproductive isolation of *Anopheles sinensis* from *Anopheles*
367 *lesteri* and *Anopheles sineroides* in Korea. *Genes & Genomics* 30: 245-252.
368 Park MH, Choochote W, Kim SJ, Somboon P, Saeung A, Tuetan B, Tsuda Y,
369 Takagi M, Joshi D, Ma YJ, Min GS. 2008b. Nonreproductive isolation
370 among four allopatric strains of *Anopheles sinensis* in Asia. *Journal of the*
371 *American Mosquito Control Association* 24: 489-495.
372 Park SJ, Choochote W, Jitpakdi A, Junkum A, Kim S, Jariyapan N. 2003. Evidence for
373 a conspecific relationship between two morphologically and cytologically
374 different Forms of Korean *Anopheles pullus* mosquito. *Molecules and Cells* 16:
375 354-360.
376 Rattanarithikul R, Harrison BA, Harbach RE, Panthusiri P, Coleman RE. 2006.
377 Illustrated keys to the mosquitoes of Thailand IV. *Anopheles*. *Southeast Asian*
378 *Journal of Tropical Medicine and Public Health* 37(suppl 2): 1-128.
379 Rattanarithikul R, Konishi E, Linthicum KJ. 1996. Detection of *Plasmodium vivax*
380 and *Plasmodium falciparum* circumsporozoites antigen in anopheline
381 mosquitoes collected in southern Thailand. *American Journal of Tropical*
382 *Medicine and Hygiene* 54: 114-121.

Reid JA, Wilson T, Ganapathipillai A. 1962. Studies on filariasis in Malaya: The mosquito vectors of periodic *Brugia malayi* in North-West Malaya. *Annals of Tropical Medicine and Parasitology* 56: 323-336.

Reid JA. 1968. Anopheline mosquitoes of Malaya and Borneo. *Studies from the Institute for Medical Research Malaysia* 31: 1-520.

Ronquist F, Teslenko M, van der Mark P, Ayres DL, Darling A, Höhna S, Larget B, Liu L, Suchard MA, Huelsenbeck JP. 2012. MrBayes 3.2: efficient Bayesian phylogenetic inference and model choice across a large model space. *Systematic Biology* 61: 539-542.

Saeung A, Baimai V, Otsuka Y, Rattanarithikul R, Somboon P, Junkum A, Tuetun B, Takaoka H, Choochote W. 2008. Molecular and cytogenetic evidence of three sibling species of the *Anopheles barbirostris* Form A (Diptera: Culicidae) in Thailand. *Parasitology Research* 102: 499-507.

Saeung A, Baimai V, Thongsahuan S, Min GS, Park MH, Otsuka Y, Maleewong W, Lulitanond V, Taai K, Choochote W. 2012. Geographic distribution and genetic compatibility among six karyotypic forms of *Anopheles peditaeniatus* (Diptera: Culicidae) in Thailand. *Tropical Biomedicine* 29: 613-625.

Saeung A, Otsuka Y, Baimai V, Somboon P, Pitasawat B, Tuetun B, Junkum A, Takaoka H, Choochote W. 2007. Cytogenetic and molecular evidence for two species in the *Anopheles barbirostris* complex (Diptera: Culicidae) in Thailand. *Parasitology Research* 101: 1337-1344.

Saitou N, Nei M. 1987. The neighbor-joining method: A new method for reconstructing phylogenetic trees. *Molecular Biology and Evolution* 4: 406-425.

Sharpe RG, Harbach RE, Butlin RK. 2000. Molecular variation and phylogeny of members of the Minimus group of *Anopheles* subgenus *Cellia* (Diptera: Culicidae). *Systematic Entomology* 25: 263-272.

Somboon P, Thongwat D, Choochote W, Walton C, Takagi M. 2005. Crossing experiments of *Anopheles minimus* species C and putative species E. *Journal of the American Mosquito Control Association* 21: 5-9.

Subbarao SK. 1998. Anopheline species complexes in South-East Asia. *World Health Organization Technical Publication Searo* 18: 1-82.

Suwannamit S, Baimai V, Otsuka Y, Saeung A, Thongsahuan S, Tuetun B, Apiwathnasorn C, Jariyapan N, Somboon P, Takaoka H, Choochote W. 2009. Cytogenetic and molecular evidence for an additional new species within the taxon *Anopheles barbirostris* (Diptera: Culicidae) in Thailand. *Parasitology Research* 104: 905-918.

Tamura K, Dudley J, Nei M, Kumar S. 2007. MEGA4: Molecular evolution genetics analysis (MEGA) software version 4.0. *Molecular Biology and Evolution* 24: 1596-1599.

Thompson JD, Higgins DG, Gibson TJ. 1994. CLUSTAL W: improving the sensitivity of progressive multiple sequence alignment through sequence weighting, positions-specific gap penalties and weight matrix choice. *Nucleic Acids Research* 22: 4673-4680.

Thongsahuan S, Baimai V, Otsuka Y, Saeung A, Tuetun B, Jariyapan N, Suwannamit, S, Somboon P, Jitpakdi A, Takaoka H, Choochote W. 2009. Karyotypic variation and geographic distribution of *Anopheles campestris*-like (Diptera: Culicidae) in Thailand. *Memorias do Instituto Oswaldo Cruz* 104: 558-566.

Thongwat D, Morgan K, O'loughlin MS, Walton C, Choochote W, Somboon P. 2008. Crossing experiment supporting the specific status of *Anopheles maculatus* chromosomal form K. *Journal of the American Mosquito Control Association* 24: 194-202.

460 **Figure legends**

461 **Figure 1.** Map of Thailand showing 2 provinces where samples of *Anopheles nitidus*
462 were collected and the number of isolines of the 5 karyotypic forms (A-E) detected in
463 each location.

464 **Figure 2.** Metaphase karyotypic forms of *Anopheles nitidus*. Phang Nga province (A-C)
465 (A) Form A (X_1, Y_1), (B) Form B (X_1, Y_2), (C) Form C (X_2, Y_3); Ubon Ratchathani
466 province (D-I) (D) Form D (X_1, Y_4), (E) Form D (X_3, Y_4), (F) Form E (X_1, Y_5), (G)
467 Form E (X_2, Y_5), (H) Form E (homozygous X_2, X_2), (I) Form E (heterozygous X_2, X_3).

468 **Figure 3.** Diagrams of representative metaphase karyotypes of Forms A, B, C, D and E
469 of *Anopheles nitidus*.

470 **Figure 4.** Synapsis in all arms of salivary gland polytene chromosome of F_1-hybrids 4^{th}
471 larvae of *Anopheles nitidus*. (A) Pg2A female x Pg5B male; (B) Pg2A female x Pg4C
472 male; (C) Pg2A female x Ur2D male; (D) Pg2A female x Ur5E male. Note: small
473 common gap of homosequential asynapsis (arrow) was found on chromosome 2L, 2R
474 and 3R; 2L and 2R; and 3L from the crosses between Pg2A female x Pg5B male; Pg2A
475 female x Pg4C male; and Pg2A female x Ur5E male, respectively.
476
477 **Figure 5.** Phylogenetic relationships among the 21 isolines of *Anopheles nitidus* by NJ
478 analysis based on ITS2 sequences compared with 8 species of the Hyrcanus Group and
479 3 Hyrcanus-group specimens (Paredes-Esquivel et al. 2011). Numbers on branches are
480 bootstrap values (%) of NJ analysis and Bayesian posterior probabilities (%). Only the
481 values higher than 50% both on bootstrap values and posterior probabilities are shown.
482 Branch lengths are proportional to genetic distance (scale bar).
483
484 **Figure 6.** Phylogenetic relationships among the 21 isolines of *Anopheles nitidus* by NJ
485 analysis based on COI barcoding sequences compared with 6 species of the Hyrcanus
486 Group. Numbers on branches are bootstrap values (%) of NJ analysis and Bayesian
487 posterior probabilities (%). Only the values higher than 50% both on bootstrap values
488 and posterior probabilities are shown. Branch lengths are proportional to genetic
489 distance (scale bar).
490
491 **Figure 7.** Phylogenetic relationships among the 21 isolines of *Anopheles nitidus* by NJ
492 analysis based on COII sequences compared with 6 species of the Hyrcanus Group.
493 Numbers on branches are bootstrap values (%) of NJ analysis and Bayesian posterior
494 probabilities (%). Only the values higher than 50% both on bootstrap values and
495 posterior probabilities are shown. Branch lengths are proportional to genetic distance
496 (scale bar).
497
498

Table 1 Locations in 2 provinces of Thailand, code of isolines, 5 karyotypic forms (A-E) of *Anopheles nitidus* and their GenBank accession numbers.

Location Geographical coordinate	Code of isoline[a]	Karyotypic form	Region	GenBank accession number			Reference
				ITS2	COI	COII	
An. nitidus							
Ubon Ratchathani	Ur2D[a]	D (X_3, Y_4)	ITS2, COI, COII	AB777782	AB777803	AB777824	This study
(15° 31′ N, 105 ° 35′ E)	Ur5E[a]	E (X_2, Y_5)	ITS2, COI, COII	AB777783	AB777804	AB777825	This study
	Ur8E	E (X_1, Y_5)	ITS2, COI, COII	AB777784	AB777805	AB777826	This study
	Ur11D	D (X_3, Y_4)	ITS2, COI, COII	AB777785	AB777806	AB777827	This study
	Ur12D	D (X_1, Y_4)	ITS2, COI, COII	AB777786	AB777807	AB777828	This study
	Ur15D	D (X_3, Y_4)	ITS2, COI, COII	AB777787	AB777808	AB777829	This study
	Ur16E	E (X_1, Y_5)	ITS2, COI, COII	AB777788	AB777809	AB777830	This study
	Ur19D	D (X_1, Y_4)	ITS2, COI, COII	AB777789	AB777810	AB777831	This study
	Ur22E	E (X_2, Y_5)	ITS2, COI, COII	AB777790	AB777811	AB777832	This study
	Ur23E	E (X_3, Y_5)	ITS2, COI, COII	AB777791	AB777812	AB777833	This study
	Ur24D	D (X_3, Y_4)	ITS2, COI, COII	AB777792	AB777813	AB777834	This study
	Ur25D	D (X_1, Y_4)	ITS2, COI, COII	AB777793	AB777814	AB777835	This study
	Ur27D	D (X_1, Y_4)	ITS2, COI, COII	AB777794	AB777815	AB777836	This study
	Ur28E	E (X_3, Y_5)	ITS2, COI, COII	AB777795	AB777816	AB777837	This study
	Ur30E	E (X_1, Y_5)	ITS2, COI, COII	AB777796	AB777817	AB777838	This study
	Ur31D	D (X_3, Y_4)	ITS2, COI, COII	AB777797	AB777818	AB777839	This study
	Ur33E	E (X_2, Y_5)	ITS2, COI, COII	AB777798	AB777819	AB777840	This study
	Ur34D	D (X_3, Y_4)	ITS2, COI, COII	AB777799	AB777820	AB777841	This study
Phang Nga	Pg2A[a]	A (X_1, Y_1)	ITS2, COI, COII	AB777800	AB777821	AB777842	This study
(08° 27′ N, 98° 31′ E)	Pg4C[a]	C (X_2, Y_3)	ITS2, COI, COII	AB777801	AB777822	AB777843	This study
	Pg5B[a]	B (X_1, Y_2)	ITS2, COI, COII	AB777802	AB777823	AB777844	This study
Hyrcanus Group	TR2	-	ITS2	HM488273	-	-	Paredes-Esquivel et al. 2011
	TR3	-	ITS2	HM488272	-	-	Paredes-Esquivel et al. 2011
	TR6	-	ITS2	HM488268	-	-	Paredes-Esquivel et al. 2011
An. belenrae	-	-	ITS2	EU789794	-	-	Park et al. 2008a
An. crawfordi	Pg4A	A (X_1, Y_1)	ITS2, COI, COII	AB779142	AB779171	AB779200	Saeung et al. unpublished data
An. kleini	-	-	ITS2	EU789793	-	-	Park et al. 2008a
An. lesteri	-	-	ITS2	EU789791	-	-	Park et al. 2008a
	ilG1	-	COI, COII	-	AB733028	AB733036	Taai et al. unpublished data
An. paraliae	Sk1B	B (X_1, Y_2)	ITS2, COI, COII	AB733487	AB733503	AB733519	Taai et al. unpublished data
An. peditaeniatus	RbB	B (X_3, Y_2)	ITS2, COI, COII	AB539061	AB539069	AB539077	Choochote 2011
An. pullus	-	-	ITS2	EU789792	-	-	Park et al. 2008a
			COI, COII	-	AY444348	AY444347	Park et al. 2003
An. sinensis	i2ACM	A (X, Y_1)	ITS2	AY130473	-	-	Min et al. 2002
	-	-	COI	-	AY444351	-	Park et al. 2003
	i1BKR	B (X, Y_2)	COII	-	-	AY130464	Min et al. 2002

a: used in crossing experiments

Table 2 Crossing experiments among 5 isolines of *Anopheles nitidus*.

Crosses (Female x Male)	Total eggs (number)[a]	Embryonation rate[b]	Hatched n (%)	Pupation n (%)	Emergence n (%)	Total emergence n (%)	
						Female	Male
Parental cross							
Pg2A x Pg2A	244 (125, 119)	88	210 (86.06)	195 (92.86)	195 (100.00)	103 (52.82)	92 (47.18)
Pg5B x Pg5B	277 (130, 147)	91	238 (85.92)	226 (94.96)	221 (97.79)	107 (48.42)	114 (51.58)
Pg4C x Pg4C	283 (118, 165)	84	218 (77.03)	218 (100.00)	211 (96.79)	106 (50.24)	105 (49.76)
Ur2D x Ur2D	292 (109, 183)	92	263 (90.07)	258 (98.10)	247 (95.74)	131 (53.04)	116 (46.96)
Ur5E x Ur5E	301 (148, 153)	88	256 (85.05)	251 (98.05)	221 (88.05)	111 (50.23)	110 (49.77)
Reciprocal cross							
Pg2A x Pg5B	289 (147, 142)	94	260 (89.97)	257 (98.85)	239 (93.00)	117 (48.95)	122 (51.05)
Pg5B x Pg2A	298 (158, 140)	90	220 (73.83)	202 (91.82)	198 (98.02)	97 (48.99)	101 (51.01)
Pg2A x Pg4C	299 (131, 168)	92	260 (86.96)	231 (88.85)	226 (97.84)	112 (49.56)	114 (50.44)
Pg4C x Pg2A	313 (162, 151)	80	225 (71.88)	218 (96.89)	209 (95.87)	112 (53.59)	97 (46.41)
Pg2A x Ur2D	211 (103, 108)	86	175 (82.94)	159 (90.86)	159 (100.00)	64 (40.25)	95 (59.75)
Ur2D x Pg2A	224 (111, 113)	91	202 (90.18)	196 (97.03)	171 (87.24)	81 (47.37)	90 (52.63)
Pg2A x Ur5E	243 (118, 125)	87	207 (85.19)	207 (100.00)	197 (95.17)	100 (50.76)	97 (49.24)
Ur5E x Pg2A	264 (139, 125)	91	235 (89.02)	235 (100.00)	204 (86.81)	108 (52.94)	96 (47.06)
F_1- hybrid cross							
(Pg2A x Pg5B)F_1 x (Pg2A x Pg5B)F_1	308 (118, 190)	85	246 (79.87)	234 (95.12)	229 (97.86)	111 (48.47)	118 (51.53)
(Pg5B x Pg2A)F_1x (Pg5B x Pg2A)F_1	312 (186, 126)	87	250 (80.13)	235 (94.00)	225 (95.74)	110 (48.89)	115 (51.11)
(Pg2A x Pg4C)F_1 x (Pg2A x Pg4C)F_1	308 (147, 161)	92	271 (87.99)	268 (98.89)	257 (95.90)	135 (52.53)	122 (47.47)
(Pg4C x Pg2A)F_1 x (Pg4C x Pg2A)F_1	329 (194, 135)	80	250 (75.99)	230 (92.00)	225 (97.83)	115 (51.11)	110 (48.89)
(Pg2A x Ur2D)F_1 x (Pg2A x Ur2D)F_1	347 (157, 190)	90	295 (85.01)	289 (97.97)	265 (91.70)	141 (53.21)	124 (46.79)
(Ur2D x Pg2A)F_1 x (Ur2D x Pg2A)F_1	287 (125, 162)	90	250 (87.11)	222 (88.80)	220 (99.10)	112 (50.91)	108 (49.09)
(Pg2A x Ur5E)F_1 x (Pg2A x Ur5E)F_1	350 (167, 183)	88	280 (80.00)	272 (97.14)	266 (97.79)	126 (47.37)	140 (52.63)
(Ur5E x Pg2A)F_1 x (Ur5E x Pg2A)F_1	339 (194, 145)	84	268 (79.06)	263 (98.13)	242 (92.02)	124 (51.24)	118 (48.76)

a: Two selective egg-batches of inseminated females from each cross; b: Dissection from 100 eggs; n = number

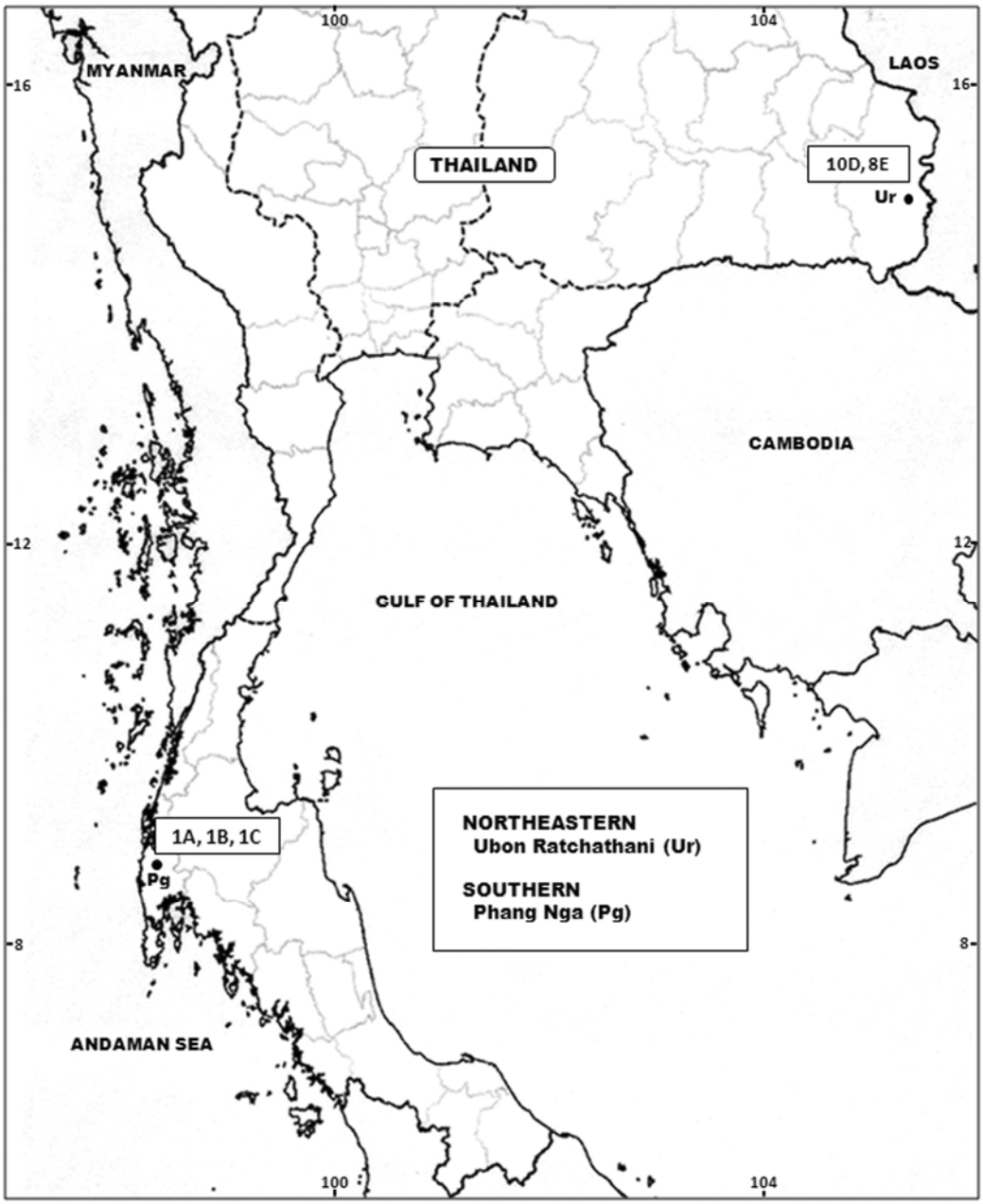

Figure 1. Map of Thailand showing 2 provinces where samples of *Anopheles nitidus* were collected and the number of isolines of the 5 karyotypic forms (A-E) detected in each location.

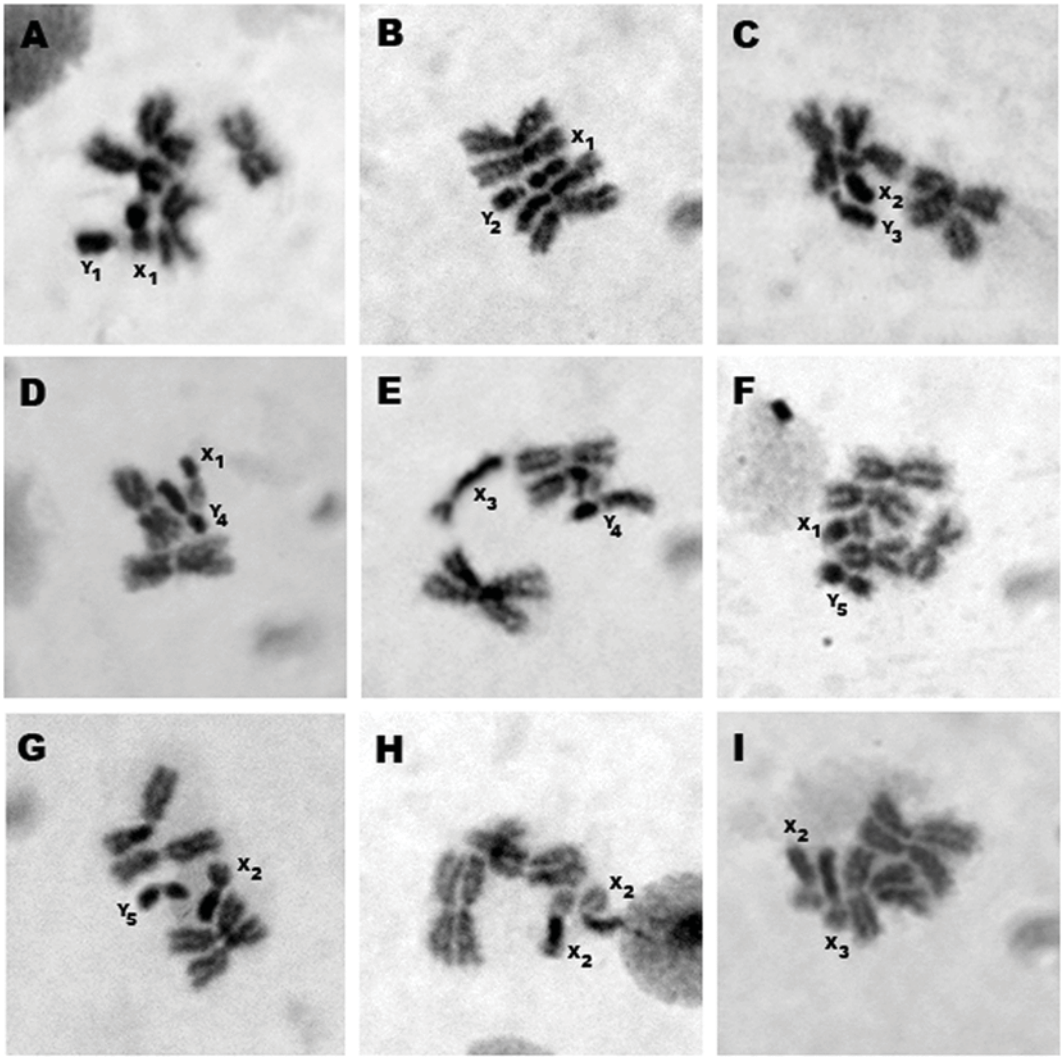

Figure 2. Metaphase karyotypic forms of *Anopheles nitidus*. Phang Nga province (A-C) (A) Form A (X_1, Y_1), (B) Form B (X_1, Y_2), (C) Form C (X_2, Y_3); Ubon Ratchathani province (D-I) (D) Form D (X_1, Y_4), (E) Form D (X_3, Y_4), (F) Form E (X_1, Y_5), (G) Form E (X_2, Y_5), (H) Form E (homozygous X_2, X_2), (I) Form E (heterozygous X_2, X_3).

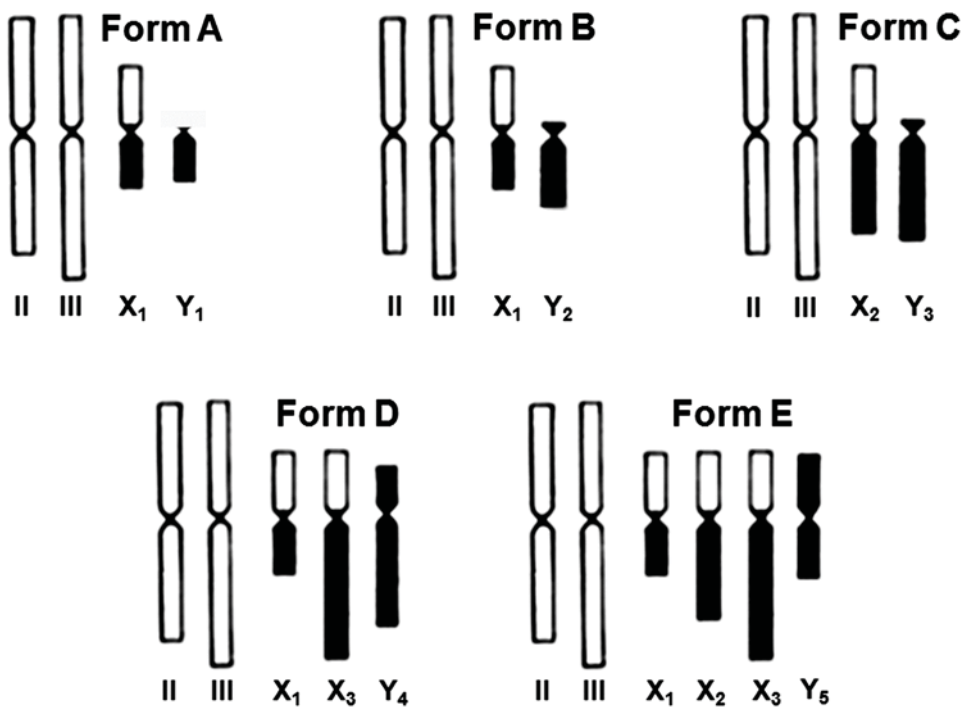

Figure 3. Diagrams of representative metaphase karyotypes of Forms A, B, C, D and E of *Anopheles nitidus*.

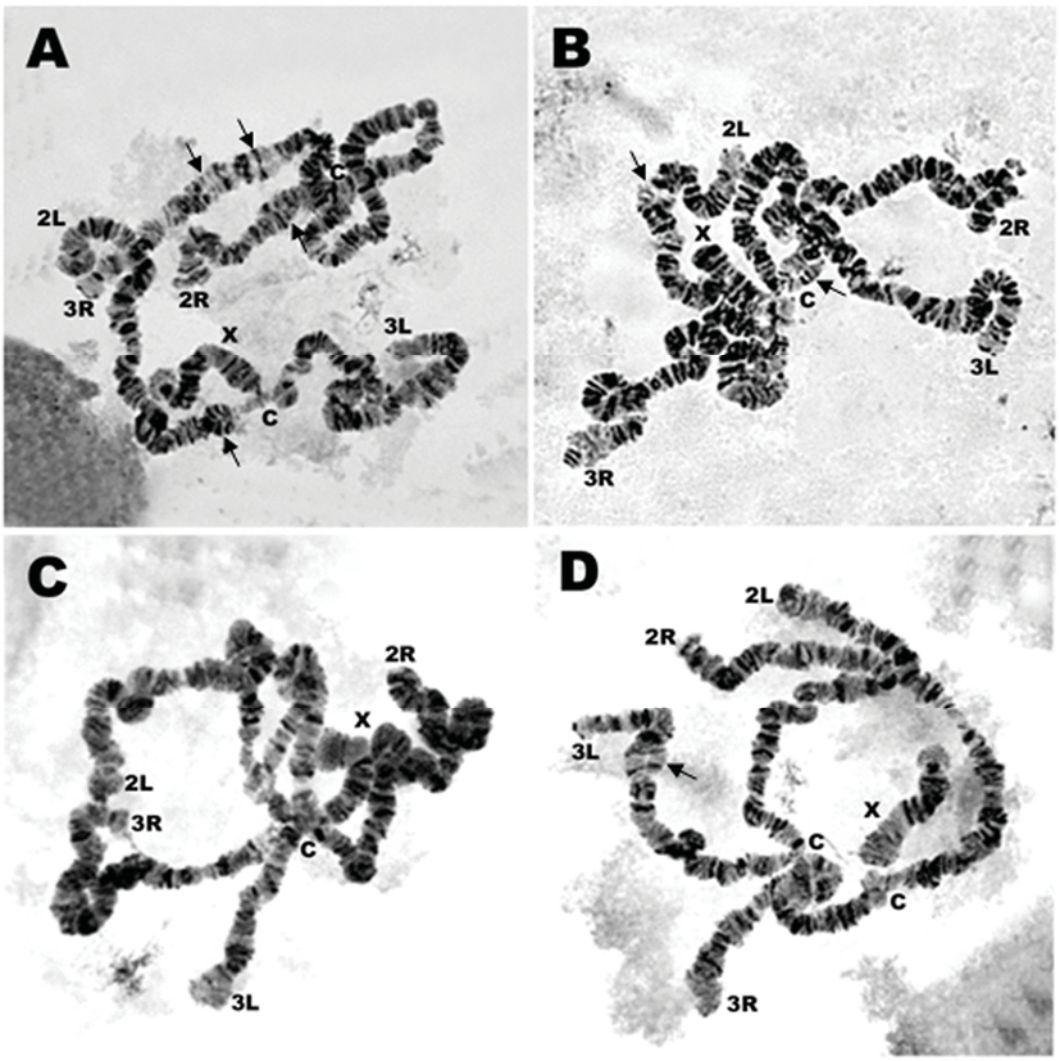

Figure 4. Synapsis in all arms of salivary gland polytene chromosome of F_1-hybrids 4th larvae of *Anopheles nitidus*. (A) Pg2A female x Pg5B male; (B) Pg2A female x Pg4C male; (C) Pg2A female x Ur2D male; (D) Pg2A female x Ur5E male. Note: small common gap of homosequential asynapsis (arrow) was found on chromosome 2L, 2R and 3R; 2L and 2R; and 3L from the crosses between Pg2A female x Pg5B male; Pg2A female x Pg4C male; and Pg2A female x Ur5E male, respectively.

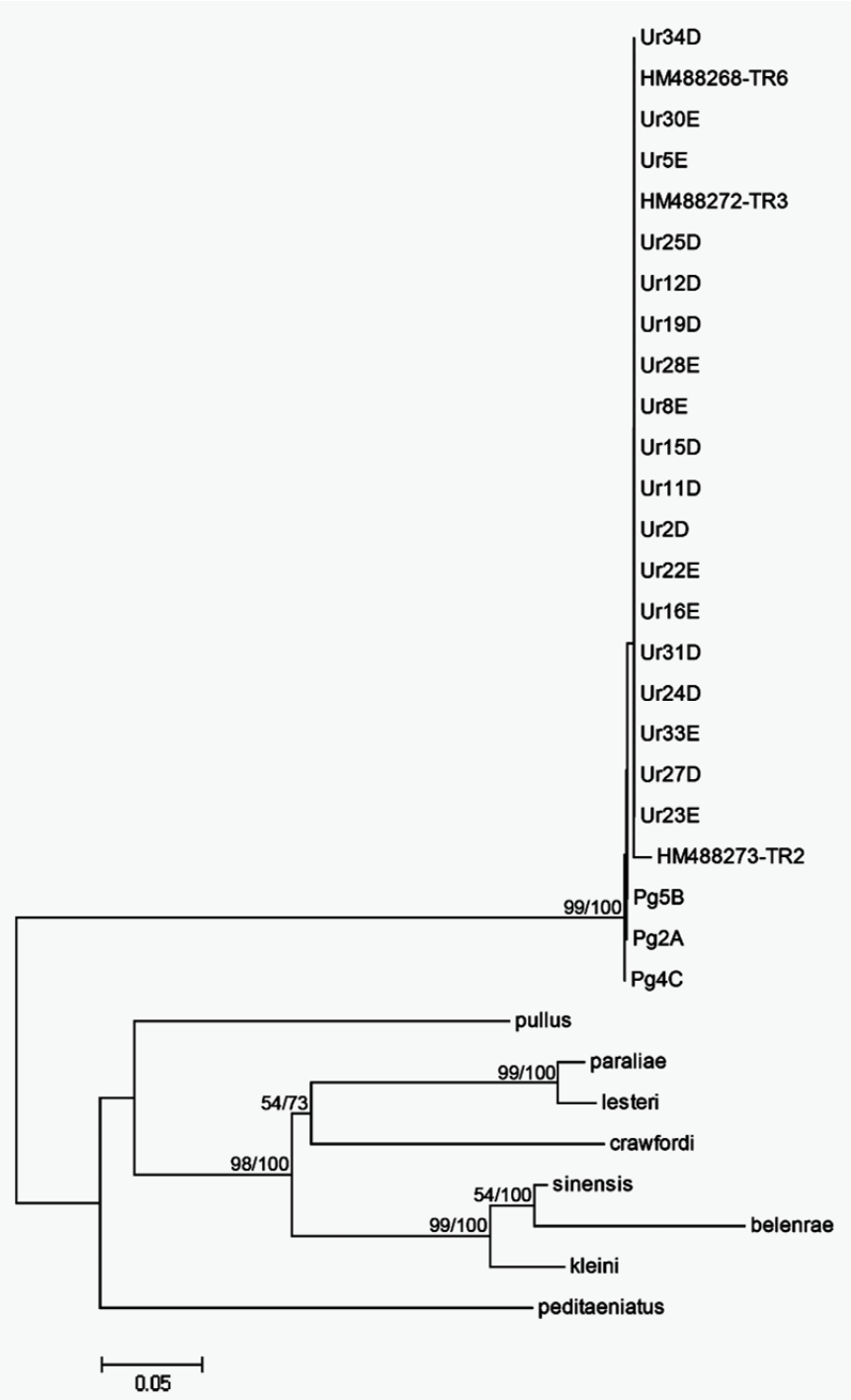

Figure 5. Phylogenetic relationships among the 21 isolines of *Anopheles nitidus* by NJ analysis based on ITS2 sequences compared with 8 species of the Hyrcanus Group and 3 Hyrcanus-group specimens (Paredes-Esquivel et al. 2011). Numbers on branches are bootstrap values (%) of NJ analysis and Bayesian posterior probabilities (%). Only the values higher than 50% both on bootstrap values and posterior probabilities are shown. Branch lengths are proportional to genetic distance (scale bar).

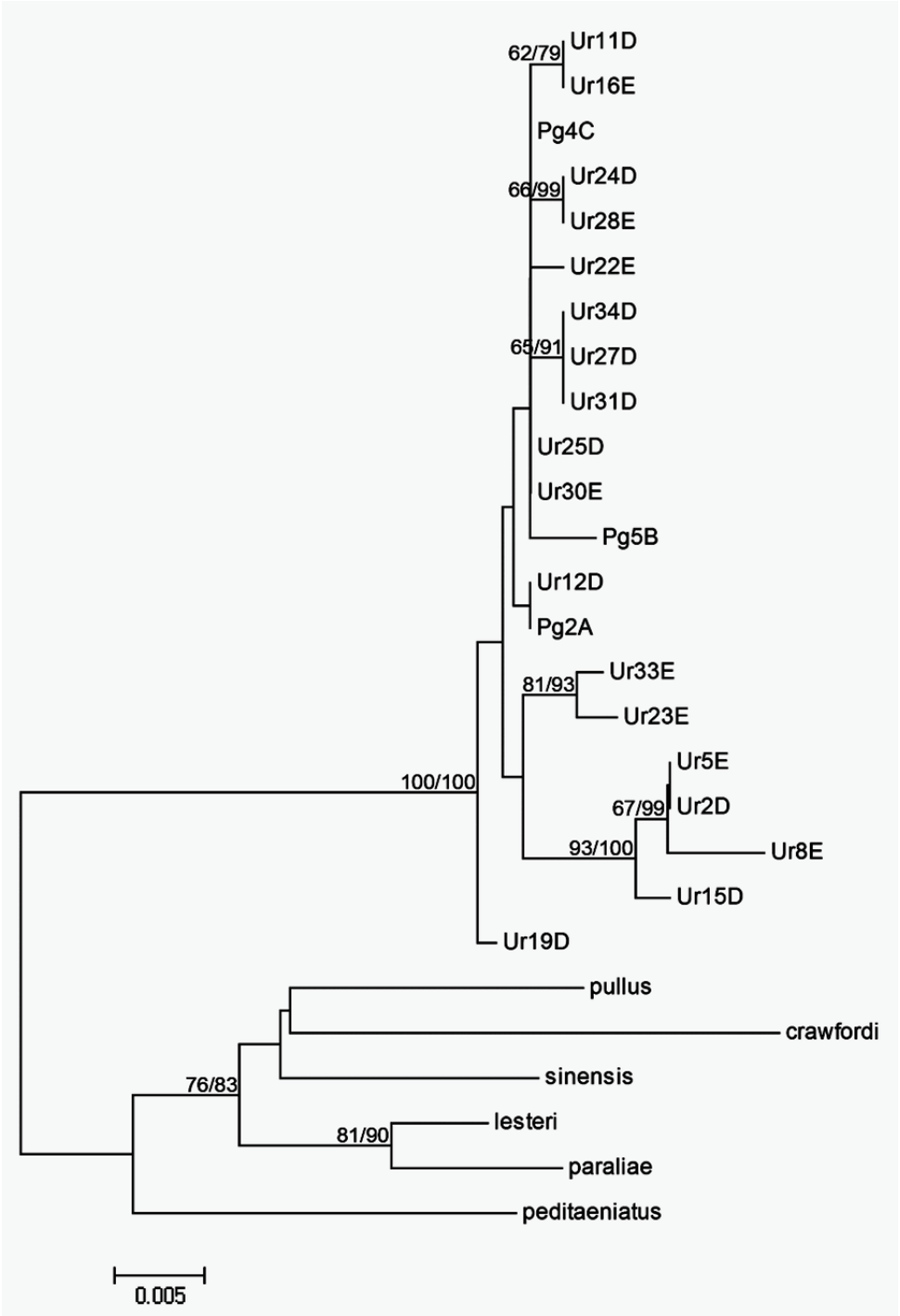

Figure 6. Phylogenetic relationships among the 21 isolines of *Anopheles nitidus* by NJ analysis based on COI barcoding sequences compared with 6 species of the Hyrcanus Group. Numbers on branches are bootstrap values (%) of NJ analysis and Bayesian posterior probabilities (%). Only the values higher than 50% both on bootstrap values and posterior probabilities are shown. Branch lengths are proportional to genetic distance (scale bar).

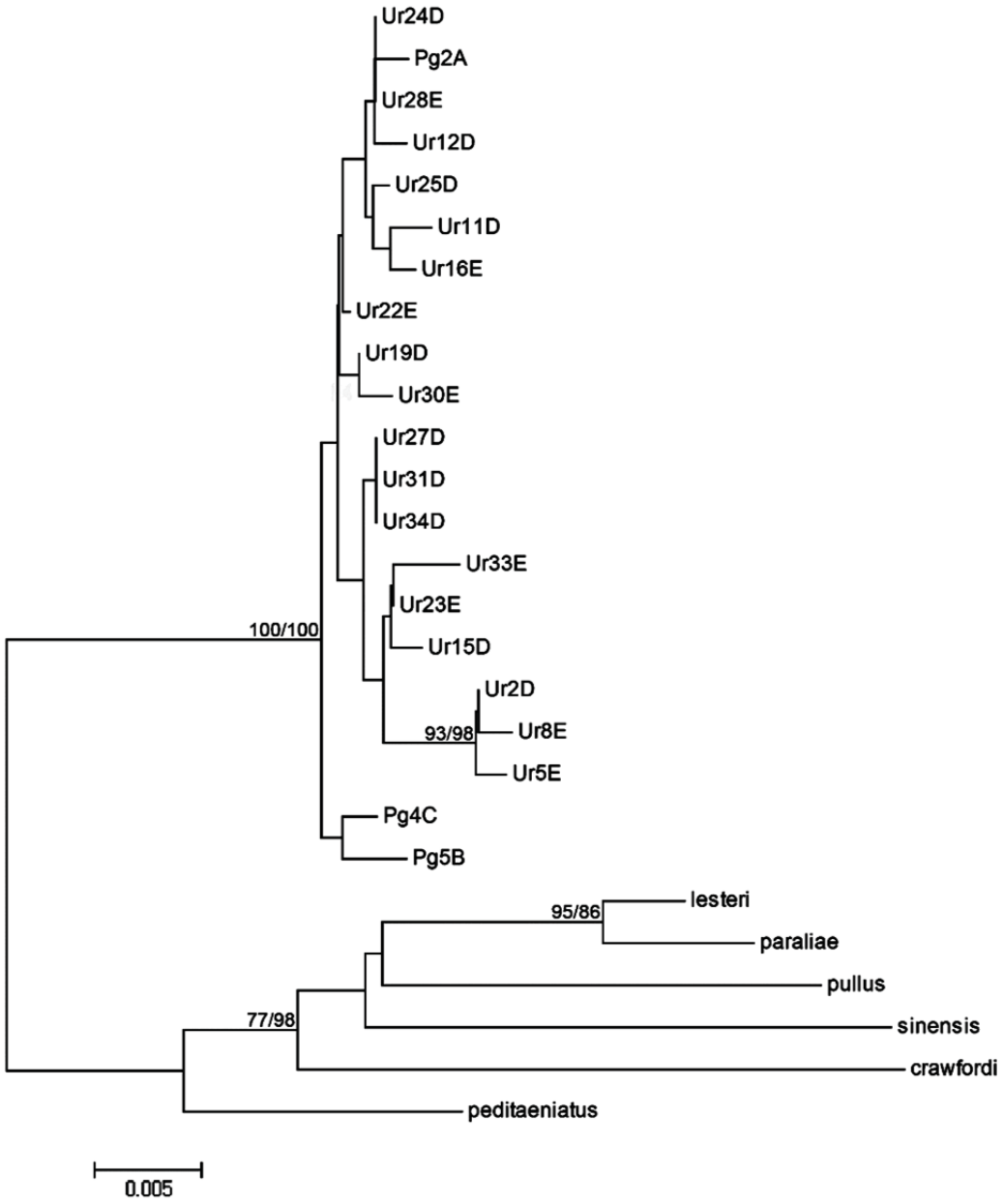

Figure 7. Phylogenetic relationships among the 21 isolines of *Anopheles nitidus* by NJ analysis based on COII sequences compared with 6 species of the Hyrcanus Group. Numbers on branches are bootstrap values (%) of NJ analysis and Bayesian posterior probabilities (%). Only the values higher than 50% both on bootstrap values and posterior probabilities are shown. Branch lengths are proportional to genetic distance (scale bar).

Peritrophic matrix formation and Brugia malayi *microfilaria invasion of the midgut of a susceptible vector,* Ochlerotatus togoi *(Diptera: Culicidae)*

Narissara Jariyapan, Atiporn Saeung, Nuchpicha Intakhan, Wetpisit Chanmol, Sriwatapron Sor-suwan, Benjarat Phattanawiboon, et al.

Parasitology Research
Founded as Zeitschrift für Parasitenkunde

ISSN 0932-0113
Volume 112
Number 7

Parasitol Res (2013) 112:2431-2440
DOI 10.1007/s00436-013-3404-5

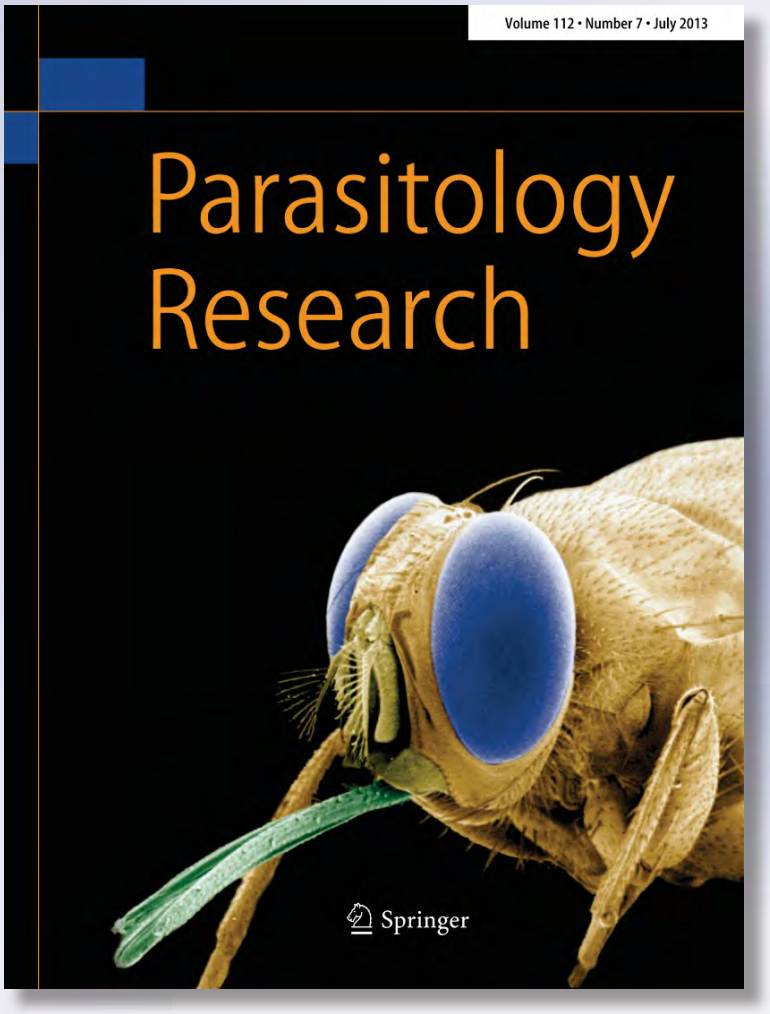

Springer

Parasitol Res (2013) 112:2431–2440
DOI 10.1007/s00436-013-3404-5

ORIGINAL PAPER

Peritrophic matrix formation and *Brugia malayi* microfilaria invasion of the midgut of a susceptible vector, *Ochlerotatus togoi* (Diptera: Culicidae)

Narissara Jariyapan · Atiporn Saeung · Nuchpicha Intakhan · Wetpisit Chanmol · Sriwatapron Sor-suwan · Benjarat Phattanawiboon · Kritsana Taai · Wej Choochote

Received: 12 January 2013 / Accepted: 15 March 2013 / Published online: 26 March 2013

Abstract The mosquito midgut is the first site that vector-borne pathogens contact during their multiplication, differentiation, or migration from blood meal to other tissues before transmission. After blood feeding, the mosquitoes synthesize a chitinous structure called peritrophic matrix (PM) that envelops the blood meal and separates the food bolus from the midgut epithelium. In this study, a systematic investigation of the PM formation and the interaction of *Brugia malayi* within the midgut of a susceptible vector, *Ochlerotatus togoi*, were performed using scanning electron microscopy (SEM). SEM analysis of the midguts dissected at different time points post feeding on a *B. malayi*-infected blood meal (PIBM) revealed that the PM was formed from 45 min PIBM and gradually thickened and matured during 8–18 h PIBM. The PM degraded from 24 to72 h PIBM, when digestion was completed. The invasion process of the microfilariae was observed between 3 and 4 h PIBM. In the beginning of the process, only sheathed microfilariae interacted with the internal face of the PM by its anterior part, and then the midgut epithelium before entering the hemocoel, after that they exsheathed. Microfilarial sheaths lying within the hemocoel were observed suggesting that they may serve as a decoy to induce the immune systems of the mosquitoes to respond to the antigens on the sheaths, thereby protecting the exsheathed microfilariae. These initial findings would lead to further study on the proteins, chemicals, and factors in the midgut that are involved in the susceptibility of *O. togoi* as a vector of filariasis.

N. Jariyapan (✉) · A. Saeung · N. Intakhan · W. Chanmol · S. Sor-suwan · B. Phattanawiboon · K. Taai · W. Choochote
Department of Parasitology, Faculty of Medicine, Chiang Mai University, Chiang Mai 50200, Thailand
e-mail: narsuwan@mail.med.cmu.ac.th

Introduction

The midgut of mosquitoes is the first site that vector-borne pathogens such as arboviruses, malaria parasites, and filarial worms contact during their multiplication, differentiation, or migration from blood meal to other tissues before transmission to a new vertebrate host. It has been proposed that the creation and release of genetically modified mosquitoes, which are refractory to parasite transmission, may be a promising new method for controlling the transmission of mosquito-borne diseases (Crampton et al. 1994; Gwadz 1994). The important role of the midgut in disease transmission implies that more research should focus on the midgut ultrastructural morphology for interpreting early events in the mosquito–pathogen interaction, the midgut physiology, and the way that it interacts with pathogens (Meis and Ponnudurai 1987; Meis et al. 1989; Syafruddin et al. 1991; Billingsley 1994; Shahabuddin et al. 1998).

Lymphatic filariasis is one of the tropical diseases targeted for elimination by the year 2020 by the World Health Organization, which has spurred vaccine and drug development, as well as new methods of vector control (http://www.who.int/neglected_diseases/NTD_RoadMap_2012). *Brugia malayi*, a filarial nematode, is a causative agent of lymphatic filariasis in humans. *B. malayi* microfilariae are transmitted by several mosquitoes in the genus *Mansonia*,

Anopheles, *Culex*, and *Aedes* (Schacher 1962; Guptavanij et al. 1978; Trpis 1981; Chang et al. 1991; Bangs et al. 1995; Kumar et al. 1998; Lek-Uthai and Tomoen 2005; Wada 2011). Filarial parasites start their life cycle in the vector when female mosquitoes ingest microfilariae during blood feeding on an infected host. The ingested microfilariae are stored within the blood meal in the mosquito midgut in order to cross a peritrophic matrix (PM) and the midgut epithelium towards the hemocoel.

In nematoceran Diptera, including mosquitoes, females produce a type 1 PM which is a chitinous structure that is composed principally of chitin, a linear N-acetyl-D glucosamine polymer (Tellam et al. 1999) and glycoproteins (Tellam et al. 1999; Terra 2001). The type 1 PM surrounds the blood meal and is induced by blood ingestion (Jacobs-Lorena and Oo 1996). PM precursors are stored in apical granules in the epithelial cells of the mosquito midgut. PM is formed by delamination from the general surface of the midgut epithelium (Lehane 1997). The major roles of the PM are associated with the prevention of midgut microvilli from the midgut contents and against pathogens and abrasion by food particles and with the compartmentalization of digestive events (Peters 1992; Lehane 1997). In mosquitoes and some hematophagous insects, the PM performs a central role in heme detoxification (Pascoa et al. 2002). O'Connor and Beatty (1936) and Iyengar (1936) have previously suggested that the PM is an efficient barrier for microfilaria migration across the midgut, by studying the interaction of *Wuchereria bancrofti* and *Brugia pahangi* microfilariae with *Mansonia annulifera* and *Culex fatigans*, respectively. However, the efficiency of the PM as a barrier depends on the kinetics of its formation and the time microfilariae takes to invade the midgut epithelium, for example, only when the PM is completely formed.

Ochlerotatus togoi (formerly known as *Aedes togoi*) is a vector of filariasis in the coastal area of Asia, i.e., China, Japan, and Taiwan (Ramachandran et al. 1963; Sasa 1976; Cheun et al. 2011). In Thailand, *O. togoi* (Chanthaburi strain) is highly susceptible to the rural strain of nocturnally subperiodic (NSP) *W. bancrofti* (Tak and Kanchanaburi strains), NSP *B. malayi* (Narathiwat strain), *B. pahangi* (Malaysia strain), *Dirofilaria immitis* (Chiang Mai strain) (Choochote et al. 1983, 1987) and urban strain or nocturnally periodic *W. bancrofti* (Myanmar strain; unpublished data). Although, invasions of the midguts of some mosquitoes by helminthes have been reported (Christensen and Sutherland 1984; Perrone and Spielman 1986; Shih and Chen 1987; Chen and Shih 1988; Santos et al. 2006), a few data of the interaction of *B. malayi* microfilariae within the midgut of a susceptible vector, *O. togoi*, is available. Therefore, in this study, details of the PM formation and the interaction of *B. malayi* microfilariae within the vector midgut were systematically investigated using scanning electron microscopy (SEM). Our finding unveiled features of the formation of the PM and the invasion of *B. malayi* microfilariae in the *O. togoi* mosquito midgut.

Materials and methods

Mosquito

O. togoi mosquitoes (Koh Nam Sao, Chantaburi Province, Southeast Thailand) were used in this study. The mosquito strain has been maintained in the insectary of the Department of Parasitology, Faculty of Medicine, Chiang Mai University, since 1983. It has been proven to be highly susceptible to NSP *B. malayi* (Choochote et al. 1987). The method for rearing of mosquitoes was followed the standard techniques described by Choochote et al. (1987).

Source of NSP *B. malayi* microfilariae

NSP *B. malayi* parasite originated from a 20-year-old woman resident of the Bang Paw district, Narathiwat Province, South Thailand. Domestic cats were then infected experimentally with the parasite, which was maintained at the Department of Medical Entomology, Faculty of Tropical Medicine, Mahidol University, Bangkok, Thailand, from 1982 to 1986, when it was transferred to Mongolian jirds (*Meriones unguiculatus*) and has since been maintained at the animal house of the Faculty of Medicine, Chiang Mai University, Chiang Mai, Thailand (Choochote et al. 1986).

Preparation of blood-containing *B. malayi* microfilaria

The jirds were deeply anesthetized with ethylene ether and intraperitoneally inoculated with infective larvae of NSP *B. malayi*. After at least 3 months (Choochote et al. 1991), the microfilariae were collected by injecting 3 ml of Hank's Balanced Salt Solution (pH 7.2–7.4) into the peritoneal cavity before withdrawal by peritoneal washing. The 0.5 ml of peritoneal-washed-rich microfilariae was mixed with 10 ml of human-heparinized blood (ten units of heparin/ml of blood), which had been taken from donors. Then, the adjusted microfilarial density ranged more or less from 200 to 300 microfilariae (mf/20 μl) by using human-heparinized blood that was used for artificial feeding of the mosquito species. The reason for adjusting microfilarial density in blood to range from 200 to 300 mf/20 μl was based on several of our proven experiments that yielded satisfactorily susceptible *O. togoi* to NSP *B. malayi* (susceptibility rates: 70–95 %). This was in agreement with experiments reporting the susceptibility of *Anopheles sinensis* to periodic *B. malayi*, i.e., using microfilarial density of 5, 10, 20, and 50 mf/20 μl, with a susceptibility rate of 30, 65, 93, and 100 %, respectively (Luo and Qu 1990).

Infection of mosquitoes with *B. malayi*

Three-day-old adult females of autogenous *O. togoi* (fasted for 12 h) were allowed to be artificially fed simultaneously on blood-containing *B. malayi* microfilariae using techniques and apparatus, as described by Chomcharn et al. (1980). Engorged mosquitoes were separated and then dissected at different time points after the blood meal: 15, 30, 45 min, and 1, 2, 3, 4, 5, 6, 8, 12, 18, 24, 36, 48, 72, and 96 h. The samples (ten samples/time point) were processed for SEM.

Preparation of samples for scanning electron microscopy

Dissected midguts were fixed overnight with a solution of 2.5 % glutaraldehyde mixed in phosphate buffer solution at a pH of 7.4 at 4 °C to accomplish primary fixation. They were then rinsed twice with phosphate buffer solution at 10-min intervals and later postfixed in a solution of 1 % osmium tetroxide for 2 h. Postfixation was followed by rinsing twice with phosphate buffer solution and dehydrating with alcohol. To replace the water in the specimens with alcohol, they were subjected to the following increasing concentrations of alcohol: 30, 50, 70, 80, 90, and 95 %. The specimens were then placed in absolute alcohol for two 12-h periods. After that, organ specimens were placed in acetone for 2 h. Finally, the specimens were subjected to critical point drying, were attached with double-stick tape to aluminum stubs, and were coated with gold in a sputter-coating apparatus before being viewed with a scanning electron microscope (JEOL JSM-5910LV, JEOL Ltd., Japan). To observe the interface between the midgut surface and the blood meal, some fixed samples were fractured before being coated with gold, while others were gently opened and the contents were washed out with phosphate buffer saline before the fixation.

Ethical clearance

The protocols were approved by the Animal Ethics Committee of Faculty of Medicine, Chiang Mai University, Chiang Mai, Thailand.

Results

Peritrophic matrix formation in *O. togoi* midgut

An analysis of *O. togoi* midguts dissected at different time points post feeding on the *B. malayi*-infected blood meal (PIBM) allowed the investigation of both the formation of the PM and the invasion of the microfilariae from the midgut into hemocoel. Figure 1 shows details of peritrophic matrix formation. The midgut epithelium from non-blood fed *O. togoi* showed numerous long microvilli (Fig. 1a). After the blood feeding, engorgement caused a great distension of the midgut. The midguts dissected at 15 min after the blood meal showed a stretched epithelium with blood cells close to it and no microvillus was observed (Fig. 1b). A very thin lamina-forming PM was visible from 45 min after the blood meal (Fig. 1c). By 1 to 3 h PIBM, an early formed PM was very attached to the blood meal and the epithelium. It was visualized separating the blood meal from the midgut epithelium in some part of the midgut (Fig. 1d, e). By 5 to 6 h after the blood ingestion, the entire abdominal midgut was uniformly covered by the PM (Fig. 1f). The PM became thicker and well formed in the 8–18 h midguts, easily separating themselves from the epithelium (Fig. 1g, h, i, j). The mature PM consisted of one thin fibrillar layer, close to the epithelium, and another thicker granular layer in contact with the blood meal (Fig. 1i, j). At 24 h after the blood feeding, the fibrillar region of the PM facing the midgut epithelium presented wavy aspects (Fig. 1k). During 36 h PIBM, the blood meal became compact and distant from the midgut epithelium. The PM looked thinner and the midgut epithelium with microvilli was observed (Fig. 2l). At 48 h PIBM, the blood meal was almost completely digested and absorbed. The PM showed a progressive shrinking in the 48-h midgut samples (Fig. 2m, n). No PM was observed in all of the 72-h midgut samples and new epithelial cells were noted (Fig. 2o). By 96 h PIBM, the midgut epithelium was mature with numerous microvilli (Fig. 2p) as seen in Figure 1a.

B. malayi microfilariae invasion

In order to observe the microfilariae interacting with the PM, fractured midguts dissected at different time points after the infected blood feeding were performed. The microfilariae were found in approximately 75 % (seven to eight from ten samples/time point) of the 30 min to 24 h midgut samples. Microfilariae with sheaths were observed inside the midgut lumens (Fig. 2a, b, c) or close to or in contact with the PM, from 30 min to 2 h PIBM. The invasion of the *B. malayi* microfilariae were observed between 3 and 4 h after being ingested (Fig. 2d, e, f, g). In the beginning of the invasion process, sheathed microfilariae interacted the internal face of the PM by its anterior part, and then penetrated across the PM and the midgut epithelium into hemocoel. Some micrographs showed sheathed microfilariae with their bodies buried inside the PM (Fig. 2d) and the epithelium (Fig. 2e). Sheathed microfilariae and microfilarial sheaths were observed on the external surface of the midgut and in the hemocoel (Fig. 2f, g). All *B. malayi* microfilariae observed penetrating the midgut epithelium were sheathed microfilariae. Figure 2h,i, j, k demonstrates the exsheathed microfilariae in the lumens of the 18 and 24 h-midguts. One microfilarial carcass inside the midgut lumen at 8 h PIBM was observed (Fig. 3). In all 36 to 96 h-midgut samples, no microfilaria was observed.

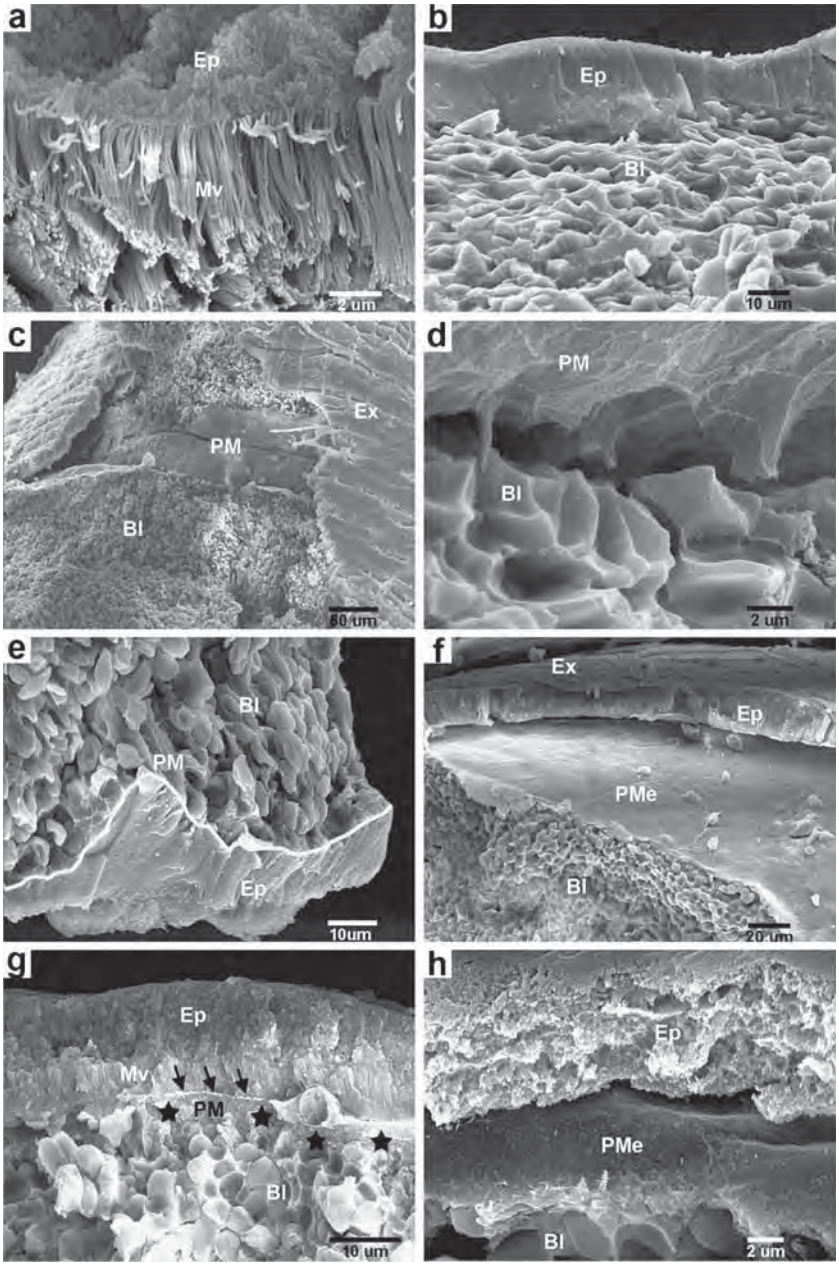

Fig. 1 Fractured midguts and peritrophic matrix (PM) of *O. togoi* female post-*B. malayi*-infected blood meal (PIBM). **a** A non-blood fed midgut showing epithelium (*Ep*) and microvilli (*Mv*) **b** At 15 min PIBM, SEM micrograph indicating the blood meal (*Bl*) and epithelium. No microvillus was observed. **c** At 45 min PIBM, a blood fed midgut showing a very thin lamina-forming PM covered some part of the blood meal. **d** One-hour blood fed midgut showing an early forming PM above the blood meal. **e** *White line* indicates the formed PM between the midgut epithelium and blood meal at 3 h PIBM. **f** At 5 h PIBM, SEM micrograph showing an external face of the PM (*PMe*). The PM is completely formed and can be separated from the epithelium. **g** Eight-hour blood fed midgut showing a thin fibrillar layer of the PM (*arrows*) and granular layer (*stars*). **h** Twelve-hour blood fed midgut showing an external face of the PM. **i** At 18 h PIBM, SEM micrograph showing a thin fibrillar layer (*arrows*). **j** Eighteen-hour blood fed midgut showing an external face of the PM bearing the impression of the epithelial cells. **k** At 24 h PIBM, SEM micrograph showing an external face of the PM with a wavy aspect between the blood meal and epithelium. **l** At 36 h PIBM, SEM micrograph showing the PM and midgut epithelium with microvilli. **m**, **n** At 48 h PIBM, an internal face of the PM (*PMi*) presents marks resulting from shrinking of the PM (*Arrows*). The blood meal was almost completely digested. **o** No PM was observed in the 72 h PIBM midguts. Marks of the format of new epithelial cells were noted. **p** At 96 h PIBM, most epithelial cells were mature with normal microvilli. External surface of the midgut (*Ex*)

Discussion

The rate of formation and the maturity of the PM seem to be related to the digestion process of the blood meal and differ according to temperature, blood source, meal size, species, and several other factors (Lehane 1997). For example, a distinct PM is visible in *Ae. aegypti* at 6 h post-blood meal (PBM), in *Anopheles gambiae* at 13 h PBM, in *Anopheles*

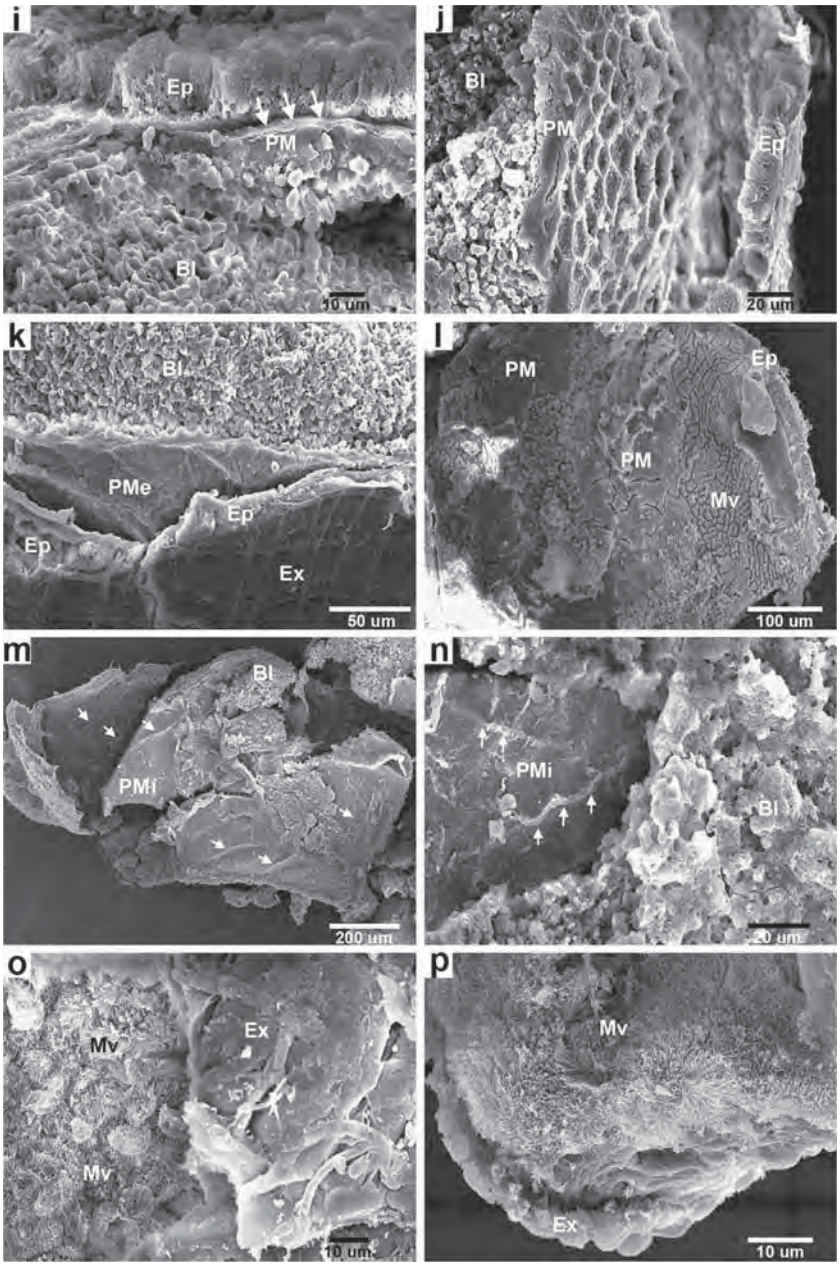

Fig. 1 (continued)

stephensi at 32 h PBM (Freyvogel and Staubli 1965), and in *Culex tarsalis* at 10 h PBM (Houk et al. 1979). Perrone and Spielman (1988) have demonstrated that the PM of *Ae. aegypti* first becomes evident at about 4 to 8 h after blood is ingested, and the membrane attains a mature texture by 12 h. The formation of PM is observed at 18 h PBM in *Anopheles darlingi* (Okuda et al. 2005). Di Luca et al. (2007) have showed that formation of PM is clearly complete after 16 h in the posterior midgut from *An. stephensi* already fed with healthy donor bloods. In sandflies, *Phlebotomus papatasi* starts the production of PM 4 h after a blood meal (Blackburn et al. 1988) whereas *Phlebotomus perniciosus* and *Lutzomyia longipalpis* start the PM synthesis as soon as 1 h after a blood meal (Walters et al. 1993; Secundino et al. 2005). In *Phlebotomus duboscqi*, the PM matures in less than 12 h (Sadlova and Volf 2009). A peritrophic membrane of *Ixodes ricinus* females is found at no later than 18 h after their placement on rabbits (Zhu et al. 1991).

This study presented details of the PM formation in *O. togoi* mosquito for the first time. The mature PM of *O. togoi* mosquito consisted of two layers, a thin fibrillar layer and a thick granular layer. Based on the data of PM formation in several mosquito species (Hegedus et al. 2009), we attribute the thin fibrillar layer to chitin, while the condensed granular layer presumably represents proteins and glycoproteins. Wrinkled, thin, and wavy phenomenon of the PM by 24 h

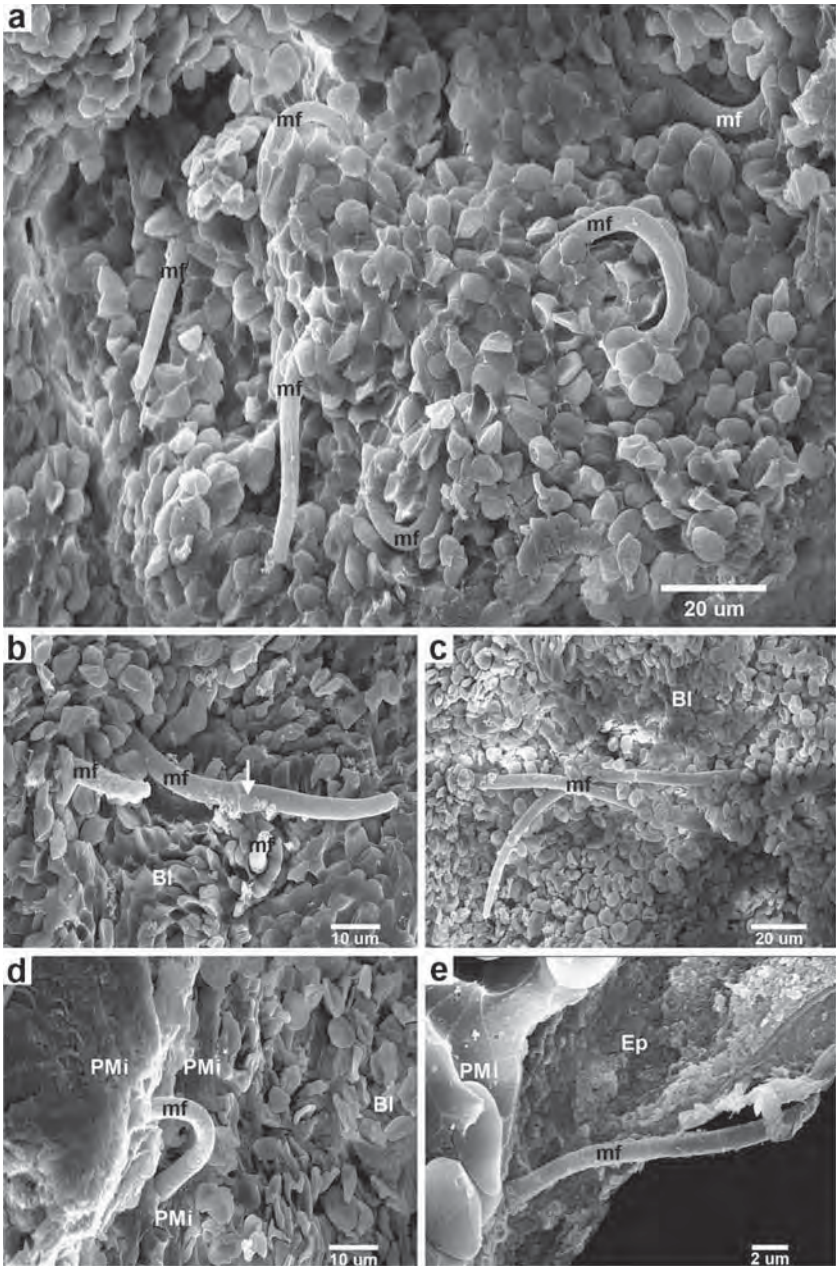

Fig. 2 SEM micrographs of fractured abdominal midguts showing the invasion process of microfilariae (*mf*) from the midgut lumen into hemocoel. **a** Sheathed microfilariae at 30 min PIBM, **b** Sheathed microfilariae at 1 h PIBM. One of the microfilariae showing its anterior portion in the process of losing its sheath (*arrow*). **c** Sheathed microfilariae at 2 h PIBM. **d** A sheathed microfilaria during invasion on the internal face of the PM (*PMi*). **e** At 3 h PIBM, SEM showing a sheathed microfilaria penetrating across the internal face of the PM and epithelium (*Ep*) into hemocoel in the final stage of invasion. **f** Sheathed microfilariae at 4 h PIBM lining on the external surface of the midgut (*Ex*). **g** Higher magnification of boxed region in (**f**) displaying the posterior portion of a microfilaria retaining contact with the sheath (*arrow*). The sheath projecting from the lesion on the external surface of the midgut produced by the penetrating microfilaria was observed (*arrowheads*). **h** An unsheathed microfilaria at 18 h PIBM. **i** Higher magnification of boxed region in (**h**) displaying an anterior portion of the microfilaria protruding from blood meal (*Bl*). *Arrow* indicates the exposed hook. **j** An unsheathed microfilaria at 24 h PIBM showing its posterior portion. **k** Anterior portion of an unsheathed microfilaria at 24 h PIBM

PIBM might be due to the degradation of the PM as pressure from the midgut distension was decreased. In addition, the absorption of digested blood meal might begin from this time. The PM disappeared in all 72 h-midgut samples suggesting that the digestion of the blood meal was complete. Also, new epithelial cells were mature by 96 h PIBM suggesting that the absorption of the products of the blood digestion was complete. The PM formation and degradation in *O. togoi* is in agreement with observations in molecular levels in several mosquitoes and sandflies. In *Ae.*

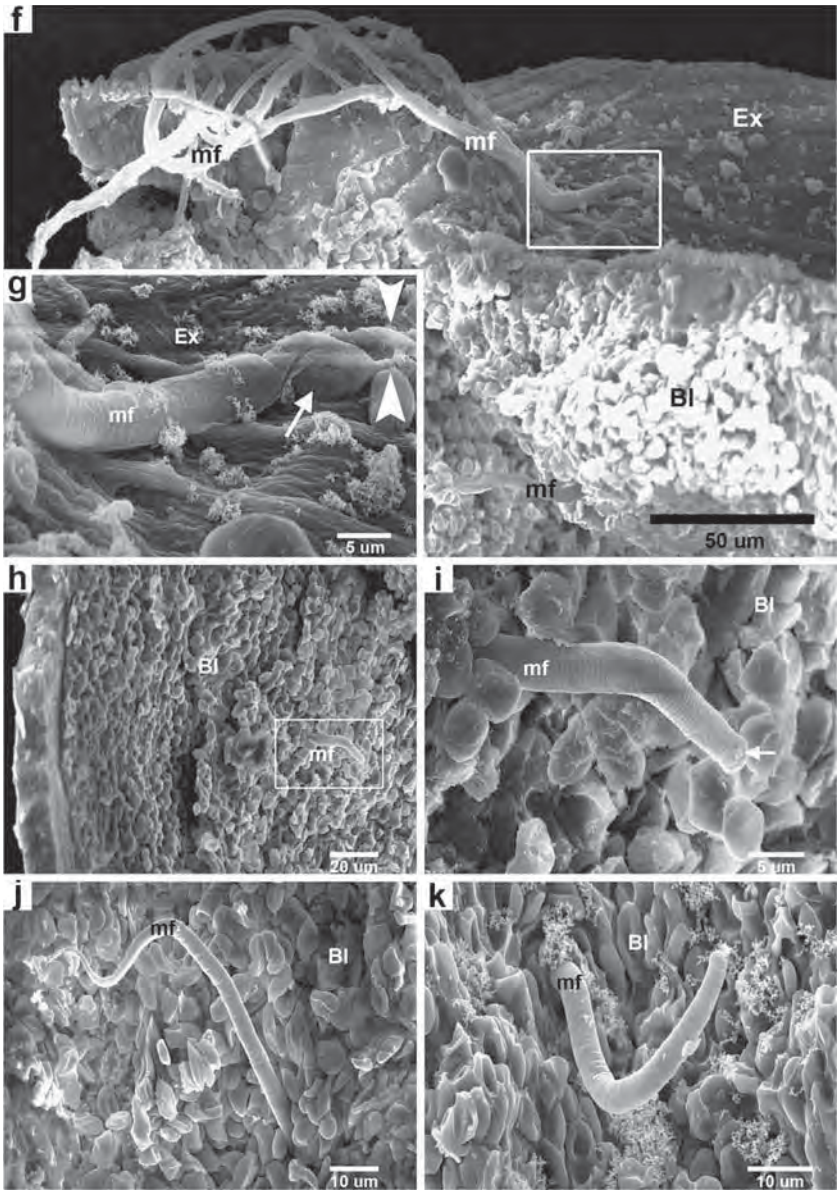

Fig. 2 (continued)

aegypti, Sanders et al. (2003) used cDNA microarrays to examine midgut gene expression on a global level in response to blood feeding and reported that transcripts of genes involved in PM formation responded immediately to blood feeding. The expression of glutamine synthetase, an enzyme that contributes to PM formation in *Ae. aegypti*, was highly induced 3–24 h post-blood meal (Smartt et al. 1998). Degradation of PM requires the activity of chitinases, which cleave the chitin microfibril components of the matrix. A chitinase expressed after a blood meal in *An. gambiae* has been proposed to partially degrade the PM (Shen and Jacobs-Lorena 1997). Villalon et al. (2003) demonstrated that feeding *Ae. aegypti* and *An. stephensi* mosquitoes with blood-containing chitinase led to accelerated blood digestion and PM degradation.

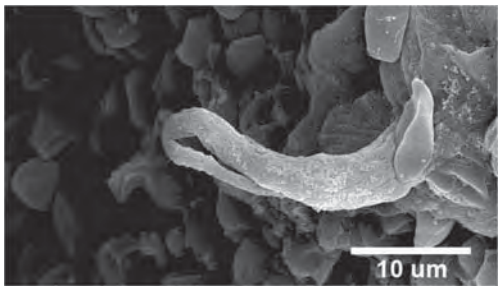

Fig. 3 SEM micrograph indicating the posterior portion of a microfilaria carcass inside the midgut lumen at 8 h PIBM

O'Connor and Beatty (1936) and Iyengar (1936) have suggested that the PM is an efficient barrier for microfilaria migration towards the midgut. They reported that *W. bancrofti*

microfilaria invades the midgut of *Culex quinquefasciatus*, at a similar time after a blood meal. In fact, the invasion of the midgut of other mosquito species by *W. bancrofti*, by other human microfilaria, such as *B. malayi* and *Brugia patei*, and *Litomosoides chagasfilhoi* are recognized to occur at 2 to 3 h after blood feeding (Laurence and Pester 1961; Bain and Brengues 1972; Petit 1978; Petit and Spitalier-Kaveh 1979; Santos et al. 2006). However, some species of microfilaria, such as *B. pahangi* (Esslinger 1962) and *Onchocerca volvulus* (Laurence 1966; Bain and Philippon 1969) can invade the vector midguts between 5 and 60 min after the blood meal. Christensen and Sutherland (1984) have suggested that *B. pahangi* microfilaria freely traverse the PM of *Ae. aegypti* within 150 min post-ingestion, with the majority (60 %) migrating out from 61–105 min. Exsheathment of microfilariae rarely occurred within the midgut and approximately 75 % retained their sheaths after midgut penetration (Christensen and Sutherland 1984).

In the present study, *B. malayi* microfilariae were able to cross the developing PM at 3 to 4 h after being ingested by the *O. togoi*. It was noted that sheaths were present on all *B. malayi* microfilariae observed penetrating the PM and the midgut epithelium into hemocoel. Our results were consistent with the results of Yamamoto et al. (1983), Christensen and Sutherland (1984), Agudelo-Silva and Spielman (1985), and Perrone and Spielman (1986) that microfilariae do not exsheath until they penetrate the midgut wall. Agudelo-Silva and Spielman (1985) studied the migration of *B. malayi* microfilariae in susceptible *Ae. aegypti* (black-eye strain) mosquitoes using SEM and concluded that the microfilariae penetrated the midgut wall of the mosquito vector while still sheathed, and that the sheath remained protruding from the gut into the hemocoel. Our present study demonstrated a clear figure of the invasion process of the *B. malayi* microfilariae in the *O. togoi* mosquito that only sheathed microfilariae penetrated the PM first and then the midgut epithelium before entering hemocoel, after that, they exsheathed. Microfilarial sheaths lying within the hemocoel may serve as a decoy to induce the immune systems of the mosquitoes to respond to the antigens on the sheaths, thereby protecting the exsheathed microfilariae.

However, some exsheathed microfilariae in the midgut lumen were observed from 1 to 24 h PIBM. From the results of our observations of *B. malayi* microfilariae, only one microfilaria carcass was observed in the 8-h midgut lumen. An explanation is that in this study, the PM of *O. togoi* midgut became thicker and well-formed during 8–18 h, therefore, the microfilariae might be detained in the PM during penetration. Santos et al. (2006) have suggested that when the entire abdominal midgut is uniformly covered by the PM, it appears to be an efficient barrier for the helminthes; and when the PM becomes thick and well-structured, microfilariae are no longer able to cross it. They stay in the midgut lumen and end up dying, probably through the activities of digestive enzymes.

In addition, the results of this study revealed that no microfilaria or carcass was observed in all 36 to 96 h-midgut samples. These may suggest that the invasion process of the sheathed microfilariae was completed during 24–36 h PIBM. For the exsheathed microfilariae in the midgut lumen, until now, the degree of exsheathment before emergence into the hemocoel remains unclear. Chen and Shih (1988) have found that *B. pahangi* microfilariae tend to carry their sheaths into the hemocoel of susceptible (Liverpool) and refractory (Bora-Bora) strains of *Ae. aegypti* within 2 h after ingestion and exsheathed within 24 h post-ingestion. Those remained microfilariae are most likely to cast off their sheaths in the midgut more than 2 h after ingestion. The percentage of microfilariae exsheathed in the midgut progressively increases to about 91 and 78 % at 24-h post-ingestion in the Bora-Bora and Liverpool strains, respectively. They have suggested that the exsheathment of *B. pahangi* microfilariae occurs both in the hemocoel and in the midgut of both strains of *Ae. aegypti* (Chen and Shih 1988). Santos et al. (2006) reported that *L. chagasfilhoi* microfilariae may cross the midgut epithelium of *C. quinquefasciatus* with or without their sheaths, depending on whether they crossed the PM or not, before reaching the midgut epithelium. Investigation on whether the exsheathed *B. malayi* microfilariae inside the *O. togoi* midgut lumen would be able to penetrate through the midgut or not are currently in progress in our laboratory. Furthermore, the mechanisms of the microfilarial penetration of the midgut epithelium are unclear if they are mechanical, enzymatic, or combined processes. As excretory–secretory products of microfilariae include several enzymes (Singh and Rathaur 2003; Wu et al. 2008), it might be possible that they secrete substances that act over the midgut epithelium to allow them to penetrate easily. Further analysis using TEM and/or immune electron microscopy to describe the *B. malayi* microfilarial penetration of the *O. togoi* midgut epithelium and the pathological processes in the epithelium caused by the penetration should be performed.

In conclusion, the PM formation and the interaction of *B. malayi* microfilariae within the *O. togoi* vector midgut were systematically investigated for the first time using SEM. Our findings unveiled features of the formation of the PM from 45 min PIBM with gradual thickening and maturing during 8–18 h PIBM. The PM degraded from 24 to72 h PIBM, when digestion completed. The invasion process of the microfilariae was observed between 3 and 4 h PIBM. Only sheathed microfilariae interacted with the internal face of the PM by its anterior part, and then the midgut epithelium before entering hemocoel, after which they exsheathed. Microfilarial sheaths lying within the hemocoel were observed suggesting that they may serve as a decoy to induce

the immune systems of the mosquitoes to respond to the antigens on the sheaths. Our data may contribute to understanding a role of the PM on insect biology and provide information that might be useful for future midgut-targeted strategies to control mosquito vector. Moreover, these initial findings can lead to further study on the proteins, chemicals, and factors in the midgut that are involved in the susceptibility of *O. togoi* as a vector of filariasis.

Acknowledgments This work was financially supported by the Thailand Research Fund (TRF Senior Research Scholar: RTA5480006 to WC, subproject to NJ) and the Faculty of Medicine, Chiang Mai University.

References

Agudelo-Silva F, Spielman A (1985) Penetration of mosquito midgut wall by sheathed microfilariae. J Invertebr Pathol 45:117–119

Bain O, Brengues J (1972) Transmission of wuchereriasis and of bovine setariasis: histological study of the passage of microfilariae through the stomach wall of *Anopheles gambiae* and *Aedes aegypti*. Ann Parasitol Hum Comp 47:399–412

Bain O, Philippon B (1969) Mechanism of passing microfilaria through the stomach wall of a vector: its importance in onchocerciasis. C R Acad Sci Hebd Seances Acad Sci D 269:1081–1083

Bangs MJ, Ash LR, Barr AR (1995) Susceptibility of various mosquitoes of California to subperiodic *Brugia malayi*. Acta Trop 59:323–332

Billingsley PF (1994) Approaches to vector control: new and trusted. 2. Molecular targets in the insect midgut. Trans R Soc Trop Med Hyg 88:136–140

Blackburn K, Wallbanks KR, Molyneux DH, Lavin DR, Winstanley SL (1988) The peritrophic membrane of the female sandfly *Phlebotomus papatasi*. Ann Trop Med Parasitol 82:613–619

Chen CC, Shih CM (1988) Exsheathment of microfilariae of *Brugia pahangi* in the susceptible and refractory strains of *Aedes aegypti*. Ann Trop Med Parasitol 82:201–206

Cheun HI, Cho SH, Lee HI, Shin EH, Lee JS, Kim TS, Lee WJ (2011) Seasonal prevalence of mosquitoes, including vectors of *Brugian filariasis*, in southern islands of the Republic of Korea. Korean J Parasitol 49:59–64

Chang MS, Chan KL, Ho BC (1991) Comparative transmission potential of three *Mansonia* mosquitoes (Diptera: Culicidae) for filariasis in Sarawak, Malaysia. Bull Entomol Res 81:437–444

Chomcharn Y, Surathin K, Bunnag D, Sucharit S, Harinasuta T (1980) Effect of a single dose of primaquine on a Thai strain of *Plasmodium falciparum*. Southeast Asian J Trop Med Public Health 11:408–412

Choochote W, Chaithong U, Somboon P, Pakdicharoen A, Tookyang B, Likitvong K, Siriprasert V, Sukontasan K, Thitasut P (1991) Small laboratory animal model for nocturnally subperiodic *Brugia malayi* (Narathiwat province, southern Thailand strain). J Trop Med Parasitol 14:51–58

Choochote W, Keha P, Sukhavat K, Khamboonruang C, Sukontason K (1987) *Aedes* (Finlaya) *togoi* Theobald 1907, Chanthaburi strain. A laboratory vector in studies of filariasis in Thailand. Southeast Asian J Trop Med Public Health 18:259–260

Choochote W, Sucharit S, Abeywickreme W (1983) A note on adaptation of *Anopheles annularis* Van Der Wulp, Kanchanaburi, Thailand to free mating in a 30×30×30 cm cage. Southeast Asian J Trop Med Public Health 14:559–560

Choochote W, Sukhavat K, Somboon P, Khamboonruang C, Maleewong W, Suwanpanit P (1986) The susceptibility of small laboratory animals to nocturnally superiodic *Brugia malayi* in Thailand. J Parasitol Trop Med Assoc Thailand 9:35–37

Christensen BM, Sutherland DR (1984) *Brugia pahangi*: exsheathment and midgut penetration in *Aedes aegypti*. Trans Amer Microscop Soc 4:423–433

Crampton JM, Warren A, Lycett GJ, Hughes MA, Comley IP, Eggleston P (1994) Genetic manipulation of insect vectors as a strategy for the control of vector-borne disease. Ann Trop Med Parasitol 88:3–12

Di Luca M, Romi R, Severini F, Toma L, Musumeci M, Fausto AM, Mazzini M, Gambellini G, Musumeci S (2007) High levels of human chitotriosidase hinder the formation of peritrophic membrane in anopheline vectors. Parasitol Res 100:1033–1039

Esslinger JH (1962) Behavior of microfilaria of *Brugia pahangi* in *Anopheles quadrimaculatus*. AmJTrop Med Hyg 11:749–758

Freyvogel T, Staubli W (1965) The formation of the peritrophic membrane in Culicidae. Acta Trop 22:118–147

Guptavanij P, Harinasuta C, Vutikes S, Deesin T, Surathin K (1978) The vectors of *Brugia malayi* in southern Thailand. Southeast Asian J Trop Med Public Health 9:543–548

Gwadz RW (1994) Genetic approaches to malaria control: how long the road? AmJTrop Med Hyg 50:116–125

Hegedus D, Erlandson M, Gillott C, Toprak U (2009) New insights into peritrophic matrix synthesis, architecture, and function. Annu Rev Entomol 54:285–302

Houk EJ, Obie F, Hardy JL (1979) Peritrophic membrane formation and the midgut barrier to arboviral infection in the mosquito, *Culex tarsalis* Coquillett (Insecta, Diptera). Acta Trop 36:39–45

Iyengar MOT (1936) Entry of filaria larvae into the body cavity of the mosquito. Parasitol 28:190–195

Jacobs-Lorena M, Oo MM (1996) The peritrophic matrix of insects. In: Beaty J, Marquardt WC (eds) The biology of disease vectors. University Press of Colorado, Boulder, pp 318–332

Kumar NP, Sabesan S, Panicker KN (1998) Susceptibility status of *Mansonia annulifera* to *Brugia malayi* parasites in Cherthala, Alappuzha district, Kerala. Indian J Exp Biol 36:829–831

Laurence BR (1966) Intake and migration of the microfilariae of *Onchocerca volvulus* (Leuckart) in *Simulium damnosum* Theobald. J Helminthol 50:337–342

Laurence BR, Pester FRN (1961) The behavior and development of *Brugia patei* (Buckley, Nelson and Heisch, 1958) in a mosquito host, *Mansonia uniformis* (Theobald). J Helminthol 35:285–300

Lehane MJ (1997) Peritrophic matrix structure and function. Annu Rev Entomol 42:525–550

Lek-Uthai U, Tomoen W (2005) Susceptibility of *Mansonia uniformis* to *Brugia malayi* microfilariae from infected domestic cat. Southeast Asian J Trop Med Public Health 36:434–441

Luo H, Qu FY (1990) Experimental infection index of *Anopheles sinensis* and melanization of periodic *Brugia malayi*. Zhongguo Ji Sheng Chong Xue Yu Ji Sheng Chong Bing Za Zhi 8:260–263

Meis JF, Ponnudurai T (1987) Ultrastructural studies on the interaction of *Plasmodium falciparum* ookinetes with the midgut epithelium of *Anopheles stephensi* mosquitoes. Parasitol Res 73:500–506

Meis JF, Pool G, van Gemert GJ, Lensen AH, Ponnudurai T, Meuwissen JH (1989) *Plasmodium falciparum* ookinetes migrate intercellularly through *Anopheles stephensi* midgut epithelium. Parasitol Res 76:13–19

O'Connor FW, Beatty H (1936) The early migrations of *Wuchereria bancrofti* in *Culex fatigans*. Trans R Soc Trop Med Hyg 30:125–127

Okuda K, Caroci A, Ribolla P, Marinotti O, de Bianchi AG, Bijovsky AT (2005) Morphological and enzymatic analysis of the midgut of

Anopheles darlingi during blood digestion. J Insect Physiol 51:769–776

Pascoa V, Oliveira PL, Dansa-Petretski M, Silva JR, Alvarenga PH, Jacobs-Lorena M, Lemos FJA (2002) *Aedes aegypti* peritrophic matrix and its interaction with heme during blood digestion. Insect Biochem Mol 32:517–523

Perrone JB, Spielman A (1986) Microfilarial perforation of the midgut of a mosquito. J Parasitol 72:723–727

Perrone JB, Spielman A (1988) Time and site of assembly of the peritrophic membrane of the mosquito *Aedes aegypti*. Cell Tissue Res 252:473–478

Peters W (1992) Peritrophic membranes. In: Bradshaw D, Burggren W, Heller HC, Ishii S, Langer H, Neuweiler G, Randall DJ (eds) Zoophysiology. Springer-Verlag, Berlin, pp 1–238

Petit G (1978) The filaria *Dipetalonema dessetae*: phenomena of regulation and parasite yield in the *Aedes* vector. Ann Parasitol Hum Comp 53:649–668

Petit G, Spitalier-Kaveh H (1979) The Filaria *Breinlia booliati* in the *Aedes togoi* adipose tissue; comparison with the couple *Dipetalonema dessetae-A. aegypti*. Ann Parasitol Hum Comp 54:653–663

Ramachandran CP, Wharton RH, Dunn FL, Kershaw WE (1963) *Aedes* (Finlaya) *togoi* Theobold, a useful laboratory vector in studies of filariasis. Ann Trop Med Parasitol 57:443–445

Sadlova J, Volf P (2009) Peritrophic matrix of *Phlebotomus duboscqi* and its kinetics during *Leishmania major* development. Cell Tissue Res 337:313–325

Sanders HR, Evans AM, Ross LS, Gill SS (2003) Blood meal induces global changes in midgut gene expression in the disease vector, *Aedes aegypti*. Insect Biochem Mol Biol 33:1105–1122

Santos JN, Lanfredi RM, Pimenta PF (2006) The invasion of the midgut of the mosquito *Culex* (*Culex*) *quinquefasciatus* Say, 1823 by the helminth *Litomosoides chagasfilhoi* Moraes Neto, Lanfredi and De Souza, 1997. J Invertebr Pathol 93:1–10

Sasa M (1976) Human filariasis: a global survey of epidemiology and control. Tokyo. University of Tokyo Press, Tokyo, p 819

Schacher JF (1962) Morphology of the microfilaria of *Brugia pahangi* and of the larval stages in the mosquito. J Parasitol 48:679–692

Secundino NFC, Eger-Mangrich I, Braga EM, Santoro MM, Pimenta PFP (2005) *Lutzomyia longipalpis* peritrophic matrix: formation, structure, and chemical composition. J Med Entomol 42:928–938

Shahabuddin M, Cociancich S, Zieler H (1998) The search for novel malaria transmission-blocking targets in the mosquito midgut. Parasitol Today 14:493–497

Shen Z, Jacobs-Lorena M (1997) Characterization of a novel gut-specific chitinase gene from the human malaria vector *Anopheles gambiae*. J Biol Chem 272:28895–28900

Shih CM, Chen CC (1987) Exsheathment of microfilariae of *Brugia pahangi* in *Anopheles quadrimaculatus* and *Culex quinquefasciatus*. Southeast Asian J Trop Med Public Health 18:521–525

Singh RN, Rathaur S (2003) *Setaria cervi*: in vitro released collagenases and their inhibition by *Wuchereria bancrofti* infected sera. J Helminthol 77:77–81

Smartt CT, Chiles J, Lowenberger C, Christensen BM (1998) Biochemical analysis of a blood meal-induced *Aedes aegypti* glutamine synthetase gene. Insect Biochem Mol Biol 28:935–945

Syafruddin AR, Kamimura K, Kawamoto F (1991) Penetration of the mosquito midgut wall by the ookinetes of *Plasmodium yoelii nigeriensis*. Parasitol Res 77:230–236

Tellam RL, Wijffels G, Willadsen P (1999) Peritrophic matrix proteins. Insect Biochem Mol Biol 29:87–101

Terra WR (2001) The origin and functions of the insect peritrophic membrane and peritrophic gel. Arch Insect Biochem Physiol 47:47–61

Trpis M (1981) Susceptibility of the autogenous group of the *Aedes scutellaris* complex of mosquitoes to infection with *Brugia malayi* and *Brugia pahangi*. Tropenmed Parasitol 32:184–188

Villalon JM, Ghosh A, Jacobs-Lorena M (2003) The peritrophic matrix limits the rate of digestion in adult *Anopheles stephensi* and *Aedes aegypti* mosquitoes. J Insect Physiol 49:891–895

Wada Y (2011) Vector mosquitoes of filariasis in Japan. Trop Med Health 39:39–45

Walters LL, Irons KP, Guzman H, Tesh RB (1993) Formation and composition of the peritrophic membrane in the sand fly, *Phlebotomus perniciosus* (Diptera: Psychodidae). J Med Entomol 30:179–198

Wu Y, Preston G, Bianco AE (2008) Chitinase is stored and secreted from the inner body of microfilariae and has a role in exsheathment in the parasitic nematode *Brugia malayi*. Mol Biochem Parasitol 161:55–62

Yamamoto H, Ogura N, Kobayashi M, Chigusa Y (1983) Studies on filariasis II: exsheathment of the microfilariae of *Brugia pahangi* in *Armigeres subalbatus*. Jpn J Parasitol 32:287–292

Zhu Z, Gern L, Aeschlimann A (1991) The peritrophic membrane of *Ixodes ricinus*. Parasitol Res 77:635–641

MIDGUT ULTRASTRUCTURE OF THE FOURTH INSTAR OF *OCHLEROTATUS TOGOI* (DIPTERA: CULICIDAE), A VECTOR OF FILARIASIS

Nuchpicha Intakhan, Narissara Jariyapan, Wetpisit Chanmol, Sriwatapron Sor-Suwan, Benjarat Phattanawiboon, Atiporn Saeung and Wej Choochote

Department of Parasitology, Faculty of Medicine, Chiang Mai University, Chiang Mai 50200, Thailand

Correspondence: Narissara Jariyapan, Department of Parasitology, Faculty of Medicine, Chiang Mai University, Chiang Mai 50200, Thailand

E-mail: narsuwan@mail.med.cmu.ac.th, njariyapan@gmail.com

Abstract. The midgut is the largest organ in the mosquito larval body sustaining ion transport, biomolecule absorption and an entry site for several pathogens. In this study, the ultrastructure of the midgut of *Ochlerotatus togoi* fourth instar was investigated by light, scanning and transmission electron microscopy. The fourth instar midgut was approximately 2 mm in length. It consisted of at least three morphologically distinct cell types including epithelial, regenerative, and endocrine cells. The midgut epithelium formed by a monolayer of epithelial cells with the plasma membrane showing multiple folding where it adjoined the basement membrane. Regenerative cells were scattered throughout the basal portion of the epithelium, along with endocrine cells. Epithelial cells containing large, microvilli-lined apical cavities were identified in most specimens. No evidence of division or differentiation was obtained for any cell types. At least six layers of peritrophic matrix (PM) were observed in the gut lumen. The PM separated foods from the midgut epithelial cells. Cytoplasmic protrusion in many areas of the luminal midgut surface and numerous autophagosomes in the epithelial cells were found in both the early and late fourth instars suggesting that autophagy involved in the degeneration process in the midguts of the fourth instars. This information provided an understanding of the normal larval midgut development for further studies on factors that control the growth and nutritional state of *Oc. togoi* larvae to reduce adult fecundity and physiological roles in the larval midgut on interaction with biological control organisms.

Keywords: *Ochlerotatus togoi*, fourth instar, larva, midgut, mosquito, ultrastructure

INTRODUCTION

The midgut is the largest organ in the mosquito larval body sustaining ion transport, biomolecule absorption and an entry site for several pathogens. Factors controlling the growth and nutritional state of mosquito larvae affect the reproductive potential of the adult (Chambers and Klowden, 1994; Soliman *et al,* 1995; Tu and Tatar, 2003; Zhou *et al,* 2004). Small, poorly fed mosquito larvae produce adults with less reproductive potential (Briegel, 1990; Renshaw *et al,* 1994; Briegel, 2003; Noriega, 2004; Telang and Wells, 2004; Telang *et al,* 2006, 2007). Interfering with the normal development of the larval midgut may possibly reduce its ability to absorb, or store, nutrients and, as a consequence, reduce adult fecundity.

One of several control tools for diseases transmitted by mosquitoes is using larvicides to kill the insect larvae. Larvicides include chemicals, such as temephos, methoprene, oils, and monomolecular films and biological insecticides, such as the microbial larvicides *Bacillus thurigiensis ssp. isaraelensis* (Bti) and *Bacillus sphaericus* (Bs). Bti is a naturally occurring soil bacterium found throughout the world. It has been developed for mosquito control. Bti larvicide product is made up of the dormant spore form of the bacterium. When Mosquito larvae eat the product, an associated pure toxin disrupts the gut in the mosquito by binding to receptor cells present in insects, but not in mammals. Bs is also a naturally occurring bacterium that has been used to kill various kinds of mosquito larvae. Mosquito larvae ingest the bacteria, and as with Bti, the toxin disrupts the gut in the mosquito by binding to receptor cells, again only present in insects not in mammals (Baumann *et al,* 1991; Lacey, 2007). The target spectrum of Bs is more limited and restricted to each mosquito genus. Most *Culex* species are highly sensitive to Bs, but within the genera *Aedes* and *Anopheles,* some species are highly

sensitive, whereas others show minimal sensitivity (Davidson *et al,* 1984; Delecluse *et al*, 2000). Although the larval midgut is a target for controlling transmission of many vector-borne diseases such as malaria and filariasis, little is known about the morphology and physiological function of the normal midguts of larvae in each mosquito species.

Ochlerotatus togoi has been reported as a vector of filariasis in the coastal area of Asia including China, Japan, and Taiwan (Ramachandran *et al,* 1963; Cheun *et al,* 2011). This mosquito species breeds year round, overwintering as the fourth stage larvae or eggs, feeds on birds and mammals and is often common enough be a pest to seaside homeowners. In Thailand, *Oc. togoi* (Chanthaburi strain) is highly susceptible to the rural strain of nocturnally subperiodic *Wuchereria bancrofti* (Tak and Kanchanaburi strains), nocturnally subperiodic *B. malayi* (Narathiwat strain), *Brugia pahangi* (Malaysia strain), and *Dirofilaria immitis* (Chiang Mai strain) (Choochote *et al,* 1983, 1987). Lymphatic filariasis is one of the tropical diseases targeted for elimination by the year 2020 (100 % of all endemic countries), which has spurred vaccine and drug development, as well as new methods of vector control (WHO, 2012).

Therefore, in this study, the ultrastructure of the midgut epithelium of the early and late fourth instars of *Oc. togoi* was examined by light, scanning and transmission electron microscopy to provide an understanding of the normal larval midgut morphology.

MATERIALS AND METHODS

Mosquito

Oc. togoi mosquitoes (Koh Nam Sao, Chantaburi Province, Southeastern Thailand) were used in this study. The mosquito strain has been maintained in the insectary of the Department of Parasitology, Faculty of Medicine, Chiang Mai University, since 1983. It has been proven to be highly susceptible to NSP *B. malayi* (Choochote *et al,* 1987). Methods for rearing of mosquitoes were followed standard techniques described by Choochote *et al,* (1987). The early fourth instars aged 8-12 h and the late fourth instars aged 92-96 h after molting (ten samples/time point) were processed for LM, SEM, and TEM.

Preparation of samples for light microscopy

The midguts of the fourth instar were dissected in PBS and allowed to settle onto slides without drying. Photographs of the glands were taken using a digital camera (Cannon, Tokyo, Japan) attached to a light microscope.

Preparation of samples for scanning electron microscopy

Dissected midguts were fixed with a solution of 2.5% glutaraldehyde mixed in phosphate buffer solution at a pH of 7.4 at 4°C for 24 h. The fixed samples were post-fixed as described for TEM and dehydrated in a crescent series of acetone. Finally, the specimens were subjected to critical point drying, were attached with double-stick tape to aluminum stubs, and were coated with gold in a sputter-coating apparatus before being viewed with a JEOL JSM-5910 scanning electron microscope (Japan). To observe the interface between the midgut surface and the blood meal, some fixed samples were fractured before coating with gold, while others were gently opened and the contents washed out with phosphate buffer saline before the fixation.

Preparation of samples for transmission electron microscopy

Dissected midguts were fixed overnight with a solution of 2.5% glutaraldehyde mixed in phosphate buffer solution at a pH of 7.4 at 4°C to accomplish primary fixation. They were then rinsed twice with phosphate buffer solution at ten minute intervals and later post-fixed in a solution of 1% osmium tetroxide for 2 h. Post-fixation was followed by rinsing twice with phosphate buffer solution and dehydrating with alcohol. To replace the water in the specimens with alcohol, they were subjected to the following increasing concentrations of alcohol: 30, 50, 70, 80, 90, and 95%. The specimens were then placed in absolute alcohol for two 12-h periods. After that, organ specimens were placed in acetone for 2 h. before transferring into ratios of resin to acetone of 1:3 for 24 h, 1:1 for 24 h, and 3:1 for 24 h, sequentially. This was followed by treatment with pure resin twice for 3 h. Each sample was then embedded in Spurr's resin by placing them into a plastic block and by incubating at 70°C for 24 h. A semithin section (0.5 μm) of each sample was made with a glass knife on an Ultramicrotome (Boeckeler®, USA). This was followed by staining with 1% methylene blue mixed with 1% Azure II (1:1) to view under a light microscope (Olympus®, Japan). The ultrathin sections (90 nm) were stained with uranyl acetate and lead citrate to observe under the ZEISS EM 10 electron microscope (Germany).

RESULTS

Ultrastructure of the midgut epithelium in the fourth instars

The fourth instar midgut was approximately 2 mm in length and formed by a monolayer of epithelial cells with the plasma membrane showing multiple folding where it adjoined the basement membrane (Fig 1A). It consisted of at least three

morphologically distinct cell types including epithelial, regenerative, and endocrine cells (Fig 1).

Epithelial cells were the major cellular component of the midgut epithelium. These cells had morphological characteristics of absorptive cells. TEM analysis revealed that the cytoplasm of the perinuclear region was rich in cisterns of rough (RER) and smooth (SER) endoplasmic reticulum and Golgi complex. In the apical region of the cytoplasm, there was an abundance of mitochondria, cisterns of RER and SER, free ribosomes, and lamellar bodies. The apical membrane was formed by densely numerous microvilli (Fig 1, 2). The basal regions of epithelial cells were rich in mitochondria (Fig 2). The nuclei of the epithelial cells were situated at one third of the cell height. Among the midgut epithelial cells, septate junctions were observed (Fig 1). SEM analysis showed that in the luminal surface of the midgut in the early fourth instars examined, two morphological features of the epithelial cells were found, one covered by a thin membrane (Fig 3C, D)and another one with long microvilli, (Fig 3F). Figure 3C and D demonstrate the luminal surface of the early fourth instar midgut which consists of a carpet of the epithelial cells being covered with a thin membrane on their surface to hinder microvilli underneath. Figure 3E shows the losing of the thin membrane from their cellular apexes. Only fully formed epithelial cells with long microvilli in almost regions in the midgut of some of the early fourth instar midguts examined were noted (Fig 3F). In the late fourth instars, a mixture of fully formed epithelial cells and epithelial cells with cytoplasmic protrusions were observed (Fig 5C, D).

Regenerative cells were scattered among the epithelial cells, throughout the basal portion of the epithelium, never reaching the lumen (Fig 1B, C). At least 70 to 80

regenerative groups were found in a transverse section through the midgut sections studied (Fig 1B). Each group was composed of three to four cells (Fig 1C, D). The cytoplasm of the regenerative cells was poor in organelles, sporadically housing mitochondria and cisternae of RER. The nucleus was oval located near the nuclear envelope and nucleolus was observed in the nucleus of the regenerative cells (Fig 2A, B).

The endocrine cells were cone-shaped and located basally in the midgut epithelium as single cells. Approximately, 30 to 40 endocrine cells were distributed in a transverse section through the midgut sections studied (Fig 1B). Midgut endocrine cells were smaller than epithelial cells. These cells displayed weakly stained cytoplasm and nuclei, contrasting with the dark digestive cells. No visible folding on the basal membranes of the endocrine cells was observed. Numerous round secretory granules were observed along the lateral and basal plasma membranes. The secretory granules were ranging in size from 60 to 120 nm (Fig 2C, D).

At least six distinct layers of peritrophic matrix (PM) were observed in the gut lumen. The PM separated foods from the midgut epithelial cells (Fig 1, 2F, 3A, B). The first layer on the luminal side was composed of electron-dense granules and was in close contact with the second layer. The second and fourth layers were very similar in their appearance longitudinally in having relatively electron-dense zones alternating with less dense zones. The second layer was somewhat thicker than the fourth layer. The third and the fifth layers were also similar to one another in consisting of loosely woven, granular strands, although both varied in thickness. The fifth layer was the thickest. Most variation in thickness of the larval PM was due to the thickness of the

fifth layer. The sixth layer appeared as a dark, solid line of varying electron density (Fig 2F).

Morphological features of epithelial cell degeneration

LM observations revealed that in the early fourth instar midgut sections, epithelial cells started to prepare for degeneration while fulfilling their functions (Fig 1C, D). Morphological features attributable to the degenerative process were observed using TEM and SEM (Fig 4, 5). In the early larval midguts, autophagic compartments (autophagosomes) were clearly seen in some epithelial cells. Autophagosomes containing organelle debris were visible in the cytoplasm of cells undergoing degeneration (Fig 4A-D). In addition, lamellar bodies which represent the result of autophagic degradation of membranous cellular components were observed (Fig 4C, D). Autophagy increased in the midgut cells of late fourth instars (Fig 4). The few organelles, such as mitochondria and vesicles near the apical membrane of the degenerated cell were observed (Fig 4E, F). SEM analysis revealed cytoplasmic protrusions of cells undergoing degeneration on the apical surface among epithelial cell borders (Fig 5A). Cytoplasmic protrusions were round and had a smooth surface (Fig 5A, C). Figure 5B shows breakage of the apical membrane and organelle debris was discharged into the midgut lumen. In the late larval midgut sections, both new epithelial cells and epithelial cells with cytoplasmic protrusions (Fig 5C, D) were found in the luminal surfaces of the midgut of the late fourth instars examined.

DISCUSSION

This present study represents the first description of the midgut of *Oc. togoi* fourth instar and morphological features of epithelial cell degeneration at the

ultrastructural level. In Diptera, Lepidoptera and Ephemeroptera, the midgut epithelium of the adult stage is always formed by two main types of cells: epithelial and regenerative cells, however, in different stages of development in some insect species endocrine and goblet cells are also found (Billingsley, 1990; Billingsley and Lehane, 1996; Leite and Evangelista, 2001; Silva-Olivares *et al,* 2003; Baton and Ranford-Cartwright, 2007; Fialho *et al,* 2009). In the fourth instar of *Oc. togoi*, three types of cells including epithelial, regenerative, and endocrine cells were found in this study but no goblet cell was observed.

Epithelial cells are predominant in the epithelium of the midgut wall of *Oc. togoi* fourth instar and show similar morphological aspects to *Aedes aegypti* (Zhuang *et al,* 1999). According to Richards and Davies (1994) and Jordao *et al* (1999), the epithelial cells present numerous and long microvilli and large quantities of mitochondria in the cell apical portion. The well-developed rough endoplasmic reticulum and Golgi complex in the middle portion, and the basal plasma membrane infoldings with associated mitochondria in the basal portion indicate that the columnar cells serve in nutrient absorption; protein synthesis, mainly related to digestive enzyme production; and ion and water transport.

It is known that regenerative cells are able to proliferate and differentiate, therefore, they might be treated as stem cells which, depending on the kind of cells forming distinct tissues, would differentiate into epithelial or even endocrine or goblet cells (Tettamanti *et al,* 2007a). Regenerative cells are either distributed as isolated cells among epithelial cells, or form regenerative groups which, depending on the shape, are called regenerative nests or crypts (Garcia *et al,* 2001; Silva-Olivares *et al,* 2003; Illa-Bochaca and Montuenga, 2006; Rost, 2006a, 2006b; Wanderley-Teixeira *et al*, 2006;

225 Baton and Ranford-Cartwright, 2007; Rost-Roszkowska *et al,* 2010a, 2010b). Similar
226 morphological aspects of regenerative cells in *Oc. togoi* were found. At this stage, no
227 proliferation and/or differentiation of the regenerative cells occurred.

228 Billingsley and Lehane (1996) and Levy *et al* (2004) have proposed that
229 endocrine cells may have functions similar to neurosecretory cells of the vertebrate
230 alimentary tract. A large variety of polypeptide hormones, which are responsible for
231 secretion of appropriate concentrations of specific enzymes after feeding and also
232 control the proliferation and differentiation of the regenerative cells, are synthesized in
233 the endocrine cells (Endo *et al,* 1982; Andries and Tramu, 1985; Zudaire *et al,* 1998).
234 The endocrine cells, presented as different types based on electron-density of their
235 granules (Raes and Verbeke, 1994; Billingsley and Lehane,1996; Jordao *et al,* 1999;
236 Cristofoletti *et al,* 2001). In some insects, for example, the desert locust *Schistocerca*
237 *gregaria* (Forskal), the stingless bee *Melipona quadrifasciata anthidioides*, and the
238 velvetbean caterpillar moth *Anticarsia gemmatalis,* glycogen granules have been
239 detected (Montuenga *et al,* 1989; Neves *et al,* 2003; Levy *et al,* 2004). Secretory
240 vacuoles and granules are mainly observed accumulated in the basal cytoplasm (Raes
241 and Verbeke, 1994; Billingsley and Lehane, 1996; Cristofoletti *et al,* 2001; Levy *et al,*
242 2004). The structure of endocrine cells in the *Oc. togoi* studied was similar to that
243 described for many insect species; granular structures were observed in the entirely
244 basal cytoplasm. The fourth instars of *Oc. togoi* are the final stages before the formation
245 of the pupa, and the organisms must be prepared for many changes associated with
246 pupation. The secretory functions of the endocrine cells are probably intensified and
247 new hormones synthesized.

Absence of goblet cells in the midgut of *Oc. togoi* fourth instars is consistent with a previous work in *Ae. aegypti* larvae (Zhuang *et al*, 1999). In the midgut of Lepidoptera larvae, goblet cells present a goblet chamber formed by an apical infolding of the plasma membrane. Cell surface basal and lateral projections into this cavity extend cell surface area, similar to the idea of microvilli but filled with mitochondria. The presence of mitochondria inside the projections is related to the active transport of potassium ions from the hemolymph to the midgut lumen, and also calcium ions from adjacent columnar cells (Klein *et al*, 1991; Koch and Moffett, 1995; Moffett *et al*, 1995). The presence of these goblet cells may be responsible for alkalization (pH 8.0-12.0) in the midgut of Lepidoptera (Dow, 1984). However, alkalization in the midgut lumen of larvae of mosquitoes occurs in the absence of goblet cells. Basolateral V-ATPases drive strong luminal alkalinization in the anterior midgut of larval *Ae. aegypti* (Zhuang *et al*, 1999; Boudko *et al*, 2001; Onken *et al*, 2008). The V-ATPase is not localized in the luminal membrane of the anterior midgut, but instead in the basolateral membrane (Zhuang *et al*, 1999). The midgut epithelium of *Ae. aegypti* larvae generates a lumen negative transepithelial voltage instead of the lumen positive voltage observed in *Manduca sexta* larvae under comparable conditions (Clark *et al*, 1999).

Our results with the PM in the fourth instars of *Oc. togoi* were similar to those of *Ae. aegypti* in that they consisted of at least six layers (Moncayo *et al*, 2005). The larval PM was of Type II and formed as a hollow posteriorly moving cylinder that forms from material secreted by a discrete ring of cells located in the larval cardia. The cardia is a distinctive organ in Diptera that encompasses the posterior end of the foregut and anterior end of the midgut. The results of our observations of *Oc. togoi* larvae show that the PM occurs continuously along the alimentary canal from the cardia to the anus. The

roles of the larval PM in the protection of the midgut epithelium from damage by food particles and also protection against pathogens have both been previously described by Peters (1992) and Lehane (1997).

Normally, cells continuously synthesize proteins, reconstruct their organelles and cellular components, renew them and take up substances from outside. Autophagy is a cellular mechanism that counteracts and controls this on-going growth of organic matter. It is also treated as a type of cell death that enables degradation of organelles that are no longer needed (Lee *et al,* 2002; Lockshin and Zakeri, 2004; Debnath *et al,* 2005; Levine and Yuan 2005; Giusti *et al,* 2007; Tettamanti *et al,* 2007b). In autophagy, two important features in the cells, autophagosome and autolysosome, have been reported (Mizushima *et al,* 2008; Tettamanti *et al,* 2011). The autophagic process begins with the formation of a membrane, called a phagophore, an isolation membrane in the cell and it progressively expands and grows to engulf a portion of cytoplasm. Afterward this double-membrane structure finally wraps around cellular components targeted for degradation and closes to become an autophagosome. By vesicle fusion, the autophagosome membrane fuses with lysosomes, small organelles surrounded by membranes that contain digestive enzymes. The contents are degraded and the resulting macromolecules are assimilated back into the cytosol (Mizushima *et al,* 2008). Degeneration of the midgut epithelial cells might carry on during digestion and new cells renew them during the entire life of insects depending on various stress and external factors such as harmful or toxic chemical compounds (Evangelista and Leite, 2003; Rost, 2006b; Baton and Ranford-Cartwright, 2007; Rost-Roszkowska *et al,* 2008). In this study, the degeneration of midgut epithelial cells by autophagosomes was observed in both the early and late fourth instars of *Oc. togoi*. Autophagy proceeded

296 intensively in the midgut epithelium of the late fourth instars of *Oc. togoi* suggesting
297 that this might be a type of elimination of harmful or toxic substances from the
298 organism. It is known that processes of degeneration, and the following regeneration, of
299 the midgut epithelium might proceed in a cyclic manner that is closely associated with
300 molting periods (Garcia *et al*, 2001; Takeda *et al*, 2001; Evangelista and Leite, 2003). In
301 this study, no mitotic activity in regenerative cells or cellular renewal due to the
302 growing digestive tube at each ecdysis was observed. An explanation is that the larvae
303 analyzed were not at a prepupal stage. However, a study on proliferation and
304 differentiation of the regenerative cells in the prepupal and pupal stages is in progress in
305 our laboratory.

306 In conclusion, this study described the ultrastructure of the midgut of *Oc. togoi*
307 fourth instar for the first time. Although the cells types found in the midgut epithelium
308 of *Oc. togoi* larvae were similar to those described for other *Aedes* or *Ochlerotatus*
309 species, further studies on factors that control the growth and nutritional state of *Oc.*
310 *togoi* larvae are required to inform on how to reduce adult fecundity and physiological
311 roles in the larval midgut on interaction with biological control organisms, for example,
312 Bti and Bs.

313

314 ## ACKNOWLEDGEMENTS

315 This work was financially supported by the Thailand Research Fund (TRF
316 Senior Research Scholar: RTA5480006 to WC, subproject to NJ) and the Faculty of
317 Medicine, Chiang Mai University.

318

319 ## REFERENCES

320 Andries JC, Tramu G. Ultrastructural and immunohistochemical study of endocrine
321 cells in the midgut of the cockroach *Blaberus craniifer* (Insecta, Dictyoptera).
322 *Cell Tissue Res* 1985; 240: 323-32.
323 Baton LA, Ranford-Cartwright LC. Morphological evidence for proliferative
324 regeneration of the *Anopheles stephensi* midgut epithelium following
325 *Plasmodium falciparum* ookinete invasion. *J Invertebr Pathol* 2007; 96: 244-54.
326 Baumann P, Clark MA, Baumann L, Broadwell AH. *Bacillus sphaericus* as a mosquito
327 pathogen: Properties of the organism and its toxins. *Microbiol Rev* 1991; 55:
328 425-36.
329 Billingsley PF. The midgut ultrastructure of haematophagous insects. *Ann Rev Entomol*
330 1990; 35: 219-48.
331 Billingsley PF, Lehane MJ. Structure and ultrastructure of the insect midgut. In: Lehane
332 MJ, Billingsley PF (eds), Biology of the insect midgut, pp 3-30. Chapman &
333 Hall, London 1996.
334 Boudko DY, Moroz LL, Harvey WR, Linser PJ. Alkalinization by chloride/bicarbonate
335 pathway in larval mosquito midgut. *PNAS* 2001; 98: 15354-9.
336 Briegel H. Fecundity, metabolism, and body size in *Anopheles* (Diptera: Culicidae),
337 vectors of malaria. *J Med Entomol* 1990; 27: 839-50.
338 Briegel H. Physiological basis of mosquito ecology. *J Vector Ecol* 2003; 28: 1-11.
339 Chambers GM, Klowden MJ. Nutritional reserves of autogenous and anautogenous
340 selected strains of *Aedes albopictus* (Diptera: Culicidae). *J Med Entomol* 1994;
341 31: 554-60.

342 Cheun HI, Cho SH, Lee HI *et al.* Seasonal prevalence of mosquitoes, including vectors
343 of Brugian filariasis, in southern islands of the Republic of Korea. *Korean J*
344 *Parasitol* 2011; 49: 59-64.
345 Choochote W, Abeyewickreme W, Sucharit S, Apiwathnasorn C, Tumrasvin W,
346 Leemingsawat S. *Aedes togoi* Koh Nom Soa, Chanthaburi, a laboratory vector
347 for *Brugia malayi* and *Brugia pahangi* in Thailand. *J Parasit Trop Med Assoc*
348 *Thai* 1983; 6: 25-31.
349 Choochote W, Keha P, Sukhavat K, Khamboonruang C, Sukontason K. *Aedes* (Finlaya)
350 *togoi* Theobald 1907, Chantaburi strain, a laboratory vector in studies of
351 filariasis in Thailand. *Southeast Asian J Trop Med Public Health* 1987; 18: 259-
352 60.
353 Clark TM, Koch A, Moffett DF. The anterior and posterior `stomach' regions of larval
354 *Aedes aegypti* midgut: regional specialization of ion transport and stimulation by
355 5-hydroxytryptamine. *J Exp Biol* 1999; 202: 247-52.
356 Cristofoletti PT, Ribeiro AF, Terra WR. Apocrine secretion of amylase and exocytosis
357 of trypsin along the midgut of Tenebrio molitor larvae. *J Insect Physiol* 2001;
358 47: 143-55.
359 Davidson EW, Urbina M, Payne J *et al.* Fate of *Bacillus sphaericus* 1593 and 2362
360 spores used as larvicides in the aquatic environment. *Appl Environ Microbiol*
361 1984; 47: 125-9.
362 Debnath J, Baehrecke EH, Kroemer G. Does autophagy contribute to cell death?
363 *Autophagy* 2005; 1: 66-74.
364 Delecluse A, Juarez-Perez V, Berry C. Vector active toxins: structure and diversity. In:
365 Charles J-F, Delecluse A, Nielson-LeRoux C (eds), Entomopathogenic Bacteria:

From laboratory to field application, pp 101-125. Kluwer Academic Publishers, Dordrecht, the Netherlands 2000.

Dow JAT. Extremely high pH in biological systems: a model for carbonate transport. *Am J Physiol* 1984; 246: R633-5.

Endo Y, Nishiitsutsuji-Uwo J, Iwanaga T, Fujita T. Ultrastructural and immunohistochemical identification of pancreatic polypeptide-immunoreactive endocrine cells in the cockroach midgut. *Biomed Res* 1982; 3: 454-6.

Evangelista LG, Leite ACR. Midgut ultrastructure of the third instar of *Dermatobia hominis* (Diptera: Cuterebridae) based on transmission electron microscopy. *J Med Entomol* 2003; 40: 133-40.

Fialho M, Zanuncio JC, Neves CA, Ramalho FS, Serrao JE. Ultrastructure of the digestive cells in the midgut of the predator *Brontocoris tabidus* (Heteroptera: Pentatomidae) after different feeding periods on prey and plants. *Ann Entomol Soc Am* 2009; 102: 119-27.

Garcia JJ, Li G, Wang P, Zhong J, Granados RR. Primary and continous midgut cell cultures from *Pseudaletia unipunctata* (Lepidoptera, Noctuidae). *In Vitro Cell Dev Biol Anim* 2001; 37: 353-9.

Giusti F, Dallai L, Beani L, Manfredini F, Dallai R. The midgut ultrastructure of the endoparasite *Xenos vesparum* (Rossi) (Insecta, Strepsiptera) during post-embryonic development and stable carbon isotopic analyses of the nutrient uptake. *Arthropod Struct Dev* 2007; 36: 183-97.

Illa-Bochaca I, Montuenga LM. The regenerative nidi of locust as a model to study epithelial cell differentiation from stem cells. *J Exp Biol* 2006; 209: 2215-23.

389 Jordao BP, Capella AN, Terra WR, Ribeiro AF, Ferreira C. Nature of the anchors of
390 membrane-bound aminopeptidase, amylase, and trypsin and secretory
391 mechanisms in *Spodoptera frugiperda* (Lepidoptera) midgut cells. *Journal of*
392 *Insect Physiology* 1999; 45: 29-37.
393 Klein U, Loffelmann G, Wieczorec H. The midgut as a model system for insect K^+
394 transporting epithelia: immunocytochemical localization of a vacuolar type H^+
395 pump. *J Exp Biol* 1991; 161: 61-75.
396 Koch A, Moffett DF. Electrophysiology of K^+ transport by midgut epithelium of
397 lepidopteran insect larvae. IV. A multicompartment model accounts for
398 tetramethylammonium entry into goblet cavities. *J Exp Biol* 1995; 198: 2115-25.
399 Lacey L. *Bacillus thuringiensis* serovariety *israelensis* and *Bacillus sphaericus* for
400 mosquito control. *J Am Mosq Control Assoc* 2007; 23: 133-63.
401 Lee CY, Cooksey BAK, Baehrecke EH. Steroid regulation of midgut cell death during
402 *Drosophila* development. *Dev Biol* 2002; 250: 101-11.
403 Levine B, Yuan J. Autophagy in cell death: an innocent convict? *J Clin Invest* 2005;
404 115: 2679-88.
405 Lockshin RA, Zakeri Z. Apoptosis, autophagy and more. *Int J Biochem Cell Biol* 2004;
406 36: 2405-19.
407 Lehane MJ. Peritrophic matrix structure and function. *Annu Rev Entomol* 1997; 42:
408 525-50.
409 Leite ACR, Evangelista LG. Ultrastructure of endocrine cells from the abdominal
410 midgut epithelium of *Lutzomyia longipalpis* (Diptera: Psychodidae). *J Med*
411 *Entomol* 2001; 38: 749-52.

412 Levy SM, Falleiros AMF, Gregorio EA, Arre-Bola NR, Toledo LA. The larval midgut
413 of *Anticarsia gemmatalis* (Hubner) (Lepidoptera: Noctuidae): light and electron
414 microscopy studies of the epithelial cells. *Braz J Biol* 2004; 64: 633-8.
415 Mizushima N, Levine B, Cuervo AM, Klionsky DJ. Autophagy fights disease through
416 cellular self-digestion. *Nature* 2008; 451: 1069-75.
417 Moffett DF, Koch A, Woods R. Electrophysiology of K^+ transport by epithelium of
418 lepidopteran insect larvae. III. Goblet valve patency. *J Exp Biol* 1995; 198:
419 2103-13.
420 Moncayo AC, Lerdthusnee K, Leon R, Robich RM, Romoser WS. Meconial peritrophic
421 matrix structure, formation, and meconial degeneration in mosquito
422 pupae/pharate adults: histological and ultrastructural aspects. *J Med Entomol*
423 2005; 42: 939-44.
424 Montuenga LM, Barrenechea MA, Sesma P, Lopez J, Vazquez JJ. Ultrastructure and
425 immunocytochemistry of endocrine cells in the midgut of the desert locust,
426 *Schistocerca gregaria* (Forskal). *Cell Tissue Res* 1989; 258: 577-83.
427 Neves CA, Gitirana LB, Serrao JE. Ultrastructure of the midgut endocrine cells in
428 *Melipona quadrifasciata anthidioides* (Hymenoptera, Apidae). *Braz J Biol* 2003;
429 63: 683-90.
430 Noriega FG. Nutritional regulation of JH synthesis: a mechanism to control
431 reproductive maturation in mosquitoes? *Insect Biochem Mol Biol* 2004; 34: 687-
432 93.
433 Onken H, Moffett SB, Moffett DF. Alkalinization in the isolated and perfused anterior
434 midgut of the larval mosquito, *Aedes aegypti*. *J Insect Sci* 2008; 8: 46.

435 Peters W. Peritrophic membranes. In: Bradshaw D, Burggren W, Heller HC, Ishii S,
436 Langer H, Neuweiler G, Randall DJ (eds), Zoophysiology, vol. 130 pp 1-238.
437 Springer-Verlag, Berlin 1992.
438 Raes H, Verbeke M. Light and electron microscopical study of two types of endocrines
439 cell in the midgut of the adult worker honeybee (Apis mellifera). *Tissue Cell*
440 1994; 26: 223-30.
441 Ramachandran CP, Wharton RH, Dunn FL, Kershaw WE. *Aedes* (Finlaya) *togoi*
442 Theobald, a useful laboratory vector in studies of filariasis. *Ann Trop Med*
443 *Parasitol* 1963; 57: 443-5.
444 Renshaw M, Service MW, Birley MH. Size variation and reproductive success in the
445 mosquito *Aedes cantans*. *Med Vet Entomol* 1994; 8: 179-86.
446 Richards OW, Davies RG. The alimentary canal, nutrition and digestion. In: Richards
447 OW, Davies RG (eds), IMMS' General Textbook of Entomology, pp 192-208.
448 Chapman & Hall, London 1994.
449 Rost MM. Ultrastructural changes in the midgut epithelium in *Podura aquatica* L.
450 (Insecta, Collembola, Arthropleona) during regeneration. *Arthropod Struct Dev*
451 2006a; 35: 69-76.
452 Rost MM. Comparative studies on regeneration of the midgut epithelium in *Lepisma*
453 *saccharina* L. and *Thermobia domestica* Packard (Insecta, Zygentoma). *Ann*
454 *Entomol Soc Am* 2006b; 99: 910-6.
455 Rost-Roszkowska MM, Poprawa I, Klag J, Migula P, Mesjasz-Przybyłowicz J,
456 Przybyłowicz W. Degeneration of the midgut epithelium in *Epilachna cf.*
457 *nylanderi* (Insecta, Coccinellidae): apoptosis, autophagy and necrosis. *Can J*
458 *Zool* 2008; 86: 1179-88.

459 Rost-Roszkowska MM, Machida R, Fukui M. The role of cell death in the midgut
460 epithelium in *Filientomon takanawanum* (Protura). *Tissue Cell* 2010a; 42: 24-
461 31.
462 Rost-Roszkowska MM, Vilimova J, Chajec L. Fine structure of the midgut epithelium
463 in *Atelura formicaria* (Hexapoda, Zygentoma, Ateluridae), with special
464 reference to its regeneration and degeneration. *Zool Stud* 2010b; 49: 10-8.
465 Silva-Olivares A, Diaz E, Shibayama M, Tsutsumi V, Cisneros R, Zuiga G.
466 Ultrastructural Study of the Midgut and Hindgut in Eight Species of the Genus
467 *Dendroctonus* Erichson (Coleoptera: Scolytidae). *Ann Entomol Soc Am* 2003;
468 96: 883-900.
469 Soliman MA, Seif AI, Hassan AN, Abdel-Hamid ME, Mansour MA, Gad AM.
470 Nutritional reserves in autogenous and anautogenous populations of *Culex*
471 *pipiens* and *Aedes caspius* (Diptera: Culicidae). *J Egypt Soc Parasitol* 1995; 25:
472 499-507.
473 Takeda M, Sakai T, Fujisawa Y, Narita M, Iwabuchi K, Loeb MJ. Cockroach midgut
474 peptides that regulate cell proliferation, differentiation and death *in vitro*. *In*
475 *Vitro Cell Develop Biol Anim* 2001; 37: 343-7.
476 Telang A, Frame L, Brown MR. Larval feeding duration affects ecdysteroid levels and
477 nutritional reserves regulating pupal commitment in the yellow fever mosquito
478 *Aedes aegypti* (Diptera: Culicidae). *J Exp Biol* 2007; 210: 854-64.
479 Telang A, Li Y, Noriega FG, Brown MR. Effects of larval nutrition on the
480 endocrinology of mosquito egg development. *J Exp Biol* 2006; 209: 645-55.
481 Telang A, Wells MA. The effect of larval and adult nutrition on successful autogenous
482 egg production by a mosquito. *J Insect Physiol* 2004; 50: 677-85.

Tettamanti G, Grimaldi A, Casartelli M *et al.* Programmed cell death and stem cell differentiation are responsible for midgut replacement in *Heliothis virescens* during prepupal instar. *Cell Tissue Res* 2007a; 330: 345-59.

Tettamanti G, Grimaldi A, Pennacchio F, de Eguileor M. Lepidopteran larval midgut during prepupal instar: digestion or self-digestion? *Autophagy* 2007b; 3: 630-1.

Tettamanti G, Cao Y, Feng Q, Grimaldi A, de Eguileor M. Autophagy in Lepidoptera: more than old wine in new bottle. *ISJ* 2011; 8: 5-14.

Tu M-P, Tatar M. Juvenile diet restriction and the aging and reproduction of adult *Drosophila melanogaster*. *Aging Cell* 2003; 2: 327-33.

Wanderley-Teixeira V, Teixeira AA, Cunha FM, Costa MKCM, Veiga AFSL, Oliveira JV. Histological description of the midgut and the pyloric valve of *Tropidacris collaris* (Stoll, 1813) (Orthoptera, Romaleidae). *Braz J Biol* 2006; 66: 1045-9.

World Health Organization (WHO). Accelerating work to overcome the global impact of neglected tropical diseases - a roadmap for implementation. Geneva: WHO, 2012 [Cited 2014 Feb 1]Available from: URL: http://www.who.int/neglected_diseases/NTD_RoadMap_2012

Zhou G, Pennington JE, Wells MA. Utilization of pre-existing energy stores of female *Aedes aegypti* mosquitoes during the first gonotrophic cycle. *Insect Biochem Mol Biol* 2004; 34: 919-25.

Zhuang Z, Linser PJ, Harvey WR. Antibody to H+ V-ATPase subunit E colocalizes with portasomes in alkaline larval midgut of a freshwater mosquito (*Aedes aegypti* L.). *J Exp Biol* 1999; 202: 2449-60.

505 Zudaire E, Simpson SJ, Montuenga LM. Effects of food nutrient content, insect age and
506 stage in the feeding cycle on the FMRF amide immune reactivity of diffuse
507 endocrine cells in the locust gut. *J Exp Biol* 1998; 201: 2971-9.
508

509 FIGURE LEGENDS

510

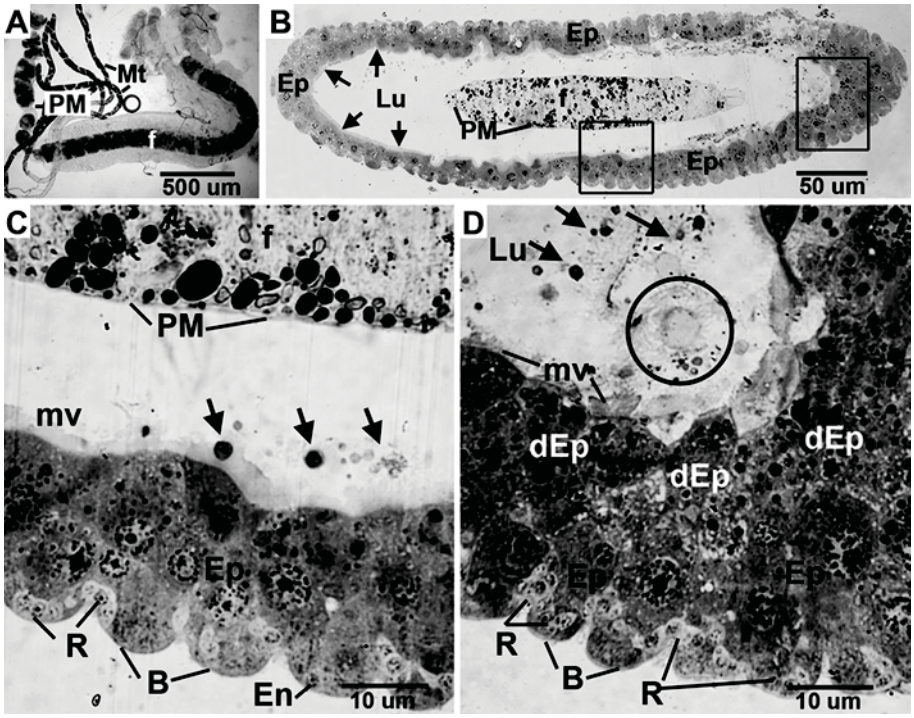

511

512 Fig 1-Morphological study of the midgut epithelium of the *Oc. togoi* early fourth instars
513 under LM. (A) A representative larval midgut before defecation showing larval
514 food (f) covered by a peritrophic matrix (PM) in the midgut lumen and
515 Malpighian tubules (Mt). (B) Transverse section through the middle region of a
516 representative larval midgut of *Oc. togoi* showing midgut epithelium composing
517 of columnar epithelial cells (Ep), larval food (f), midgut lumen (Lu), and
518 peritrophic matrix (PM). Arrows indicate microvilli. (C) Higher magnification of
519 square boxed region in (B) displaying basement membrane (B), endocrine cells
520 (En), epithelial cells (Ep), larval food (f), microvilli (mv), peritrophic matrix
521 (PM), and groups of regenerative cells (R). Arrows indicate degenerated
522 organelles and nuclei discharged into the midgut lumen. (D) Higher
523 magnification of rectangular boxed region in (B) displaying basement membrane

(B), degenerated epithelial cells (dEp), epithelial cells (Ep), microvilli (mv), and groups of regenerative cells (R). Arrows indicate degenerated organelles and nuclei discharged into the midgut lumen (Lu). Circle indicates a transverse section of an apical membrane of a degenerated epithelial cell protruding into the midgut lumen.

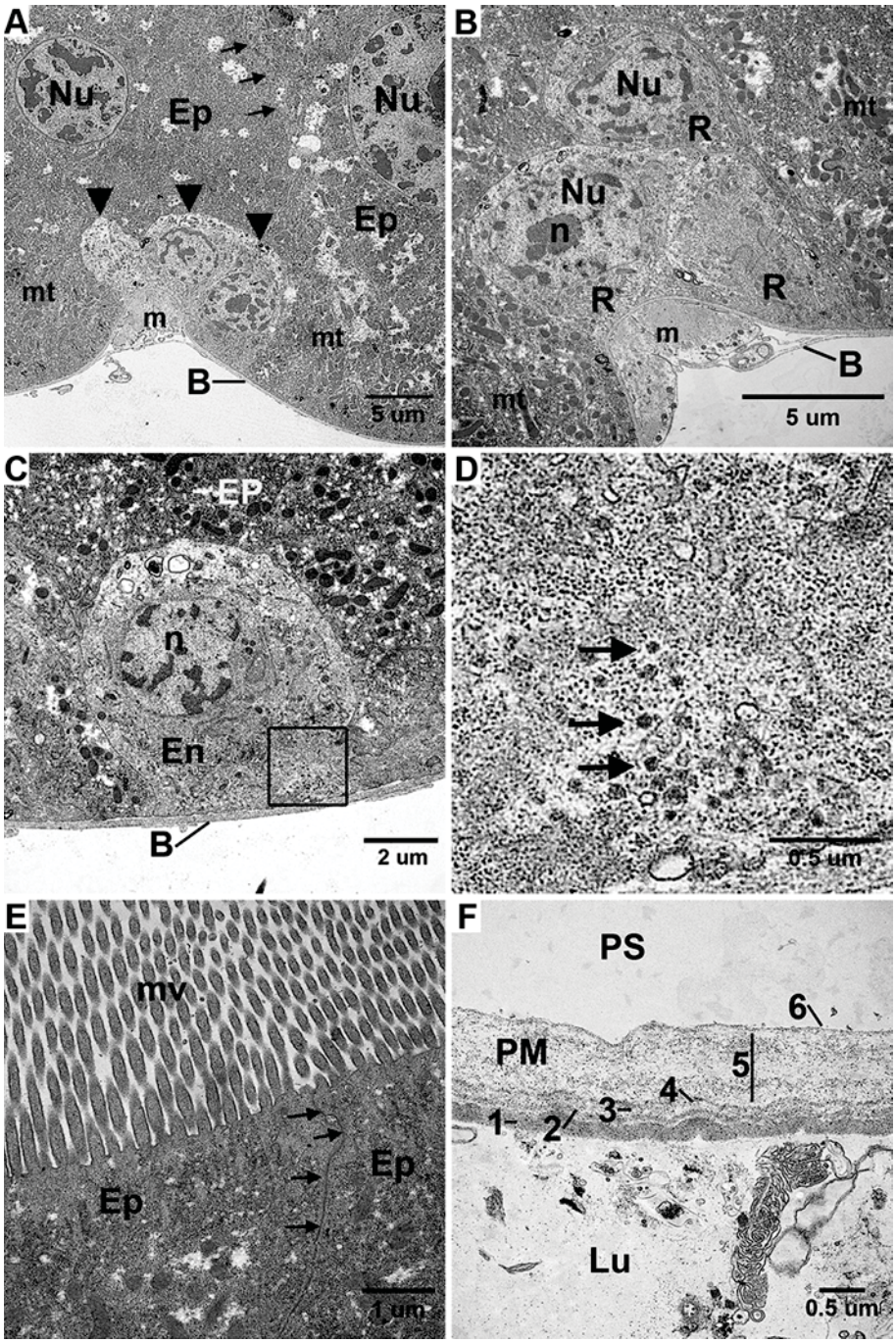

Fig 2-Ultrastructural aspects of the midgut epithelium of the *Oc. togoi* early fourth instars under TEM. (A) A region of the epithelium showing epithelial cells (Ep), a group of regenerative cells (arrowheads), septate junction (arrows), basement membrane (B), muscle (m), mitochondria (mt), and nucleus of epithelial cell (Nu). (B) TEM micrograph displaying a group of regenerative cells (R), basement

membrane (B), muscle (m), mitochondria (mt), nucleus of regenerative cell (n), and nucleus of epithelial cell (Nu). (C) An endocrine cell with many secretory granules in the basal region (square). (D) Higher magnification of square boxed region in (C) displaying the secretory granules (arrows). (E) An apical part of the midgut epithelial cells (Ep), microvilli (mv), and septate junction (arrows). (F) A peritrophic matrix (PM) consisting of at least six layers, peritrophic space (PS), and ingested food and food debris in the lumen of a larval midgut (Lu).

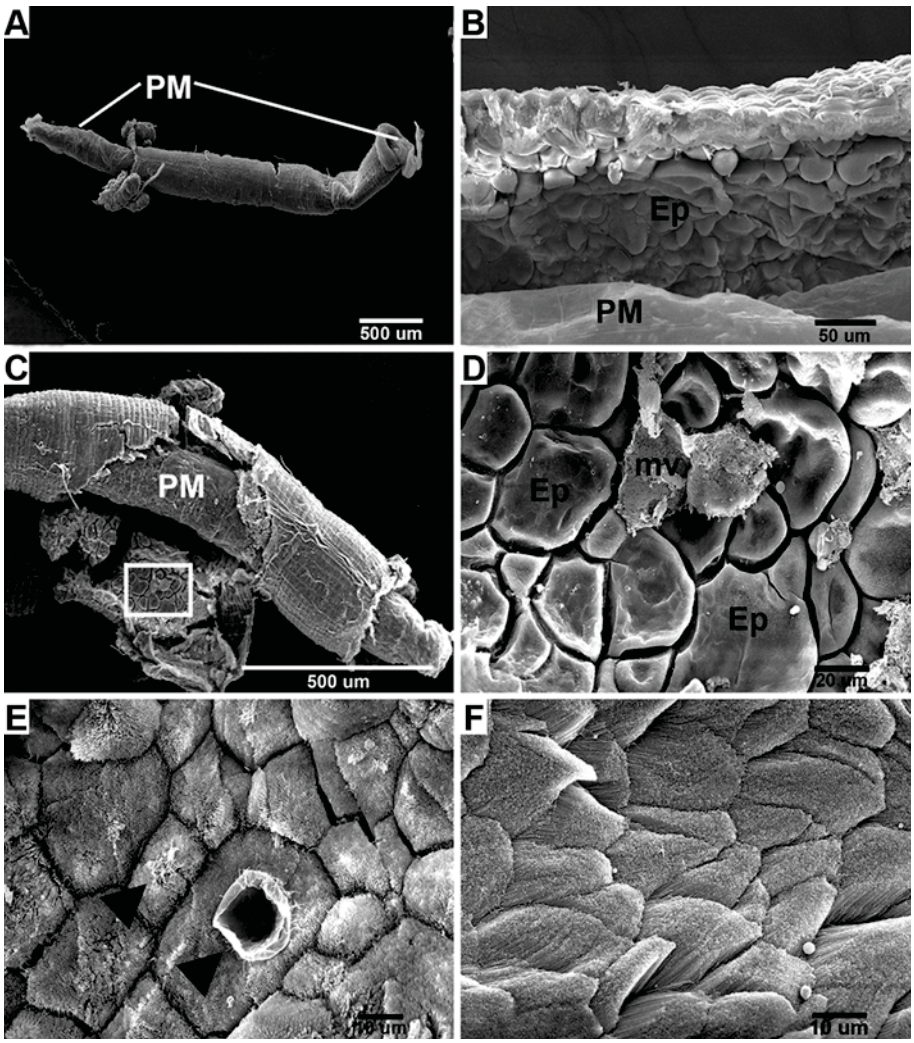

Fig 3-Ultrastructural aspects of *Oc. togoi* epithelium in early fourth instars under SEM. (A) A representative midgut of an early fourth instar with a peritrophic matrix

(PM). (B) A middle part of a larval midgut showing epithelial cells (Ep) and a peritrophic matrix (PM) separated from the midgut epithelium. (C) A posterior part of a larval midgut a peritrophic matrix (PM) and a group of epithelial cells (rectangle). (D) Higher magnification of boxed region in (C) displaying a group of epithelial cells (Ep) with microvilli covered by a thin membrane. (E) A group of epithelial cells (Ep) after the thin membrane gradually loosen from cellular apexes (arrowheads). (F) A region in the midgut with fully formed epithelial cells.

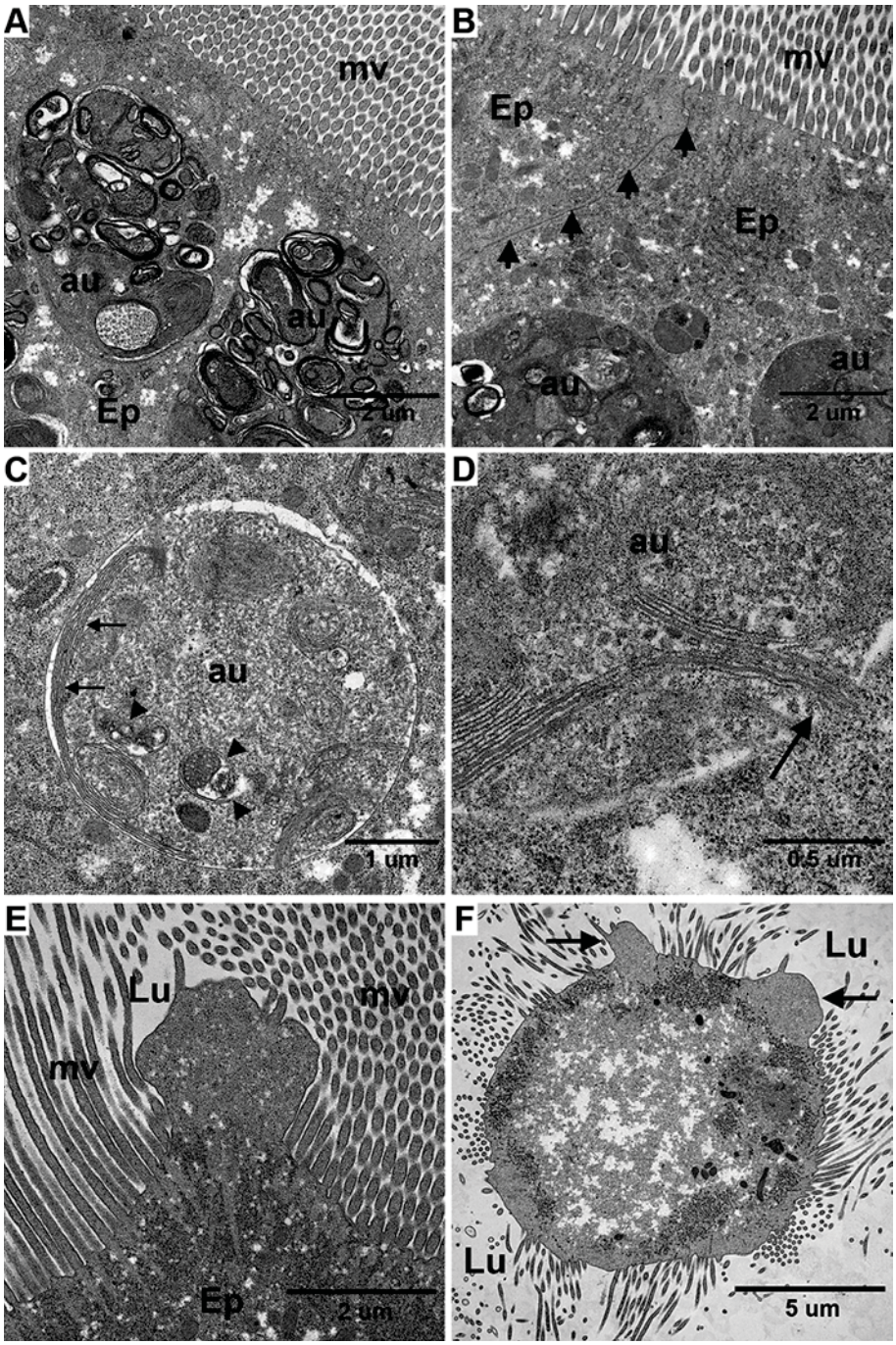

555

556 Fig 4-Autophagy in the midgut epithelium of the *Oc. togoi* late fourth instars under
557 TEM. (A), (B) TEM micrographs showing epithelial cells (Ep) with apical
558 cytoplasm rich in autophagosomes (au). Arrows indicate septate junction.
559 Microvilli (mv). (C) An autophagosome (au) with degenerated organelles and
560 lamellae of rough endoplasmic reticulum (arrows). Two small autophagosomes

(arrowheads) forms inside the autophagosome (au). (D) Higher magnification of an autophagosome (au) remaining in contact with the cytoplasm (arrow) by lamellae. (E) Protrusion of an apical membrane of a degenerated epithelial cell (Ep) into the midgut lumen (Lu). Microvilli (mv). (F) A transverse section of an apical membrane of a degenerated epithelial cell protruding into the midgut lumen (Lu) showing the accumulation of degenerated organelles inside the cells and two regions of the apical membrane evaginated into the lumen (arrows).

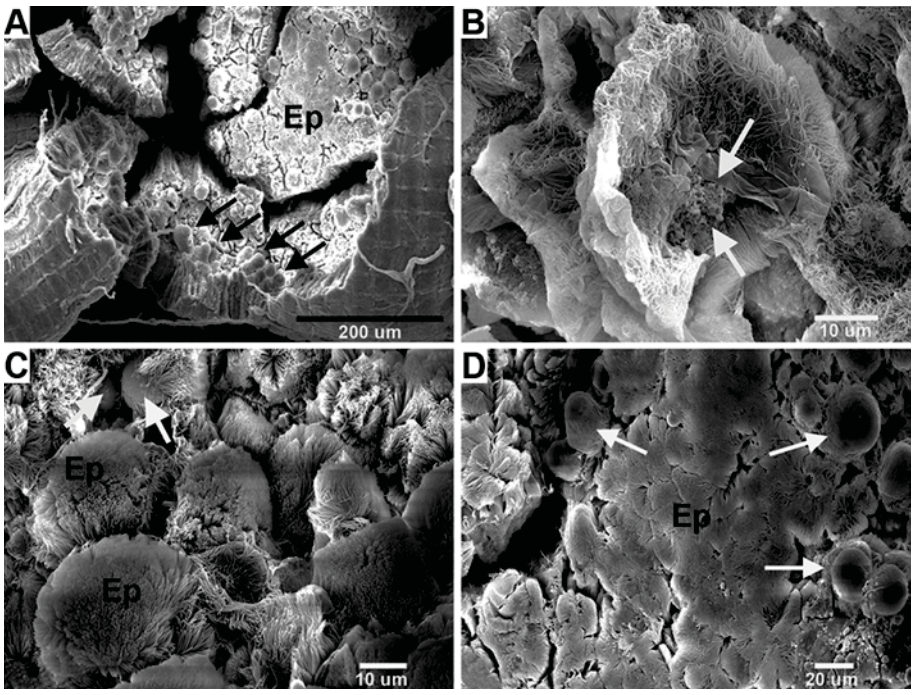

Fig 5-Ultrastructural aspects of *Oc. togoi* epithelium in late fourth instars with peritrophic matrix removed under SEM. (A) Numerous degenerated epithelial cells with cytoplasmic protrusions (arrows) in the midgut lumen were noted. (B) An apical membrane of a degenerated epithelial cell broke and organelle debris (arrows) was discharged into the midgut lumen. (C), (D) SEM micrographs showing fully formed epithelial cells (Ep) and epithelial cells with cytoplasmic protrusions (arrows).

Morphological and protein analyses of adult female salivary glands of *Anopheles barbirostris* species A1 (Diptera: Culicidae)

Phattanawiboon, B.[1], Jariyapan, N.[1*], Roytrakul, S.[2], Paemanee, A.[2], Sor-suwan, S.[1], Intakhan, N.[1], Chanmol, W.[1], Siriyasatien, P.[3], Saeung, A.[1] and Choochote, W.[1]

[1]Department of Parasitology, Faculty of Medicine, Chiang Mai University, Chiang Mai 50200, Thailand

[2]National Center for Genetic Engineering and Biotechnology (BIOTEC), National Science and Technology Development Agency, Pathumthani 12120, Thailand

[3]Department of Parasitology, Faculty of Medicine, Chulalongkorn University, Bangkok 10330, Thailand

*Corresponding author email: njariyapan@gmail.com

Abstract. Morphology and protein profiles of female salivary glands of *Anopheles barbirostris* species A1 were analyzed. Female glands consisted of a distinctive tri-lobed structure connected to a main salivary canal, a single medial and two lateral lobes with proximal and distal portions. Cellular architecture was similar among the lobes, with secretory material appearing as large masses. Cells of the proximal-lateral lobes contained secretory masses with a finely filamentous aspect. In the distal-lateral lobes, cells had a dense secretory product with mottled pattern. Cells of the medial lobe had secretory masses which were uniformly stained and highly electron dense. Following emergence, the glands accumulated secretory material rapidly and developed completely within three days. Degenerative changes including loss of stored secretion and increase of cytoplasmic vacuolation and concentric lamellar structures were observed from day 16 post emergence that correlated with total amount of the salivary gland proteins determined during development. SDS-PAGE, nanoLC-MS, and glycoprotein analysis revealed at least eleven major protein bands, of which each morphological region contained different major proteins. Two glycoproteins, apyrase/5'-nucleotidase and D7, were identified. These results form a basis for further studies on details of cytopathological changes of malarial infected glands and roles of the proteins in disease transmission.

Keywords. *Anopheles*; mosquito; salivary gland; proteins; morphology

INTRODUCTION

Malaria is an ongoing problem for people in the world, especially children. It affects 200 million people worldwide causing up to 500 million clinical cases annually and 1.5 to 2.7 million deaths per year (WHO, 2012; Raghavendra *et al*., 2011). Malaria is exclusively transmitted by female *Anopheles* mosquitoes. Mosquito female salivary glands are being investigated because of their important role in the transmission of pathogens and assisting both blood and sugar meal feeding (James & Rossignol, 1991; James, 1994). The saliva of mosquitoes contains pharmacologically active molecules, such as vasodilators, anti-coagulants, and platelet aggregation inhibitors, to counteract the host's defense against blood loss (hemostasis) (Law *et al*., 1992; Stark & James, 1996). In addition, antigenic and immunogenic molecules in the mosquito saliva involving immunoglobulin E, immunoglobulin G and T-lymphocyte mediate hyposensitivity response in the vertebrate host (Ribeiro & Arca, 2009; Ribeiro *et al*., 2010).

Previous works on the morphological aspects of mosquito salivary glands has been described for *Aedes aegypti*, *Anopheles stephensi*, *Culex pipiens*, *Anopheles darlingi*, and *Culex quinquefasciatus* (Orr *et al*., 1961; Wright, 1969; Janzen & Wright, 1971; Barrow *et al*., 1975; Moreira-Ferro *et al*., 1999; da Cunha Sais *et al*., 2003). However, histological sections of adult female salivary glands related to the age of mosquitoes have only been studied in *Ae. aegypti* and *Aedes togoi* (Beckett, 1990). Results have shown that the salivary gland morphology varies from less than one day to 48 days post emergence. For salivary gland proteins, the following hematophagous mosquitoes have been analyzed: *Ae. aegypti* (Orr *et al*., 1961; Janzen & Wright, 1971; Valenzuela *et al*., 2002), *An. stephensi* (Suwan *et al*., 2002), *An. gambiae* (Arca *et al*., 1999; Franceschetti *et al*., 2002), *An. darlingi* (Moreira *et al*., 2001), *An. barbirostris* complex (Jariyapan *et al*., 2010), *Anopheles cracens*, formerly *Anopheles dirus* B, (Jariyapan *et al*., 2007), *Anopheles albimanus* (Cazares-Raga *et al*.,

2007), *Cx. pipiens* (Barrow *et al*., 1975), *Cx. quinquefasiatus* (Nascimento *et al*., 2000), *Ae. togoi* (Jariyapan & Harnnoi 2002), *Armigeres subalbatus* (Siriyasatien *et al*., 2005), and *Mansonia uniformis* (Phumee *et al*., 2011). These analyses have revealed at least 19 major polypeptides in the mosquito salivary glands using SDS-PAGE but a few proteins have been identified (Suwan *et al*., 2002; Jariyapan *et al*., 2007, 2010). So far, no systematic investigation on changes in salivary gland morphology and proteins during adult development has been performed in *Anopheles* mosquitoes.

In Thailand, *Anopheles barbirostris* species A1, a member of the *An. barbirostris* complex (Saeung *et al*., 2007), has been reported as a potential vector for *P. vivax* (Thongsahuan *et al*., 2011). However, only preliminary analysis of female salivary gland proteins of *An. barbirostris* species A1 has performed using sodium dodecyl sulphate polyacrylamide gel electrophoresis (SDS-PAGE). Nano-liquid chromatography-mass spectrometry (nanoLC-MS) analysis has revealed only a major protein band matched with a protein involved in blood feeding, gSG6, of *An. gambiae* (Jariyapan *et al*., 2010). No other study has been performed in this mosquito species. Therefore, in this study, the ultrastructural morphology of the salivary glands of female *An. barbirostris* species A1 mosquitoes and the total amount of salivary gland proteins during adult development were analyzed. In addition, identification of the major salivary gland proteins using SDS-PAGE followed by nanoLC-MS and glycoprotein analysis were performed. These results provided information helpful for further study on the roles of salivary proteins of this mosquito species in disease transmission and hematophagy.

MATERIALS AND METHODS

Mosquito

An. barbirostris species A1 colonies (Saeung *et al*., 2007) successfully maintained for many consecutive generations in an insectary at the Department of Parasitology, Faculty of Medicine, Chiang Mai University, Thailand and were utilized in this study. The methods for rearing mosquitoes described by Choochote *et al*. (1983) and Kim *et al*. (2003) were used. The mosquitoes were reared and maintained in the insectary at 27±2°C with 70±10% relative humidity, and a photo-period of 12:12 (light/dark) h. Adult mosquitoes were given continuous access to a 10% sucrose solution and fed on blood from immobilized mice when required. Mosquitoes aged 0-25 days post emergence and fed on sucrose solution were used in this study.

Salivary gland dissection

Salivary gland dissection was performed utilizing the method described by Jariyapan *et al.* (2010). Adult mosquitoes between three to five days of age were cold anaesthetized on ice before salivary gland dissection. Salivary glands of the mosquitoes were dissected in phosphate-buffered saline [PBS; 10 mM Na_2SO_4, 145 mM NaCl (pH 7.2)] using fine entomological needles under a stereoscopic microscope at 4X magnification and transferred to a microcentrifuge tube with a small volume of PBS. The samples were then kept at -80°C until use. Dissection of the various regions of the female salivary glands was performed. The medial lobes were cut at the junction of the medial lobes and the lateral lobes. The distal-lateral and proximal-lateral lobes were cut at the intermediate region separating the two lobes. The gland parts were immediately removed to separate tubes to avoid possible protein contamination between the different sections of the glands. The gland parts were placed in a small volume of PBS and stored at -80°C until use.

Protein quantification

The protein content of each salivary gland pair was determined using a Micro BCA Protein Assay Kit (Pierce, Rockford, IL) according to the manufacturer's instruction. The protein concentration was determined based on a bovine serum albumin (BSA) standard curve.

Light microscopy

Salivary glands of female mosquitoes were dissected in PBS and allowed to settle onto slides without drying. Photographs of the glands were taken using a digital camera attached to a light microscope.

Transmission electron microscopy (TEM)

Salivary glands were dissected in PBS and fixed for two h at room temperature with 2.5% glutaraldehyde in PBS buffer (pH 7.4). The glands were then washed twice in buffer and post-fixed for one h with 1% osmium tetroxide. Thereafter, the glands were dehydrated in a crescent series of graded ethanol, incubated overnight in an epoxy resin (PolyBed 812)/acetone solution (1:1), and then embedded in pure resin and polymerized for 48 h at 60°C. Ultra-thin sections were stained with uranyl acetate and lead citrate and observed in a Zeiss EM10C transmission electron microscope, operated at 60 kV.

SDS-Polyacrylamide gel electrophoresis

Salivary gland samples were thawed on ice and mixed in 1:2 (v/v) 1XSDS gel loading buffer (50mM Tris-HCl, pH 6.8, 100 mM DTT, 2% SDS, 0.1% Bromphenol blue, 10% glycerol). Then, the samples were heated for five min in a boiling water bath and loaded on 15% SDS polyacrylamide gels. Molecular weight markers (Bio-Rad Laboratories; Hercules, CA) were applied in each gel.

In-gel digestion

Protein bands of interest were excised from the SDS-polyacrylamide gels using sterile surgical blades with aseptic technique. The gel pieces were subjected to in-gel digestion using an in-house method developed by Proteomics Laboratory, National Center for Genetic Engineering and Biotechnology (BIOTEC), National Science and Technology Development Agency (NSTDA), Thailand. The gel plugs were dehydrated with 100% acetonitrile (ACN), reduced with 10 mM DTT in 10 mM ammonium bicarbonate at room temperature for one h and alkylated at room temperature for one h in the dark in the presence of 100 mM iodoacetamide (IAA) in 10 mM ammonium bicarbonate. After alkylation, the gel pieces were dehydrated twice with 100% ACN for five min. To perform in-gel digestion of proteins, 10 µl of trypsin solution (10 ng/µl trypsin in 50% ACN/10 mM ammonium bicarbonate) was added to the gels followed by incubation at room temperature for 20 minutes, and then 20 µl of 30% ACN was added to keep the gels immersed throughout digestion. The gels were incubated at 37°C for a few hours or overnight. To extract peptide digestion products, 30 µl of 50% ACN in 0.1% formic acid (FA) was added into the gels, and then the gels were incubated at room temperature for ten min in a shaker. Peptides extracted were collected and pooled together in a new tube. The pool extracted peptides were dried by vacuum centrifuge and kept at -80°C for further mass spectrometric analysis.

NanoLC-MS analysis and protein identification

The protein digest was injected into an Ultimate 3000 LC System (Dionex, Sunnyvale, CA) coupled to an ESI-Ion Trap MS (HCT Ultra PTM Discovery System, Bruker, Germany) with electrospray at a flow rate of 300 nl/min to a nanocolumn (Acclaim PepMap 100 C18, 3 µm, 100A, 75 µm id x 150 mm). A solvent gradient (solvent A: 0.1% formic acid in water; solvent B: 80% of 0.1% formic acid in 80% acetonitrile) was run for 40 min. Mascot from

Matrix Science Ltd. (London, UK) was used to search all of the tandem mass spectra (Perkins *et al*., 1999). The data were sent to the National Center for Biotechnology nonredundant (NCBInr) protein database. The search was performed taking Other Metazoa as taxonomy. The other search parameters were enzyme of specificity strict trypsin; one missed cleavage; fixed modifications of Carbamidomethyl (C); oxidation (Met); peptide tolerance of 100 ppm; Fragment Mass Tolerance of ± 0.5 Da; peptide change of 1+; and monoisotopic. Protein identification was made on the basis of a statistically significant Mowse score (≥ 30).

Coomassie Brilliant Blue (CBB) and glycoprotein staining

Following the electrophoresis, the gels were CBB stained. First, the gels were fixed in 50% methanol and 10% acetic acid for 30 min, then stained with 1% CBB in 10% methanol and 5% acetic acid for 2 h, and finally de-stained in 10% methanol and 5% acetic acid until dark protein bands were visible. The gels were scanned with the Imagescanner III (GE Healthcare, UK). For glycoproteins, the gels were stained with Pro-Q Emerald 300 glycoprotein stain (Invitrogen, OR) according to the manufacturer's instruction.

RESULTS

Morphology of female salivary glands of *An. barbirostris* species A1 mosquitoes

An adult female salivary gland of *An. barbirostris* species A1 consisted of a distinctive tri-lobed structure connected to a main salivary canal, a single medial and two lateral lobes with proximal and distal secretory portions. The proximal portion of the median lobe was short and served to link this lobe with the two lateral lobes. A cuticular duct extended through it from the distal portion and connected to the ducts of the lateral lobes (Figure 1).

Ultrastructural analysis revealed that all lobes were acinar structures, organized as a unicellular epithelium that surrounded a salivary canal and surrounded by a very thin basal

lamina. In general, cellular architecture was similar among the lobes, with secretory material appearing as large masses that pushed the cellular structures to the periphery of the organ. In the cytoplasm of all secretory cells, rough endoplasmic reticulum cisternae with several mitochondria were observed. Nuclei were also basally located and exhibited a more or less prominent central nucleolus. In cells of the proximal-lateral lobes, secretory cavities contain secretory mass with finely filamentous aspect (Figure 2). Numerous short microvilli extended from the apical cell membrane into the cavities. The secretory cavities opened into a periductal space and the secretory product seemed to reach the duct lumen through irregular channels that perforate the cuticular wall of the proximal salivary duct (Figure 2). In the distal-lateral lobes, cells had secretory cavities filled with a dense secretory product with a mottled pattern (Figure 3). A large number of mitochondria, rough endoplasmic reticulum, and free ribosomes were found in the cytoplasm of the cells. The secretory masses of the distal lateral portion appeared to open directly into the duct, whose cuticle is perforated by broad channels; the dark secretory product completely filled the duct lumen. The apical cell membrane forms a very intricate network that surrounds the secretory cavities (Figure 3b). Cells of the medial lobe hold large secretory cavities containing secretory masses uniformly stained and highly electrondense (Figure 4). Short membrane projections protruding from the apical cell membrane into the secretory cavities were observed. The cytoplasm of the cells contained abundant cisternae of rough endoplasmic reticulum and mitochondria with large nucleoli noted (Figure 4). Figure 5 shows non-secretory cells of the proximal portion of the medial lobe. Seven to eight cells make up the circumference of the proximal portion epithelium. The apical cell membranes are united by septate desmosomes. A high number of mitochondria and a large nucleus in the basal cytoplasm of each non-secretory cell were thrown into numerous deep membrane infoldings penetrating into one-fourth to one-third of the depth of the cells. A very dense and ruffled cuticular wall with no channels limited the

salivary duct, which had its lumen occupied by a very uniform and electron-dense secretory material (Figure 5a, b).

Following emergence, the glands of newly emerged females were poorly developed but their growth was progressive from the time of emergence. The glands accumulated secretory material rapidly and developed completely within three days post emergence. In all lobes, degenerative changes including loss of stored secretion and increase of cytoplasmic vacuolation and concentric lamellar structures were observed from 16 days post emergence (Figure 2-5).

Total amount of the salivary gland proteins during adult development

Total salivary gland protein contents of female *An. barbirostris* species A1 during adult development were determined (table 1). The protein content in a newly emerged female was 0.12 ± 0.01 μg/gland pair. After day one post emergence, the total protein content increased gradually and reached the highest level on day three (1.26 ± 0.04 μg/gland pair) and remained almost constant for two weeks. The content started to gradually decrease from day 16.

Identification of major salivary gland proteins and glycoprotein analysis

SDS-PAGE analysis revealed at least 11 major protein bands in the female glands. In newly emerged females, protein bands of molecular masses higher than 32 kDa were weakly visualized. Then the number of protein components gradually increased with age (Figure 6a). The different morphological regions of the female salivary glands displayed different electrophoretic protein profiles. The major protein bands with molecular masses of 65, 37, 34, 20, 18, and 10 kDa appeared predominantly in the distal portions of the lateral lobes (Figure 6a, lane D), while protein bands with molecular masses of 45, 39, 35, 33, and 14 kDa were predominant in the medial lobe (Figure 6a, lane M). As the proximal portions of the

lateral lobes were very small, 50 proximal portions from 25 females were used to analyze on a SDS gel. The protein profile shows a number of minor protein bands (Figure 6a, lane P). Five major proteins were identified by nanoLCMS including 5' nucletidase/apyrase (65 kDa), antiplatelet protein (37 kDa), D7 protein (34 kDa), D7r1 (18 kDa), and gSG6 (10 kDa) (Fig. 6a). Glycoprotein analysis showed that at least five major glycoprotein bands were detected and two were identified as apyrase/5'-nucleotidase (65 kDa) and D7 protein (34 kDa) (Figure 6b).

DISCUSSION

Our morphological studies of adult female *An. barbirostris* species A1 salivary glands revealed similarities with the salivary glands of *Aedes, Culex* and *Anopheles* species (Orr *et al*., 1961; Wright, 1969; Janzen & Wright, 1971; Barrow *et al*., 1975; Moreira-Ferro *et al*& 1999). As described for *Anopheles* mosquitoes, the salivary glands of adult female *An. barbirostris* species A1 were composed of three identical lobes, one short medial lobe and two longer lateral ones. However, in the salivary glands of the female *Ae. aegypti*, *Culex quinquefasciatus* and *Culex tritaeniorhynchus*, the cuticular canal extends throughout the full length of all the three lobes (Clements, 1992). In *An. barbirostris* species A1, only the lateral lobes have a cuticular canal corresponding to the study in *An. stephensi* and *An. darlingi* (Wright, 1969; Moreira-Ferro *et al*., 1999).

Although, the cellular architecture was similar among the lobes, the secretory products of each particular region were different between cells of the portions. The secretory cavities of the proximal lateral lobes contained secretory mass with finely filamentous aspect, possibly due to coagulation of a dispersed material (probably protein and carbohydrate complexes). The secretory products in the distal lateral and medial lobes were uniformly dense and extremely dark when stained with uranyl/lead, suggesting a high hydration state

and high protein content. A similar pattern of secretory materials in the salivary glands of *An. stephensi* and *An. darlingi* has been reported, respectively (Wright, 1969; Moreira-Ferro *et al*., 1999). It was established that the distal lateral and medial lobes are female specific, while the proximal lateral lobes produce enzymes involved in sugar feeding and are morphologically and functionally similar to adult male glands (Stark & James, 1996). Short microvilli extended from the apical cell membrane in the three lobes into the secretory cavities might be related to surface enlargement as described for *Cx. quinquefasciatus, Ae. aegypti, Ae. albopictus*, and *An. darlingi* (Rossignol *et al*., 1984; Marinotti & James, 1990; Marinotti *et al*., 1996; Moreira-Ferro *et al*., 1998; Nascimento *et al*., 2000). Abundant cisternae of rough endoplasmic reticulum and mitochondria with large nucleoli in cytoplasm of the cells were related to protein synthesis and high-energy requirement.

In addition, non-secretory cells with numerous mitochondria enclosed by cell membrane infoldings observed in the proximal portion of the medial lobe of *An. barbirostris* species A1 is consistent with a previous work by Moreira-Ferro *et al.* (1999) on the female salivary glands of *An. darlingi*. In *An. stephensi*, *Ae. aegypti*, and *Cx. quinquefasciatus* salivary glands, a region without acini in the proximal-medial lobe has been reported with its proposed role in water and ion transport (Wright, 1969; Janzen & Wright, 1971; Nascimento *et al*., 2000).

Following emergence, development of the glands of newly emerged *An. barbirostris* species A1 females was progressive. The glands accumulated secretory material rapidly and developed completely within three days which is consistent with previous studies on salivary gland proteins in *Ae. aegypti*, *An. cracens*, and *Cx. quinquefasciatus* (Beckett, 1990; Nascimento *et al*., 2000; Jariyapan *et al*., 2007). Degenerative changes including loss of stored secretion and increase of cytoplasmic vacuolation and concentric lamellar structures were observed from 16 days post emergence that correlate with total amount of the salivary

gland proteins determined during adult development. This result suggests that the cytological changes in the salivary glands are a natural phenomenon due to aging as reported in *Ae. aegypti* and *Ae. togoi* (Beckett, 1990). However, study on details of morphological and cytopathological changes of long-term malarial infected salivary glands of *An. barbirostris* species A1 using TEM would improve our understanding on the mosquito cellular respond to malarial infection as they relate to pathogen transmission as a study in *Cx. quinquefasciatus* infected with West Nile virus (Girard *et al*., 2005).

In most of mosquito species, on the first day post emergence, adult *Anopheles* spp. females need to feed on sugar to meet the energy demands of basal metabolism and flight. After the third day of adult life, they must feed on human or animal blood as they require nutrients in the blood to stimulate growth of ovaries and encourage creation of eggs (Clements, 1992). The rate of protein accumulation in the salivary glands is highest on day two of adult development, reaching a peak in week two and then beginning to decline at week three (Racioppi *et al*., 1987). For female *An. barbirostris* species A1, the protein accumulation in the salivary glands is highest on day three post emergence and then begins to decline at week two indicating that the salivary glands of this mosquito species became mature on the third day of adult life. Jariyapan *et al.* (2012) have demonstrated that proteins involved in blood feeding in the salivary glands of female *An. barbirostris* species A2 started to accumulate from zero hours after emergence and gradually increased and became predominant within two days.

SDS-PAGE analyses of several *Anopheles* mosquito salivary glands have demonstrated that approximately 12-15 major and several minor proteins are detected in *An. stephensi* (Suwan *et al*., 2002), *An. carcens* (formerly *An. dirus* B) (Jariyapan *et al*., 2007), *Anopheles albimanus* (Cazares-Raga *et al*., 2007), *An. barbirostris* species A2 (Jariyapan *et al*., 2012), and *An. campestris*-like (Sor-suwan *et al*., 2013). For *An. barbirostris* species A1,

we used SDS-PAGE followed by Nano-LCMS to identify the major proteins in this study. Results show that at least 11 major proteins were found in the female salivary glands and each morphological region of the female glands contained different major proteins. Our results confirm accumulation of proteins involved in blood feeding, i.e., putative 5'-nucleotidase/apyrase, anti-platelet protein, long form D7 salivary protein, D7-related one protein, and gSG6, in the distal-lateral lobes and/or medial lobes of the female glands. Specific proteins produced in different parts of the salivary glands of female *An. barbirostris* species A1 are consistent with previous studies on salivary gland profiles of *An. stephensi*, *Ae. togoi*, *Ar. subalbatus* and *An. cracens* (Suwan *et al*., 2002; Jariyapan & Harnnoi, 2002; Siriyasatien *et al*., 2005; Jariyapan *et al*., 2007). Moreover, at least five glycoproteins were detected in the female salivary glands of *An. barbirostris* species A1, however, only two were identified including apyrase/5'-nucleotidase and D7.

Secretory proteins that pass through the Golgi apparatus are often glycosylated or modified by phosphorylation. Glycoproteins contain three major types of oligosaccharides: N-linked, O-linked, and glycosylphosphatidylinositol (GPI) lipid anchors and are involved in a wide range of biological functions such as receptor binding, cell signaling, immune recognition, inflammation, and pathogenicity. In insects, for examples, mucins, which are found in the sialotranscriptomes of *Anopheles funestus* (Calvo *et al*., 2007) and *Glossina morsitans morsitans* (Alves-Silva *et al*., 2010), contain many short O-linked glycans. Mucins increase the viscosity of the fluids and are postulated to help maintain the insect mouthparts (Alves-Silva *et al*., 2010). For apyrase/5'-nucleotidases, most 5' nucleotidases are typically extracellular proteins bound to the membrane by GPI anchors attached to their carboxyterminal domain. In some insects including the *Ae. aegypti*, *Ae. albopictus*, *Culex pipiens quinquefasciatus*, *L. longipalpis*, and *G. morsitans morsitans*, however, the 5' nucleotidases lack the GPI anchor attachment domain, either through mutation or truncation,

thus inferring that these proteins are secreted (Champagne *et al*., 1995; Charlab *et al*., 1999; Ribeiro *et al*., 2004; Ribeiro *et al*., 2007; Alves-Silva *et al*., 2010; Dong *et al*., 2012). This enzyme helps the acquisition of blood meals by the degradation of adenosine diphosphate (ADP), a mediator of platelet aggregation and inflammation (Ribeiro & Francischetti, 2003) and prevents neutrophil activation (Sun *et al*., 2006). Long form D7 proteins contain glycosylation sites found in *An. gambiae*, *An. stephensi*, *Anopheles arabiensis*, *An. funestus*, and *An. darlingi* mosquitoes (Francischetti *et al*., 2002; Suwan *et al*., 2002; Valenzuela *et al*., 2002; Calvo *et al*., 2007; Calvo *et al*., 2009). D7 proteins are one of the abundant proteins in the saliva of female mosquitoes and able to bind biogenic amines and leukotrienes, in addition to various components of the coagulation cascade, thus interfering with the hemostatic and host immune responses (Calvo *et al*., 2006). Structure and specific biological functions of these glycoproteins in the salivary glands of female mosquitoes should be studied for their involvement in pathogen transmission. In conclusions, morphology and protein profiles of female salivary glands of *An. barbirostris* species A1 were analyzed. The adult female salivary glands revealed similarities with the salivary glands of *Aedes*, *Culex* and *Anopheles* species. Following emergence, development of the glands of newly emerged females was progressive. The glands accumulated secretory material rapidly and developed completely within three days. Degenerative changes including loss of stored secretion and increase of cytoplasmic vacuolation and concentric lamellar structures were observed from day 16 post emergence that correlated with total amount of the salivary gland proteins determined during adult development. SDS-PAGE, nanoLC-MS, and glycoprotein analysis revealed at least eleven major protein bands, of which each morphological region contained different major proteins and two were glycoproteins including apyrase/5’-nucleotidase and D7. From day one post emergence, similar major protein profiles of females were detected in all ages suggesting that aging may have no effect on the major proteins. Our data indicated

that the salivary glands of *An. barbirostris* species A1 present different morphological aspects, probably reflecting different biochemical compositions and activities. Further biochemical and molecular studies are needed to demonstrate the real composition and function of each salivary gland lobe. Furthermore, distinct physiological aspects of the gland cells must be approached, by using insects with different feeding status. These results are foundational for further studies on details of morphological and cytopathological changes of long-term malarial infected salivary glands and roles of the saliva proteins in disease transmission and hematophagy.

Acknowledgments. This work was financially supported in part by the Thailand Research Fund through the Royal Golden Jubilee Ph.D. Program (PHD/0350/2552), the Thailand Research Fund (TRF Senior Research Scholar: RTA5480006 to WC, subproject to NJ), and the Faculty of Medicine Endowment Fund, Chiang Mai University.

REFERENCES

Alves-Silva, J., Ribeiro, J.M., Van Den Abbeele, J., Attardo, G., Hao, Z., Haines, L.R., Soares, M.B., Berriman, M., Aksoy, S. & Lehane, M.J. (2010). An insight into the sialome of *Glossina morsitans morsitans*. *BMC Genomics* **11**: 213.

Arca, B., Lombardo, F., De Lara Capurro, M., Della Torre, A., Dimopoulos, G., James, A.A. & Coluzzi, M. (1999). Trapping cDNAs encoding secreted proteins from the salivary glands of the malaria vector *Anopheles gambiae*. *Proceedings of the National Academy of Sciences of the United States of America* **96**: 1516-1521.

Barrow, P.M., McIver, S.B. & Wright, K.A. (1975). Salivary glands of female *Culex pipiens*: morphological changes associated with maturation and blood-feeding. *Canadian entomologist* **107**: 1153-1160.

383 Beckett, E.B. (1990). Development and ageing of the salivary glands of adult female *Aedes*
384 *aegypti* (L.) and *Aedes togoi* (Theobald) mosquitoes (Diptera:Culicidae).
385 *International Journal of Insect Morphology and Embryology* **19**: 277-290.
386 Calvo, E., Dao, A., Pham, V.M. & Ribeiro, J.M. (2007). An insight into the sialome of
387 *Anopheles funestus* reveals an emerging pattern in anopheline salivary protein
388 families. *Insect Biochemistry and Molecular Biology* **37**: 164-175.
389 Calvo, E., Mans, B.J., Andersen J.F. & Ribeiro, J.M. (2006). Function and evolution of a
390 mosquito salivary protein family. *Journal of Biological Chemistry* **281**: 1935-1942.
391 Calvo, E., Pham, V.M., Marinotti, O., Andersen, J.F. & Ribeiro, J.M. (2009). The salivary
392 gland transcriptome of the neotropical malaria vector *Anopheles darlingi* reveals
393 accelerated evolution of genes relevant to hematophagy. *BMC Genomics* **10**: 57.
394 Cazares-Raga, F.E., Gonzalez-Lazaro, M., Montero-Solis, C., Gonzalez-Ceron, L., Zamudio,
395 F., Martinez-Barnetche, J., Torres-Monzon, J.A., Ovilla-Munoz, M., Aguilar-Fuentes,
396 J., Rodriguez, M.H. & de la Cruz Hernandez-Hernandez, F. (2007). GP35 ANOAL,
397 an abundant acidic glycoprotein of female *Anopheles albimanus* saliva. *Insect*
398 *Molecular Biology* **16**: 187-198.
399 Champagne, D.E., Smartt, C.T., Ribeiro, J.M. & James A.A. (1995). The salivary gland-
400 specific apyrase of the mosquito *Aedes aegypti* is a member of the 5'-nucleotidase
401 family. *Proceedings of the National Academy of Sciences of the United States of*
402 *America* **92**: 694-698.
403 Charlab, R., Valenzuela, J.G., Rowton, E.D. & Ribeiro, J.M. (1999). Toward an
404 understanding of the biochemical and pharmacological complexity of the saliva of a
405 hematophagous sand fly *Lutzomyia longipalpis*. *Proceedings of the National Academy*
406 *of Sciences of the United States of America* **96**: 15155-15160.

Choochote, W., Sucharit, S. & Abeywickreme, W. (1983). Experiments in crossing two strains of *Anopheles barbirostris* Van der Wulp 1884 (Diptera: Culicidae) in Thailand. *Southeast Asian Journal of Tropical Medicine and Public Health* **14**: 204-209.

Clements, A.N. (1992). Devevelopment, nutrition and reproduiction. In: The biology of mosquitoes, 1st ed, Chapman & Hall, London, pp.272-291.

da Cunha Sais, T., de Moraes, R.M., Ribolla, P.E., de Bianchi, A.G., Marinotti, O. & Bijovsky, A.T. (2003). Morphological aspects of *Culex quinquefasciatus* salivary glands. *Arthropod Structure and Development* **32**: 219-226.

Dong, F., Fu, Y., Li, X., Jiang, J., Sun, J. & Cheng, X. (2012). Cloning, expression, and characterization of salivary apyrase from *Aedes albopictus*. *Parasitology Research* **110**: 931-937.

Francischetti, I.M., Valenzuela, J.G., Pham, V.M., Garfield, M.K. & Ribeiro, J.M. (2002). Toward a catalog for the transcripts and proteins (sialome) from the salivary gland of the malaria vector *Anopheles gambiae*. *Journal of Experimental Biology* **205**: 2429-2451.

Girard, Y.A., Popov, V., Wen, J., Han, V. & Higgs, S. (2005). Ultrastructural study of West Nile virus pathogenesis in *Culex pipiens quinquefasciatus* (Diptera: Culicidae). *Journal of Medical Entomology* **42**: 429-444.

James, A.A. & Rossignol, P.A. (1991). Mosquito salivary glands: parasitological and molecular aspects. *Parasitology Today* **7**: 267-271.

James, A.A. (1994). Molecular and biochemical analyses of the salivary glands of vector mosquitoes. *Bulletin de I'Institut Pasteur* **92**: 133-150.

Janzen, H.G. & Wright, K.A. (1971). The salivary glands of *Aedes aegypti* (L.): an electron microscope study. *Canadian Journal of Zoology* **49**: 1343-1346.

Jariyapan, N., Choochote, W., Jitpakdi, A., Harnnoi, T., Siriyasatein, P., Wilkinson, M., Junkum, A. & Bates, P.A. (2007). Salivary gland proteins of the human malaria vector, *Anopheles dirus* B (Diptera: Culicidae). *Revista do Instituto de Medicina Tropical de São Paulo* **49**: 5-10.

Jariyapan, N., Baimai, V., Poovorawan, Y., Roytrakul, S., Saeung, A., Thongsahuan, S., Suwannamit, S., Otsuka, Y. & Choochote, W. (2010). Analysis of female salivary gland proteins of the *Anopheles barbirostris* complex (Diptera: Culicidae) in Thailand. *Parasitology Research* **107**: 509-516.

Jariyapan, N., Roytrakul, S., Paemanee, A., Junkum, A., Saeung, A., Thongsahuan, S., Sor-Suwan, S., Phattanawiboon, B., Poovorawan, Y. & Choochote, W. (2012). Proteomic analysis of salivary glands of female *Anopheles barbirostris* species A2 (Diptera: Culicidae) by two-dimensional gel electrophoresis and mass spectrometry. *Parasitology Research* **111**: 1239-1249.

Jariyapan, N. & Harnnoi, T. (2002). Preliminary study of salivary gland proteins of the mosquito *Aedes togoi* (Theobald). *Chiang Mai Medical Bulletin* **41**: 21-28.

Kim, S.J., Choochote, W., Jitpakdi, A., Junkum, A., Park, S.J. & Min, G.S. (2003). Establishment of a self-mating mosquito colony of *Anopheles sinensis* from Korea. *Korean Journal of Entomology* **33**: 267-271.

Law, J.H., Ribeiro, J.M.C. & Wells, M.A. (1992). Biochemical insights derived from diversity in insects. *Annual Review of Biochemistry* **61**: 87-111.

Marinotti, O., Brito, M. & Moreira, C.K. (1996). Apyrase and alpha-glucosidase in the salivary glands of *Aedes albopictus*. *Comparative Biochemistry and Physiology* **113B**: 675-679.

Marinotti, O. & James, A.A. (1990). An α-glucosidase in the salivary glands of the vector mosquito, *Aedes aegypti*. *Insect Biochemistry* **20**: 619-623.

457 Moreira-Ferro, C.K., Daffre, S., James, A.A. & Morinotti, O. (1998). A lysozyme in the
458 salivary glands of malaria vector *Anopheles darlingi*. *Insect Molecular Biology* **7**:
459 257-264.
460 Moreira-Ferro, C.K., Marinotti, O. & Bijovsky, A.T. (1999). Morphological and biochemical
461 analyses of the salivary glands of the malaria vector, *Anopheles darlingi*. *Tissue and*
462 *Cell* **31**: 264-273.
463 Moreira, C.K., Marrelli, M.T., Lima, S.L. & Marinotti, O. (2001). Analysis of salivary gland
464 proteins of the mosquito *Anopheles darlingi* (Diptera: Culicidae). *Journal of Medical*
465 *Entomology* **38**: 763-767.
466 Nascimento, E.P., dos Santos Malafronte, R. & Marinotti, O. (2000). Salivary gland proteins
467 of the mosquito *Culex quinquefasciatus*. *Archives of Insect Biochemistry and*
468 *Physiology* **43**: 9-15.
469 Orr, C.W.M., Hudson, A. & West, A.S. (1961). The salivary glands of *Aedes aegypti*,
470 histological-histochemical studies. *Canadian Journal of Zoology*. **39**: 265-272.
471 Perkins, D.N., Pappin, D.J.C., Creasy, D.M. & Cottrell, J.S. (1999). Probability-based protein
472 identification by searching sequence databases using mass spectrometry data.
473 *Electrophoresis* **20**: 3551-3567.
474 Phumee, A., Preativatanyou, K., Kraivichain, K., Thavara, U., Tawatsin, A., Phusup, Y. &
475 Siriyasatien, P. (2011). Morphology and protein profiles of salivary glands of filarial
476 vector mosquito *Mansonia uniformis*; possible relation to blood feeding process.
477 *Asian Biomedicine* **5**: 353-360.
478 Racioppi, J.V. & Spielman, A. (1987). Secretory proteins from the salivary glands of the
479 adult *Aedes aegypti* mosquitoes. *Insect Biochemistry* **17**: 503-511.
480 Raghavendra, K., Barik, T.K., Reddy, B.P., Sharma, P. & Dash, A.P. (2011). Malaria vector
481 control: from past to future. *Parasitology Research* **108**: 757-779.

Ribeiro, J.M.C. & Arca, B. (2009). From sialomes to the sialoverse: An insight into the salivary potion of blood feeding insects. *Advances in Insect Physiology* **37**: 59-118.

Ribeiro, J.M., Arca, B., Lombardo, F., Calvo, E., Pham, V.M., Chandra, P.K. & Wikel, S.K. (2007). An annotated catalogue of salivary gland transcripts in the adult female mosquito, *Aedes aegypti*. *BMC Genomics* **8**: 6.

Ribeiro, J.M., Charlab, R., Pham, V.M., Garfield, M. & Valenzuela, J.G. (2004). An insight into the salivary transcriptome and proteome of the adult female mosquito *Culex pipiens quinquefasciatus*. *Insect Biochemistry and Molecular Biology* **34**: 543-563.

Ribeiro, J.M.C. & Francischetti, I.M. (2003). Role of arthropod saliva in blood feeding: sialome and post-sialome perspectives. *Annual Review of Entomology* **48**: 73-88.

Ribeiro, J.M., Mans, B.J. & Arca, B. (2010). An insight into the sialome of blood-feeding Nematocera. *Insect Biochemistry and Molecular Biology* **40**: 767-784.

Rossignol, P.A., Ribeiro, J.M.C. & Spielman, A. (1984). Increased intradermal probing time in sporozoite-infected mosquitoes. *American Journal of Tropical Medicine and Hygiene* **33**: 17-20.

Saeung, A., Otsuka, Y., Baimai, V., Somboon, P., Pitasawat, B., Tuetun, B., Junkum, A., Takaoka, H. & Choochote, W. (2007). Cytogenetic and molecular evidence for two species in the *Anopheles barbirostris* complex (Diptera: Culicidae) in Thailand. *Parasitology Research* **101**: 1337-1344.

Siriyasatien, P., Tangthongchaiwiriya, K., Jariyapan, N., Kaewsaitiam, S., Poovorawan, Y. & Thavara, U. (2005). Analysis of salivary gland proteins of the mosquito *Armigeres subalbatus*. *Southeast Asian Journal of Tropical Medicine and Public Health* **36**: 64-67.

Sor-suwan, S., Jariyapan, N., Roytrakul, S., Paemanee, A., Saeung, A., Thongsahuan, S., Phattanawiboon, B., Bates, P.A., Poovorawan, Y. & Choochote, W. (2013). Salivary

gland proteome of the human malaria vector, *Anopheles campestris*-like (Diptera:Culicidae). *Parasitology Research* **112**: 1065-1075.

Stark, K.R. & James, A.A. (1996). Salivary gland anticoagulants in culicine and anopheline mosquitoes (Diptera:Culicidae). *Journal of Medical Entomology* **33**: 645-650.

Sun, D., McNicol, A., James, A.A. & Peng, Z. (2006). Expression of functional recombinant mosquito salivary apyrase: a potential therapeutic platelet aggregation inhibitor. Platelets **17**: 178-184.

Suwan, N., Wilkinson, M.C., Crampton, J.M. & Bates, P.A. (2002). Expression of D7 and D7-related proteins in the salivary glands of the human malaria mosquito *Anopheles stephensi*. *Insect Molecular Biology* **11**: 223-232.

Thongsahuan, S., Baimai, V., Junkum, A., Saeung, A., Min, G.S., Joshi, D., Park, M.H., Somboon, P., Suwonkerd, W., Tippawangkosol, P., Jariyapan, N. & Choochote, W. (2011). Susceptibility of *Anopheles campestris*-like and *Anopheles barbirostris* species complexes to *Plasmodium falciparum* and *Plasmodium vivax* in Thailand. *Memórias do Instituto Oswaldo Cruz* **106**: 105-112.

Valenzuela, J.G., Charlab, R., Gonzalez, E.C., de Miranda-Santos, I.K., Marinotti, O., Francischetti, I.M. & Ribeiro, J.M. (2002). The D7 family of salivary proteins in blood sucking diptera. *Insect Molecular Biology* **11**: 149-155.

World Health Organization. (2012). The World Malaria Report 2012. World Health Organization, Geneva.

Wright, K.A. (1969). The anatomy of salivary glands of *Anopheles stephensi* Liston. *Canadian Journal of Zoology* **47**: 579-587.

530 Figure legends

531

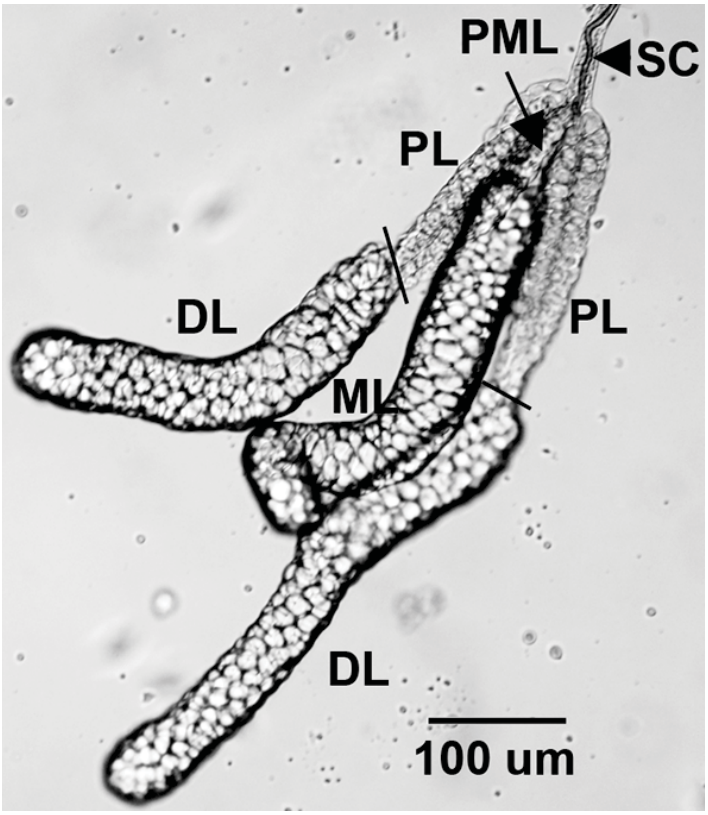

532

533

534 Figure 1. Representative adult female salivary glands of the mosquito, *An. barbirostris*
535 species A1, 7 days post emergence. PL: proximal portion of the lateral lobe; DL: distal
536 portion of the lateral lobe; ML: medial lobe; PML: proximal portion of medial lobe (arrow);
537 SC: salivary canal (arrowhead)

538

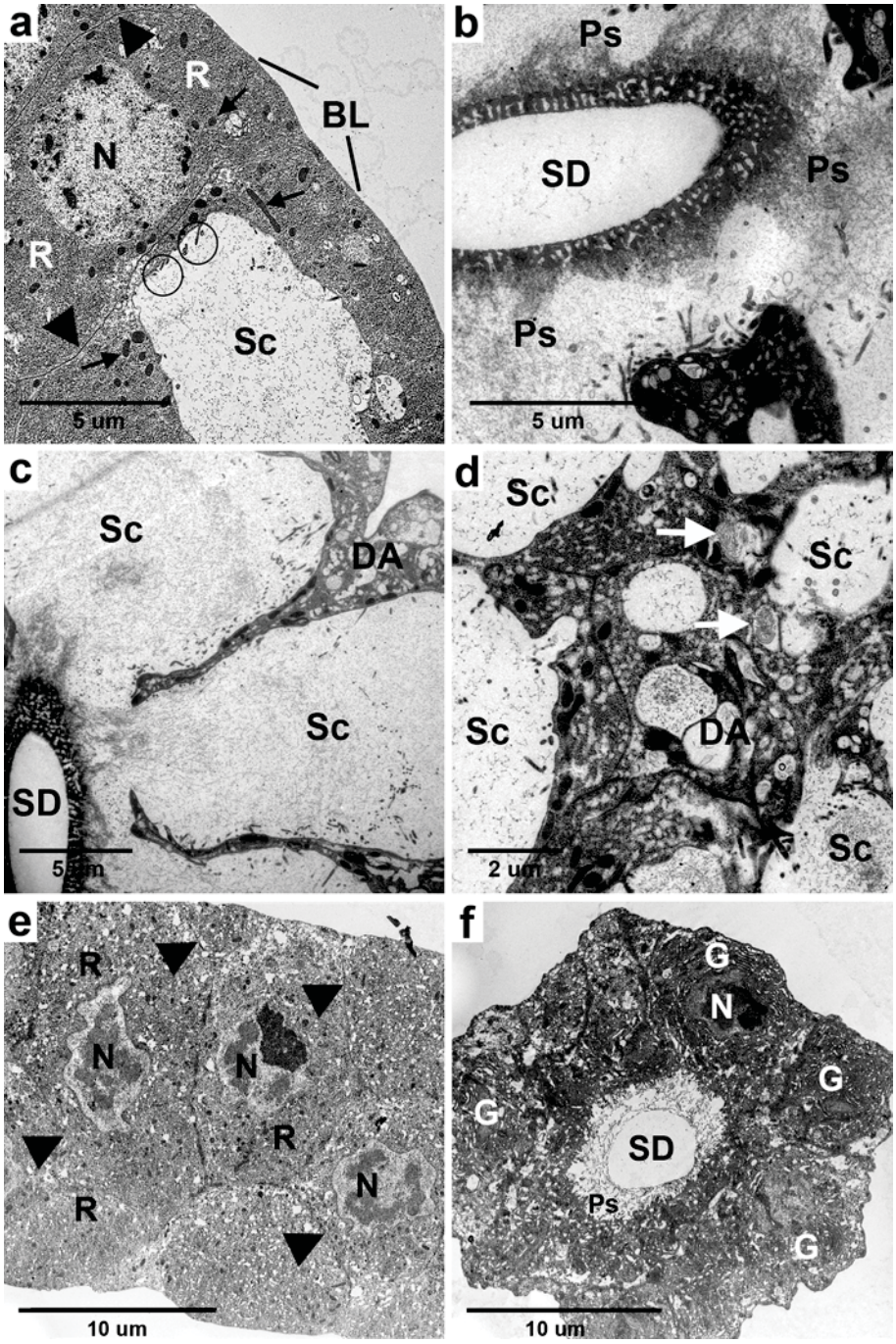

Figure 2. Electron micrograph of proximal-lateral lobes of adult female glands. (a) TEM micrograph of a proximal-lateral lobe of an adult female gland of a newly emerged female. The epithelial cells contain rough endoplasmic reticulum (R), mitochondria (arrows) and nucleus (N) with masses of condensed chromatin. Short microvilli (circles) protrude into a secretory cavity (Sc). The secretory cavity is filled with finely granular secretion. A thin basal

laminar (BL) encompasses the cell periphery. Arrowheads indicate septate desmosomes which unite the lateral cell membranes of the epithelial cells. (b) TEM micrograph showing the duct and periductal space (Ps) of the proximal-later portion. A filamentous meshwork surrounding the granular material similar to the secretion product filled the periductal space. (c, d) TEM micrographs of the proximal-lateral lobes of mosquitoes aged 16 and 21 day post emergence, respectively, showing degenerative areas (DA) with cytoplasmic vacuoles and concentric lamellar structures (white arrows)

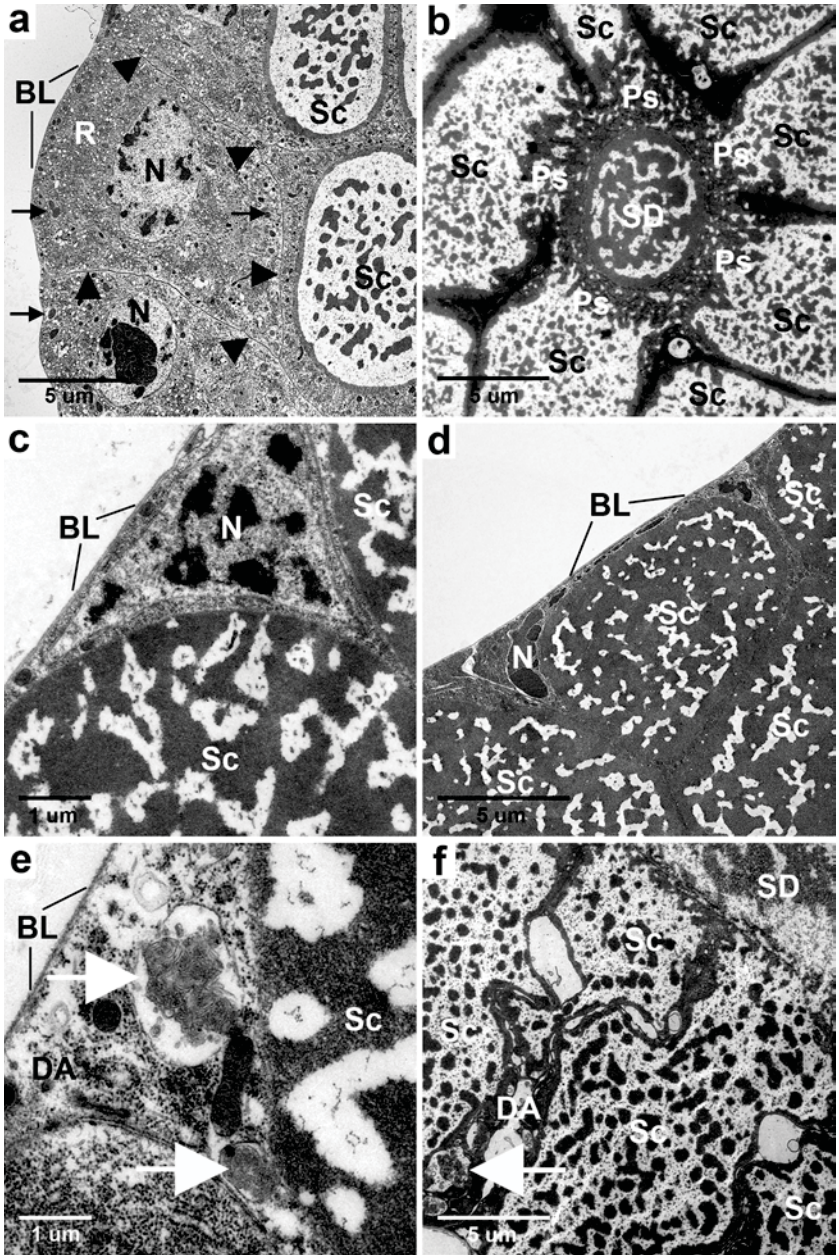

Figure 3. Electron micrograph of distal-lateral lobes of adult female glands. (a) TEM micrograph of a newly emerged female. The epithelial cells contain rough endoplasmic reticulum (R), mitochondria (arrows) and nucleus (N). A nucleoli with large condensed chromatin masses was noted. Secretory cavities (Sc) were filled with coarsely granulated material. The secretory material has a mottled pattern. A thin basal laminar (BL) encompasses the cell periphery. Arrowheads indicate septate desmosomes of the epithelial cells. (b) TEM micrograph showing a salivary duct and periductal space (Ps) of the distal-later portion. The duct surrounds with at least seven epithelial cells. Each cell has a large secretory cavity. A filamentous meshwork and granular material similar to the secretion product fills the periductal space. (c) TEM micrographs of an epithelial cell from a mosquito aged seven days post emergence showing a nucleus (N) with condensed chromatin masses, secretory cavities (Sc) filled with coarsely granulated material, and a thin basal laminar (BL). (d) Epithelial cells from a mosquito aged 16 days post emergence showing a nucleus (N) with large condensed chromatin masses, secretory cavities (Sc), and a thin basal laminar (BL). (e, f) Shrinking epithelial cells with loss of stored secretion and degenerative areas (DA) with vacuoles and concentric lamellar structures (white arrows) were observed in from the mosquitoes aged 21 days post emergence

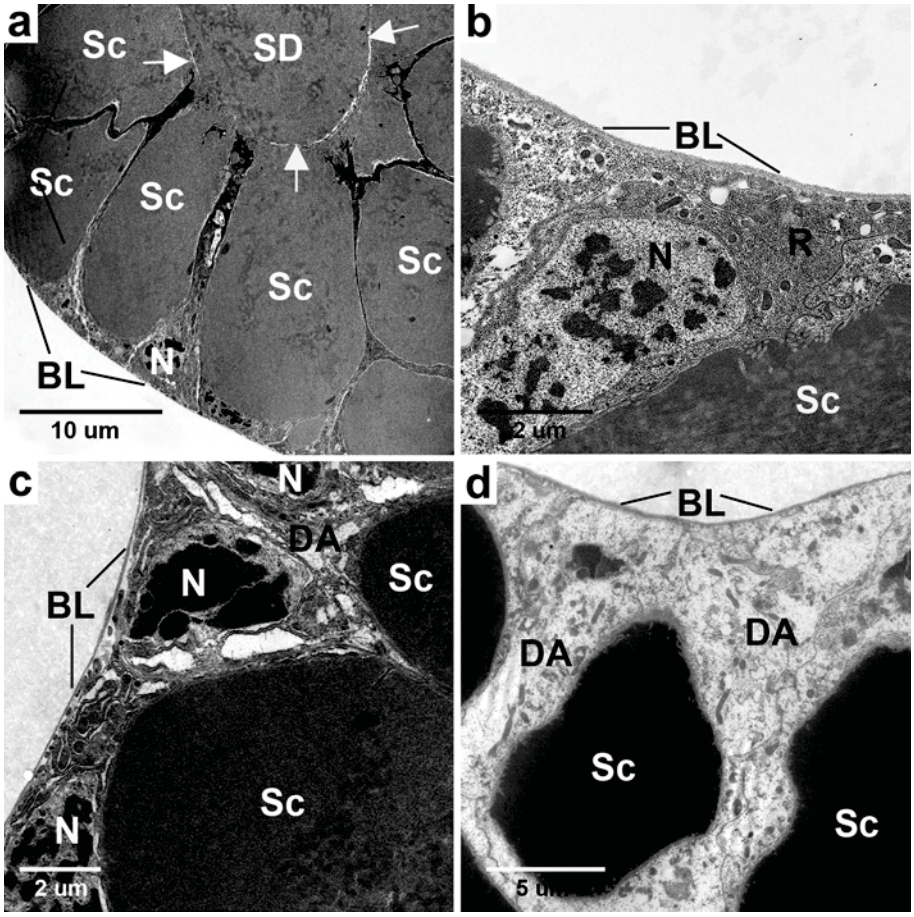

574

575

576 Figure 4. Electron micrograph of cells in the medial lobe of adult female glands. (a) TEM
577 micrograph of epithelial cells from a mosquito aged three day post emergence. The epithelial
578 cells contain nucleus (N) and secretory cavities (Sc) filled with dark homogeneous material.
579 A thin basal laminar (BL) encompasses the cell periphery. (b) TEM micrograph of cells from
580 a mosquito aged seven day post emergence showing a nucleus (N) with condensed chromatin
581 masses, rough endoplasmic reticulum (R), secretory cavities (Sc) and a thin basal laminar
582 (BL). (c) Epithelial cells from a mosquito aged 16 days post emergence showing nucleus (N)
583 with large condensed chromatin masses, secretory cavities (Sc), and a thin basal laminar
584 (BL). Degenerative areas (DA) is noted. (d) Shrinking epithelial cells with loss of stored
585 secretion and degenerative areas (DA) with vacuoles and concentric lamellar structures
586 (white arrows) were observed in cells from the mosquitoes aged 21 days post emergence

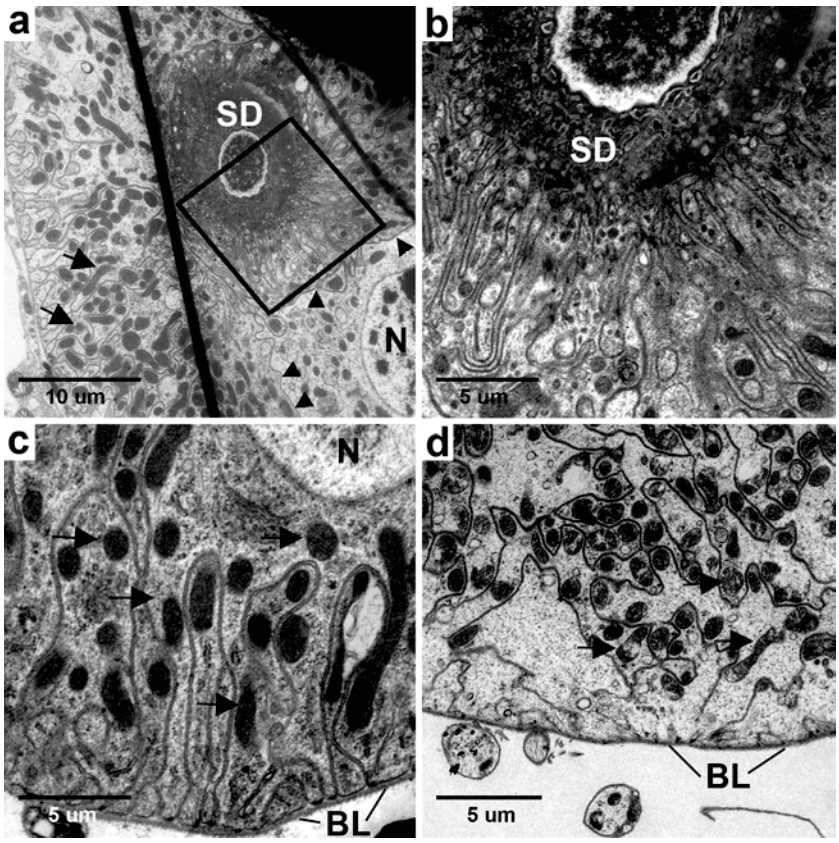

Figure 5. Electron micrograph of the proximal portion of the medial lobe. (a) TEM micrograph showing the salivary duct (SD) with a ruffled wall. Cells surrounding the duct display numerous and deep infoldings of membrane extended from the basal region to the periductal space. The infoldings contain a high number of mitochondria (arrows) and almost no cytoplasm. Arrowheads indicate septate desmosomes. (b) Higher magnification of boxed region in (a) displaying a part of the salivary duct (SD) and infolded apical cell membranes. (c) A part of a large nucleus (N) and the presence of numerous tubular mitochondria (arrows) associated with basal membrane invaginations were observed. (d) At 21 days post emergence, degradation of mitochondria (arrows) and vesicles were observed. Basal laminar (BL)

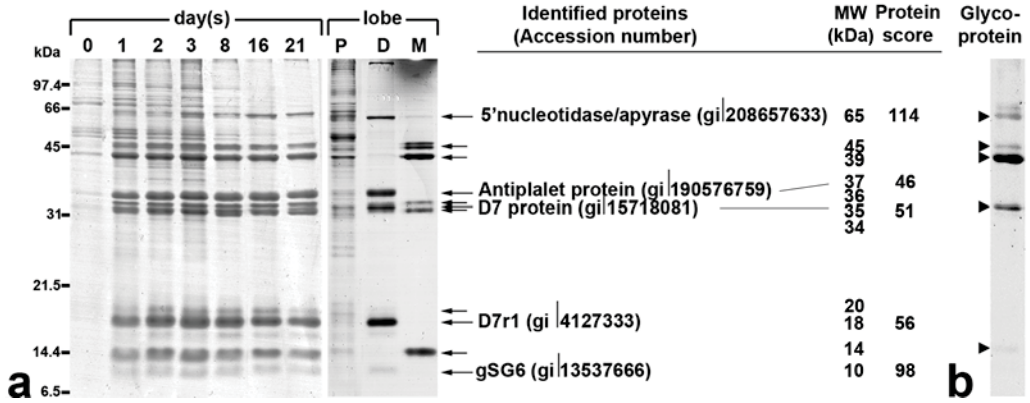

Figure 6. Electrophoretic protein profiles of salivary glands of female *An. barbirostris* species A1 mosquitoes. (a) A pair of female salivary glands was dissected from a mosquito kept on a sugar diet with ages varying from 0 to 21 days post emergence. Lane P: fifty proximal portions of the lateral lobes; lane D: two distal portions of the lateral lobes; lane M: two medial lobes. Proteins were analyzed by SDS-PAGE in a 15% polyacrylamide gel and CBB stained. Molecular mass markers are indicated on the left in kDa. Numbers at the top indicate age in days post emergence. Arrows indicate major salivary gland proteins of female mosquitoes. Long arrows indicate proteins identified by nanoLC-MS. (b) representative of SDS polyacrylamide gels stained with Pro-Q Emerald 300 glycoprotein stain. Arrowheads indicate salivary gland glycoproteins of female mosquitoes

613 Table 1. Total salivary gland content in female *An. barbirostris* species A1 during adult
614 development

	Day (s) post emergence								
	0	1	2	3	5	8	16	21	25
Protein content (µg/gland pair)[1]	0.12 ± 0.01	0.57 ± 0.02	0.73 ± 0.03	1.26 ± 0.04	1.22 ± 0.03	1.20 ± 0.05	0.81 ± 0.02	0.55 ± 0.02	0.46 ± 0.05

615 [1]Mean±SD, Number of samples = 30

616

6. Takaoka H, Srisuka W, Saeung A, Otsuka Y, **Choochote W**. *Simulium* (*Simulium*) *lomkaoense*, a new species of black fly (Diptera: Simuliidae) from Thailand. Zootaxa (impact factor 2012 = 0.974).

Identification and characterisation of *Aedes aegypti* aldehyde dehydrogenases involved in pyrethroid metabolism

Nongkran Lumjuan[1]*, Jureeporn Wicheer[1], Posri Leelapat[1], Wej Choochote[2] and Pradya Somboon[2]

[1]Research Institute for Health Sciences, Chiang Mai University, PO Box 80, Chiang Mai, 50202, Thailand
[2]Department of Parasitology, Faculty of Medicine, Chiang Mai University, Chiang Mai, 50200, Thailand

*Corresponding author: Tel: +66-5394-5055-8 ext. 235, Fax: +66-5322-1849, +66-5389-2298 E-mail address: nklumjuan@yahoo.com, Research Institute for Health Sciences, Chiang Mai University, Chiang Mai, 50200, Thailand

Short title: *Aedes aegypti* aldehyde dehydrogenases and pyrethroid metabolism

Abstract

Background: Pyrethroid insecticides, especially permethrin and deltamethrin, have been used extensively worldwide for mosquito control. However, insecticide resistance can spread through a population very rapidly under strong selection pressure from insecticide use. The upregulation of aldehyde dehydrogenase (ALDH) has been reported upon pyrethroid treatment. In *Aedes aegypti*, the increase in ALDH activity against the hydrolytic product of pyrethroid has been observed in DDT/permethrin-resistant strains. The objective of this study was to identify the role of individual ALDHs involved in pyrethroid metabolism.

Methodology/Principal Findings: Three ALDHs were identified; two of these, ALDH9948 and ALDH14084, were upregulated in terms of both mRNA and protein levels in a DDT/pyrethroid-resistant strain of *Ae. aegypti*. Recombinant ALDH9948 and ALDH14084 exhibited oxidase activities to catalyse the oxidation of a permethrin intermediate, phenoxybenzyl aldehyde (PBald), to phenoxybenzoic acid (PBacid).

Conclusions/Significance: ALDHs have been identified in association with permethrin resistance in *Ae. aegypti*. Characterisation of recombinant ALDHs confirmed the role of this protein in pyrethroid metabolism. Understanding the biochemical and molecular mechanisms of pyrethroid resistance provides information for improving vector control strategies.

Keywords: Aldehyde dehydrogenase, *Aedes aegypti*, pyrethroid, permethrin, metabolism insecticide resistance**.**

Introductions

Pyrethroids, synthetic insecticides analogous to natural pyrethrin, have been widely used throughout the world for the control of insects. Pyrethroids are divided into two groups based on their chemical structures. Type I pyrethroids, such as permethrin, lack an α-cyano group, whereas type II pyrethroids, such as deltamethrin and cypermethrin, contain an α-cyano group. However, the extensive use of these insecticides has led to insecticide resistance in insect populations [1,2,3]. Resistance to pyrethroids can be divided into two main mechanisms: an alteration in the target site of the insecticide or increased expression of metabolic detoxification enzymes. Pyrethroids act by targeting sodium channels, leading to neurotoxic effects [4]. Several point mutations in the voltage-gated sodium channel gene are associated with DDT and pyrethroid resistance [5,6,7,8,9]. In metabolic resistance, enhanced activity of enzymes in metabolic pathways in insects leads to insecticides being detoxified or sequestered before they reach the target site. Overexpression of detoxification enzymes such as cytochromes P450 (CYPs), glutathione S-transferases (GSTs) and carboxylesterases (CEs) have been well documented in pyrethroid resistance in insects [10,11,12].

Pyrethroids are mainly metabolised through the hydrolysis of the ester linkage followed by the oxidation of their component alcohol and acid moieties [13]. Pyrethroids have been extensively studied in humans and rats, indicating that both types are mainly hydrolysed by CEs to produce 3-phenoxybenzyl alcohol (PBalc) [14,15], whereas they are mainly oxidised by P450s, alcohol dehydrogenases (ADHs) and aldehyde dehydrogenases (ALDHs) [16,17]. ALDHs have been investigated as enzymes that are important in the oxidation of permethrin in mammals for their oxidation of intermediate products of pyrethroid to carboxylic acid [18]. In the

mosquito *Anopheles gambiae*, the up-regulation of ALDH after exposure to permethrin has been reported [19]. Enzyme-based metabolite assays also indicated that the catalytic activity of P450s, ADHs and ALDHs were increased in microsomal fractions of a DDT/permethrin-resistant strain (PMD-R) of *Aedes aegypti* from Thailand [20]. In our preliminary study using a proteomic approach, crude homogenates of 4th instar larvae of *Aedes* mosquitoes were partially purified using glutathione agarose columns. Bound fractions were collected, concentrated and separated by 2-dimensional gel electrophoresis. The result indicated that a detoxification enzyme, ALDH (AAEL014080 in VectorBase), was upregulated in the PMD-R strain relative to the laboratory susceptible strain (unpublished data). However, the ability of individual ALDHs isoforms to metabolise permethrin in mosquito has not yet been investigated.

The present study aimed to identify the ALDH genes responsible for permethrin resistance in *Ae. aegypti.* The individual ALDHs that are involved in permethrin resistance were characterised, and their expression patterns were analysed. Recombinant proteins were produced, and the in vitro metabolism of permethrin and its hydrolysis products were determined.

Materials and Methods

Materials

Cis/Trans-permethrin was purchased from Chem Service (West Chester, PA). Permethrin metabolites, 3-phenoxybenzyl alcohol (PBalc, 98% purity), 3-phenoxybenzylaldehyde (PBald, 98% purity) and 3-phenoxybenzoic acid (PBacid, 98% purity) including β-Nicotinamide adenine dinucleotide (NAD^+) were purchased from Sigma (St. Louis, MO).

Mosquito strains

The PMD and PMD-R strains originated from Chiang Mai Province, Thailand [21]. The PMD strain was resistant to DDT, whereas the PMD-R strain was resistant to both DDT and permethrin. The New Orleans strain was an insecticide-susceptible laboratory strain of *Ae. aegypti.*

Database search and sequence alignment

A preliminary study using 2-dimensional gel electrophoresis demonstrated that expression of ALDH (AAEL014080) was increased in the PMD-R strain relative to the NO and PMD strains at the larval stage (unpublished data). The protein sequence of a known ALDH (AAEL014080) was used as a query for a BLAST search of the *Aedes aegypti* sequences in VectorBase. Deduced amino acid sequences of ALDHs were aligned using ClustalW [22].

Identification of ALDH genes

The oligonucleotide primers were designed based on the sequences of ALDH in VectorBase (Table S1). The full-length cDNAs of ALDH genes from *Ae. aegypti* were amplified using Taq DNA polymerase (Qiagen) as described by the manufacturer's protocol. PCR parameters consisted of 35 cycles of 30 s at 95 °C, 30 s at 55 °C, and 1.5 min at 72 °C. PCR products were cloned into the pGEM-T easy Vector (Promega) and then transformed into JM109 competent *Escherichia coli* cells. The plasmid DNA was submitted to 1st BASE Laboratories (Malaysia) for sequencing to verify the integrity of genes.

Quantitative PCR analysis

Total RNA was extracted from 3 biological replicate sets (10 mosquitoes per replicate) of 4th instar larvae, pupae, and one-day-old adult males or females from

each of the three strains using the TRIzol plus RNA Purification System (Invitrogen). Complementary DNA was synthesised using SuperScript III reverse transcriptase (Gibco) as described in the manufacturer's protocol. Quantitative PCR was performed as previously described, using QuantiFast SYBR Kit's protocol (Qiagen) [23].The primers used are shown in Table S2.The PCR parameters consisted of 2 steps of 95ºC for 5 min and 35 cycles of 95ºC for 10 s, 60ºC for 35 s, followed by a dissociation step.

Construction of plasmids and expression of ALDHs

Total RNA was extracted from whole mosquitoes of the PMD-R strain using Trizol reagent (Sigma). Complementary DNA was synthesised using SuperScript III reverse transcriptase (Gibco) as described in the manufacturer's protocol. PCR products generated with ProofStart DNA polymerase (Qiagen) using gene specific primers (Table S1) were cloned into the pET 100-D/TOPO vector using the Champion pET directional TOPO Expression kit according to the manufacturer's instruction (Invitrogen). The construct was verified by DNA sequencing. The plasmids containing the ALDH genes were transformed into *E. coli* BL21 Star (DE3). The recombinant proteins were produced after induction with isopropyl β−D-thiogalactoside at 37ºC or room temperature for 4 h.

Protein purification

The pET 100-D/TOPO vector encodes an N-terminal polyhistidine (6xHis) fused to the recombinant protein. Protein purification was performed using HisTrap Ni affinity column (GE Healthcare) as described previously [23]. The protein purity was verified by 12.5% polyacrylamide gel electrophoresis and Coomassie staining.

The protein concentration was determined by the Bradford method using the Bio-Rad protein-assay dye reagent and bovine serum albumin as a standard [24].

Western Blot analysis

Western blot analysis was performed as previously described [21]. The membrane was probed with 1:50,000 and 1:100,000 dilutions of polyclonal antibodies against ALDH9948 and ALDH14080, respectively. The bound antiserum was detected by incubation with a 1:50,000 dilution of Peroxidase-labelled Anti-Rabbit Antiserum followed by visualisation using ECL Advanced Blotting Detection Kit (Amersham Bioscience).

Enzyme activity

ALDH activity against PBald was measured as described previously [16]. Briefly, the substrate mixture contained 1 mM EDTA, 0.1 mM pyrazole and 2.5 mM $NAD(P)^+$ in 33 mM Phosphate buffer, pH 8.2. The enzyme was incubated with the substrate mixture at 37ºC, and the reaction rate was determined by the formation of NAD(P)H at 340 nm in 4 min. The esterase assay was conducted as described previously, by measuring the hydrolysis of p-nitrophenyl acetate (pNPA) to the products p-nitrophenol (pNP) and acetate [25]. Kinetic studies were performed by varying the concentration of PBald in the presence of NAD^+. The results were analysed by non-linear regression analysis using GraphPad Prism 4 software.

PBald oxidation by recombinant ALDHs

ALDH activity was measured by the oxidation of PBald to PBacid, as detected by HPLC. The assay was modified from the method described previously [17]. Briefly, 20 μg of recombinant ALDHs were incubated with 0.4 mM PBald in the presence of 3 mM NAD^+ in 0.1 M Tris-Cl buffer, pH 7.4 at 37°C for 10 min.

Pyrene was then added as an internal control. The reaction mixture was extracted with 1.5 ml of chloroform. This procedure was repeated in triplicate. The chloroform extracts were then pooled, air-dried and analysed with HPLC.

HPLC was performed with a Shimadzu LC 20-A Series (Shimadzu) using a Nova-Pak C18 column (3.9 x 150 mm; Waters). The extract was resuspended in 200 µl of acetonitrile. The mixture (10 µl) was injected into the column at a flow rate of 1 ml/min. The gradient elution was performed at 35ºC, and the detection wavelength was 230 nm. Peaks were integrated into peak area with the LC Solution (Shimadzu). ALDH activity was calculated as the formation of PBacid/min/mg protein. The concentration of PBacid was determined by comparison with a known concentration of PBacid.

Results

Identification of *Ae. aegypti* ALDHs

The DNA sequence of ALDH (AAEL014080) in *Ae. aegypti* was retrieved from VectorBase (http://www.vectorbase.org), and it is located in supercontig 1.1002. Close paralogues of ALDH (AAEL014080), ALDH (AAEL009948) and ALDH (AAEL009029) were included in the experiment to expand for genes of interest that were found on supercontigs 1.440 and 1.363, respectively. The deduced amino acid sequences of these three ALDHs are shown in Figure 1.

Quantitative PCR analysis

To determine whether the ALDH genes were overexpressed at the transcriptional level, real-time PCR was performed in three *Ae. aegypti* strains, the NO susceptible strain and the PMD and PMD-R strains, at three developmental stages. *ALDH14080* was significantly upregulated in the larvae and females of the

PMD-R strain relative to the NO strain. *ALDH9948* and *ALDH9029* were also overexpressed in almost all developmental stages except in the adult male for *ALDH9948* (Figure 2). *ALDH9948* mRNA levels were significantly upregulated in all life stages except the adult male ($p< 0.001$ in larva and adult female, and $p< 0.05$ in pupa) when compared to the PMD strain. *ALDH14080* expression was significantly higher in the larval stage of PMD-R only relative to PMD (Table S3). In contrast, there is no evidence of upregulation of *ALDH9029* mRNA in the PMD-R strain when compared to the PMD strain in any life stage (Table S3). These results show that upregulation of *ALDH9948* and *ALDH1408*0 may confer resistance to permethrin.

Western Blot analysis

To confirm the expression of ALDHs at the protein level, western blots were performed using specific polyclonal antibodies against ALDH9948 and ALDH14080. To validate the specificity of these polyclonal antibodies, immuno-cross-reactivity between ALDH9948 and ALDH14080 was investigated. The polyclonal antibody for ALDH9948 exhibited low-level cross-reactivity with ALDH14080 (Figure 3B), whereas the anti-ALDH14080 antibody was observed to have high specificity. Protein expression profiles of ALDH were investigated in crude homogenates of four developmental stages of three *Ae. aegypti* strains. Expression levels of ALDH9948 and ALDH14080 were increased in the PMD-R strain in almost all developmental stages (pupae and adult males and females), except for larvae when compared to the NO and PMD strains (Figure 3A). In all three strains, no visible bands of ALDHs were detected in the larval stage, whereas strong bands were presented in pupae and adult males and females. Meanwhile, crude homogenates from the larval stage gave no smearing bands when stained with Coomassie blue, indicating no protein degradation. The expression of rat ALDH has been reported to increase with age

[26]. This might indicate that early stages express ALDH proteins at low levels that could not be detected in the small number of larvae used in this study.

Recombinant protein expression

To determine whether the *Ae. aegypti* ALDHs contribute to permethrin metabolism, recombinant ALDHs were produced, and the ability of these proteins to metabolise permethrin was determined. The full-length sequences of two ALDHs, ALDH9948 and ALDH14080, were amplified by PCR using cDNA templates from the PMD-R strain and subcloned into the *E. coli* expression vector pET 100-D/TOPO. Expression of His_6-tagged ALDHs in *E. coli* BL21 Star (DE3) yielded soluble recombinant proteins at the 37ºC expression temperature. The purity of His_6-tagged recombinant ALDHs was verified in 12.5% SDS-PAGE and corresponded to the predicted size of approximately 65 kDa (data not shown).

Biochemical characterisation of ALDHs

Both His_6-tagged recombinant ALDHs possess ALDH activity to catalyse the oxidation of intermediate aldehyde of permethrin, PBald. The ALDH activity was measured by spectrophotometry, mediated by the formation of NAD(P)H as products of the reaction. The oxidation reactions of recombinant ALDH9948 and ALDH14080 required either NAD^+ or $NADP^+$ as a cofactor; however, these enzymes prefer NAD^+ to $NADP^+$ (Table 1). It has been noted that most ALDHs prefer to use NAD^+ over $NADP^+$ as a cofactor [27]. Generally, ALDHs exhibit esterase activity in vitro [28]. In this study, recombinant ALDHs also have esterase activities that catalyse the hydrolysis of p-nitrophenyl acetate to produce p-nitrophenol and acetate (Table 1). The highest esterase activity belongs to recombinant ALDH14080, with a specific activity of 13.11 ± 0.98 μmole/min/mg proteins.

Kinetic parameters of purified ALDHs were determined using PBald and NAD^+ as substrate and cofactor, respectively. Michaelis-Menten constants (K_m) for ALDH9948 and ALDH14080 were 153.8 ± 30.0 and 34.4 ± 6.8 nM, respectively, in respect to PBald (Table 2). The ($V_{max}/K_{m\ PBald}$) value of ALDH14080 was higher than that of ALDH9948, indicating the catalytic efficiency of this enzyme against PBald.

To determine whether recombinant ALDHs readily oxidised PBald, HPLC was performed to identify the product of PBacid. The metabolite profile of *trans*/*cis*-permethrin is shown in Figure S1. Pyrene was spiked as an internal control, given the extraction recovery range of 81-97%. The HPLC results indicated that PBald was oxidised by recombinant ALDH9948 and ALDH14080 with specificities of 1192 ± 55 and 1119 ± 14 nmole PBacid formed/min/mg protein, respectively (Table 3). Because recombinant ALDHs exhibit esterase activity, the ability of these enzymes to catalyse the hydrolysis of the parent permethrin was investigated. The incubation of recombinant ALDHs with *trans*/*cis* permethrin did not produce PBalc, suggesting that ALDHs are not associated with permethrin hydrolysis (data not shown). The incubation of denatured recombinant ALDHs with PBald in the presence of NAD^+ did not produce PBacid, indicating that the oxidation of PBald was mediated by recombinant ALDHs.

Discussion

Overexpression of detoxification genes has been well documented in association with insecticide resistance of many insect species. P450s, GSTs and CEs are primarily implicated in the detoxification of insecticides in insects. It has been reported that P450s contribute to resistance in all classes of insecticides [29]. The upregulation of several P450s, particularly those belonging to the CYP6Z, CYP6M or

CYP9J subfamilies, has been reported to be involved in resistance to pyrethroids in mosquitoes [30,31,32]. Some species, including *Ae. aegypti* CYP9J32, *An. gambiae* CYP6M2 and *An. gambiae* CYP6Z8, have the ability to metabolise pyrethroids [32,33,34]. GSTs, especially GSTE2, GSTE4 and GSTE7, were also observed to be overexpressed in resistant populations [30,31,35]. Recombinant GSTE2-2 showed DDT dehydrochlorinase activity to metabolise DDT, but the recombinant GSTE7-7 did not appear to metabolise DDT. Therefore, the role of GSTE7 in insecticide resistance remains unclear [21]. Many genes encoding CE enzymes were identified to be upregulated in organophosphate-, carbamate- and pyrethroid-resistant insects [36].

However, other genes that are responsible for insecticide resistance cannot be excluded. To date, microarray technology has been utilised to expand the number of detoxification genes and has identified new relevant genes that might be involved in metabolic resistance [19,30,31,37,38,39]. Aside from P450s, GSTs and CEs, microarray data also identified secondary detoxification genes that may confer insecticide resistance. For example, aldo-ketoreductase, an NAD(P)(H) oxidoreductases that catalyse the reduction of aldehydes to alcohols, was over-transcribed in temephos-selected strain of *Ae. aegypti*[40]. UDP-glucuronosyltransferases (UGTs), phase II detoxification enzymes involved in the conjugation of xenobiotics, were also identified as upregulated after permethrin exposure and in response to carbamate, respectively. ALDHs were also found to be upregulated in insecticide resistance in insects [19,37]. However, the functions of these enzymes in insecticide detoxification require further investigation. In mammals, the oxidation of pyrethroids was catalysed by ALDH [16]. A recent study in insecticide metabolism revealed the important role of ALDH in the detoxification of pyrethroid in mosquito [20]. Aldehyde dehydrogenases are a family of enzymes that

oxidise a broad range of endogenous, xenobiotic and lipid peroxidation products that contain the highly reactive aldehyde to their corresponding carboxylic acid [25]. In mammals, ALDHs are involved in both the detoxification of aldehydes and the biosynthesis of pheromones [27]. However, few studies of ALDHs have been reported in insects. In *Drosophila*, ALDHs play a vital role in ethanol metabolism by mediating the oxidation of acetaldehyde to acetate, which is involved in ethanol resistance [28,29,31].

In this study, transcript levels for three of the *Ae. aegypti* ALDH genes were quantified. *ALDH9948* was significantly overexpressed in the insecticide-resistant PMD-R strain in almost all developmental stages, except adult males, when compared to the susceptible PMD line. In contrast, *ALDH14080* was upregulated relative to the PMD strain only in the larval stage. Quantitative PCR results revealed that insecticide selection increased the expression of these ALDHs, although the overexpression was not observed in all life stages. The altered expression of ALDH9948 and ALDH14080 was confirmed at the protein level, indicating that the increase in these proteins is strongly associated with resistance to permethrin. Inconsistencies between the mRNA and protein levels of the same gene may be caused by differences in post-translational regulation between the different developmental stages. Although high levels of ALDH mRNA were found in the larval stage, there was no protein detected by western blot, suggesting that the protein may be expressed at a level below the detection limit in early stages. However, low-abundance ALDH was detected by 2D-gel electrophoresis from a large sample of larvae used in combination with the sub-proteome approach for the enrichment of low-abundance proteins. The recombinant ALDH isoforms exhibited oxidase activity to catalyse the oxidation of aldehyde moiety of pyrethroids, but subcellular localisation of individual ALDHs was not

investigated further in this study. These experiments support a role for *ALDH9948* and *ALDH14080* in conferring resistance to permethrin in the PMD-R strain of *Ae. aegypti*.

Collectively, in *Aedes aegypti*, it has been reported that parental permethrin can be hydrolysed in vitro. Our previous study demonstrated that the formation of PBacid was decreased in the presence of an esterase inhibitor, BNPP, suggesting the function of esterases in permethrin metabolism [20]. The importance of particular CEs in pyrethroid detoxification has not yet been studied. However, it has been proposed that non-specific esterases may be involved in pyrethroid hydrolysis in insects [41]. A recent study demonstrated that both PBalc and PBald were oxidised by *Aedes aegypti* CYP6Z8 [32]. In addition, our finding also clearly revealed that recombinant *ALDH9948* and *ALDH14080* have the ability to catalyse the oxidation of PBald. The results of this study will improve our ability to detect and hence manage insecticide resistance.

In conclusion, we identified two ALDHs that are upregulated in permethrin-resistant *Ae. aegypti* mosquitoes in Thailand. Functional characterisation of recombinant ALDHs clearly demonstrates that these enzymes are capable of metabolising PBald. This report indicates the importance of *Ae. aegypti* ALDHs in permethrin degradation.

Acknowledgements

This study was supported by grants from the National Research Council of Thailand (NRTC) to NL and Thailand Research Fund (TRF) to WC and NL (TRF Senior Research Scholar: RTA5480006).

References

1. Chareonviriyaphap T, Bangs MJ, Suwonkerd W, Kongmee M, Corbel V, et al. (2013) Review of insecticide resistance and behavioral avoidance of vectors of human diseases in Thailand. Parasit Vectors 6: 280.
2. Hemingway J, Field L, Vontas J (2002) An overview of insecticide resistance. Science 298: 96-97.
3. Maharaj R (2011) Global trends in insecticide resistance and impact on disease vector control measures. Open Access Insect Physiol 3: 27-33.
4. Soderlund DM, Clark JM, Sheets LP, Mullin LS, Piccirillo VJ, et al. (2002) Mechanisms of pyrethroid neurotoxicity: implications for cumulative risk assessment. Toxicology 171: 3-59.
5. Brengues C, Hawkes NJ, Chandre F, McCarroll L, Duchon S, et al. (2003) Pyrethroid and DDT cross-resistance in *Aedes aegypti* is correlated with novel mutations in the voltage-gated sodium channel gene. Med Vet Entomol 17: 87-94.
6. Martins AJ, Lima JB, Peixoto AA, Valle D (2009) Frequency of Val1016Ile mutation in the voltage-gated sodium channel gene of *Aedes aegypti* Brazilian populations. Trop Med Int Health 14(11): 1351-1355.
7. Rajatileka S, Black WCt, Saavedra-Rodriguez K, Trongtokit Y, Apiwathnasorn C, et al. (2008) Development and application of a simple colorimetric assay reveals widespread distribution of sodium channel mutations in Thai populations of *Aedes aegypti*. Acta Trop 108: 54-57.
8. Saavedra-Rodriguez K, Urdaneta-Marquez L, Rajatileka S, Moulton M, Flores AE, et al. (2007) A mutation in the voltage-gated sodium channel gene associated with pyrethroid resistance in Latin American *Aedes aegypti*. Insect Mol Biol 16: 785-798.
9. Yanola J, Somboon P, Walton C, Nachaiwieng W, Somwang P, et al. (2011) High-throughput assays for detection of the F1534C mutation in the voltage-gated sodium channel gene in permethrin-resistant *Aedes aegypti* and the distribution of this mutation throughout Thailand. . Trop Med Int Health 16: 501-509.
10. Feyereisen R (2005) Insect Cytochrome P450; In: Gilbert LI IK, Gill SS, eds. Comprehensive Molecular Insect Science Elsevier,pp 1-77, editor.
11. Oakeshott JG, Devonshire AL, Claudianos C, Sutherland TD, Horne I, et al. (2005) Comparing the organophosphorus and carbamate insecticide resistance mutations in cholin- and carboxyl-esterases. Chem Biol Interact 157-158: 269-275.
12. Ranson H, Hemingway J (2005) Glutathione transferases. Comprehensive Molecular Insect Science – Pharmacology (ed. by L.I.Gilbert, K.Iatrou & S.S.Gill), Vol. 5, pp. 383–402. Elsevier, Oxford.
13. Kaneko H (2011) Pyrethroids: Mammalian Metabolism and Toxicity. Journal of Agricultural and Food Chemistry 59: 2786-2791.
14. Nishi K, Huang H, Kamita SG, Kim IH, Morisseau C, et al. (2006) Characterization of pyrethroid hydrolysis by the human liver carboxylesterases hCE-1 and hCE-2. Arch Biochem Biophys 445: 115-123.
15. Ross MK, Borazjani A, Edwards CC, Potter PM (2006) Hydrolytic metabolism of pyrethroids by human and other mammalian carboxylesterases. Biochem Pharmacol 71: 657-669.

16. Choi J, Rose, RL. and Hodgson, E. (2002) In vitro human metabolism of permethrin: the role of human alcohol and aldehyde dehydrogenase. . Pest Biochem Physiol 22: 249-261.
17. Nakamura Y, Sugihara K, Sone T, Isobe M, Ohta S, et al. (2007) The in vitro metabolism of a pyrethroid insecticide, permethrin, and its hydrolysis products in rats. Toxicology 235: 176-184.
18. Hodgson E (2003) In vitro human phase I metabolism of xenobiotics I: pesticides and related compounds used in agriculture and public health, May 2003. J Biochem Mol Toxicol 17: 201-206.
19. Vontas J, Blass C, Koutsos AC, David JP, Kafatos FC, et al. (2005) Gene expression in insecticide resistant and susceptible *Anopheles gambiae* strains constitutively or after insecticide exposure. Insect Mol Biol 14: 509-521.
20. Somwang P, Yanola J, Suwan W, Walton C, Lumjuan N, et al. (2011) Enzymes-based resistant mechanism in pyrethroid resistant and susceptible *Aedes aegypti* strains from northern Thailand. Parasitol Res.
21. Lumjuan N, McCarroll L, Prapanthadara LA, Hemingway J, Ranson H (2005) Elevated activity of an Epsilon class glutathione transferase confers DDT resistance in the dengue vector, *Aedes aegypti*. Insect Biochem Mol Biol 35: 861-871.
22. Thompson JD, Higgins DG, Gibson TJ (1994) CLUSTAL W: improving the sensitivity of progressive multiple sequence alignment through sequence weighting, position-specific gap penalties and weight matrix choice. Nucleic Acids Res 22: 4673-4680.
23. Lumjuan N, Rajatileka S, Changsom D, Wicheer J, Leelapat P, et al. (2011) The role of the *Aedes aegypti* Epsilon glutathione transferases in conferring resistance to DDT and pyrethroid insecticides. Insect Biochem Mol Biol 41: 203-209.
24. Bradford MM (1976) A rapid and sensitive method for the quantitation of microgram quantities of protein utilizing the principle of protein-dye binding. Anal Biochem 72: 248-254.
25. Marchitti SA, Brocker C, Stagos D, Vasiliou V (2008) Non-P450 aldehyde oxidizing enzymes: the aldehyde dehydrogenase superfamily. Expert Opin Drug Metab Toxicol 4: 697-720.
26. Yoon M, Madden MC, Barton HA (2006) Developmental expression of aldehyde dehydrogenase in rat: a comparison of liver and lung development. Toxicol Sci 89: 386-398.
27. Morse D, Meighen E (1984) Aldehyde Pheromones in Lepidoptera: Evidence for an Acetate Ester Precursor in *Choristoneura fumiferana*. Science 226: 1434-1436.
28. Fry JD, Bahnck CM, Mikucki M, Phadnis N, Slattery WC (2004) Dietary Ethanol Mediates Selection on Aldehyde Dehydrogenase Activity in *Drosophila melanogaster*. Integr Comp Biol 44: 275-283.
29. Fry JD, Donlon K, Saweikis M (2008) A worldwide polymorphism in aldehyde dehydrogenase in *Drosophila melanogaster*: evidence for selection mediated by dietary ethanol. Evolution 62: 66-75.
30. Strode C, Wondji CS, David JP, Hawkes NJ, Lumjuan N, et al. (2008) Genomic analysis of detoxification genes in the mosquito *Aedes aegypti*. Insect Biochem Mol Biol 38: 113-123.

31. Fry JD, Saweikis M (2006) Aldehyde dehydrogenase is essential for both adult and larval ethanol resistance in *Drosophila melanogaster*. Genet Res 87: 87-92.
32. Chandor-Proust A, Bibby J, Regent-Kloeckner M, Roux J, Guittard-Crilat E, et al. (2013) The central role of mosquito cytochrome P450 CYP6Zs in insecticide detoxification revealed by functional expression and structural modelling. Biochem J 455: 75-85.
33. Stevenson BJ, Pignatelli P, Nikou D, Paine MJ (2012) Pinpointing P450s associated with pyrethroid metabolism in the dengue vector, Aedes aegypti: developing new tools to combat insecticide resistance. PLoS Negl Trop Dis 6: e1595.
34. Stevenson BJ, Bibby J, Pignatelli P, Muangnoicharoen S, O'Neill PM, et al. (2011) Cytochrome P450 6M2 from the malaria vector Anopheles gambiae metabolizes pyrethroids: Sequential metabolism of deltamethrin revealed. Insect Biochem Mol Biol 41: 492-502.
35. Ding Y, Hawkes N, Meredith J, Eggleston P, Hemingway J, et al. (2005) Characterization of the promoters of Epsilon glutathione transferases in the mosquito *Anopheles gambiae* and their response to oxidative stress. Biochemical Journal 387: 879-888.
36. Montella IR, Schama R, Valle D (2012) The classification of esterases: an important gene family involved in insecticide resistance--a review. Mem Inst Oswaldo Cruz 107: 437-449.
37. Silva AX, Jander G, Samaniego H, Ramsey JS, Figueroa CC (2012) Insecticide resistance mechanisms in the green peach aphid *Myzus persicae* (Hemiptera: Aphididae) I: A transcriptomic survey. PLoS One 7: e36366.
38. Saavedra-Rodriguez K, Suarez AF, Salas IF, Strode C, Ranson H, et al. (2012) Transcription of detoxification genes after permethrin selection in the mosquito *Aedes aegypti*. Insect Mol Biol 21: 61-77.
39. Grisales N, Poupardin R, Gomez S, Fonseca-Gonzalez I, Ranson H, et al. (2013) Temephos resistance in *Aedes aegypti* in Colombia compromises dengue vector control. PLoS Negl Trop Dis 7: e2438.
40. Strode C, de Melo-Santos M, Magalhaes T, Araujo A, Ayres C (2012) Expression profile of genes during resistance reversal in a temephos selected strain of the dengue vector, *Aedes aegypti*. PLoS One 7: e39439.
41. Hemingway J, Hawkes NJ, McCarroll L, Ranson H (2004) The molecular basis of insecticide resistance in mosquitoes. Insect Biochem Mol Biol 34: 653-665.

Tables

Table 1. Substrate specificity of *Ae. aegypti* recombinant ALDH isoforms**.**

	Substrate/cofactor	ALDH 9948	ALDH 14080
Esterase activity (μmole/min/mg)	pNPA	13.11 ± 0.98	0.14 ± 0.02
ALDH activity (nmole/min/mg)	PBald/NAD^+	483 ± 9	254 ± 24
	PBald/$NADP^+$	58 ± 4	19 ± 2

ALDH activity was performed in the presence 4 mM PBald and 2.5 mM $NAD(P)^+$. The oxidation of PBald was monitored by the formation of NAD(P)H.

Table 2. Kinetic parameter of *Ae. aegypti* recombinant ALDH isoforms.

Enzyme	V_{max} (nmole NADH/min/mg)	PBald		NAD^+	
		K_m (nM)	V_{max}/K_m	K_m (nM)	V_{max}/K_m
ALDH 9948	627.4 ± 34.0	153.8 ± 30.8	4.1	139.1 ± 27.9	3.2
ALDH 14080	208.2 ± 9.8	34.4 ± 6.8	6.1	193.8 ± 34.5	1.3

Kinetic studies were performed by varying the concentration of PBald and cofactor NAD^+ at fixed saturated concentrations of NAD^+ and PBald, respectively. The oxidation of PBald to PBacid was monitored by the formation of NADH in the reaction at 37ºC for 4 min. Three independent assays were performed. The results are shown as the mean± SE.

Table 3. Specific activity of *Ae.aegypti* recombinant ALDH isoforms to oxidise PBald**.**

Enzyme	Specific activity (nmole PBacid formed/min/mg protein)
ALDH 9948	1192 ± 55
ALDH 14080	1119 ± 14

Recombinant ALDH (5 μg) was incubated with 2 mM PBald in the presence of 3 mM NAD+ in 0.1 M Tris-Cl buffer, pH 7.4 at 37ºC for 10 min. PBacid formation was determined by HPLC as described. Three independent assays were performed. The results are shown as the mean± SE.

FIGURE LEGENDS

Figure 1. Deduced amino acid sequences of *Ae. aegypti ALDH 9948* and *ALDH 140809*. Sequences shown are from the PMD-R strain. The amino acid sequences were aligned using ClustalW. Letters in bold indicate 100% conservation between the 3 sequences. Dashes are used to denote gaps introduced for maximum alignment.

Figure 2. Transcription profiles of ALDH9029, *ALDH9948* and *ALDH140809* in three strains of *Ae. aegypti*. Complementary DNA from three different biological replicates (ten mosquitoes each) was used as templates. Four life-stages were analysed: larvae (L), pupae (P), adult male (M), and adult female (F). Each sample was analysed in duplicate in each experiment, and the results were averaged from three independent experiments. The mRNA copy numbers were determined by comparison with known concentrations of standard plasmids and normalised against the copy number of the ribosomal S7 transcript. Error bars indicate standard error of the mean. Statistically significant differences were evaluated with ANOVA ($p < 0.001$ indicated by ** and $p < 0.05$ as * relative to New Orleans strain.

Figure 3. Western blot analysis of ALDH9948 and ALDH14080. (A) Elevated protein of ALDH9948 and ALDH14080 in PMD-R strain. Fifty micrograms of protein from New Orleans (NO), PMD and PMD-R strains in four life stages (larvae, pupae, and adult males and females) including purified recombinant His-tagged ALDH9948 and 14080 (25 ng each) were resolved by SDS-PAGE. Proteins were transferred to a nitrocellulose

membrane and probed with anti-ALDH9948 and anti-ALDH14080. Peroxidase labelled anti-rabbit antibody was used as a secondary antibody. Proteins were visualised by enhancing the chemiluminescence using ECL Advanced Blotting Detection Kit (Amersham Biosciences). (B) Determination of antibodies specificity by western blot. Fifty nanograms of non-fusion ALDH9948 and ALDH14080 (Lane1, 2 and 3, respectively) were resolved in SDS-PAGE. Western blotting was performed as described.